Bioactive alginates and macronutrient digestion

Peter Chater BSc

Thesis submitted for the Degree of Doctor of Philosophy

Institute for Cell and Molecular Biosciences

Medical School

Newcastle University

September 2013

Abstract

Macronutrient digestion is a major factor in health and metabolic diseases such as obesity and diabetes and presents a huge global challenge.

Modulating macronutrient digestion with food additives and pharmaceuticals has been shown to be a fruitful approach to the treatment of obesity (Orlistat) and diabetes (Acarbose). Previous work has shown that bioactive agents have novel modulatory effects on the major enzymes of digestion, and work in this lab has shown that specific alginates can inhibit pancreatic lipase up to 70%. Alginates are now being investigated as a potential anti-obesity agent.

The purpose of this thesis was to develop *in vitro* methodologies and an analytical approach for investigating the effects of exogenous compounds on the major digestive enzymes; α-amylase, pepsin, trypsin, and lipase. A 3-step process was developed consisting of; higher-throughput single enzyme analysis, selected enzyme kinetics and model gut analysis.

Alginates were shown to inhibit the action of pepsin, but have no effect on trypsin activity *in vitro*. The structure of alginate is key to the inhibition of pepsin, and rheological and viscometric data suggested that this effect was due to a pH dependent interaction between alginate and protein substrate as well as direct enzyme-inhibitor interactions. A similar effect was observed with Fucoidan and sulphated carrageenans. In the model gut analysis, these effects manifested as inhibition of proteolysis in the simulated gastric phase, but not in the small-intestinal phase.

Alginates were shown to increase the activity of α-amylase during *in vitro* single enzyme analysis, but have no significant affect on carbohydrate digestion in a model gut simulation. Fat digestion in the model gut simulation was inhibited by specific alginates, adding further weight to the potential use of alginates as a therapeutic treatment of obesity.

There was never a sound beside the wood but one,
And that was my long scythe whispering to the ground.
What was it it whispered? I knew not well myself;
Perhaps it was something about the heat of the sun,
Something, perhaps, about the lack of sound—
And that was why it whispered and did not speak.
It was no dream of the gift of idle hours,
Or easy gold at the hand of fay or elf:
Anything more than the truth would have seemed too weak
To the earnest love that laid the swale in rows,
Not without feeble-pointed spikes of flowers
(Pale orchises), and scared a bright green snake.
The fact is the sweetest dream that labor knows.
My long scythe whispered and left the hay to make.

Robert Frost

Acknowledgements

Decleration

This thesis is based on research performed at the Institute for Cell and Molecular Biosciences, Newcastle University. I performed all laboratory work and analysis of results, with the exception of NMR characterisation of alginate structural characteristics which was carried out by FMC Biopolymer & Technostics Ltd.

Contents

List of Figures

xvi

List Of Tables

Chapter 1
Introduction

1.1 Introduction & Justification of Research

The digestion and absorption of the major macronutrients fat, protein and carbohydrate is a major factor in health and metabolic diseases such as obesity and diabetes. By 2015 it is projected that 2.3 billion people will be overweight and 700 million obese [1]. This presents a huge global challenge in terms of health, cost and sustainability. Obesity already currently costs the NHS around £5 Billion annually [2].

Modulating macronutrient digestion with food additives and pharmaceuticals has been shown to be a fruitful approach to the treatment of obesity (Orlistat [3]) and diabetes (Acarbose [4]). Previous studies have shown a number of dietary fibres to have regulatory effects on the activity of digestive enzymes and work in this lab has shown that specific alginates can inhibit pancreatic lipase up to 70%. This is now being investigated as a potential anti-obesity agent.

Alginates are bio-active dietary fibres commonly used at low levels in the food industry which have been shown to have inhibitory action on both pepsin and lipase [5-7]. As current approaches to obesity treatment and management are often ineffective, high-risk or carry with them side-effects the prospect of alginate inhibition of lipase is an exciting and important area of research.

The aim of this project was therefore to develop methodologies for the practical examination of bioactive exogenous compounds on the major digestive enzymes; pepsin, trypsin, α-amylase and lipase. These studies were undertaken with a view to explore the potential to develop novel therapeutics which would modulate the activity of these digestive enzymes.

Nutrition research is a key strategic priority for bioscience research both in terms of food security and in understanding the role of diet and the mechanisms that underpin health and disease [8]. This approach aims to provide a system for analysis of macronutrient digestion and the screening of novel therapeutics, which will aid food

research and present an ethical alternative to animal models and a cost effective pre-trial system that can be used to inform and improve human trials.

Furthermore the introduction of EFSA (European Food Standards Agency) requires a much higher threshold of scientific evidence for food health claims in the EU. This means that costly and financially risky human studies must be undertaken to support health claims.

A potential benefit of the methodological approach which has been developed, and particularly a model gut system is that it provides a robust and physiologically relevant *in vitro* system of analysis which can be used to improve and inform human studies. The methodology may potentially be used to provide data that can be used to investigate efficacy, dosage, delivery methods and allow them to make decisions that will potentially save costs and improve results.

1.2   *Bioactive alginates and obesity*

In 2010 Wilcox et al showed that specific alginates were capable of inhibiting pancreatic lipase by a maximum of 72.2% (± 4.1) using a synthetic substrate DGGR (1,2-o-dilauryl-rac-glycero-3-glutaric acid-(6'-methylresorufin) ester) and 58.0% (± 9.7) with a natural substrate (olive oil triglyceride) [5, 6]. Pancreatic lipase is responsible for the breakdown of the major dietary fat triacylglycerol and inhibition of triglyceride breakdown with alginate may reduce fat breakdown and provide a potential treatment for obesity.

The inhibitory effect was shown to be related to alginate structure, alginates are composed of guluronic and mannuronic acid residues, and alginates high in guluronic acid were shown to be more potent inhibitors of pancreatic lipase. High-G alginates extracted from the *Laminaria hyperborea* seaweed inhibited pancreatic lipase to a significantly higher extent than High-M alginates from the *Lessonia nigrescens* species (Figure 1). The invention of alginate as an inhibitor of pancreatic lipase is now under patent, and is being investigated as an anti-obesity agent in human trials [6].

As the *in vitro* assays for lipase activity have already been developed, the purpose of this study was to develop methodologies to analyse the effects of bioactive compounds on the other enzymes of macronutrient digestion
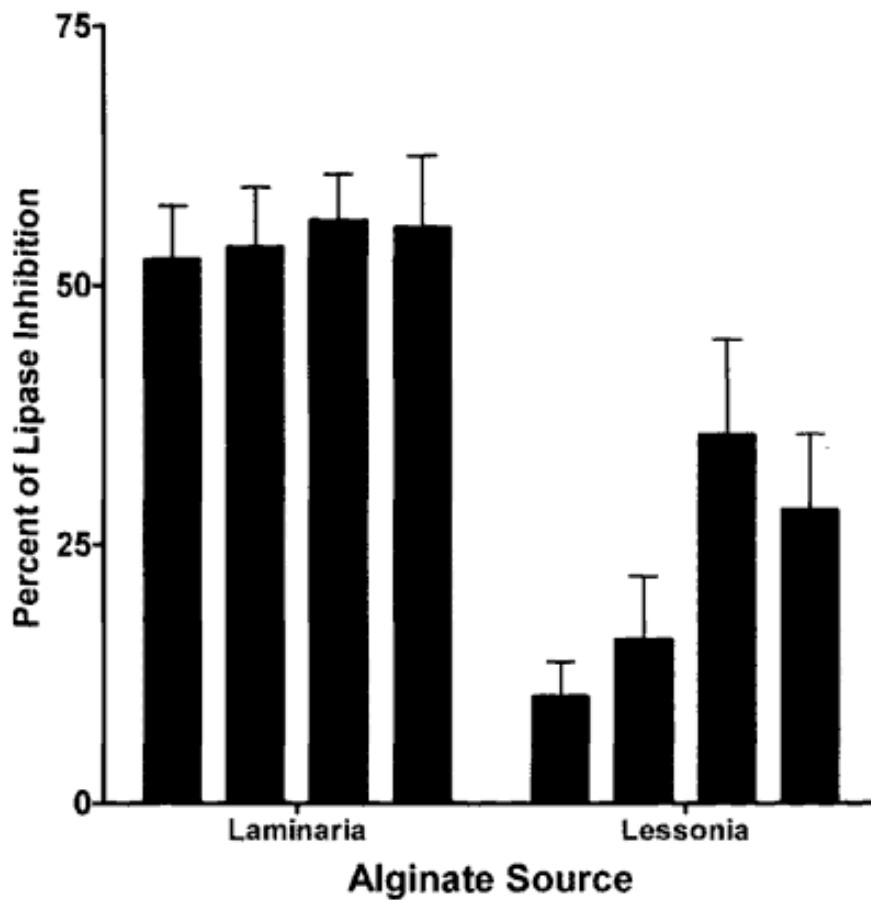
Figure 1   Comparison of lipase inhibition by Lamanaria and Lessonia alginates. Inhibition is shown as a percentage reduction in the presence of 2.43mg/ml alginate as compared to normal lipase activity. The alginates in order as shown are LFR5/60, SF120, SF/LF, LF10L, LF120L, SF60 and H120L. Error bars are shown as the standard error of the mean (n=6). Taken from Wilcox, 2010 [5].

1.2.1   Current Treatments Of Obesity

Obesity and metabolic diseases are a significant and growing problem, particulary in the developed world with obesity and diabetes at epidemic levels. As of 2005, almost 25% of the worlds population (1.6 billion people) were considered overweight by BMI (BMI $\geq$ 25 kg/m^2) and 400 million obese (BMI $\geq$ 30 kg/m^2)[1]. This is projected to rise to 2.3 billion overweight and 700 million obese by 2015 [1].

---

[1] BMI has been observed to correlate with body fat percentage (BF%) and therefore provides a 'surragate measure' of body fat. The relationship between BMI and BF% has however been shown to be dependent on age, gender and ethnicity so universal cut off points between weight categories may not be appropriate . Furthermore cut-off points between weight categories are defined relative to populations, overweight generally corresponding to $\geq$85th percentile and obesity to $\geq$95th percentile. BMI therefore offers a crude but useful surrageate measure of BF% [9].

Obesity, excess fat storage and high energy, high fat diets are associated with an array of health complications (Table 1). Finding effective treatments and interventions for obesity and associated diseases is therefore paramount.

Metabolic Disease	*Cancer*
Type II Diabetes	Kidney cancer
Cardiovascular disease	Endometrial cancer
Hypertension	Postmenopausal breast cancer
Stroke	Oesophageal Cancer
Hyperlipidaemia	Gall bladder cancer
Nonalcaholic fatty liver disease	Colon Cancer
Reproductive Disorders	*Other*
Infertility	Osteoarthritis
Stillbirth	Sleep apnoea
Miscarriage	Asthma
Birth defects	Depression
Fetal Macrosomia	
Pre-eclampsia	
Maternal death	

Table 1   Health issues associated with obesity. Adapted from Power & Schulkin, 2009 [9].

Obesity and weight gain in general are caused by a sustained imbalance of energy intake and expenditure, more calories are consumed than burned off and the excess energy is stored as fat. Treatments of obesity therefore aim to restore this energy balance through either increasing activity or reducing calorie intake.

Managing obesity through exersise and diet is the preferred treatment due to lower cost and risk of complications [10]. However, the long term efficacy of dieting as a treatment of obesity has been questioned, in a review of dietary studies, Ayyad *et al* 2000, suggest an average long term success rate of just 15% for dietary treatment [11].

Bariatric surgery has proved to be the most succesful intervention. Gastric bands, gastric bypass, gastric reduction surgery and intra gastric balloons all seek to physically reduce the capacity of the stomach so that smaller meals can satiate, thereby reducing calorific intake. A meta-analysis of 136 studies accounting for 22,000 patients showed that significant weight loss was achieved in 61.2% of all types of bariatric surgey [12]. A comorbid improvement of diabetes, hyperlipidaemia, hypertension and sleep apnoea was also observed. However, on the NHS, barriatric surgery is normally only considered for those with a BMI greater than 40, or for patients with a BMI between 35 and 40 and a comorid condition which would benefit.

A number of anti-obesity agents have been suggested as medical treatments of obesity. Haddock *et al* conducted a meta-analysis of suggested drug treatments, showing most of the drugs studied to have a moderate effect with none showing particular superiority [13]. However, due to side effects, many of these agents are not approved for use (e.g. amphetamine, fenfluramine, methamphetamine, phenylpropanolamine) [13]. Orlistat, a pancreatic lipase inhibitor, is the most commonly prescribed obesity medication in the UK [14]. A randomised double-blind study showed that when used in conjunction with a calorie restricted diet orlistat can cause a mean weight loss of 5.9% of body mass compared with 2.3% for those on a calorie restricted diet and placebo [15]. However, side effects including sterrathorea and incontinence, can make it an unpleasant treatment for the patient [16].

Bariatric surgery and orlistat provide effective treatment options for obesity, they are however not without risk or side effect and bariatric surgery is only appropriate in the most severe and advanced cases of obesity. Furthermore, the questionable long term efficacy of traditional dietary interventions suggest a need for new approaches to obesity management.

1.2.2   Treatment Of Obesity With Enzyme Inhibitors

Orlistat (Tetrahydrolipstatin) was developed from Lipstatin, a natural lipase inhibitor isolated from *Streptomyces toxytricin* and is capable of reducing fat absorption by up to 35% [17]. Orlistat has been shown to irreversibly inhibit lipase by covalently binding to the active site, inducing a conformational change in the enzyme. The lactone ring of Orlistat (Figure 2) forms a covalent bond with the catalytic serine residue in the lipase active site inhibiting lipase activity in a 'quasi-irreversible' manner [18-22].The term quasi-irreversible is used as the enzyme-inhibitor complex can be unstable in low levels of bile salts, suggesting that bile salts stabilise the reaction [23].
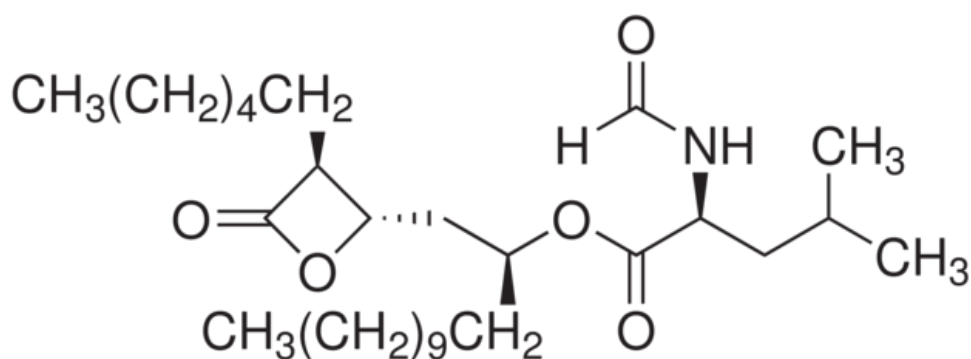
Figure 2   Structure of Orlistat (Tetrahydrolipstatin).

As orlistat demonstrates, inhibition of digestive enzymes presents a therapeutic target for obesity treatment and orlistat is neither the first nor the only anti-obesity agent that works through enzyme inhibition. In the 1980's starch blockers became a leading area of research in the treatment of obesity and other 'carbohydrate-dependent' diseases such as diabetes and insulin resistance as researchers sought to find ways of inhibitting α-amylase in order to block carbohydrate digestion. Although starch blocker tablets are still widely marketed, their efficacy is the subject of dispute [24-26].

The active agents in starch blockers are proteins extracted from a number of plants; *Phaseolus vulgaris* (Common bean) [27], *Triticum aestivum* (wheat flour) [28] and Type 1 α-amylase Iinhibitor (α-AI) from *Amaranthus hypochondriacus* seeds [29]. It is thought that these natural amylase inhibitors evolved as a defense mechanism to protect the plant against predation [30]. Relatively recent work has again supported the use of *Phaseolus vulgaris* extract. In a small human trial weight-loss with *Phaseolus vulgaris* extract was shown to be higher than placebo when 25 healthy individuals were fed *Phaseolus vulgaris* extract or placebo with meals [25].

The α-glucosidase inhibitor acarbose has been shown to significantly reduce development of Type 2 Diabetes in patients with glucose intolerance [31]. In a randomised control trial involving 714 patients, 32% of patients taking acarbose went on to develop diabetes as compared to 42% on placebo, furthermore acarbose significantly increased reversion to normal glucose tolerance (p<0.0001). By slowing carbohydrate digestion, acarbose reduces the glycaemic-hit of a meal and reduces post-prandial insulin secretion with benefits for the treatment of insulin resistance [32]. Acarbose is a pseudooligosaccharide similar in structure to maltotetraose (Figure 3) and

is effectively absorbed through the maltose-maltodextrin transport system. Acarbose is however a poor substrate for α-glucosidases and can not be metabolised [33].

Acarbose is derived from the *Actinoplanes* fungus and inhibits α-glucosidase by reversible competitive inhibition by competing for the active site. It is effective against the brush border α-glucosidases of the small intestine and is a weaker but effective inhibitor of pancreatic α-amylase. This reduces the rate at which monosaccharides are cleaved from carbohydrates [34].

In a 5-year study of nearly 2000 individuals with Type II diabetes, 4.7% showed adverse effects believed to be linked to acarbose. Side effects included; flatulance, diarrhoea, nausea, abdominal pain, loss of appetite and heart burn [35].
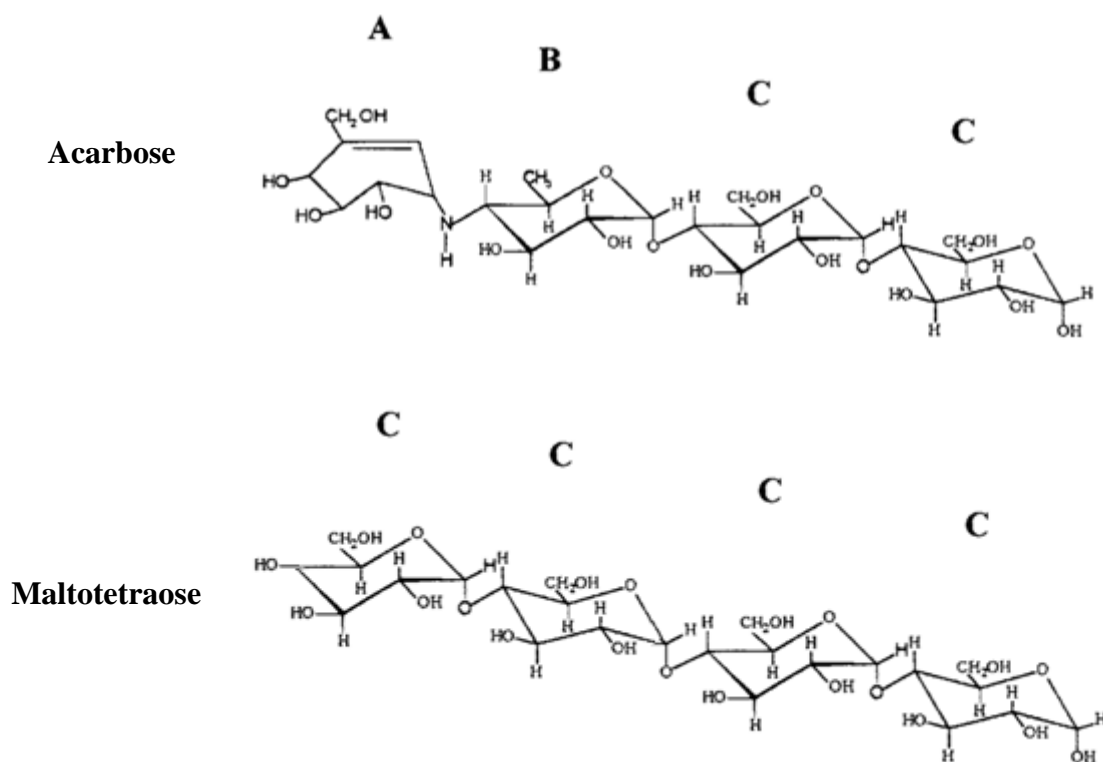
Figure 3   Structure of Acarbose: (A) amino-cyclitol moiety (B) deoxyhexose (C and Maltose

1.3 Dietary Fibre

1.3.1 Overview

Dietary Fibre is not a discrete and chemically identifiable nutrient, but a nutritional concept referring to a group of dietary constituents sharing similar characteresitics. There is no single agreed upon definition and it is therefore important to clearly define what is included as dietary fibre.

Trowell *et al* 1976, define fibre "simply as the plant polysaccharides and lignin which are resistant to hydrolysis by the digestive enzymes of man." [36]. This definition would however exclude fibres of animal origin such as chitin and chitosan. For the purposes of this report, dietary fibre shall therefore be defined as the carbohydrate constituents of the diet that are resistant to digestion and absorption in the human small intestine (i.e. escapes pre-colonic digestion and absorption) [37].

Dietary fibres are widely used in the food industy as gelling, thickening and stabilising agents, as well as as prebiotics and as such they can be incorporated into a wide range of foods.

1.3.2 Health Benefits of Dietary Fibre (DF)

DF is recommended because of its known benefits to digestive physiology; stool bulking, gastro-intestinal motility, stool frequency and maintainance of intestinal flora [38]. Recommendations for daily intake vary from country to country between 15-40g/day however these levels of intake are consistently not met in the general population [38]. DF is also considered to have wider health benefits and a high intake of DF is inversely associated with total mortality risk and reduced risk in a number of diseases [39, 40].

High long term intake of DF is associated with decreased risk of coronary heart disease [41], hypertension [42, 43], diabetes [44], obesity [45] and colorectal cancer [46]. A study in a subgroup of 632 Israelis showed those consuming more than 25g of DF a day had a 43% lower mortality risk [47].

However, when considering the health benefits of DF in epidemiological studies it must be noted that high fibre intake is associated with a generally healthier lifestyle; more physically active, lower likelihood of smoking and a generally healthier diet including more vegetables and less fat [48]. Therefore a causal link can not be assumed.

1.3.3   Dietary fibre as an Enzyme Inhibitor

Research into fibres as inhibitors of digestive enzymes began in the late 70's and early 80's. The inhibitory effects of a number of dietary fibres against trypsin, chymotrypsin, amylase and pepsin were investigated *in vitro* by Ikeda *et al* 1983. The investigation claimed to show *in vitro* inhibitory activity from a number of dietary fibres; Hemicellulose, pectin and xyal were shown to inhibit trypsin (up to 80% inhibition). Pectin and cellulose showed inhibition of α-amylase of up to 35%, and pectin and cellulose demonstrated inhibitory activity against pepsin of up to 60% [49].

Rats fed a high fibre diet containing 20% cellulose have shown a significant decrease in intestinal proteolytic, lipolytic and amylolytic enzyme activity upon analysis of intestinal contents [50]. Dilution of stomach contents with DF has been suggested as a possible factor during *in vivo* studies of enzyme activity [50]. However, the same investigators were also able to demonstrate *in vitro* inhibiton of pancreatic enzymes in samples of human pancreatic juice. Activity of lipase, amylase, trypsin and chymotrypsin was compared in samples of human pancreatic juice incubated with or without a range of DFs. With the exception of pectin, the fibres examined (alfalfa fibre, oat bran, hemicellulose, wheat bran and cellulose) all brought about a reduction in enzyme activity, with cellulose and hemicellulose producing the largest effect [51].

As well as the work from the 1980s, more recent work has also looked into the potential of DFs as inhibitors of digestive enzymes. El Kossiri *et al* 2000, measured casein digestion with pancreatin in the presence of DF. A range of soluble fibres including carrageenan, locust bean gum, alginate and pectin brought about a reduction of protein digestion [52].

The observation of pectin inhibition of casein digestion contradicts the results of Dunaif *et al* 1983, who suggested pectin had no inhibitory effect on proteolytic activity [51]. Pectins are an heterogenous group of molecules with diverse structure and the degree of methyl esterification of pectin carboxyl groups has been suggested to affect the inhibitory activity of pectins, this may offer an explanation for the conflicting evidence

and it is discussed later in the report how esterification of pectins affects viscosity and gellation of pectins. which may explain the varying results of pectin inhibition [53]. The current reasearch aims to address this conflicting evidence of pectin inhibition by designing a robust high-throughput methodology which, may be able to link the regulatory properties of pectins (and any other fibres) to their structure and properties.

El Kossiri *et al* 2000, also investigated a viscosity effect as the potential mechanism for inhibition. A direct relationship between fibre viscosity and inhibition would suggest a viscosity effect reducing the pedesis of solutes therefore reducing substrate-enzyme contact. As no significant correlation was found between viscosity and inhibition, the author argues viscosity alone is insufficient to explain the inhibition [52].

As stated previously, current work in this lab is investigating alginate inhibition of pancreatic lipase. A key benefit of using alginate as an inhibitor of lipase is that the properties of the DF may help mitigate the side effects seen with Orlistat. DF is generally beneficial to digestive health, causing stool bulking and improved gastro-intestinal motility and stool frequency which may help to prevent the incontinence seen with Orlistat. It is also thought that DF may bind up some of the undigested lipids reducing sterrathoroea. Two groups of 30 obese women were treated with orlistat, one group was also given DF supplement (*Psyllium mucilloid*) and the other placebo. Both groups showed significant weight loss, but while 71% of placebo group suffered GI side effects, in the DF group this figure was 29% [54].

1.3.4   Mechanisms of Dietary Fibre Inhibition

While there is a clear body of evidence showing that DFs can regulate the activity of digestive enzymes, the mechanism of this regulation is unclear and is an area into which further work is needed. A number of mechanisms have been proposed (Figure 4), and it is likely that there are a number of different ways in which enzyme activity is affected by the presence of DF.

As stated previously dilution of digesta has been suggested as an explanation of reduced digestive enzyme activity *in vivo*. However, DF has also been shown to inhibit enzyme activity *in vitro* where dilutions are controlled and can therefore not be responsible for the loss of activity.

DFs can be highly viscous, and it is for their gelling and thickening properties that they are often used as food additives. *In vivo*, the viscosity of DF opposes the peristaltic mixing process, slowing enzyme access to substrate [55]. Both *in vitro* and *in vivo*, viscous DF slows the pedesis of solutes, decreasing the rate of enzyme-substrate interactions. However, as El Kossiri *et al* and others have shown, viscosity effects cannot offer a full explanation of the inhibitory action that DF.

A number of other inhibitory mechanisms have been suggested; fibre binding of enzyme/substrate causing reduced enzyme-substrate binding [56, 57], interaction with fibre causing a conformational change to the enzyme and sequestering of calcium ions [52]. Sequestering of calcium ions by DF is suggested as a mechanism by which enzyme activity is reduced. A number of enzymes require calcium ions for stability or activity (e.g. trypsin, α-amylase). DF with a higher affinity for calcium than the enzyme would sequester calcium from the enzyme and could lead to decreased activity or an increased rate of enzyme degredation [58].

In vitro & In vivo	*In vivo*

Direct Binding Of Enzyme or Substrate

Binding of substrate or enzyme leading to reduced enzyme-substrate interaction

Reduced Peristaltic Mixing

Viscosity of fibre in solution opposes the action of peristaltic mixing

Viscosity Effect

Addition of viscous dietary fibre slows the pedesis of solutes, decreasing the rate of enzyme-substrate interactions

Dilution of Digesta

Increased fibre content and reduce water absorption for gut causing dilution of digesta leading to reduced rate of digestion

Sequestering of ions

Many enzymes bind ions for stability, and/or activity. Sequestering of ions by DF my lead to reduced activity by or degradation.

Unknown Mechanism

Figure 4   *Potential mechanisms of DF mediated enzyme inhibition*

1.4 Fibres Included In this study

For the purpose of the literature review the focus shall be on alginates as previous work in this lab has centred around alginates. Other fibres including fucoidan, carrageenan, pectin and agar have also been included in the study and are discussed in **Error! Reference source not found.**.

1.5 Alginate

1.5.1 Overview

Alginate is an indigestible polysaccharide and as such can be considered a DF. Found in cell walls and intercellular space of brown seaweed (*Phaeophyceae*) alginate is involved in cell structure and ion exchange [59]. Alginate is also produced by some bacteria of the *Azotobacter* and *Pseudomonas* genii as a component of the extracellular matrix [60, 61].

Commercially, alginates are produced from the harvesting of brown seaweed off the coasts of the British Isles (Outer Hebrides), Norway, Iceland, France, and Canada (east coast) where it grows in the colder waters of the Northeren Hemisphere and Australia, Chile and New Zeeland in the Southern Hemisphere [62, 63]. Alginates are commonly harvested from Giant Kelp, a *Laminarialean* algae in the class *Phaeophyceae* (Brown algae) which can reach a maximum length of 40m. Kelp is collected by kelp mowers; boats with large rotary blades similar to a lawn mower which cut and collect the fronds of the seaweed. Harvesting just the fronds rather than the whole seaweed allows for regrowth. Harvested kelp lanes have been shown to recover the same biomass and kelp density as control (unharvested) lanes within two years, making it a very sustainable method of production [64]. The same study showed that cutting close to the base of the fronds (less than 20cm) can seriously hamper regrowth.

Seaweeds can be correctly referred to as multicellular benthic[2] marine algae. While they are sometimes referred to as primitive plants or algal plants because of their relative complexity, seaweeds are algae and therefore belong to *Kingdom Protista* and are

---

[2] Living in sedimentary zones on or near the sea bed or in tidal pools

distinct from the 'higher' plants in that they do not form true leaves, stems or roots [65]. There are four groups of seaweed algae; green algae (Chlorophyceae), red algae (*Rhodophycae*), blue-green algae (*Cyanophyceae*) and brown algae (*Phyophyceae*) from which alginates are harvested (Figure 5).
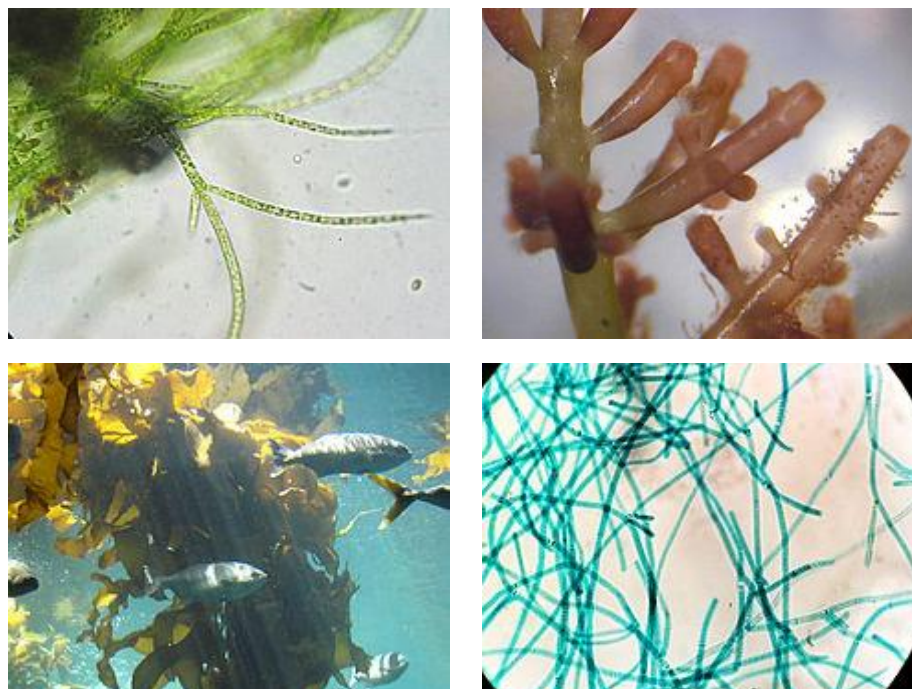
Figure 5   The four species of seaweed algae from which alginates are harveste, clockwise from top-left; green algae (Chlorophyceae), red algae (*Rhodophycae*), blue-green algae (*Cyanophyceae*) and brown algae (*Phyophyceae*).

Alginates have a number of industrial uses. In the food industry they are used variously as thickening, gelling, foaming, emulsifying and stabilisation agents [65]. Alginates also have medical and scientific applications; cell encapsulation, drug encapsulation as a controlled delivery system adsorbent wound dressings and anti-reflux therapies [7, 66] They are also thought to have a number of bioactive properties; Induction of pro inflammotary cytokines tumour necrosis factor (TNF) and interleukin-1 (IL-1)[67]. Oligo-G alginates have also been shown to have anti-bacterial properties, distrupting biofilm structure and growth [68].

1.5.2   Alginate Structure

Alginates are unbranched polysaccharides composed of (1-4)-α-L-guluronic acid (G-Residues) and (1-4)-β-D-mannuronic acid residues (M-Residues). In seaweeds these polyuronans are found as salts of different metals (usually sodium and calcium). The polyuronic chains are composed of blocks of about 20 residues which are either G-rich,

M rich, or MG rich (Figure 6). The characteristics of the alginate are dictated by the arrangement of these blocks [59].

G-rich blocks form relatively stiff blocks as there is limited rotation around the glycosidic bond. The presence of mannuronic acid residues increases chain flexibility with M blocks and MG blocks forming relatively flexible chains because of freer rotation around the glycosidic bonds [69].
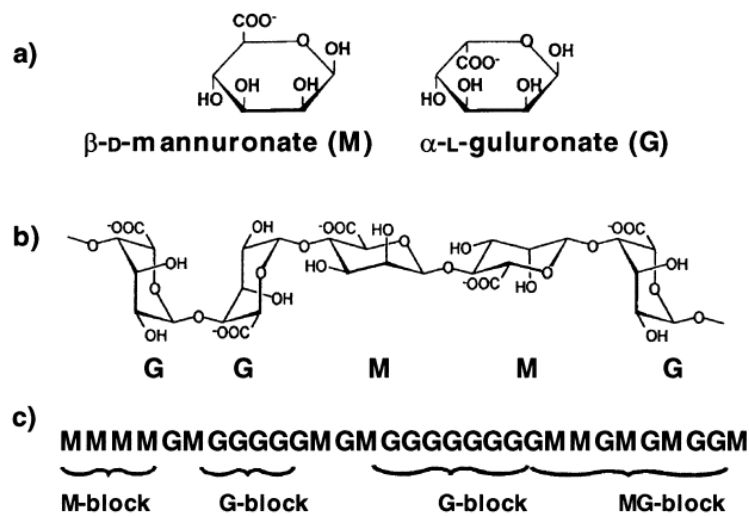
Figure 6   Suggested sturucture of alginate. (a) β-D-mannuronic acid and α-L-guluronic acid, (b) chain conformation, (c) block structure. Taken from Draget et al (2002) [69]

Alginates are hydrocolloids and are able to form gels, there are two mechanisms by which they can do this. Interchain binding of cations causes the formation of ionic gels and lowering the pH of an alginate solution below the pK_a of the alginate can cause acid-gel formation [70]

1.5.3 Ionic-Gel

Alginates are able to form ionic gels through the binding of cations and the formation of interchain associations between fibres [71]. Homopolymeric regions (M or G blocks) better support the formation of junction zones between adjacent polmers and therefore increase viscosity in solution, with G-Blocks forming the most stable gels [72]. The affinity of an alginate for cations increases with G content as G-blocks have a greatly

increased selectivity for divalent cations. Alternating blocks (MG blocks) increase the flexibility of the polysaccharide chain and therefore decrease alginate gel viscosity [73, 74]

As well as being related to overall G-Content, mechanical strength is also influenced by the length of G-Blocks. Polymannuronan forms a flat ribbon-like chain, whereas polyguluronon forms a 'buckled' ribbon-like structure [65]. This buckled ribbon forms regular folds into which calcium ions can fit. The binding of cations and formation of interchain associations were described by Rees as the "egg-box model" with the (1-4)-α-L-guluronic acid forming regular folds between chains within which ions can be bound [75]. Figure 7 shows the egg box structure, and a schematic model of calcium binding which has generally been accepted as the structural mechanism of gellation [76].
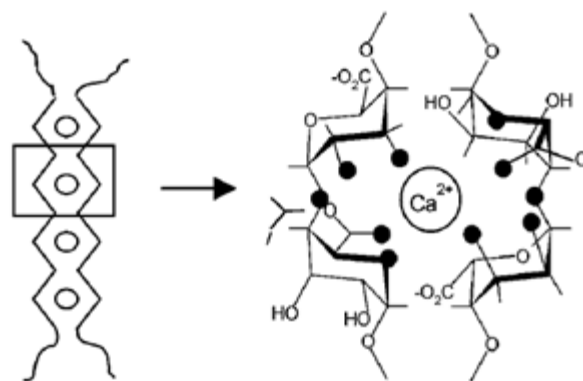
Figure 7 "Egg-box" structure in alginate junction zone and suggested model for calcium co-ordination in a calcium (Black circles represent oxygen atoms". Taken from Braccini et al (2001) [76]

1.5.4 Acid-Gel Formation

Although the model for ionic gels has been well characterised, less is known about acid gels. Acid gels are formed when the pH of an alginate solution is lowered below the pK_a of the alginate polymer. It is believed that the gel is stabilised by intermolecular hydrogen bonds connecting the polyuronan chains [77, 78]. The carboxyl group of the alginate monosaccharide residue becomes protonated at low pH forming carboxylic acid, which is then able to form hydrogen bods.

Tests of gel strength through measurements of Young's Modulus[3] in longitudinal deformation tests have shown that as with ionic gels, the strength of alginate gels formed by polyuronan blocks is in the order GG>MM>GM/MG [79] . It is believed that the arrangement of the monomers within the chain effects the formation of intermolecular bonds. Draget *et al* also showed acid gel formation has a dependence on molecular weight. A clear relationship was demonstrated whereby high molecular weight alginates form the strongest gels, and low MW alginates the weakest as measured by Young's modulus [79].

1.5.5 Modification of Alginates

Alginates are biosynthesised predominately as polymannuronic acid in the cytoplasm and are modified by acetylation and epimerisation during periplasmic transfer [66]. During epimerisation M-residues are converted to G-residues by Mannuronan C-5 epimerases [60].The extent and distribution of epimerisation determines the alginates characteristics which is important in algae and bacteria for controlling the mechanical properties of alginate. Epimerases therefore have applications both in research and industry as the gelling properties of alginates are dictated by the M:G ratio and organisation of these residues [80].

Ertesvag *et al* 1999, characterised the activity of alginate epimerses AlgE1-7 from *Azotobacter vinelandii.* The seven AlgE epimerases were expressed in E. coli and epimerase activity ascertained by H NMR (Nuclear Magnetic Resonance) measurement of M and G content. AlgE4 was shown to convert solely to MG blocks, all other epimerases were shown to convert to a mixture of G and MG blocks [60].

Knowledge of alginate epimerases opens up the potential for 'designing' alginates. If alginates are found to have regulatory activity towards digestive enzymes, alginate epimerases could be used to manufacture the 'optimum' alginate which provides the most inhibition or activation.

---

[3] Young's Modulus provides a measure of elasticity/stiffness calculated by the ratio of tensile strength to tensile strength in N/m^2 and can be calculated by the gradient of a stress-strain curve.

1.6   Overview of digestive physiology and macronutrient breakdown

The primary function of the gastrointestinal tract is to process ingested food into a form that can be absorbed across the gut lumen and in to the blood stream and lymphatic system. The mechanical breakdown of food through chewing in the mouth and churning in the stomach eases the movement of food through the digestive tract, mixes the food with digestive secretions and increases the surface area for enzyme action. Peristaltic action keeps the digesta moving and mixing as it is passed throught the organs of the GI tract.   Digestive secretions from accesory glands mediate the chemical breakdown of food through the catalytic action of enzymes aided by the emulsifying effects of bile and optimisation of pH through acid/bicarbonate secretions.

The GI tract is a succession of functionally and structurally distinct organs adapted to provide the optimum environment for its role in the digestive process. pH variation throughout the GI tract allows for optimum activity of digestive enzymes at distinct sites. This pH variation has been profiled in healthy subjects using a pH sensitive 'radiopill' capable of transmitting pH readings during passage through the GI tract [81]. Secretion of HCl from parietal cells in the gastric pit makes the gastric juice highly acidic with a pH range of 1.0-2.5. In the small intestine the pH is raised to near neutral by bicarbonate secretion from the pancreas, bile ducts and intestinal mucosa. Proximal small intestine was measured at an average of pH 6.6, rising to around 7.4 in the distal and mid small intestine. Measurements of pH in the large intestine ranged from 6.6 to 7.5.

The major sites of digestive secretions are the salivary glands, gastric glands, the pancreas and the liver. A fuller list of these digestive secretions is available in Table 3 below.

As summarised by Pedersen *et al* 2002, in Table 2 saliva contributes to a number of important roles in GI function; taste, mastication, bolus formation, enzymatic digestion and swallowing [82]. Saliva is produced by serous and mucus acinar cells and secreted from the parotid, sublingual and submandibular salivary glands (90%) and hunreds of minor salivary glands in the wall of the mouth and pharynx (10%) [83]. Saliva is a watery solution containing salivary amylase which begins carbohydrate digestion,

mucus to lubricate food and protect the mouth and bicarbonate to create a slightly alkaline environment [84]. Saliva also contains lysozyme, an enzyme which is active against bacteria. In humans, 0.9-1.5L of saliva is produced daily [83].

Mechanical cleansing of food and bacteria
Lubrication of oral surfaces
Protection of teeth and oro-esophageal mucosa
Oral acid neutralization and dilution of detritus
Antimicrobial activity
Dissolution of taste compounds
Facilitation of speech, mastication and swallowing
Formation of food bolus conducive for swallowing
Initial digestion of starches and lipids
Esophageal clearance and gastric acid buffering

Table 2   Functions of saliva in the upper gastrointestinal tract. Taken from Pedersen et al, 2002 [82].

Chewing of food (mastication) acts to breakdown food, increasing the surface area upon which enzymes can act. Mastication also serves to form food into a bolus by mixing food with saliva, a bolus is a portion of food that has been softened and lubricated through mechanical breakdown and mixing with saliva. Bolus formation allows food to be more easily swallowed; water in saliva makes the food moist and softens it, salivary mucins serve to bind the bulus together and give it a slippery surface for swallowing.

After passing through the lower oesophageal sphincter salivary amylase is inactivated by the acidic conditions of the stomach. The acidic conditions of the stomach favour pepsin mediated proteolysis, this is assisted by the 'antral pump' action of the stomach which breaks up the food particles and forms a chyme which is passed into the duodenum through the pyloric sphincter. The wall of the fundus and body of the stomach contain gastric pits composed of various secretory cells. Mucus is secreted by neck cells and surface mucosal cells, pepsinogen by chief peptic cells and parietal cells (also known as oxyntic cells) secrete HCl to acidify the stomach.

In the duodenum the acidic chyme is neutralised upon mixing with the pancreatic juices which are rich in bicarbonate (secreted by duct cells). The pancreas secretes a whole range of digestive enzymes as shown in Table 3.

Although digestion is well underway by the time food reaches the small intestine, the majority of food is digested by pancreatic enzymes which are secreted into the

pancreatic duct by acinar cells of the exocrine pancreas [85]. Before the pancreatic juices are released into the duodenum through the sphincter of Oddi, they are mixed with bile in the ampulla of Vater, where the pancreatic duct and common bile duct merge [86].

The common bile duct transports bile from the gallbladder where it is stored after secretion from the liver. Bile is composed of bicarbonate, phospholipids, inorganic ions and bile salts [84]. Bile aids the digestion of dietary fats through its detergent effect, dispersing fats into micelles thereby increasing the surface area upon which digestive lipases can act.

Bile acids are cholesterol derivatives. Primary bile acids cholic acid and chenodeoxycholic acid are synthesised in the hepatocytes of the liver, these form either glycine or taurine conjugates. The amphiphillic nature of bile acids causes them to form into micelles with the hydrophobic steroid side of the molecule pointing inwards [87]. In the colon the primary bile acids are deconjugated and can then be converted to the secondary bile acids lithocholic acid and deoxycholic acid by the bacterial flora. Bile acids are recycled through enterohepatic circulation and trasported back to the liver where they are reconjugated [88].

The small intestine is also the major site where the products of these combined digestive processes are absorbed by cells of the mucosal epithelia. The absorbative capacity is increased by folding of the mucosal membrane in to villi, and the brush border membranes of the epithelial cells, microvilli.

Most of the energy and nutrient content of food is ingested in polymeric form as protein, carbohydrate and triglycerides, macronutrients must therefore be broken down by these processes of digestion for uptake and transport around the blood stream; amino acids and glucalogues in the case of protein and polysaccharides respectively. Or in the case of triglycerides reconstitued in to chylomicrons – water soluble lipoprotein particles that allow for the transport of fats and cholesterol in the bloodstream. The surface area of the small intestine is specialised to provide a large absorbative surface. Kerckrings folds, villi and microvilli together result in a 600 fold increase in surface area as compared to a smooth cylidircal tube [89]. Absorption across the small intestinal epithelium occurs through a number of processes; passive diffucion, carrier mediated diffusion, active transport and pinocytosis (a form of non-specific endocytosis). The

intestinal epithelium is coated with an 'unstirred layer', composed of adherent mucus protecting the intestinal epithelia and the associated solution which resist peristaltic motion. The unstirred layer has the effect that only dissolved substrates can diffuse across for uptake, and that the rate of this diffusion and therefore uptake is affected by the thickness and constitution of the unstirred layer. It has been shown that by thickening the unstirred layer, the gelling agent guar can reduce intestinal absorption rates [90].

Finally the colon then re-absorbs water, salts and salvages any other useful products from the digesta prior to removal of waste by defacation.

Site	Source	Enzyme	Substrate	Effect
Mouth	Saliva	α-amylase	Starch	Catalyses cleavage of α1→4 glycosydic bonds
Stomach	Gastric Secretions	Pepsin	Protein	Catalyse cleavage of peptide bonds
		Gastric Lipase	Lipids	Catalyse hydrolysis of dietary fats
Small Intestine	Pancreas	α-amylase	Starch	Catalyses cleavage of α1→4 glycosydic bonds
		Pancreatic Lipase	Lipids	Catalyse hydrolysis of dietary fats
		Proteases	Protein	Catalyse cleavage of peptide bonds
		Trypsin	Polypeptides	Hydrolyses peptide bonds prefferentially of arginine and lysine residues
		Chymotrypsin	Polypeptides	Hydrolyses polypeptides at the carboxyl end of hydrophobic amino acids
		Elastase	Polypeptides	Hydrolyses peptide bonds containing the carboxyl group of alanine, glycine, isoleucine, leucine or valine
		Carboxypeptidase A and B	Polypeptides	Cleave amino acids from the carboxyl end of polypeptides with the exception of arginine, lysine and proline
	Gall Bladder	Bile Salts	Lipids (fatty acids and triglycerides)	Formation of micelles and emulsification of dietary lipids
	Brush Border Cells	Lactase (β-galactosidase)	Lactose	Cleaves lactose into glucose and galactose
		Maltase (α-D-glucosidase)	α1→4 glycosidic linked limit dextrins	Cleaves into glucose
		Sucrase	Sucrose	Cleaves into glucose and fructose
		Isomaltase	Maltose Maltotriose	Cleaves into glucose
		Amino-oligopeptidases	Oligopeptides of 2-6 amino acids	Cleaves N-terminal amino acids
		Dipeptidyl peptidases	Peptides and oligopeptides	Cleaves N-terminal amino acids

Table 3   Adapted from Vickerstaff Jonega (2004) [91]

1.7 Overview of Enzymatic Breakdown of Macronutrients

This section contains an overview of the sites and processes of enzymatic breakdown of macronutrients and uptake of metabolites, more detailed explanations of enzyme structure and mechanism are included in Chapter 3Chapter 5.

1.7.1 Fat Digestion and Uptake

Fat is thought to constitute approximately 40% of energy intake in the western world [92]. The major source of dietary fat is triacylglycerol (TAG) which makes up 90-95% of dietary fat [93]. Remaining fat sources comprise a mixture of phospholipids, glycolipids and sterols (eg cholesterol). [92, 93]

Triacylglycerol consists of a glycerol backbone with three fatty acid side chains of varying length, in the human diet fatty acid chains can vary in length from C2 to C24 [92]. The fatty acids may be saturated, containing only single bonds between carbon atoms in the fatty acid side chains, or unsaturated, containing one or more double bond between carbons.

Fat digestion is initiated in the mouth, mastication begins the mechanical dispersion of fats and the formation of food in to a bolus. Lingual lipase is secreted from a set of lingual serous glands on the tongue called von Ebner's glands in response to a meal [94]. Chewing serves to mix lingual lipase in with food bolus which is passed into the stomach through swallowing [92, 95]. Lingual lipase has a pH optimum of 5.5 and is resistant to acid inactivation. Lipase activity is therefore retained in the stomach when the pH environment is buffered with the intake of a meal [95, 96].

Gastric lipase is also secreted into the stomach from gastric chief cells [94]. It is believed that 10-30% of dietary fat is digested in the stomach before passage into the small intestine [97]. The stomach is also responsible for creating a crude emulsion of dietary fats, through peristaltic action and initial lypolysis [93]. Fats therefore pass into the duodenum as a crude emulsion of fine lipid droplets, an important aspect of pre-duodenal fat digestion which aids small-intestinal fat breakdown. It has been shown that droplet size of the fat emulsion influences the rate of fat digestion, with emulsions of fine droplet size being hydrolysed at a faster rate [98].

The first step of triglyceride digestion is the hydrolysis of TAG to diacylglycerol (DAG). Gastric and Lingual Lipase both preferentially cleave the fatty acid at the SN3 position, Figure 8.

$$sn2 - \begin{cases} sn1 \\ \\ sn3 \end{cases}$$
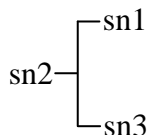
Figure 8   Orientation of Fatty Acids in triglyceride molecule. Taken from Mu et al [92]

This release of fatty acids from TAG stimulates the secretion of cholecystokinin, a peptide hormone synthesised in the mucosal epithelium of the duodenum. The secretion of pancreatic juice and release of bile is triggered by Cholecystokinin. Secretin release is also triggered in the duodenum by the entrance of gastric acid with the chyme, this in turn triggers bicarbonate and water secretion [93] .

Bile aids the digestion of dietary fats through its detergent effect. Bile acids are amphipathic molecules synthesised in liver hepatocytes and are vital to the emulsification of dietary fats [88]. As lipase acts at the lipid-water interface, the level of emulsification is an important factor in the rate of fat digestion as it determines the area over which lipase can act [85]. With the breakdown products of lipids including fatty acids, cholesterol and phospholipids bile acids form mixed micelles [99] . As the mixed micelles pass through the small intestine pancreatic lipase acts to further digest dietary fats. In the illeum up to 95% of bile acids are reabsorbed, and passed back to the liver through enterhepatic circulation, this process can occur several timess during a single meal [99].

Pancreatic lipase acts at the lipid-aqueous interface of TAGs and DAGs, its presence is stabilised by the co-enzyme co-lipase which is secreted as precolipase and activated by trypsin in the duodenum. The typical digestion system is that after TAGs have been hydrolised to DAGs by cleavage of the fatty acid at the SN3 position, the SN1 fatty acid is cleaved, leaving an SN2-Monoacylglycerol sn2-MAG. The spontaneous rearrangement of the SN2-FFA to position SN1 Allows for the complete hydrolysis into glycerol and FFAs.

The first step of the uptake of fat metabolites is the diffusion of mixed micelles across the unstirred layer to the brush-border membrane. Some free metabolites may diffuse indipendently to the membrane, but the poor solubility of lipid metabolites means micellar solubilisation is required to enhance uptake. Models of both protein dependent and protein independent uptake have been described for transport of fat metabolites across the brush border epithelium [93].

Within the smooth endoplasmic recticulum cholesterol, monoacylglycerol and retinol are esterified by cholesterol acyltransferase, diacylglycerol acyltransferase and lecithin:retinol acyltransferare respectively so that they can be incorpotated into chylomicrons and low density lipoprotreins. Chylomicrons and LDLs exit the cell via exocytosis and for transport through the lymphatic system.

Phospholipid digestion is predominantly carried out by pancreatic phospholipase A2; Cholestrerol esterase hydrolyses free sterols to cholesterol for incorporation into micelles and uptake; micelles are also important for the uptake of fat soluble vitamins such as Vitamin E.

1.7.2 Carbohydrate Digestion

Carbohydrates may be digestable or indigestable (DF) depending upon their glycosidic bonding. Of the nutritionally available carbohydrates, a reported 3-6% of carbohydrate consumed is in the form of monosacharides, the vast majority of carbohydrate is in the form of starch (53-64%) and the remainder oligosaccharides (33-42%), and therefore must be broken down for absorption (See

Table 4) [100]. Starch is composed of amylose and amylopectin. Amylose is a linear α(1-4) polysaccharide and amylopectin; α(1-4) polysaccharide chains with α(1-6) branching side-chains.

Carbohydrate	Compostion (%)
Polysaccharides	
Starch	52.6-64
Glycogen	0.5
Oligosaccharides	
Sucrose	26-33.2
Lactose	6.5-6.6
Maltose	1.8
Monosaccharides	
Glucose	4.2
Fructose	1.6-3

Table 4   Carbohydrate composition of the human diet. Adapted from Elsenhans *et al* 1983 [100]

Carbohydrate breakdown can be thought of as a two step process; the initial breakdown of starch by α-amylases, and then the cleavage of oligosaccharides by membrane bound glucosidases into monosaccharides (hexoses, predominantly glucose, galactose and fructose).

Physiologically amylolysis begins in the mouth with the action of salivary α-amylase, also referred to as ptyalin which is secreted from serous acinar cells of the parotid and submandibular gland. Salivary α-amylase is mixed throughout the food bolus during chewing and begins carbohydrate breakdown by cleavage of α (1-4) glycosidic bonds. Salivary amylase is thought to be of limited significance in the digestion of carbohydrates, due to the preompt deactivation in the acid environment of the stomach. However Rosenblum *et al*, 1998 have suggested that starch polymers can protect α-amylase from acid and pepsin inactivation, so that amylase may maintain some activity in the stomach, and therefore remain active through to the small intestine [101].
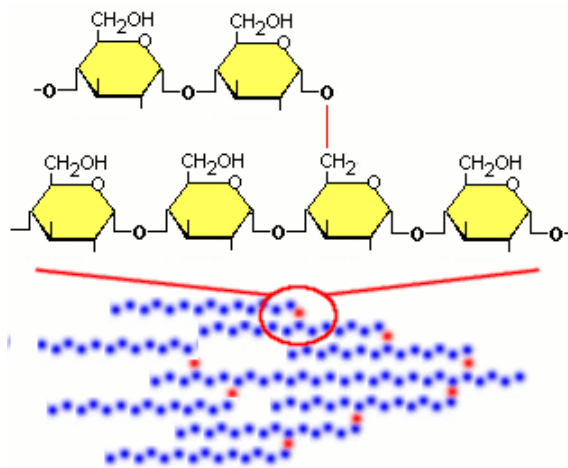
Figure 9   α(1-6) linkages in amylopectin

After passage through the stomach, further carbohydrolysis occurs in the small intestine. Small intestinal α-amylase is synthesised in the pancreas. Both pancreatic and salivary α-amylases only have activity towards α (1-4) glycosidic bonds. The cleavage of starch predominantly generates maltose and maltotriose from both amylose and amylopectin. In addition the cleavage of amylopectin generates the α-limit dextrins; oligosaccharides composed of approximately 6 residues which are created because of the limited cleavage of α(1-4) bonds in the proximity of α(1-6) linkages (Figure 9).

Starch breakdown into maltose, maltotriose and α-limit dextrin is thought to occur very rapidly and within 10 minutes of transit into the duodenum [100]. The next phase of carbohydrate digestion occurs at the brush border membrane of intestinal enterocytes.

Brush border enzymes are localised to the apical membrane in close proximity to glucose carrier proteins [102]. Maltase is responsible for the breakdown of maltose to D-Glucose. Glucoamylase cleaves end terminal glucose residues from maltotriose and α-limit dextrin. Isomaltase and sucrose have been shown to form a single enzyme complex; sucrase cleaves sucrose to D-Glucose and D-Fructose, Isomaltase has activity towards α (1-6) glycosidic bonds and is responsible for cleaving α-limit dextrin down into maltose. Finally lactase is responsible for the breakdown of lactose in to D-Glucose and D-Galactose. Lactase deficiencies can result in lactose intolerance [103].

Carbohydrates are broken town to hexose monosaccharides. Glucose, fructose and galactose are the most common monosaccharide products of carbohydrate digestion. Following absorption, galactose and fructose are converted to glucose for metabolism,

transport and storage [104]. The uptake of monosaccharides is a highly regulated process, with both specific and non-specific mechanisms of regulation. The rate limiting step of sugar absorption from the lumen are brush border membrane transport into enterocytes and basolateral membrane transport into the blood stream [105]. Nonspecific mechanisms of sugar uptake regulation have been shown to be regulation of the number and length of intestinal villi during pregnancy and lactation [106]. Specific regulation is achieved by the regulation of glucose transporters, and this process has been shown to be highly responsive to dietary carbohydrates.

The paths of possible monosaccharide uptake are shown in Figure 10 below. Monosaccharides may transit the enterocytes by transcellular transport or paracellular transport through tight junctions.
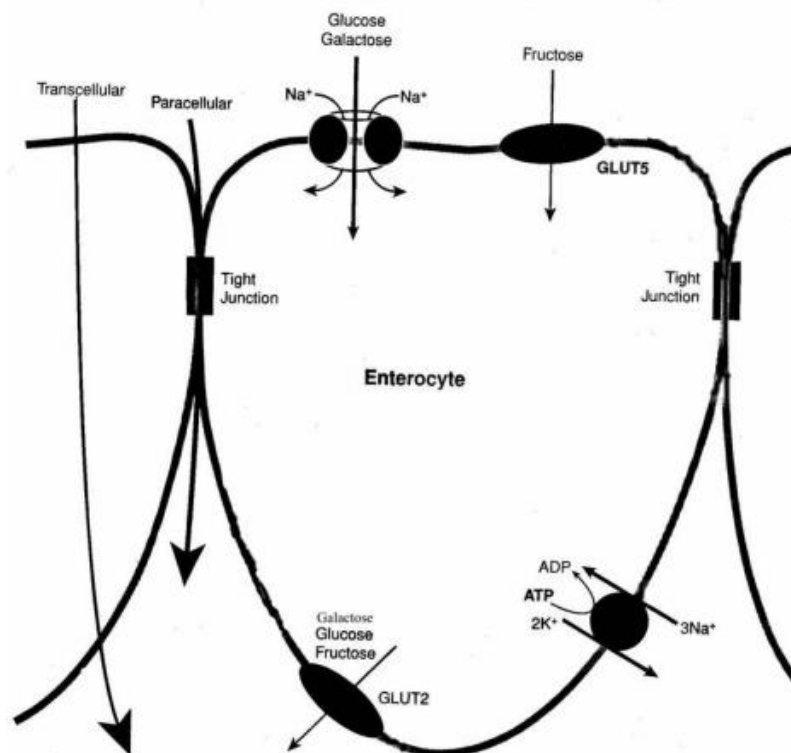
Figure 10   Taken from Traber, 2004 [107] The classical model of sugar absorption. Glucose and galactose are actively transported across the brush border membrane by the Na+-dependent glucose transporter. Fructose is transported by facilitative GLUT 5 and GLUT2 transports glucose, galactose, fructose across the BLM via facilitative diffusion.

Intestinal brush border membrane uptake of glucose and galactose into the cell cytoplasm is governed by the Na^+/glucose co-transporter SGLT1, passive fructore transport occurs through the GLUT5 uniporter. Glucose, galactose and fructose all exit the cell via passive dffucsion through GLUT2 and GLUT5 uniporters [108]. SGLT1

27

also contains a number of phosphorylation sites. PKA activation has been shown to increase glucose transport by 30% and PKC to reduce glucose transport by 60% [104] While SGLT1 is predominantly a glucose transporter, it has affinity for other sugars in the order; D-Glucose > α-methyl-D-Glucose > D-galactose > 3-O-methyl glucose> L-glucose and 2 deoxyglucose [109].

1.7.3   Digestion and absorption of protein

The gastrointestinal proteases of the stomach, pancreas and small intestine result in the efficient hydrolysis of polypeptides into amino-acids and small oligopeptides that can be absorbed by small intestinal enterocytes [74]. Luminal protein digestion occurs in both the stomach and small intestine. Gastric protein digestion of polypeptides is mediated by gastric pepsin in the acid environment of the stomach and results in a mixture of large polypeptides, smaller oligopeptides and some free amino acids [74].

Pepsin is part of the aspartate protease super family (EC 3.4.23.-) [110]. As the major proteolytic enzyme in gastric juice, pepsins are responsible for protein digestion. Pepsins are broad specificity endopeptidases with a preferance for cleavage between hydrophobic amino acids. Pepsin is an acid protease secreted as the zymogen pepsinogen from Chief/Peptic Cells in the Gastric Glands of the stomach. Pepsinogen is activated to pepsin only in acidic conditions. Pepsinogen is reported to be stable within the pH range 6-9 [111]. Above pH 9.0 pepsinogen is reversibly denatured, and below pH 6.0 pepsinogen is activated by an autocatalytic mechanism. This activation of pepsin occurs faster at lower pH [112]. Further information about the structure, classification and catalytic mechanism of pepsin is included in Chapter 3. Patients with a full gastrectomy are capable of digesting and absorbing protein without difficulty, therefore gastric protein digestion may not be critical to protein digestion [113]

Protein digestion is completed in the small intestine. Caspary 1992, characterises small intestinal protein digestion as consisting of three phases; 1) luminal protein digestion 2) brush border membrane digestion and 3) Cytoplasmic assimilation of polypeptides. An array of proteolytic enzymes are secreted into the small intestine from the pancreas as zymogens which are activated during the proteolytic enzyme cascade (Figure 11) which also causes the activation of pancreatic lipase and colipase [114]. Trypsinogen,

proelastase, chymotrypsinogen, procarboxypeptidases and kallikreinogen are secreted from the pancreas. The mucosal enzyme enterokinase catalyses the activation of trypsinogen to trypsin. Enterokinase is a glycosylated protein synthesised by small intestinal enterocytes. While trypsinogen is capable of autocatalytic activation, activation by enterokinase is reported to be 2000 times more efficient [115].

Activated trypsin then activates the secreted pancreatic zymogens to their active forms. Small intestinal zymogen activation is likely a far more complicated process than Figure 11 suggests, with autocatalytic and secondary activation of zymogens as well as the influence of various factors including zymogen concentrations, levels of active trypsin, total luminal protein content, pH, presence of ions and length of incubation.
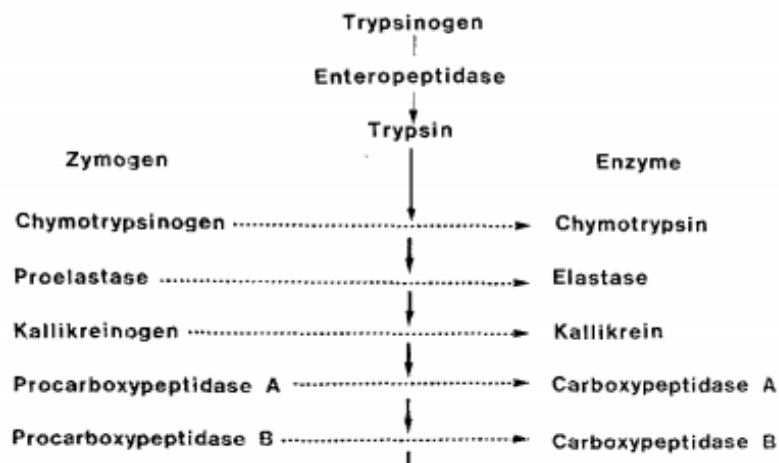
Figure 11   The pancreatic enzyme cascade of protease activation Taken from Rinderknecht, 1986 [115].

The endopeptidases trypsin, elastase and chymotrypsin are serine proteases that cleave interior peptide bonds. The carboxypeptidases are zinc-containing metallopeptidases with exopeptidase activity and cleave single amino acids from the carboxyl terminal of polypeptides [115]. Protease specificity and activity is described in Table 5 below.

Enzyme Family	Enzyme	Favoured Site of Activity
Serine proteases (endopeptidases)	Trypsin	cleaves on the carboxyl side of basic amino acids (Arg, Lys)
	chymotrypsin	cleaves on the carboxyl side of amino acids with aromatic carbonyl groups (Tyr, Phe, Trp)
	Elastase	cleaves on the carboxyl side of

		aliphatic amino acids residues (Ala, Leu, Gly, Val, Ile)
Zinc-containing metallopeptidases (exopeptidases)	Carboxypeptidases A and B	single amino acids from the carboxy terminal ends of proteins and oligopeptides

Table 5   Pancreatic proteases. Adapted from Erickson *et al* 1990 [74]

Luminal digestion of polypeptides by proteolytic enzymes results in short oligopeptides of 2-8 amino acids in length which can then diffuse to the brush border membrane for further hydrolysis by brush border peptidases. Short oligopeptides are further hydrolysed by brush border amino oligopeptidases to their constituent amino-acids, or small di and tri-peptides for uptake by specialised amino-acid and peptide transporters. The brush border peptidases are summarised in Table 6, of particular significance are the prolyl-peptidases; Dipeptidyl aminopeptidase IV, Aminopeptidase P, Carboxypeptidase P and Angiotensin converting enzyme which can cleave peptide bonds involving proline, to which luminal peptidases have limited activity [74].

Aminopeptidase N	Cleaves amino acids from the N-terminal of short chain oligopeptides
Dipeptidyl aminopeptidase IV	Cleaves Prolyl peptides from the N-Terminal of oligopeptides
Aminopeptidase P	Cleaves Prolyl peptides from the N-Terminal of oligopeptides
Carboxypeptidase P	Cleaves Prolyl peptides from the Carboxyl Terminal of oligopeptides
Angiotensin converting enzyme	Cleaves Prolyl peptides from the Carboxyl Terminal of oligopeptides
Neutral Metalloendopeptidases	Cleave internal peptide bonds of large proteins such as α-casein, fibrinogen and histone
Glutamyl aminopeptidase	Cleaves peptides containing glutamic or aspartic acid at the N-Terminal.

Table 6   Brush-border peptidases. Adapted from Caspary 1992 [114]

These brush border metabolites are absorbed in to the enterocytes. Di and tri-peptides are transported through peptide carriers and further hydrolysed to free amino acids in the cytoplasm of enterocytes, only highly resistant peptides such as glycyl-proline pass in to the blood stream without having undergone complete hydrolysis [116]. A wide

array of amino acid transport systems have been characterised and are summarised in Table 7. Broer *et al* 2008, categorise these carrier systems in to 5 groups; 1) Neutral amino acids, 2) Cationic amino acids and cysteine, 3) Anionic amino acids,) Proline, hydroxyproline and glycine and 5) Taurine and other β-amino acids.

TABLE 1. *Epithelial amino acid transport systems and their mediators*

System	cDNA	SLC	Amino Acid Substrates	Analogs	Affinity	Mechanism	Ions	Expression*
A	SNAT2	SLC38A2	G,P,A,S,C,Q,N,H,M	MeAIB	Medium	S	Na^+	Ub
	SNAT4	SLC38A4	G,A,S,C,Q,N,M,AA^+	MeAIB	Medium	S	Na^+	K
ASC	ASCT1	SLC1A4	A,S,C	Cysteic acid	High	A	Na^+	K
	ASCT2	SLC1A5	A,S,C,T,Q		High	A	Na^+	K,I (AM)
asc	4F2 hc/asc1	SLC3A2/SLC7A10	G,A,S,C,T	D-AA^0	High	A		K
B^0	B^0AT1	SLC6A19	AA^0	BCH	Low	S	Na^+	K,I (AM)
	B^0AT2	SLC6A15	P,L,V,I,M	BCH	High	S	Na^+	K
$B^{0,+}$	$ATB^{0,+}$	SLC6A14	AA^0, AA^+, β-Ala	BCH	High	S	Na^+, Cl^-	I (AM)
$b^{0,+}$	rBAT/$b^{0,+}$AT	SLC3A1/SLC7A9	R,K,O,cystine		High	A		K,I (AM)
β	TauT	SLC6A6	Tau, β-Ala		High	S	Na^+, Cl^-	K (AM,BM)
Gly	XT2	SLC6A18	G		NR	NR	NR	K (AM)
IMINO	IMINO	SLC6A20	P, HO-P	MeAIB	Medium	S	Na^+, Cl^-	K,I (AM)
L	4F2hc/LAT1	SLC3A2/SLC7A5	H,M,L,I,V,F,Y,W	BCH	High	A		
	4F2hc/LAT2	SLC3A2/SLC7A8	AA^0 except P	BCH	Medium	A		K,I (BM)
	LAT3	SLC43A1	L,I,M,F	BCH	Low	U		K
	LAT4	SLC43A2	L,I,M,F	BCH	Low	U		
N	SNAT3	SLC38A3	Q,N,H		Low	S	Na^+(S), H^+(A)	K (BM)
	SNAT5	SLC38A5	Q,N,H,S,G		Low	S	Na^+(S), H^+(A)	K
PAT (Imino acid)	PAT1	SLC36A1	P,G,A GABA, β-Ala	MeAIB	Low	S	H^+	K,I (AM)
	PAT2	SLC36A2	P,G,A	MeAIB	Medium	S	H^+	K
T	TAT1	SLC16A10	F,Y,W		Low	U		K,I (BM)
X^-_{AG}	EAAT2	SLC1A2	E,D	D-Asp	High	S	Na^+,H^+(S), K^+(A)	K (BM)
	EAAT3	SLC1A1	E,D	D-Asp	High	S	Na^+,H^+(S), K^+(A)	K,I (AM)
x^-_c	4F2 hc/xCT	SLC3A2/SLC7A11	E, cystine$^-$		High	A		Ub
y^+	CAT-1	SLC7A1	R,K,O,H		Medium	U		Ub
y^+L	4F2hc/y^+LAT1	SLC3A2/SLC7A7	K,R,Q,H,M,L		High	A	Na^+(S-AA^0)	K,I (BM)
	4F2hc/y^+LAT2	SLC3A2/SLC7A6	K,R,Q,H,M,L,A,C		High	A	Na^+(S-AA^0)	K,I (BM)

NR, not reported; A, antiport; AA^0, neutral amino acids; AA^+, cationic amino acids; U, uniport; S, symport; S-AA^0, symport together with neutral amino acids; K, kidney; I, intestine; AM, apical membrane; BM, basolateral membrane; Ub, ubiquitous. Amino acids are given in one-letter codes. O, ornithine; HO-P, hydroxyproline. Affinity: high, <100 μM; medium, 100 μM to 1 mM; low, >1 mM. * Expression in epithelial cells of kidney and intestine.

Table 7   Epithelial amino acid transport systems and their mediators. Taken from Broer et al 2008 [116].

The resulting amino acids are then passed into the portal venous system for transport to the liver and on to the whole body.

Chapter 2
Aims & Approaches

"Thus the body is in a constant state of flux; we do not consist of particular molecules but of a pattern imposed on continuously changing molecules. The dynamic state enables us to adapt to a continually changing environment, which presents now an excess of one type of food, now an excess of another; which demands different levels of activity at different times, and which is apt to damage the organism" **Tanner, 1989 [117].**

2.1 Macronutrient Regulation

2.1.1 Introduction

The human body is in a constant state of energy and nutrient turnover. Metabolism and homeostatic control have evolved to maintain healthy body function and meet the nutrient and energy requirements of the body under constantly changing levels of energy intake and expenditure and varying nutrient supply.

A range of behavioural and biological controls of eating behaviour, macronutrient digestion and processing have been identified which are involved in maintaining energy and nutrient homeostasis. The macronutrients protein, fat and carbohydrate play an essential role in this balance, both as the major source of energy, and as a source of the chemical compounds and elements required for anabolism of organic compounds and cell components. As such, ensuring appropriate supply and processing of macronutrients is absolutely essential to health.

Excess, shortage or impaired processing of macronutrients can and will lead to disease and ill health. This is particularly apparent with the modern day epidemics of diabetes and obesity, driven by a mismatch between the biological systems that humans have evolved to regulate diet and activity and the modern environment of readily available energy dense food and sedentary lifestyles. The human and economic costs of metabolic disease and other diet related syndromes is immense and as discussed herein current treatments, whilst effective have limitations and risks.

Researchers therefore aim to find therapeutic targets for treatment both in terms of digestive physiology and appetite and exercise regulation which can be exploited for disease treatment and management.

As has been shown with enzyme inhibitors such as Orlistat, Acarbose, and latterly alginate, using exogenous agents as regulators of digestive enzyme activity and therefore macronutrient availability provides a way of affecting and regulating this balance as a paradigm for disease treatment and control of nutrient intake.

2.2 *Overview of dietary control, Energy Balance and Nutritional State*

The major behavioural influences of nutrition state are an individual's eating behaviour and level of physical activity. Dietary behaviour and physical activity are influenced by the complex interaction of multiple biological, genetic, behavioural, psychological, social and environmental factors. These factors are incorporated in to a complex decision making process which determines food choice and physical activity levels [118].

Booth et al 2009, have developed a framework model of the 'Determinants of Physical Activity and Eating Behaviour' which describes the varying influences that interact to determine exercise and eating behaviour. The authors argue that physical activity and eating behaviour are influenced 'by a wide variety of internal and external factors, and all should be considered when planning interventions' [119]. At the centre of the model is **(i) The Psychobiological Core** – The individuals genetic makeup and early conditioned behaviour. This also includes the phenotypic response to environment. Then comes **(ii) Cultural** and **(iii) Societal** influences – how the values and beliefs of an individual, and roles, relationships and trends can influence behaviour. **(iv) Enablers of choice** are described as environmental factors that can seen as barriers or enhancers of change which can be targeted in interventions to influence an individual's behaviour and lifestyle. **(v) Behaviour settings** are the physical and social settings of the individual within which choices are made. The Leverage points described in the model are those influences which the authors believe present targets for interventions to 'leverage'/change behaviour. **(vi) Proximal Leverage Points** are the 'close' micro-environmental points which directly influence the individual **(vii) Distal Leverage points** describe the more indirect factors which influence behaviour such as politics, economics and industry.

The use of exogenous enzyme inhibitors clearly aims to target the psychobiological core by aiming to modify the energy and nutrient yield of a meal while aiming to minimise effects on satiety, enjoyment of a meal and lifestyle. However as stated by Booth et al diet and exercise choices and behaviours are pervasive through life and interventions must be considered within the wider context to improve effectiveness [119]. In particular therapeutic interventions targeting digestive enzymes must be considered with regard to the body's natural control, of diet and activity.

2.2.1   Satiety and Feeding

Blundell *et al* 1994, characterise three levels of appetite control in their model of the satiety cascade; (i) Psychological and behavioural events (ii) peripheral physiology and metabolic events (iii) Neurotransmitter function and metabolic interactions with the brain [120]. Appetite is dictated by the interactions of these processes and appetite and food intake is therefore the result of both biological and environmental forces.

The sight, smell and taste of food provide pre-ingestive inputs that influence eating behaviour and stimulate digestive secretions to prepare the digestive organs for the receipt of food. During feeding and digestion, chemo-receptors and mechano-receptors supply information about meal size, nutrient content and digestion which provide post-ingestive satiety signals; and metabolites absorbed across the intestinal epithelia provide post absorptive satiety signals. All of these stages therefore represent targets for dietary interventions.
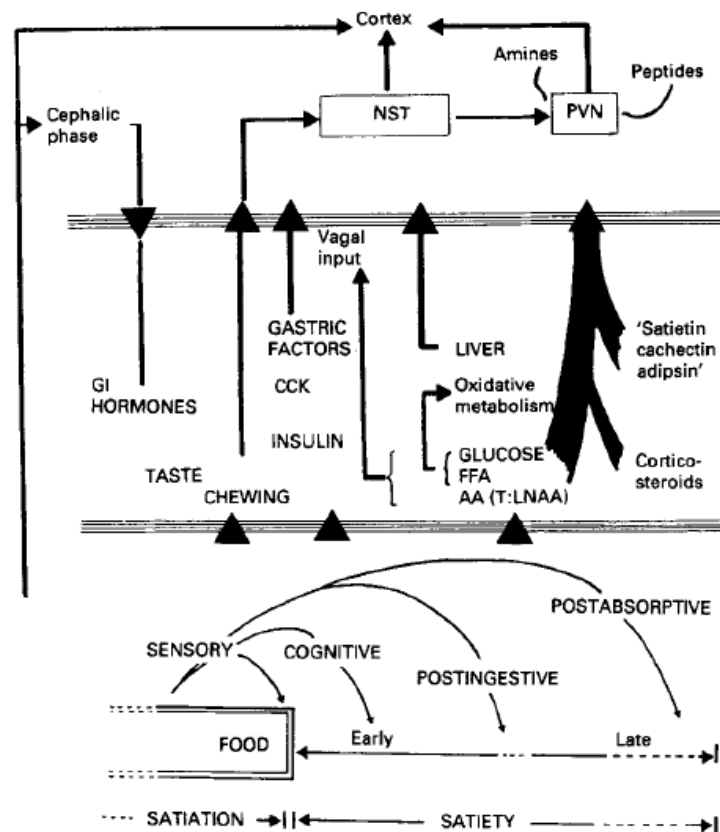
Figure 12 The Blundell Appetite model, taken from Blundell, 2001 [121]. The model shows the three levels ofappetite control: the behavioural pattern, peripheral physiology and metabolism, and brain activity.

Cephalic phase responses occur as a result of the pre-ingestive inputs provided by the sight smell and taste of food. Cephalic phase responses begin before and during eating to stimulate digestive secretions and prepare the digestive tract for food to be ingested. Rather than being satiety signals, these processes give a positive feedback for eating and ready the digestive tract. Smith *et al* 1990, state that 'afferent information from ingested food acting in the mouth provides primarily positive feedback for eating; that from the stomach and small intestine is primarily negative feedback'[122].

During digestion, chemo and mechano-receptors located throughout the digestive tract supply afferent information to the brain through the vagus nerve. These post-ingestive satiety signals feedback information about meal size, nutrient content and digestion which provide and act as post-ingestive negative feedback. Finally post-absorbative satiety signals are provided when digested nutrients cross the intestinal wall and enter circulation.

Digestion and satiety signalling is regulated by the enteric nervous system, which innervates the GI tact, hormonal and chemical signalling from cells of the GI tract and post-absorbative nutrient interactions [123]. Woods 2004, argues that eating patterns are regulated primarily by habit, behaviour and environment, the regulatory control mechanisms of the body must therefore control how much food is consumed once feeding has begun, allowing flexibility over eating patterns [123].

Woods defines three categories of signalling influencing food intake; satiety signals, adiposity signals and central effectors. Satiety signals function to promote a sense of fullness and reduce food intake. Sham feeding using a closed/open fistula in animal studies have shown that sight, smell and taste are not sufficient to estimate meal size and energy consumption. In a 'sham feed' where swallowed food is removed from the fistula, animals eat continuously as their appetite remains unsated [122]. There are therefore more complex methods of feedback for estimating portion size.

Mechanical satiety signals detect stomach distention, stretch receptors and mechanoreceptors signal satiety to the brain [124]. Chemical signals may act on the brain either by acting on receptors in the GI tract and signalling through the vagus nerve, or by circulating hormones in the bloodstream and acting on the brain [123]. A number of anoretic satiety-inducing peptides have been identified which suppress hunger. The release of the hormone cholecystokinin (CCK) in response to protein or fat is thought to play an important role in satiety. CCK activates CCK-A receptors in the pylorus of the stomach which act on the hypothalamus. CCK administration and CCK-A agonists have been shown to have a suppressive effect on the appetite [125]. Other sensing mechanisms have also been suggested, for example, the activation of procolipase to colipase by cleavage of the activation peptide enterostatin has been shown to decrease food intake in rats.

Reduce Meal Size	Increase Meal Size
CCK	Ghrelin
Bombesin family (bombesin, gastrin releasing peptide or GRP, and neuromedin B)	
Glucagon	
Glucagon-like peptide-1	
Glucagon-like peptide-2	
Apolipoprotein A-IV	
Amylin	
Somatostatin	
Enterostatin	
Peptide YY-(3–36)	

Table 8   Gastrointestinal peptides that influence food intake. Taklen from Woods 2004 [123]

Ghrelin is the only pro-appetite peptide which has so far been identified. Ghrelin is 28 amino acid chain esterified on the Serine at position 3 with octanoic acid [126]. It acts as a ligand for the growth hormone secretagogue receptor and plasma ghrelin levels have been shown to increase between meals, peaking immediately before a meal and decrease afterwards [127]. Ghrelin has been demonstrated to be appetite and hunger stimulating, intravenous injection of ghrelin into human subjects stimulated appetite and caused a significant increase in thought and 'imagination' of meals [128]. As shown in Figure 13 Ghrelin acts in the arcuate nucleus of the hypothalamus to stimulate the release of Neuropeptide-Y a potent appetite stimulator. NPY also acts to inhibit secretion of GABA (gamma-aminobutyric acid), inhibition of which results in increasing stimulation of corticotrophin-releasing hormone expressing neurons which results in secretion of Adrenocorticotropic hormone and cortisol [129].
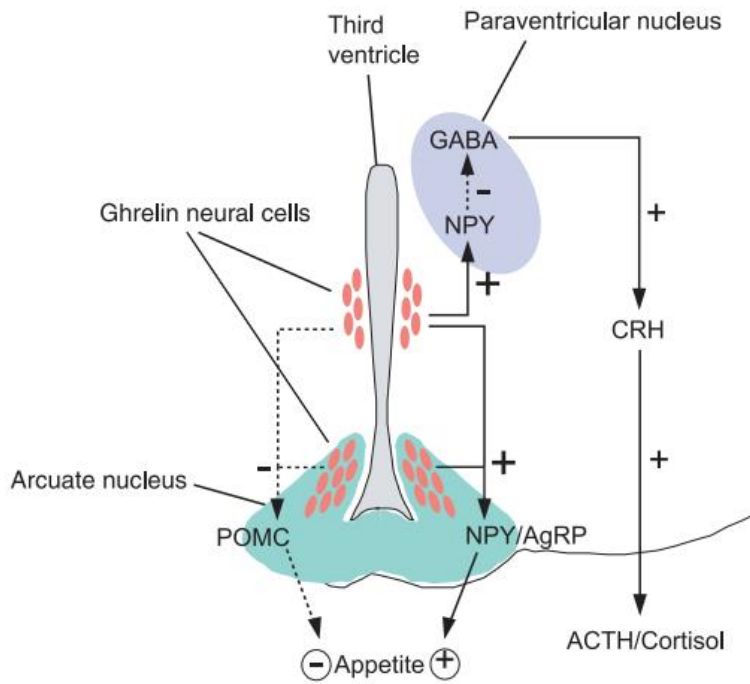
Figure 13   Peptides regulation of appetite in hypothalamic neural networks. Neurons in the arcuate nucleus (ARC) produce ghrelin which act to presynaptically induce neuropeptide Y (NPY) release from NPY neurons, which stimulates food intake, increase GABA secretion (which may postsynaptically modulate the release of the an anorexigenic neuropeptide POMC). Ghrelin stimulates NPY release in the paraventricular nucleus (PVN), which suppresses GABA release, simulating corticotropin releasing hormone (CRH)-expressing neurons, leading to ACTH and cortisol release. Taken from Kojima et al 2005 [129]

Leptin acts as a negative feedback in appetite regulation. Leptin is a 16kD protein produced by adipocytes which acts on the hypothalamus to suppress appetite. As shown in Figure 14 increased circulating leptin encourages increased energy expenditure and sympathetic tone and decreased energy intake. Conversely decreasing leptin acts to stimulate appetite and reduce energy expenditure [130].
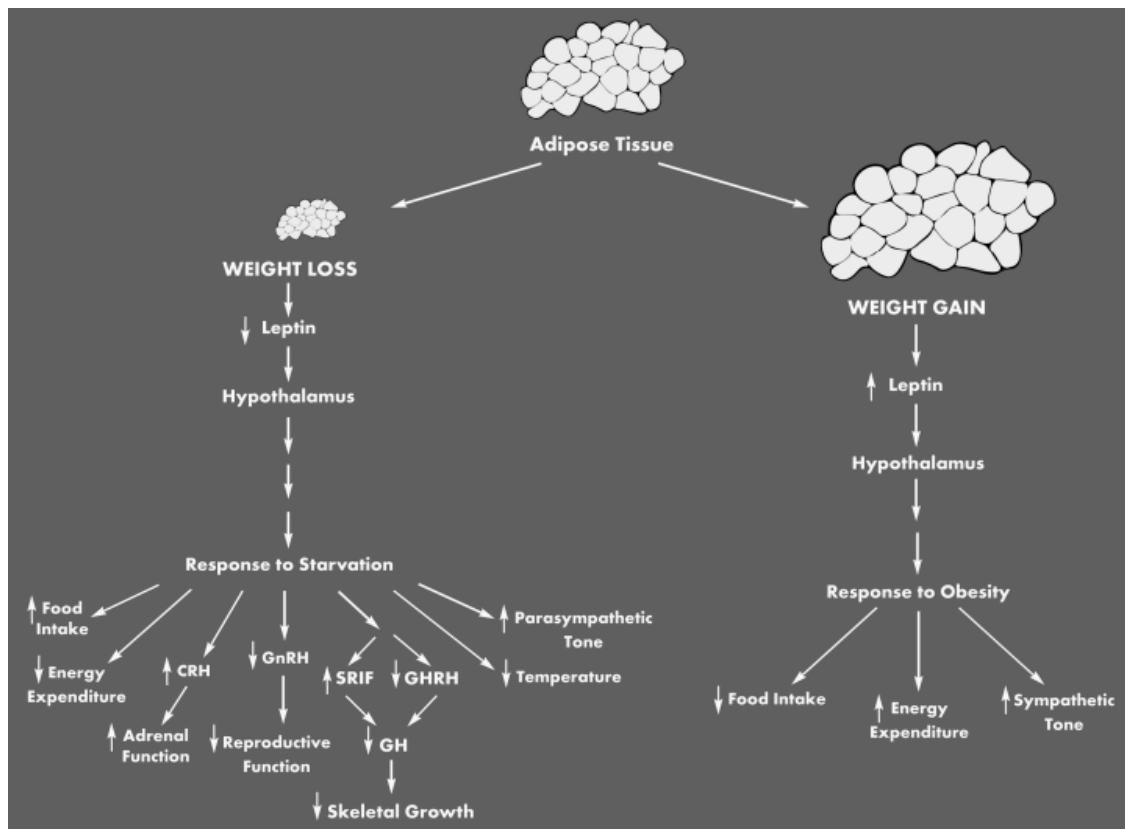
Figure 14   Leptin response in vivo Taken from Friedman 2002 [130].

Carbohydrate intake has been shown to be well regulated and accurately sensed by the body. Pre-load studies with carbohydrate have shown that after a polysaccharide pre-load meal there is an equivalent reduction of energy intake at later free feeding [131].

2.3   Impairment of regulation

A range of behavioural and biological controls of eating behaviour, macronutrient ingestion and processing have been identified which maintain energy and nutrient homeostasis. However impairments to the regulatory mechanisms of digestion can lead to disease. Using exogenous agents as regulators of digestive enzyme activity and therefore macronutrient availability provides a way of affecting and regulating this balance as a paradigm for disease treatment and control of nutrient intake.

2.3.1   Obesity.

Obesity presents a prime example of how multiple environmental, social and cultural factors can interact with a susceptible 'Psychobiological Core' leading to sustained over eating and under exercising in segments of the population. In a review of the Human Obesity Epedemic, 2009, Power describes three types of obesity: (i) metabolic obesity; where identifiable syndromes or diseases result in weight gain, (ii) socio-cultural obesity; where historically obesity may have been seen as a status symbol or sign of

wealth and (iii) Environmental obesity; which encompasses the modern epidemic where otherwise physiologically normal individuals become obese [9].

Regulation of appetite and eating is a key control of macronutrient supply, and in an ideal state, eating behaviour is controlled and maintained relative to the biological need. However it is observed by Blundell *et al* 1994 that in a state of overconsumption and accumulation of body fat, there is a failing of homeostasis, and there does not seem to be a drive towards under-eating as a response, therefore weight gain can occur passively without a biological feedback. As Blundell et al put it, 'biological defences against overconsumption are weak or inadequate' [120].

Fat is an essential aspect of our diet and fats/lipids are essential throughout the body as structural components, in cell membranes, as hormones and certain fatty acids which are integral to brain development and function. Adipose tissue therefore exists as a store of fat, however excessive fat storage as has been discussed can become pathological.

Not only are the negative feedbacks against fat accumulation inadequate, but the picture is complicated by the function of adipose tissue as an active endocrine organ. Adipose tissue secretes cytokines and hormones including leptin, adiponectin, interleukins (IL-6, Il-8 and Il-10) and is also involved in steroid hormone metabolism. The hormones secreted by adipose tissue influence a range of processes including appetite, eating behaviour, energy metabolism neuroendocrine function and the immune system [9]. Excess adipose tissue is therefore associated with insulin resistance, hyperglycemia, dyslipidemia, hypertension, and prothrombotic and proinflammatory states [132].

Lipid deficiency can also associated with aspects of metabolic syndrome and pathology characterised by insulin resistant diabetes [132, 133].

As discussed in the introduction, obesity and metabolic diseases are a significant problem, particulary in the developed world, with obesity and diabetes at epidemic levels. In 2005, almost 25% of the worlds population (1.6 billion people) were considered overweight and 400 million obese and in 2010 the global prevelance of Diabetes was 6.4% (285 million) people, with 90% of these cases being Type 2 Diabetes [1, 134].

The health effects and co-morbdities of obesity and current treatments were discussed at length in the introduction. Obesity is caused by a positive energy balance maintained

over a period of time and treatments aim to redress this balance. Downregulation of digestive enzyme activity in order to reduce the energy yield of a meal and could play a part in restoring this energy balance, furthermore the calorific load could be decreased without affecting the sensation of satiety.

Downregulation of lipase activity would reduce dietary availability of fatty acids. Acetyl CoA which is required for cholesterol biosynthesis is produced during fatty acid metabolism, so reducing dietary fatty acids could hypothetically reduce cholesterol synthesis with benefits to cardiovascular health. Bile acids are derivatives of cholesterol, therefore reduced cholesterol production could potentially lead to reduced bile acid production. For the efficient digestion of lipids, bile acid is required for emulsification. Reducing bile acid production would reduce emulsification, resulting in a smaller lipid-water interface and therefore lower lipase activity.

2.3.2 TTDM

In 2010 the global prevelance of Diabetes was 6.4% (285 million) people, with 90% of these cases being Type 2 Diabetes [134]. It is estimated that this figure will rise to 7.7% of the population, or approximately 439 million people by 2030 [135]. As with obesity Type 2 Diabetes is seen as a disease of the developed world, with the rise in prevelance occuring much more rapidly in the developed world. In the year 2000, 2.9 million people died as a result of diabetes [136]. Diabetes is also related to the co-morbidities of heart disease, stroke, blindness, renal failure and limb amputations.

Type 2 Diabetes is estimated to have a heritability of over 50% however chronic overeating is the leading cause of diabetes. Insulin resistance, insuficient insulin secretion or a combination of the two leave type-2 diabetics unable to maintain normal blood glucose levels. In over-eating, non-susceptible individuals are able to process excess energy into subqutaneous fat. However in susceptible individuals, the β-islet cells can not produce enough insulin to compensate leading to increased glucose release, adipose tissue inflamation and ultimately insulin resistance. As the energy is not deposited as sub-cutaneous fat, it is deposited elsewhere as Visceral adipose tissue around the organs and can cause tissue damage [135].

In nature, sugars are stored predominantly as the polysaccharides cellulose, starch and glycogen; the ability to hydrolyse polysaccharides is therefore of great importance to biological organisms as it confers access to a vast supply of glucose, and a major source of energy [137] .

β(1-4) linked cellulose remains resistant to human digestion as humans do not produce β(1-4) hydrolysing enzymes. Starch and glycogen on the other hand are both α(1-4) linked and can be cleaved by a number of human enzymes, principally the α-amylases. Starch, the major carbon reserve of plants and as the most common polysaccharide found in food, accounts for more than half of the carbohydrate ingested by humans [138].

Modulation of α-amylase activity is therefore a target for regulation of carbohydrate digestion. Downregulation of carbohydrase activity would reduce the glycaemic load following a meal and therefore lower the insulin response; this has potential application

in the management of Type 2 Diabetes as is seen with the α-glucosidase inhibitor acarbose which is a poor substrate for α-glucosidases and competetively inhibits them [31].

As mentioned in the introduction, the α-glucosidase inhibitor acarbose has been shown to significantly reduce development of Type 2 Diabetes in patients with glucose intolerance and promote a return to normal glucose tolerance [31]. By slowing carbohydrate digestion, acarbose reduces the glycaemic-hit of a meal and reduces post-prandial insulin secretion. [32].

Furthermore, dietary fibres have also been investigated as potential treatments of diabetes and metabolic disease. The dietary fibre guar gum was shown to have anti-hyperlipidaemic and anti-hyperglycaemic effects when given as a dietary supplement to diabetic rats [139]. Partially Hydrolysed Guar Gum has been investigated as a human intervention in a randomised clinical trial and was shown to have benneficial effects towards markers of metabolic syndrome with a significant reduction in waist circumferance in the intervention group (average 1.2cm) and a significant hypoglycaemic effect and was shown to blunt the post-prandial increases in blood glucose and insulin [140].

Dietary fibre including pectin, alginate, xantham gum and guar gum have been shown to attenuate post-prandial blood glucose response and to be an effective treatment of diabetes [141]. It has been argued that this is due to the soluble dietary fibres increasing the viscosity of the meal which slows digestion and delays gastric emptying. Alginate has been investigated as a dietary additive to be used in diabetes management.

2.3.3 Pancreatic Insuficiency

A loss of pancreatic function will lead to pancreatic insufficiency: the insufficient production of digestive enzymes leading to an inability to properly digest food. Pancreatic insufficiency may result from pancreatitis, cystic fibrosis, pancreatic duct obstruction, tumours of the pancreas, coeliacs disease, alcoholic pancreatitis and acid-mediated enzyme inactivation [142]. The main symptoms are malnutrition, weight loss, steatorrhea, abdominal pain and micronutrient deficiency.

Treatments for pancreatic insufficiency aim to relieve symptoms and to restore a normal nutrition state with enzyme supplementation. A fat restricted diet may be recommended to reduce steatthorrhea resulting from undigested fats. Dietary fibres have been shown to reduce the side-effects of undigested fats in the case of Orlistat treatment [143]. Psyllium mucilloid was effective in controlling the gastro-intestinal side-effects of orlistat administration.

In pancreatic enzyme replacement therapy, exogenous enzymes are supplemented orally [143]. The common delivery is in 'enteric-coated' minimicrospheres which deliver a high lipase activity enzyme load to the small intestine to avoid acid inactivation. These treatments have been shown to increase fat digestion and absorption, reduce fat excretion and improve stool consistency [144, 145]. Proton pump inhibitors have been shown to improve the efficacy of enzyme replacement therapy, this is done by increasing the pH of the stomach and reducing the activity of gastric pepsin [146].

Pancreatic secretion has been shown to respond to the diet and interestingly in a study of six healthy subjects supplemented with 20g dietary fibre (predominantly pectin) per day over four weeks resulted in significantly increased levels of lipase secretion in response to a meal. Lipase secretion 120 minutes after a test meal was increased by 64% [147]. However, another study showed that dietary fibre could inhibit pancreatic enzyme activity *in vitro*, and led to increased fat excretion *in vivo* and gastro-intestinal side-effects [148]. This suggests that increases in lipase secretion as observed in the Dukehart et al 1989, study may have occurred as a response to lipase inhibition by the dietary fibre.

Pancreatic enzyme supplementation has been shown to improve outcomes in pancreatic adenocarcinoma as part of a programme of nutrition supplementation and detoxification

support, with one year survival in a group of 11 patients increasing to 81% as compared to a normal one year survival of 25% [149].

Exogenous compounds which increase the activity of digestive enzymes may have potential for improving remaining pancreatic enzyme function, and increase the efficacy of enzyme replacement therapy.

2.3.4 Protein disregulation

Proteolytic enzymes catalyse the breakdown of dietary proteins into amino acids and short oligopeptides capable of crossing the small intestinal epithelia to be circulated through the blood and resynthesised to proteins in cells. Due to this central role in protein metabolism, protease activity is impicated in many downstream effects on health and disease.

From a nutrition perspective, the ability to affect protein digestion and absorption by eliciting an increase or decrease in pepsin activity has potential therapuetic benefits for protein deficiency and hyperproteinaemia respectively. Modulation of protein digestion and alteration of luminal protein and amino acid levels may also have effects on digestive regulation through the amino acid sensing system. Luminal amino-acid sensing is thought to contribute to control of digestive processes, sensory stimuli from within the digestive tract can initiate signalling pathways which are involved in regulating digestion, absorption gut motility, food intake and satiety [150].

The proteolytic enzyme pepsin is an agressor in gastro-oesophagul reflux with the ability to cause damage up to pH6.0, inhibition of pepsin is thererfore seen as a potential treatment [151]. It is thought that alginate based treatments of heartburn and acid reflux may be in part effective both through inhibition of pepsin as well as their raft-forming mechanism [7].

Protoeolytic activity is also important in drug delivery, with luminal metabolism and first-pass intestinal metabolism affecting the oral bioavailability of protein based drugs during pre-systemic metabolism [152]. Inhibition of gastrointestinal enzymes has been shown to increase the bioavailability of orally administered drugs [153].

2.4 Experimental Approach

Given the need for novel therapies for a range of metabolic and nutrition related diseases and the growing evidence of dietary fibres as novel interventions for enzyme inhibition it is the aim of this study to develop a methodological approach for the testing of exogenous bioactive compounds. Within this, the project has had three major goals:

 i.   Identify and develop assays for single enzyme analysis in order to carry out high throughput screening of a library of bioactive compounds
 ii.   Develop a model gut system in order to investigate the effects of any compounds identified in (i) on macronutrient digestion in an *in vitro* simulation of the human GI tract
 iii. Investigate the mechanisms of enzyme regulation through enzyme kinetics and enzyme/substrate interactions with bioactive agents

A 3-step process has been developed to test the action of biopolymers on the major enzymes of macronutrient digestion, pepsin, trypsin, α-amylase and lipase:

Selected Kinetic Analysis

Model Gut Analysis

High Throughput Analysis
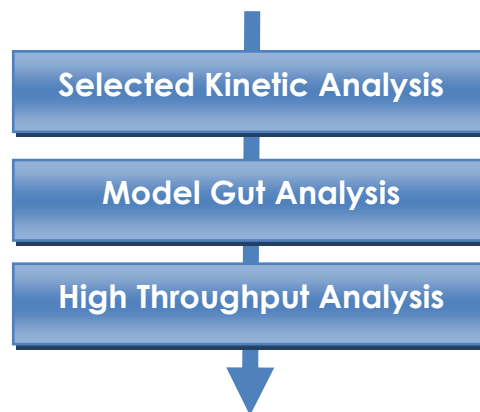
2.5 Higher throughput analysis

Methods for higher throughput analysis of biopolymer samples will be developed on 96 well microplates in order to quickly and efficiently screen a library of biopolymers for regulatory effects. The observed effects will be compared and correlated to structural characteristics and properties of the samples in order to find the optimum candidates for enzyme regulators and to attempt to define their mechanisms.

Eighteen alginates provided by Technostics Ltd and FMC biopolymer were tested in a pepsin activity assay. Alginates are linear biopolymers composed of guluronic and mannuronic acid, their structural and bioactive properties are dictated by the proportion and arrangement of guluronnate and mannuronate. The eighteen samples tested provide a catalogue of alginates of varying degrees of F[G]. F[G] represents the frequency of guluronic acid residues in the alginate backbone, therefore the remaining residues in the backbone are mannuronate. As can be seen in Figure 15, this catalogue of alginates provides a range of samples from Low-F(G) to High-F(G).
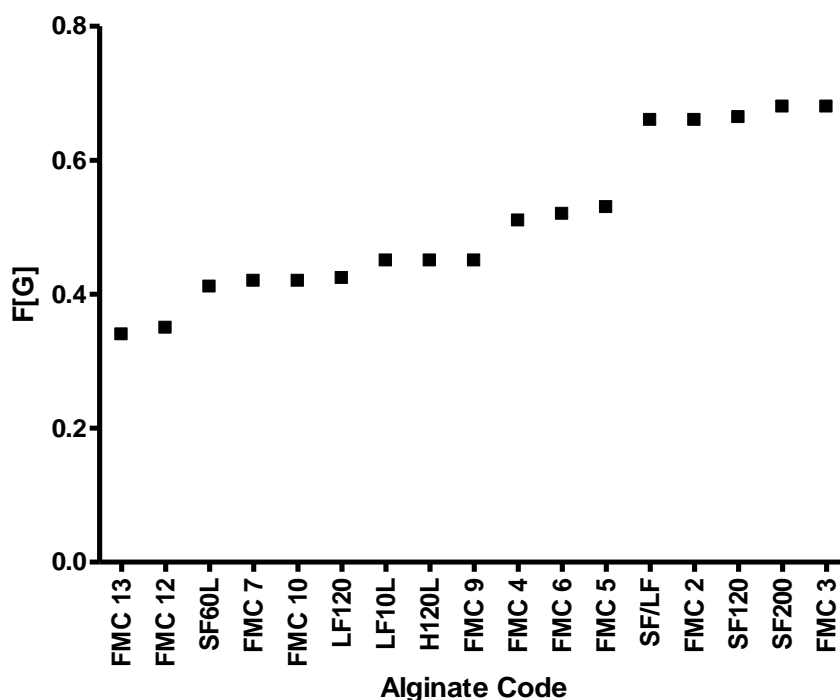
Figure 15   Freguency of guluronic residues in alginate backbone F(G) for all sample alginate biopolymers.

The structures of the alginate samples were characterised by ^{13}C-NMR neighbour diad analysis and the full characteristics of all samples are shown in

Table 9 and represented in Appendix 8.1

	F(G)	F(M)	F(GG)	F(MG/G M)	F(MM)	F(MGG/G GM)	F(MGM)	F(GGG)	N (G>1)
FMC 2	0.66	0.34	0.54	0.11	0.23	0.038	0.076	0.51	15.47
FMC 3	0.68	0.32	0.57	0.11	0.21	0.042	0.069	0.53	14.66
FMC 4	0.51	0.49	0.34	0.17	0.32	0.043	0.124	0.3	8.97
FMC 5	0.53	0.47	0.36	0.16	0.31	0.042	0.123	0.32	9.67
FMC 6	0.52	0.48	0.35	0.17	0.31	0.048	0.122	0.3	8.15
FMC 7	0.42	0.58	0.24	0.18	0.4	0.044	0.133	0.2	6.47
FMC 9	0.45	0.55	0.26	0.19	0.36	0.054	0.136	0.2	5.78
FMC 10	0.42	0.58	0.21	0.21	0.37	0.07	0.14	0.14	3.96
FMC 12	0.35	0.65	0.19	0.16	0.49	0.053	0.111	0.13	4.54
FMC 13	0.34	0.66	0.17	0.17	0.49	0.046	0.124	0.12	4.63
LF120	0.424	0.576	0.24	0.185	0.391	0.057	0.156	0.183	4.7
LFR560	0.633	0.367	0.505	0.128	0.239	0.054	0.096	0.45	9.9
LF10L	0.45	0.553	0.257	0.19	0.362	0.068	0.153	0.19	4.4
H120L	0.45	0.551	0.276	0.173	0.379	0.051	0.15	0.22	5.9
SF120	0.664	0.336	0.545	0.119	0.218	0.061	0.083	0.484	9.6
SF200	0.68	0.322	0.573	0.105	0.218	0.036	0.079	0.537	16.7
SF/LF	0.66	0.336	0.548	0.116	0.22	0.042	0.081	0.506	13.8
SF60L	0.411	0.589	0.219	0.195	0.393	0.077	0.155	0.133	3.3

Table 9   Codes and molecular characteristics for alginates used in this study. F(G) is the fraction of the alginate polymer composed of guluronate and F(M) the fraction of mannuronate. N(G>1) is the number of consecutive guluronate residues above 1.

2.6   Enzyme Kinetics

Microplate assays will be modified to allow for selected kinetic analysis. Michaelis Menten and Lineweaver Burke analysis of samples will be carried out in order to study mechanisms and potency of regulatory effects.

2.6.1   Michaelis Menten Kinetics

In single molecule enzymology, the reaction is a two-step process, firstly the enzyme [E] and substrate [S] combine to form an enzyme-substrate complex [ES] before being converted to product [P]. The Michaelis-Menten equation as represented by Briggs and Haldane in 1925 shows this reaction.

$$E + S \underset{K_3}{\overset{K_1}{\longleftrightarrow}} ES \underset{K_4}{\overset{K_2}{\longleftrightarrow}} P + E$$
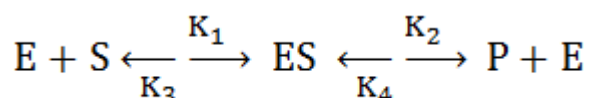
As this equation shows, the rate of product formation, and therefore velocity of the reaction will be restricted by the rate of formation of ES complex. The rate of ES formation will increase from when enzyme and substrate are initially mixed until a steady state is reached in which ES formation and dissociation in equilibrium.

Michaelis and Menten observed that the kinetics of this reaction alters with substrate concentration (or ratio of substrate to enzyme). Enzyme catalysed reactions increase in velocity with substrate concentration until saturation is achieved and addition of further substrate can no longer increase the reaction rate as all active sites are saturated with
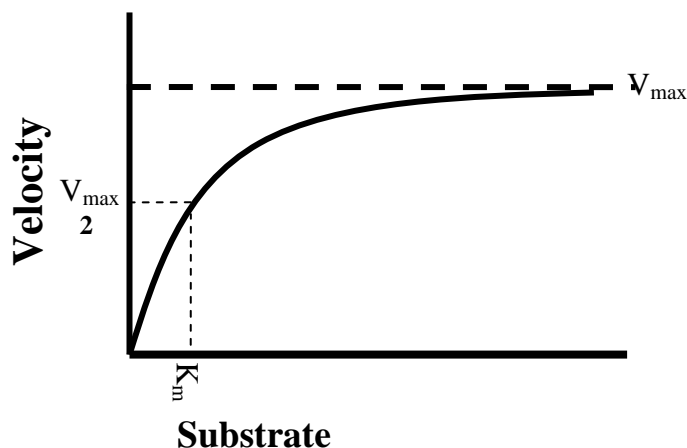
substrate. This can be graphically represented by a Michaelis-Menten plot (Figure 16).

Figure 16   Generalised example of a michaelis menten plot.

49

This plot can also provide useful information about the kinetics of an enzyme catalysed reaction. The maximum velocity of the reaction (V_{max}), is the theoretical concentration of substrate at which all active sites are saturated with substrate and functioning at a maximal rate. This value can be determined from where the Michaelis-Menten curve plateaus, this levelling of reaction rate occurs due to substrate saturation.

The constant V_{max} can be used to calculate the Michaeles Constant (K_m), which is the substrate concentration required for half of maximal enzyme activity. As such the K_m provides an important measure of the affinity of an enzyme for its substrate. A low K_m means high affinity. Inversely a higher K_m would indicate a lower affinity.

The Michaelis Constant can be described as the rate of enzyme-substrate complex dissociation (either in to product and enzyme or back in to substrate and enzyme) divided by the rate of enzyme-substrate complex formation:

$$K_m = \frac{(K_2 + K_3)}{K_1}$$

2.6.2   Lineweaver Burk Plots

As well as deriving kinetics constants from Michaelis Menten plots and the formulas listed above, Lineweaver and Burk stated that by drawing a double reciprocal plot of the substrate velocity data it is possible to establish the K_m and V_{max} from the x and y intercepts of a linear regression (Figure 17).
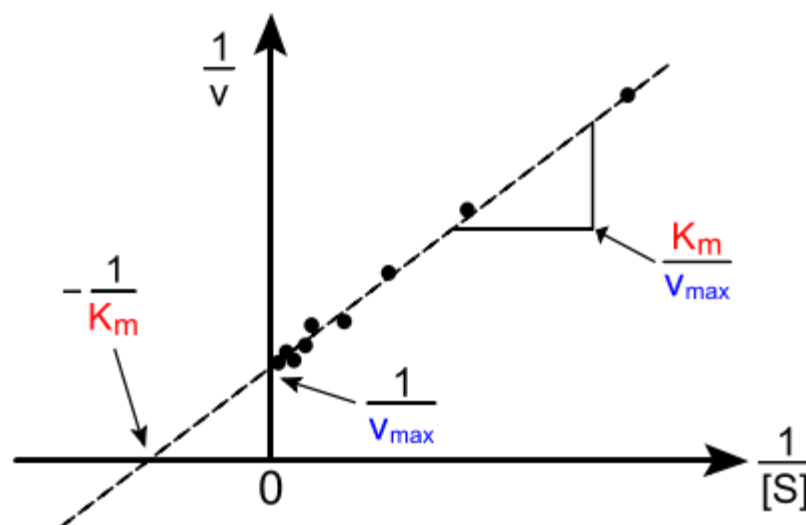
Figure 17   Generalised example of a lineweaver-burke plot

50

2.6.3 Regulation of enzyme reactions

The rate of enzyme reaction can be influenced by many factors such as enzyme concentration, substrate concentration, substrate-enzyme affinity, temperature and pH. As well as this, certain extrinsic compounds may have effects on the rates and kinetics of an enzyme catalysed reaction. Inhibition and activation can be described in a number of ways; linear or non-linear, reversible or irreversible and competitive, non-competetive, uncompetetive or mixed. In the presence of a 'regulator' either the K_m, V_{max} or both will be changed and the Michaelis Menten and Lineweaver-Burk profiles will be altered. The way in which these factors are changed can tell us a lot about the type of regulation that is being seen.

2.6.4 Enzyme Inhibition

2.6.5 Reversible Competitive inhibition

Reversible Competitive Inhibition occurs when an inhibitor [I] combines with the enzyme, blocking substrate binding to the active site. Likewise, a competitive inhibitor cannot bind to the enzyme when substrate is bound. This is why this method of inhibition is referred to as competitive. However, as the binding is reversible, the inhibitor will dissociate from the enzyme, and all substrate will eventually be converted.

In competitive inhibition rate of enzyme action is slowed by the competition of inhibitor for enzyme active sites and so K_m is increased. The V_{max} however will not be altered, because addition of sufficient substrate will overcome the competition of the inhibitor.

The model of reversible competitive inhibition and all other models of inhibition is included in the appendix (Chapter 8, Figure 166a-d).

2.6.6 Non-Competitive Reversible inhibition

In Non-Competitive Reversible inhibition, the inhibitor binds the enzyme at a point other than the active site, either when the enzyme is free of in complex. As substrate binding is unaffected the K_m will be unaltered as [ES] complex formation and dissociation will be unhindered. V_{max} will however be reduced as the presence of inhibitor blocks the formation of product.

2.6.7   Uncompetetive Inhibition

In uncompetitive inhibition, binding of substrate modifies the enzyme such that an inhibitor binding site is exposed. Inhibitor can then bind to the enzyme substrate complex, preventing product formation.

Binding of inhibitor to the [ES] complex reduces the rate of [ES] dissociation. As such the K_m will be decreased as can be seen from the equation below:

$$K_m \quad = \quad \frac{(k2+k3)}{k1}$$

Therefore in the case of uncompetitive inhibition neither the K_m nor V_{max} correspond on the MM and LB plots.

2.6.8   Mixed Inhibition

Mixed inhibition may be a combination of the inhibitor binding the active site and binding the [ES] complex. So the inhibitor can compete with substrate for the active site, but when the active site is occupied with substrate, the inhibitor may also act upon the enzyme substrate complex. This therefore results in both a decreased V_{max} and an increase in K_m. The two routes of inhibition are shown in the appendix (Chapter 8, Figure 166d).

2.6.9   Irreversible Inhibition

Irreversible inhibitors act by covalently binding to the enzyme and modifying its structure such that it is no longer active either through blocking the active site or inducing a conformational change that renders the enzyme inactive. For example, Penicillin covalently modifies the transpeptidase enzyme in bacteria preventing cell wall synthesis. They are referred to as irreversible due to the slow disassociation of inhibitor from the enzyme [154].

2.7 Quantification of Regulatory effects

The kinetic constants K_m and V_{max} provide useful indicators of the type of inhibition or activation. Using V_{max} and K_m it is possible to calculate the K_i or inhibition constant. The K_i is the amount of inhibitor required to halve the V_{max}.

K_i therefore describes the relationship between the uninhibited and inhibited enzyme, and is best understood using a Lineweaver Burk plot (Figure 18).
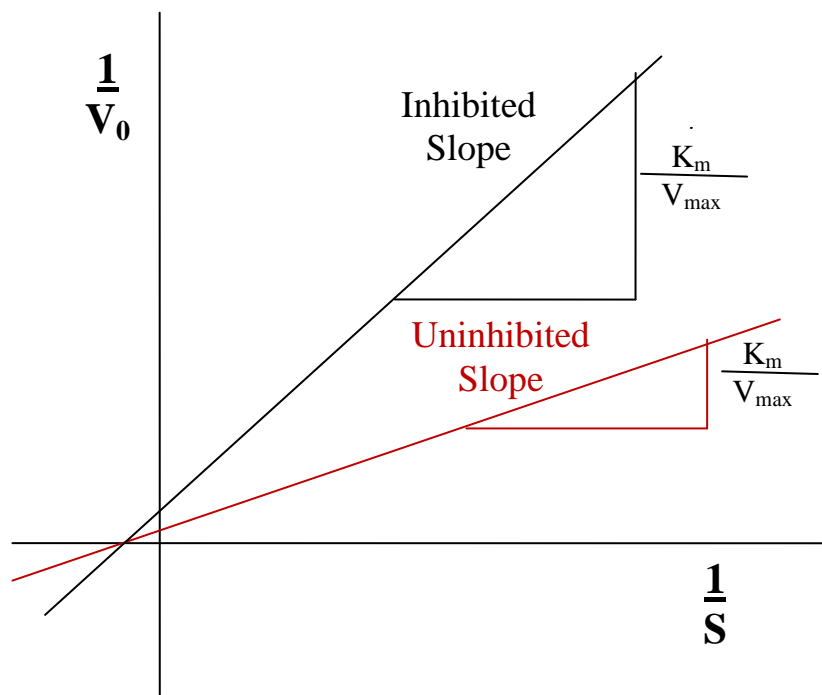
Figure 18   Generalised representation of inhibition on a Lineweaver-Burk plot

The gradient of the line on the double-reciprocal Lineweaver Burk plot can be calculated as the Michaelis Constant (K_m) divided by the Maximum Velocity (V_{max}).

The relationship between these two slopes is determined by the Inhibitor Concentration [I] and Inhibitor Constant K_i as shown below:

$$New\ Slope = Old\ Slope \times \left(1 + \frac{[I]}{K_i}\right)$$

$$\frac{K_{m1}}{V_{max1}} = \left(\frac{K_{m2}}{V_{max2}}\right)\left(1 + \frac{[I]}{K_i}\right)$$

53

$$\left(\frac{\left(\frac{K_{m1}}{V_{max1}}\right)}{\left(\frac{K_{m2}}{V_{max2}}\right)}\right) = \left(1 + \frac{[I]}{K_i}\right)$$

$$K_i = \frac{[I]}{\left(\frac{\left(\frac{K_{m1}}{V_{max1}}\right)}{\left(\frac{K_{m2}}{V_{max2}}\right)} - 1\right)}$$

While there is not specifically such thing as an 'activation constant', a negative inhibition constant can be taken to indicate an activation, or increase in enzyme activity. Although the relationship between K_i and activation is somewhat more complicated than in the case of inhibition, as is discussed in Appendix 8.3.

2.8 Model Gut analysis

A physiologically relevant *in vitro* Model Gut System (MGS) has been developed which simulates the digestive processes of the gastrointestinal tract from mouth to terminal small intestine. This model can be used to study the chemical and enzymatic digestion of the macronutrients fat, protein and carbohydrate and to analyse the effects of exogenous compounds on digestion with a view to developing novel therapeutics. The model has been validated with known inhibitors, and used to characterise novel modulators of digestive enzyme activity. The efficacy of the MGS has been demonstrated by the role it has played in building a case for the novel lipase inhibitor alginate as a weight loss treatment, which has now progressed to the BBSRC funded human weight-loss trial titled "Designing the most effective vehicle to deliver alginate to effectively reduce fat digestion and absorption".

An artificial model of the human upper GI tract was designed to simulate the conditions of macronutrient digestion *in vitro*. The model gut system provides a methodology for the investigation of fat, protein and carbohydrate digestion and a tool for quantitatively analysing the effects of exogenous regulators on digestion. As such the model provides an *in vitro system* that can be used to validate effects seen with bioactive compounds in single enzyme analysis in a physiologically relevant mixed model.

Model gut analysis provides a well controlled, reproducible and cost-effective alternative to *in vivo* studies.

Chapter 3

Modulation of Pepsin Activity

3.1 Pepsin

3.1.1 Categorisation

Pepsin is part of the aspartate protease super family (EC 3.4.23.) [110]. As the major proteolytic enzymes in gastric juice, pepsins are responsible for the digestion of dietary protein in the low pH environment of the stomach. Pepsins are broad specificity endopeptidases with a preferance for cleavage between hydrophobic amino acids.

There are 5 types of pepsin, pepsins A, B, C, F and Y. Of these pepsins A and C are found in humans, derived from two immunological pepsinogen groups PGI and PGII respectively. PGI and PGII comprise 7 pepsinogens that are each activated to a unique pepsin. PGI comprises pepsinogens 1-5 and is secreted in the stomach by oxynitic glands. PGII consists of pepsinogens 6 and 7 and is secreted in the stomach by the pyloric glands of the antrum as well as the fundus oxynitic glands, and in the proximal duodenum by 'pepsin secreting tissue'[112].

3.1.2 Structure

Pepsinogen, the zymogen precursor of pepsin is a protein of approximately 40kDa, and the active form of pepsin is in the region of 35kDa, although there is a wide variation in this with sub-species of active human pepsin varying from 31-44kDa.

Like all aspartate-proteases pepsin is a monomeric enzyme. Native human pepsin is composed of 2,438 atoms which make up the protein structure, co-ordinated with 102 water molecules [155].

Pepsin is composed of two lobes (Figure 19), of similar size and structure, referred to as the N-terminal lobe and C-terminal lobe, in porcine pepsin these comprise amino acids 1-175 and 176-326 respectively [156]. The active site region backbone (Residues Val 1-Leu 6, Asp 149-Val 184 and Gln 308-Ala 326) consists of a six-stranded antiparallel beta sheet containing the active site which is formed by a deep 30 Angstrom cleft

between the two lobes. All pepsins contain two conserved aspartate residues in the middle of this cleft [157]. In porcine pepsin the two aspartates Asp32 and Asp215 are about 3 Angstrom (0.3nm) apart, close enough to share a proton [157]. The two aspartic residues are covered by an N-terminal flap (aa 60-90 in porcine pepsin) which forms a hairpin loop with a highly conserved Tyr 75 residue at the tip.
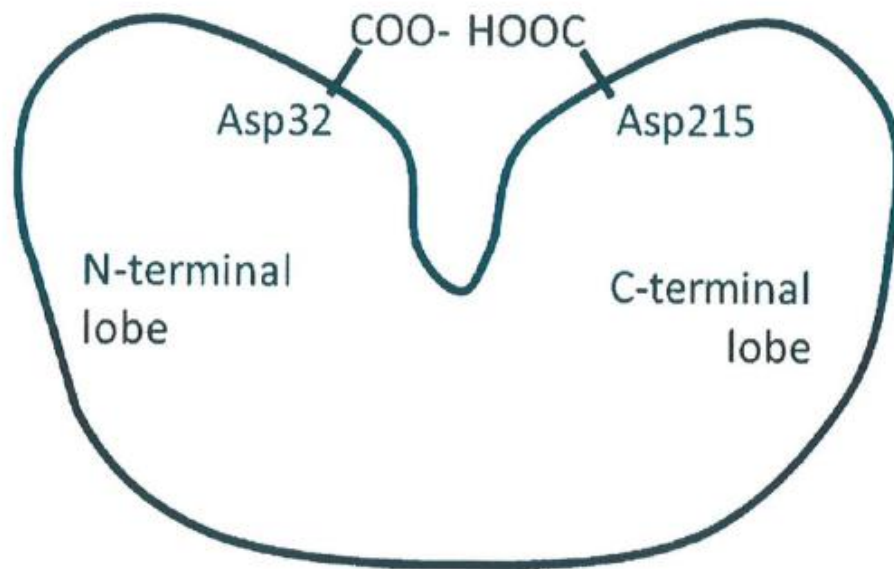
Figure 19   Diagrammatic representation of pepsin structure. Taken from Pepsins, Pearson et al 2010 [158]

An extensive hydrogen-bonding network, and the co-ordination of seventeen water molecules stabilise the active site. Both the hydrogen bond network and the water molecules within the active site are essential for pepsin structure and function [155]. Outside of the active site region, the N-terminal lobe consists of three layers of β-Sheets (GLn 308-Ala 326), and a C-terminal lobe consisting of 2 layers of β-Sheets (Thr185-Arg148) [155].

3.1.3   Activation

The major site of pepsin activity is the stomach. Pepsin is secreted as the inactive zymogen pepsinogen from Chief/Peptic Cells in the Gastric of the stomach. Pepsinogen is reported to be stable within the pH range 6-9 [111], above pH 9.0 pepsinogen is irreversibly denatured.

Pepsinogen is activated to pepsin below pH6 by a pH-driven auto-catalytic mechanism. This activation of pepsin occurs faster at lower pH [112].

In porcine pepsinogen the active site is blocked by a 44 amino acid N-terminal peptide. Pepsin is highly acidic and therefore negatively charged, the 44 aa propeptide is highly basic and therefore positively charged. Therefore at neutral pH this propeptide is held over the active site by electrostatic interactions between the amino groups of basic amino acids, and carboxyl groups of acidic amino acids [151]. Below pH 5.0 carboxyl groups become protonated, disrupting charge-charge interactions and allowing the N-terminal peptide to move into the active site where there are two possible activation pathways; 1) a 16 amino-acid peptide is cleaved and the enzyme/protein becomes a partially active 'pseudo-pepsin', a further 28 amino-acid peptide is then cleaved from the N-terminal by either a partially or fully active pepsin. 2) alternatively pepsinogen can be activated to active pepsin by complete cleavage of the 44 amino-acid chain blocking the active site.

Site directed mutagenesis has shown that the catalytic aspartate residues are essential for auto-catalytic activation of pepsinogen. When substituted with glutamate, the mutant pepsin retains proteolytic activity as a glutamyl protease, however lacks the ability of autocatalytic activation. The relative size of glutamate residues block alignment of the N-terminal segment for autocatalytic cleavage [159].

3.1.4   Catalytic Mechanism

The two aspartate residues (Asp32 and 215 in pig pepsin) which form an acid base pair in the middle of the active site cleft hold between them a water molecule which facilitates nucleophillic attack on the peptide bond. Asp32 is the basic partner and Asp215 the acid. The extensive hydrogen bonding network is required to maintain the basic Asp32 in the COO^- state. Nucleophillic attack by the water molecule on the peptide bond NH-CO generates $-NH2$ and $-COOH$. The six-stranded antiparallel beta sheet between the N and C-terminal lobes contains an active site binding region which can bind a peptide region of 7-9 amino acids [160].

Pepsins are endopeptidases and therefore preferentially cleave peptide bonds within the polypeptide chain as opposed to cleaving amino acids from the terminal ends. Pepsins are of broad specificity, but preferentially cleave bonds between hydrophobic and aromatic amino acids [161]. The residue at the P1 position at the cleavage site has been shown to have the strongest influence on pepsin cleavage, with the enzyme favouring Phe, Leu, Met, Cys, Glu, Trp and Tyr residues at P1. Little pepsin cleavage occurs after

a charged amino acid at P1 such as His, Lys or Arg, or after the cyclic amino acid Pro. Aromatic residues are also favoured at the P1' position such as Tyr, Trp or Phe. The same study showed that pepsin favours cleavage of smaller peptides to larger ones Further data is available for favourable cleavage sites [162]. Figure 20 shows an explanation for the P1 and P1' terminology with P1 representing the residue on the amino side of the cleavage site and P1' on the carboxyl side.
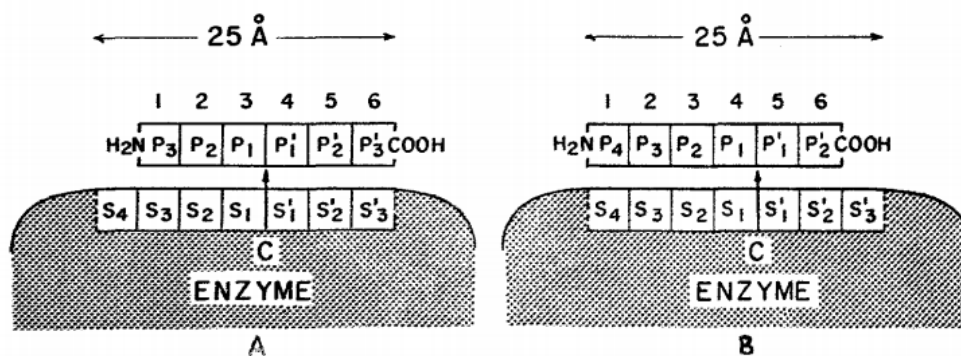
Figure 20 The two possible enzyme-substrate complexes of papain with a hexapeptide molecule. There are 7 subsites in the enzyme active site. Complex A yields two tripeptide molecules, and B one tetrapeptide and one dipeptide. Taken from Schechter et al 1967 [163].

3.1.5   pH Optima and Inactivation

The pH optima of human pepsin has been shown to be in the range pH1.5-2.5 depending on both substrate and pepsin sub-family [164]. Figure 21 shows an activity and stability curve for human pepsin against serum albumin. In this study, pH optimum is reported as 1.5-2.5, with pepsin maintaining approximately 60-70% activity up to pH5. The range pH5 to 7.5 represents the range within which pepsin has little or no activity, but a return to acidic pH will fully restore activity. Above pH 7.5 pepsin is irreversibly inactivated [165].
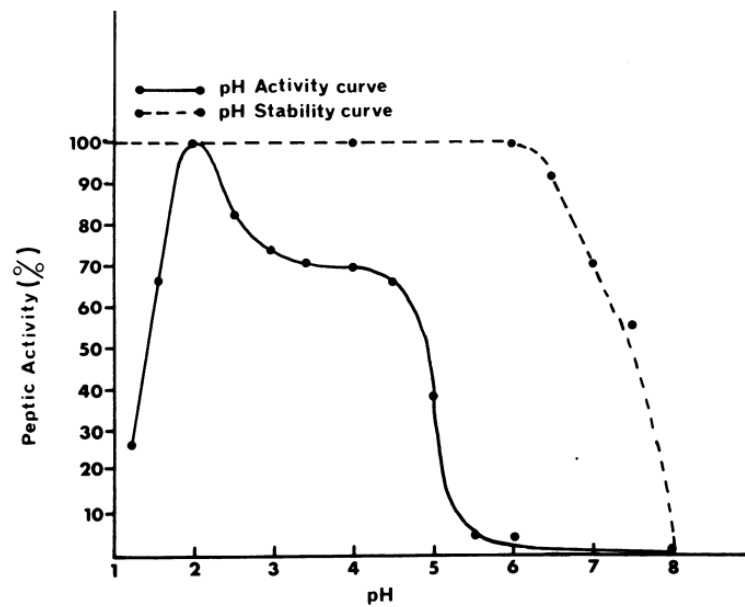
Figure 21   pH stability and activity curve of pepsin Piper et al, 1965 [165]

Interestingly, pepsin is denatured at pHs above neutral, whereas pepsinogen is not. It is thought that the N-terminal pro-peptide domain is essential for stability of the N-terminal domain at high pH. After activation of pepsinogen to active pepsin, while the C-terminal domain retains the capability of reversible folding after pH denaturation, the cleaved N-terminal domain will misfold upon return to a lower pH [166].

In addition to functioning as a digestive proteinase, pepsin also has a key role in the innate immune protection in conjunction with the acid environment of the stomach, creating a bacteriocidal barrier to protect the body from infection via the digestive tract. Pepsins are also an important biomarker of, and believed to be an aggressor in gastric reflux.

3.2 Alginate inhibition of Pepsin

In 2000, Sunderland *et al* showed alginates could inhibit pepsin activity by 52% *in vitro* [57]. Subsequent studies suggested that the levels of inhibition were related to the molecular weight of the alginates. Highest inhibition was shown to occur between molecular weights of 40,000 and 350,000, with a peak inhibition between 150,000 and 200,000 MW [167]. However, a subsequent study by Strugala *et al* 2005, found no correlation between levels of inhibition and molecular weight and suggested the inhibitory effect was related to alginate structure [7]. A catalogue of well characterised alginates were tested which showed inhibition levels in the range 39-81% reduction in activity by 5mg/ml alginate. In this study, significant correlations were shown between alginate structure and levels of inhibition, with high F[M] alginates tending to inhibit better than those high in F[G], although as can be seen from Figure 22, the data points are spread widely around the line of best fit.
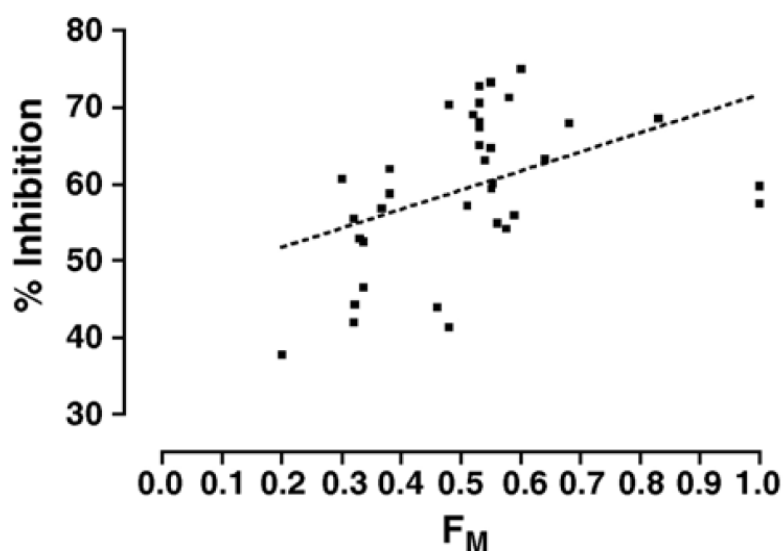
Figure 22   Scatter plot of correlation between percentage pepsin inhibition anf frequency of mannuronic acid residues Strugala *et al*, 2005 [7]

The Strugala et al study used a colourimetric assay of proteolytic activity originally described by Lin et al [168]. The assay is based on the detection of newly generated N-terminals from a succinylated albumin substrate. Trinitrobenzo Sulfonic Acid (TNBS) is used to detect N-terminals exposed through proteolysis by reacting and forming a coloured product. Colour development is measured spectrophotometrically and is proportional to the rate of cleavage. The assay was performed using pepsin and

substrate titrated to pH2.2 with HCl, however the alginates tested in the study were made up as aqueous solutions. Alginates have pK_a's in the range 3.38 to 3.65 and an aqueous alginate will have a pH of approximately 6-7 [169]. Addition of aqueous alginates to a reaction mixture will affect the pH and therefore affect the rate of enzyme activity. This chapter aims to investigate this issue.

Sunderland *et al* 2000, carried out some simple binding studies to investigate the mechanism of alginate inhibition [57]. An alginate-pepsin mixture was centrifuged and the pepsin content of the supernatent was assayed to determine if pepsin had bound to alginate and been pulled out of solution. These results showed levels of pepsin to be significantly lower after centrifugation with alginate. It was therefore suggested that alginate binding of pepsin was a possible mechanism of inhibition.

Alginates have been shown to inhibit the activity of pepsin, and have been utilised in the treatment of reflux. The alginate based anti-reflux agent Gaviscon has proved an effective treatment of GORD (Gastro-Oesophagul Reflux Disease) [57]. Reflux is the retrograde flow of gastric and/or duodenal contents into the oesophagus [170]. The primary mechanism of alginate based reflux suppressants was originally thought to be the viscous acid-gel formed by alginate upon contact with stomach acid. The alginate raft that is formed creates a physical barrier to the reflux by floating on the top of the stomach contents [171].

Acid alone will not cause experimental damage in animal models, and pepsin is thought to be a major aggressor in reflux [172]. In experimental animal mode is addition of pepsin results in reflux-like oesophagitis [173]. As stated previously, pepsin retains activity up to pH5.5, so still has potential to cause damage to the oesophagus in the refluxate. Alginate has been shown to inhibit pepsin *in vitro,* it is therefore thought that alginate inhibition of pepsin may be a secondary mechanism for the anti-reflux activity of alginate based agents [172].

3.2.1 Protein Digestion Kinetics

Postprandial protein utilisation and retention has been shown not just to depend upon protein quantity and amino acid composition, but also upon rate of protein digestion [174]. Dangin *et al* 2001, showed a relationship between the kinetics of protein digestion, and subsequent absorption, utilisation and retention. In a comparison of the

digestion and utilisation of 'slow and fast-digested' protein meals, 22 healthy male volunteers were fed slow and fast digested protein meals matched for weight and content. One group was fed either slow or fast digested casein (30g casein or 30g free Amino-Acids matching casein composition) and another group slow or fast whey protein (30g whey protein in one sitting or 30g whey protein in 13 feeds over 4 hours). All meals contained ^{13}C radio-labelled leucine, and blood and breath samples were taken over 300mins after feeding. Circulating plasma Leucine levels and radio-labelled $[^{13}C]CO_2$ expiration were measured.
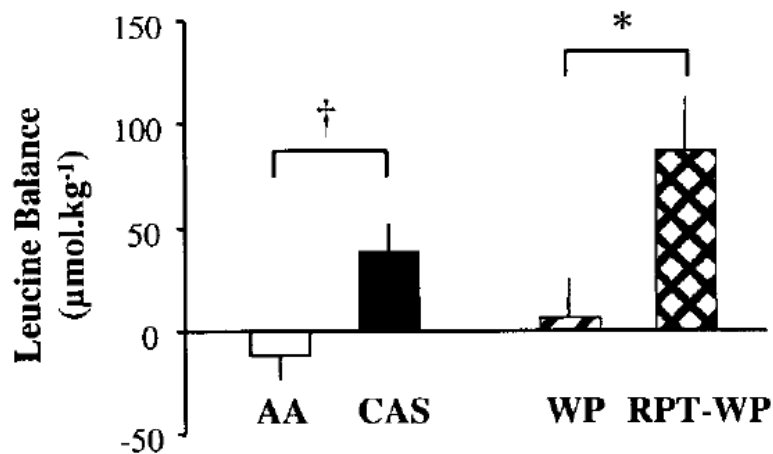
Figure 23   Postprandial leucine balance 7 hours after a meal. Protein digestion rates differed between AA and CAS mealsand between WP and RPT-WP meals, but amino acid profiles were identical. Taken from Dangin et al 2001 [174].

With both casein and whey protein, the fast digested meals showed rapid peaks in circulating leucine as would be expected, however these increases were transient and fell back to resting levels. Whereas with the slow digested protein, the increase in circulating leucine was much less pronounced, but was maintained through to the final measurement at 300min. Furthermore, the rapid peak in circulating amino acids was mirrored by a similar rapid increase in protein synthesis, as measured by NOLD (Non oxidative Leucine Disposal) which is thought to have stimulated protein synthesis. In the slow-digested protein meals, there was not a similar stimulation of the rate of protein synthesis. However, in both test cases, overall total postprandial leucine balance 420mins after feeding was higher in the patients who had been fed the slow-digested protein meals. From this data, Dangin *et al* 2001, calculated that there was an overall better rate of protein utilisation in the slow digested meals than the fast over a 7 hour period (Slow casein $0.78\pm0.04\mu mol\cdot kg^{-1}\cdot min^{-1}$, fast casein AA, 0.62 ± 0.06

μmol·kg^{-1}·min^{-1}; slow whey protein 0.80±0.07 μmol·kg^{-1}·min^{-1}, fast whey protein 0.66±0.03μmol·kg^{-1}·min^{-1})[174].

Therefore rate of protein digestion may be of consequence to the efficacy of protein supplementation in the diet. There is a variation in protein digestibility and utilisation which depends on protein structure, and the behaviour of different proteins in the gastrointestinal tract. Whey protein is much more rapidly digested than casein. This is thought to be due to the fact that casein coagulates in the acidic conditions of the stomach, and therefore the accessibility of the substrate to pepsin is greatly reduced, whereas whey protein remains soluble and is easily available for pepsin digestion in the stomach [175]. Furthermore, the coagulation of casein delays gastric emptying [176].

3.2.2   Proteinase Inhibition and Drug Delivery

Protoeolytic activity is also important in drug delivery, with luminal metabolism and first-pass intestinal metabolism affecting the bioavailability of orally delivered protein based drugs during pre-systemic metabolism [152]. Drug vehicles such as nanoparticles, microparticles and liposomes are commonly used to protect drugs from proteolytic degradation, but co-administration of enzyme inhibitors is becoming increasingly commonplace to reduce proteolytic degradation and increase the bioavailability of drugs. Langguth *et al* 1994, showed that inhibition of gastrointestinal enzymes increased the bioavailability of the pentapeptide drug Metkephamid 20-fold in a rat model [153].

Many peptide based drugs are administered parenterally in order to bypass pre-systemic metabolism. Insulin is a prime example of this. Yamamoto et al 1994, looked at the oral delivery of insulin, co-administered with the proteinase inhibitors both in animal models and in ex vivo tissue homogenates [177]. In the rat model, aprotinin, Soybean trypsin inhibitor, Na-glycocholate, camostat mesilate and bacitracin all promoted insulin absorption from the large intestine, with 20mM Bacitracin being the most effective. The degradation of insulin in mucosal homogenates was studied and it was found that Na-glycocholate, camostat mesilate and bacitracin were most effective in reducing insulin degradation.

3.3 *Aims*

The aim of this chapter therefore was to investigate the effects of bioactive compounds on pepsin activity. A library of bioactive alginates, was tested in high throughput assays to screen for regulatory effects, and structure-function relationships were investigated. Selected enzyme kinetics were carried out to attempt to elucidate the nature of any regulatory effects.

3.4 Experimental Section

3.4.1 Materials

All biopolymer samples tested were supplied by FMC Biopolymer and Technostics Ltd (Hull, UK). cBovine Serum albumin was purchased from VWR Jencons. Unless otherwise stated, all other chemicals and reagents were purchased from Sigma Aldrich (Poole, UK).

3.4.2 Equipment

A Biotek 96 well plate reader set at 340nm was used for spectrophotometric measurements (Elx808 Biotek, Bedfordshire, UK). An Autoblot microhybridization oven was used for temperature incubations at 37°C and 55°C (Bellco Glass Inc, Vineland, NJ). A Martini Mi150 pH meter was used for all pH measurements, (Milwaukee Instruments, Inc. NC, U.S.A.).

3.4.3 Preparation of Succinyl albumin

Succinyl albumin was prepared following the method described by Hutton et al 2003 [178]. 20g Bovine serum albumin (Fraction V) was dissolved in 200ml phosphate buffer pH7.5. 2.8g of Succinic anhydryde was slowly added while stirring, maintaining pH at 7.5 with dropwise addition of 2M Sodium hydroxide. This solution was then exhaustively dialysed against deionised water at 4°C and freeze dried.

Protein + Succinic Anhydride → Succinyl albumin + Water

$$COOH\text{-}[CH\text{-}R^1\text{-}NH\text{-}CO]_n\text{-}CH\text{-}R^2\text{-}NH_2 + CO\text{-}CH_2\text{-}CH_2\text{-}COO$$

$$\rightarrow$$

$$COOH\text{-}[CH\text{-}R^1\text{-}NH\text{-}CO]_n\text{-}CH\text{-}R^2\text{-}NHCO\text{-}CH_2\text{-}CH_2\text{-}COH$$
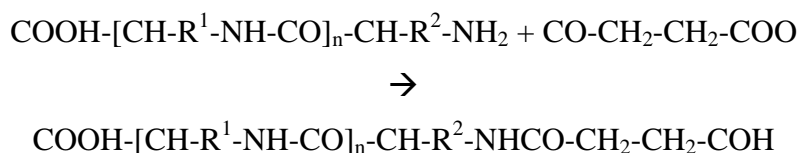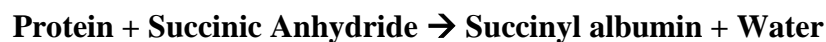
3.4.4   Preperation of TNBS

TNBS was prepared according to the method described by Hutton et al. 1.5ml of 1M 2,4,6-trinitrobenzenesulphonic acid (TNBS) from Fluka was mixed with 10mg of activated charcoal. Charcoal was removed by centrifugation at 5000rpm for 10 minutes. The resulting supernatant was then diluted to the required concentration.

3.4.5   Assay Principle

Activity of pepsin was measured using the N-terminal assay developed by Lin *et al* 1969 [168] and modified by Hutton *et al* 1986 [178]. Pepsin activity can be measured through the generation of new terminal amino groups formed during peptide hydrolysis. As pepsin cleaves peptides, new terminal carboxyl and amino groups are exposed. At pH7 and above primary amine groups are trinitrophenylated with Trinitrobenzosulphonic Acid (TNBS) to generate a yellow colouration which can be measured at 340nm. The trinitrophenylation reaction is shown below. A flow diagram of the N-Terminal methodology is shown in Figure 24.

TNBS Reaction With Protein:

Protein + TNBS $\rightarrow$ Trinitrophenylated Protein + Sulphorous acid

$COOH\text{-}[CH\text{-}R^1\text{-}NH\text{-}CO]_n\text{-}CH\text{-}R^2\text{-}NH_2 + C_6H_2(NO_2)_3SO_3H$
$\rightarrow$
$COOH\text{-}[CH\text{-}R^1\text{-}NH\text{-}CO]_n\text{-}CH\text{-}R^2\text{-}NHC_6H_2(NO_2)_3 + H_2SO_3$
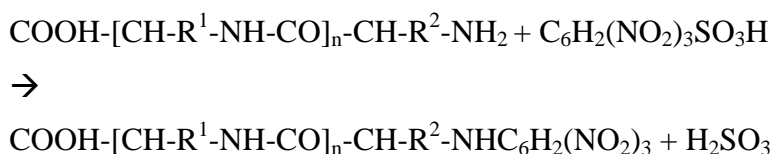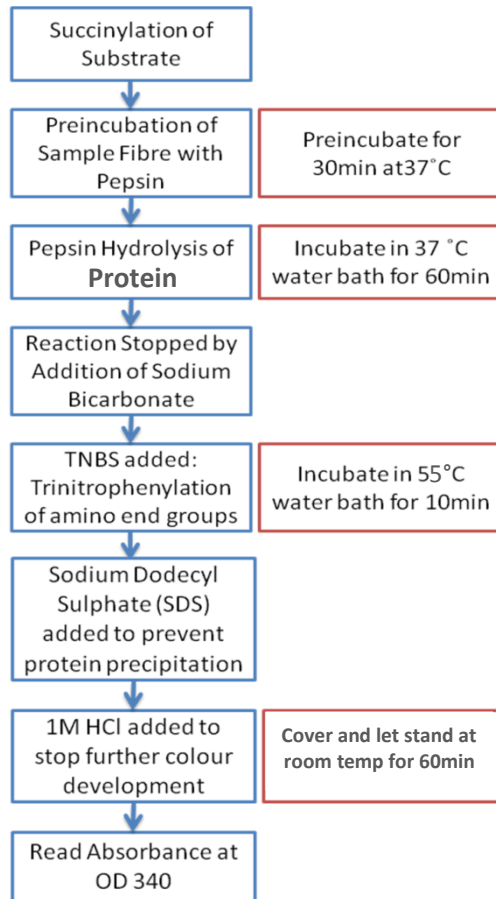
Figure 24   Schematic representation of Pepsin N-Terminal Reaction

3.4.6   Modification of Assay

Following the methodology of Strugala et al 2005, biopolymer samples are made up in deionised water before being mixed 1:1 with 5µg/ml pepsin (in 0.01M HCl at pH 2.2) to give concentrations of 2mg/ml and 2.5µg/ml respectively and samples were pre-incubated for 30 minutes at 37˚C. Substrate (8mg/ml) succinyl albumin was also made up in 0.01M HCl titrated to pH2.2 [7].

Alginates themselves are weakly acidic, and have a pH of ~5.75-7.25 in deionised water depending upon concentration as shown in Figure 25. Strugala et al 2005, argued that this did not have a significant effect on the overall pH of the reaction solution, raising the mean pH to 2.3 and having little effect on the rate on the reaction [7].
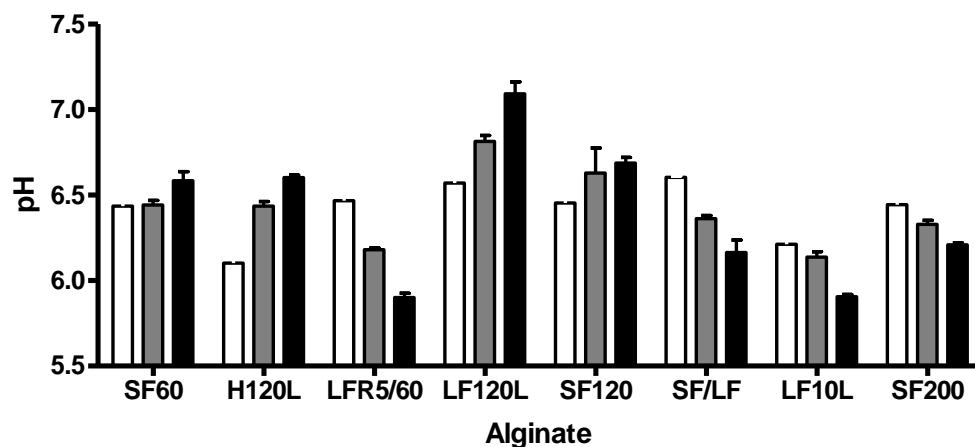
Figure 25   pH variation of aqueous alginates. ☐0.25mg/ml, ▦1mg/ml, ■4mg/ml.

Measurements in this lab however have shown a greater variation in pH of the reaction mixture than previously reported, especially at higher concentrations of biopolymer as shown in Figure 26. Furthermore, in the reaction solutions, addition of aqueous alginate causes a precipitant to form , as seen in Figure 27. This may be either the alginate or substrate coming out of solution or a precipitate formed through interaction between the two.
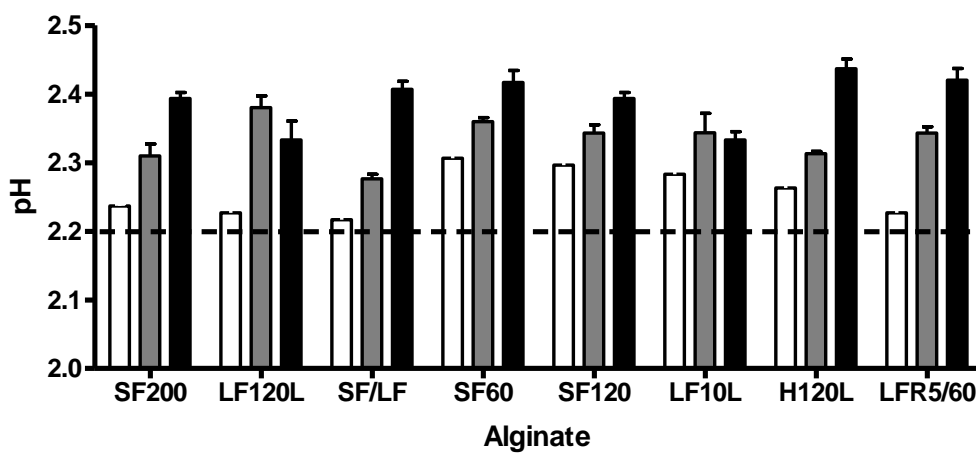
Figure 26   pH variation of N-terminal reaction mixture with addition of aqueous alginate. ☐0.25mg/ml, ▦1mg/ml, ■ 4mg/ml.
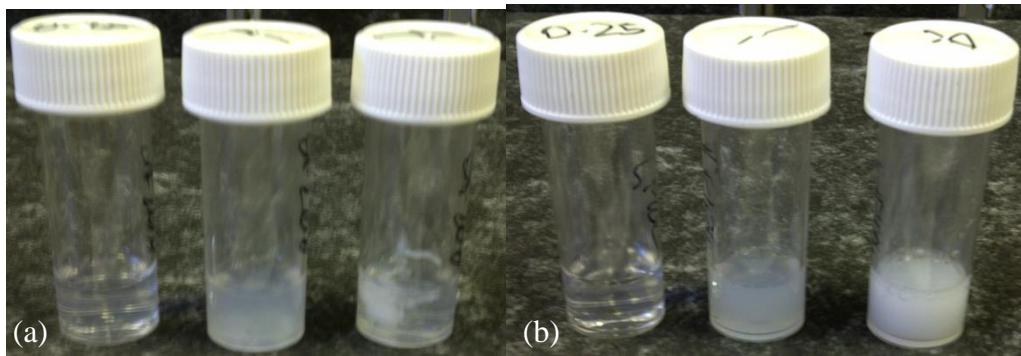
Figure 27   Picture of reaction mixture of N-terminal assay with aqueous alginates. (a) SF200 alginate - 0.25mg/ml, 1mg/ml and 4mg/ml from left to right. (b) LF10L alginate - 0.25mg/ml, 1mg/ml and 4mg/ml from left to right.

3.4.7   Adaptation of methodology with orthophosphate/phosphoric acid buffer

A variation of 0.2 units of pH would have significant effects on the rate of reaction reaction. Variations in pH could affect this assay in two specific ways: firstly pepsin activity is pH dependent, and moving away from the optimum pH would lower pepsin activity; secondly succinyl albumin substrate is soluble only within a certain pH range and alteration of pH may cause succinyl albumin to come out of solution, which may cause a reduction in substrate digestion.

In the Strugala methodology 0.01M HCl acid (pH2.2) is used as a diluent for other solutes in the assay (i.e. pepsin and succinyl albumin) [7]. However 0.01M HCl is ineffective at buffering pectins, and will not take alginates into solution. This is presumably why Strugala et al chose to work with aqueous alginates.

Finding a buffering system for the N-terminal assay presented a number of difficulties. The N-terminal Assay is pH dependent and requires a number of pH changes and running the assay in a buffer may affect the pH changes required for trinitrophenylation and colour development. Furthermore, succinyl albumin must be taken fully into solution at pH 2.2 and dietary fibres, particularly alginates, can be difficult to get into solution at low pH.

A number of buffer systems were investigated and the method had to be adjusted slightly to accommodate the buffer.

Substrate (8mg/ml) and pepsin (5μg/ml) were made up in a 0.05M potassium dihydrogen orthophosphate/phosphoric acid buffer pH2.2. All fibres were made up at 4mg/ml in buffer. Alginates added to buffer at pH2.2 will not go into solution. The alginates were therefore made up in the basic component of the buffer initially and then mixed with the acidic component of the buffer. As can be seen from Figure 28 that in this system the final reaction mixture is buffered within 0.05 units of pH.

The methodology of Lin *et al* was followed with 0.05% TNBS, 10% (w/v) sodium bicarbonate, 10% (w/v) SDS (Sodium Dodecyl Sulphate) and 1M HCl. Note that the sodium bicarbonate concentration has been raised to accommodate for the effect of the buffer.
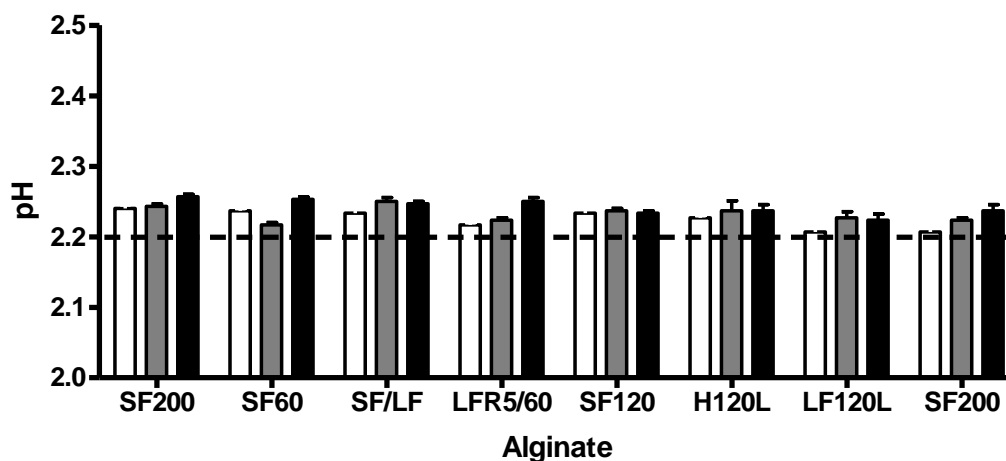
Figure 28   pH variation of reaction solution with addition of buffered alginate. □ 0.25mg/ml, ▦ 1mg/ml, ■ 4mg/ml.
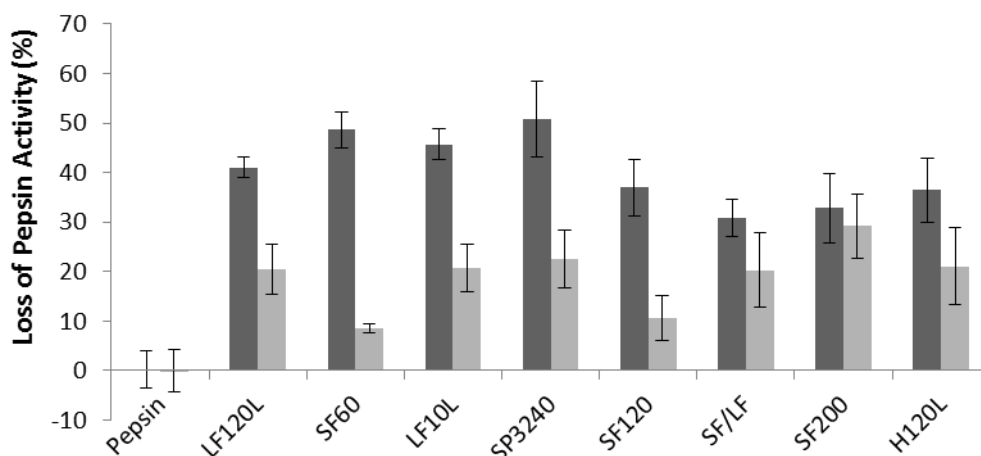
Figure 29   Comparison of alginate mediated pepsin inhibition in buffered and unbuffered systems.
■ Unbuffered system ▨ Buffered system.

Alginate inhibition of pepsin was compared in a buffered and unbuffered system (Figure 29). These results indicate that some of the inhibition effect observed were due to changes in the pH of the reaction mixture and that a buffered N-Terminal Assay system offers a more robust method of analysis of pepsin inhibition.

3.4.8   Scaling down to 96 well microplate

The assay was scaled down to a 96 well microplate from the original methodology, modifications were made to concentrations and volumes of substrates and reagents. Buffering of the assay was shown not to affect the validity of the assay.

30µl of buffer sample was pre-incubated with pepsin at a range of concentrations (2.5-17.5µg/ml) for 30 minutes. At T_0 50µl of succinyl albumin solution (10mg/ml) was added and the plate was incubated for 30min at 37˚C. At T_{30} 50µl NaHCO3 (10% w/v) and 50µl TNBS at a range of concentrations (0-5%v/v) was added and the plate incubated at 55˚C for 15 minutes. At T_{45} 50ul SDS (10%) and 50ul 1M HCl were added. The plate was then left to stand for 15 minutes until effervesce had stopped.

Absorbance was then measured at 340nm on the Biotek plate reader.

Figure 30 shows the assay tested at a range of pepsin and TNBS concentrations in order to work out optimal reaction conditions. It was determined from this data that a concentration of pepsin of 10µg/ml and TNBS of 2µl/ml would give sufficient colour development to be reliably detected at 340nm.
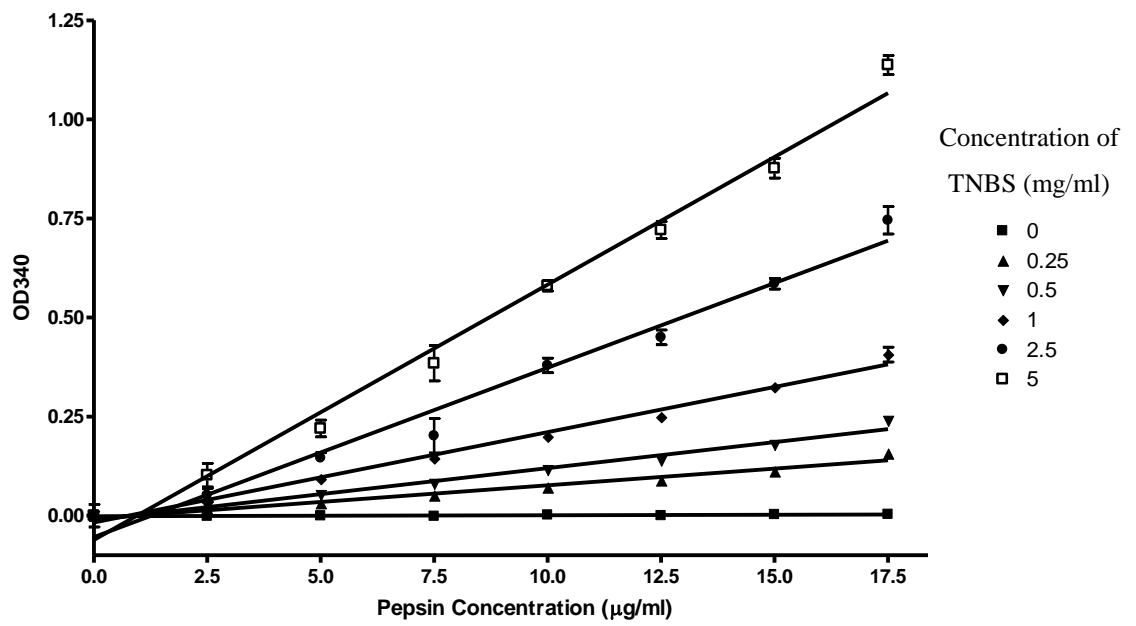
Figure 30   Colour development with Pepsin N-Terminal assay at varying pepsin and TNBS concentrations.

3.5   96-Well Plate N-Terminal Method

3.5.1   Preperation of Solutions

For high-throughput analysis, biopolymer samples were prepared at 10mg/ml in the acidic side of the buffer (5.7988ml Phosphoric Acid in 500ml) and then diluted at a 1:1 ratio with the basic side of the buffer (32.646g KH_2PO_4 in 500ml). 10mg/ml succinyl albumin was prepared in 0.05mM phosphate buffer and the solution was to pH 2.5.

Trinitrobenzosulfonic acid (TNBS) was prepared at 2µl/ml in deionised water.

10µg/ml pepsin was prepared 10 minutes prior to T0.

3.5.2   Method

30µl fibre sample was pre-incubated with 50µl Succinyl albumin substrate for 60 minutes on a shaker. At T_0 30µl pepsin solution or buffer blank was added as appropriate and the plate was incubated for 30min at 37˚C (Figure 31).

After 30 minutes, 50µl sodium bicarbonate and 50µl TNBS was added, mixed and the plate was incubated for 15 minutes in Autoblot Microhybridisation oven at 55˚C.

At T_{45}, 50µl SDS and 50µl 1M hydrochloric acid were added and the plate was left to stant until all wells had stopped effervescing, and samples were read at 340nm.

To calculate percentage pepsin inhibition the following formula was used:

$$\text{Percentage pepsin inhibition} = \frac{Polymer\ Sample - Sample\ Control}{Pepsin\ Control - Background\ Control} \times 100$$

All data is presented as the mean of at least three repeats with error bars as standard deviation.

3.5.3 Plating – Higher Throughput Microplate Assay

| | Blank | Pepsin Control | Sample A | | | Sample B | | | Sample C | | | Blank |
| | | | 5 mg/ml | 2.5 mg/ml | 1.25 mg/ml | 5 mg/ml | 2.5 mg/ml | 1.25 mg/ml | 5 mg/ml | 2.5 mg/ml | 1.25 mg/ml | |
	1	2	3	4	5	3	4	5	3	4	5	12
A	60ul Buffer	30ul Buffer 30ul Pepsin	30ul Pepsin 30ul Sample	30ul Pepsin 30ul Sample	30ul Pepsin 30ul Sample	30ul Pepsin 30ul Sample	30ul Pepsin 30ul Sample	30ul Pepsin 30ul Sample	30ul Pepsin 30ul Sample	30ul Pepsin 30ul Sample	30ul Pepsin 30ul Sample	60ul Buffer
B	60ul Buffer	30ul Buffer 30ul Pepsin	30ul Pepsin 30ul Sample	30ul Pepsin 30ul Sample	30ul Pepsin 30ul Sample	30ul Pepsin 30ul Sample	30ul Pepsin 30ul Sample	30ul Pepsin 30ul Sample	30ul Pepsin 30ul Sample	30ul Pepsin 30ul Sample	30ul Pepsin 30ul Sample	60ul Buffer
C	60ul Buffer	30ul Buffer 30ul Pepsin	30ul Pepsin 30ul Sample	30ul Pepsin 30ul Sample	30ul Pepsin 30ul Sample	30ul Pepsin 30ul Sample	30ul Pepsin 30ul Sample	30ul Pepsin 30ul Sample	30ul Pepsin 30ul Sample	30ul Pepsin 30ul Sample	30ul Pepsin 30ul Sample	60ul Buffer
D	60ul Buffer	60ul Buffer	30ul Buffer 30ul Sample	30ul Buffer 30ul Sample	30ul Buffer 30ul Sample	30ul Buffer 30ul Sample	30ul Buffer 30ul Sample	30ul Buffer 30ul Sample	30ul Buffer 30ul Sample	30ul Buffer 30ul Sample	30ul Buffer 30ul Sample	60ul Buffer
E	60ul Buffer	60ul Buffer	30ul Buffer 30ul Sample	30ul Buffer 30ul Sample	30ul Buffer 30ul Sample	30ul Buffer 30ul Sample	30ul Buffer 30ul Sample	30ul Buffer 30ul Sample	30ul Buffer 30ul Sample	30ul Buffer 30ul Sample	30ul Buffer 30ul Sample	60ul Buffer
F												
G												
H												

Figure 31   Plating layout for Pepsin N-Terminal microplate assay.

3.5.4 Kinetic assay of Pepsin Activity

The kinetics of dietary fibre interactions with pepsin was measured using a modification of the 96 well-plate N-Terminal method previously described. Trinitrobenzosulfonic Acid was prepared fresh at 2µl/ml in deionised water.

Succinyl albumin substrate was prepared fresh at 25mg/ml in Phosphate Buffer (Phosphoric Acid (30mM)/Monopotassium Phosphate (47mM)) and 50µl plated out as below. Substrate dilutions were prepared from a stock of 25mg/ml Succinyl Albumin and plated out as shown in Figure 32, including a control and blank lane both at 10mg/ml succinyl albumin. 200µl was added into each well so that there would be sufficient substrate for 3 plates to be run in triplicate.

Blank Lane	Control Lane	Substrate Dilutions									
10	10	25	20	15	10	5	2.5	1.25	0.625	0.3125	0
10	10	25	20	15	10	5	2.5	1.25	0.625	0.3125	0
10	10	25	20	15	10	5	2.5	1.25	0.625	0.3125	0

Table 10   Substrate dilutions for Pepsin N-Terminal Kinetic assay.

In sample plates 30µl of sample (4mg/ml) was pre-incubated with 30µl pepsin (10µg/ml) for 15 minutes at 37˚C to give sample concentrations of 2mg/ml and 5µg/ml respectively.

At T_0 50µl of of substrate was added into the appropriate wells and incubated for 30 minutes. After 30 minutes 50µl $NaHCO_3$ and 50µl of TNBS was added and the temperature raised to 55°C for colour development.

After 15 minutes at 55˚C, 50µl SDS and 50µl HCl was then added and the plate was left to stand until effervescence had stopped. Absorbance was then read at 340nm.

All samples tested were compared to a control pepsin digestion of 10mg/ml Succinyl albumin. The absorbance reading for the control lane at 30minutes was taken as 100%, and all test samples were converted to fractions of this 100% absorbance reading. These data was then converted into velocities. This standardisation was necessary to account for variations in backround absorbance of succinyl albumin substrate. Because of this

the raw absorbance data would not give an accurate comparison between replicates. However, by standardising to an internal control before conversion to a velocity, comparisons could be made between replicates. These percentage values were then divided to give percentage change per minute.

$$\text{Percentage Change in OD per Minute (\%/min)} = \frac{\frac{Polymer\ Sample - Sample\ Control}{Pepsin\ Control - Background\ Control} \times 100}{Time}$$

3.5.5 Plating Kinetic assay

	Blank Lane	Control Lane 10mg/ml	Substrate Dilutions 25mg/ml	Substrate Dilutions 20mg/ml	Substrate Dilutions 15mg/ml	Substrate Dilutions 10mg/ml	Substrate Dilutions 5mg/ml	Substrate Dilutions 2.5mg/ml	Substrate Dilutions 1.25mg/ml	Substrate Dilutions 0.625mg/ml	Substrate Dilutions 0.3125mg/ml	Substrate Dilutions 0mg/ml
A												
B	60ul Buffer	30ul Sample 30ul Pepsin	30ul Sample 30ul Pepsin	30ul Sample 30ul Pepsin	30ul Sample 30ul Pepsin	30ul Sample 30ul Pepsin	30ul Sample 30ul Pepsin	30ul Sample 30ul Pepsin	30ul Sample 30ul Pepsin	30ul Sample 30ul Pepsin	30ul Sample 30ul Pepsin	30ul Sample 30ul Pepsin
C	60ul Buffer	30ul Sample 30ul Pepsin	30ul Sample 30ul Pepsin	30ul Sample 30ul Pepsin	30ul Sample 30ul Pepsin	30ul Sample 30ul Pepsin	30ul Sample 30ul Pepsin	30ul Sample 30ul Pepsin	30ul Sample 30ul Pepsin	30ul Sample 30ul Pepsin	30ul Sample 30ul Pepsin	30ul Sample 30ul Pepsin
D	60ul Buffer	60ul Sample	30ul Sample 30ul Buffer	30ul Sample 30ul Buffer	30ul Sample 30ul Buffer	30ul Sample 30ul Buffer	30ul Sample 30ul Buffer	30ul Sample 30ul Buffer	30ul Sample 30ul Buffer	30ul Sample 30ul Buffer	30ul Sample 30ul Buffer	30ul Sample 30ul Buffer
E												
F												
G												
H												

Figure 32   Plating layout for Pepsin N-Terminal Kinetic microplate assay.

3.6   Alginate and pepsin

3.6.1   Higher-throughput assays

As described in the experimental section, pepsin activity in the presence of dietary biopolymers was measured using a 96 well microplate adaptation of the N-Terminal Proteolysis assay. Succinylated bovine serum albumin was used as the substrate, cleavage of polypeptides generates new terminal amino groups, which are trinitrophenylated above pH7 at 50°C. Trinitrophenylation causes a yellow-orange spectrophotometrically quantifiable coloration, and pepsin activity was measured as an increase in optical density at 340nm.

Colour development was measured in the presence of dietary bioplolymers and pepsin inhibition was calculated as a percentage change in optical density as compared to uninhibited pepsin control. The assay system was validated using pentosan polysulphate (SP54) as a positive inhibition control. SP54 is a heparin analogue with a molecular weight of 4000-6000 Daltons and like heparin is a highly sulphated polysaccharide. Heparin and other highly sulphated polysaccharides are known to inhibit pepsin activity [179, 180]. The structure of a Pentosan polysulphate subunit is shown in Figure 33 below.
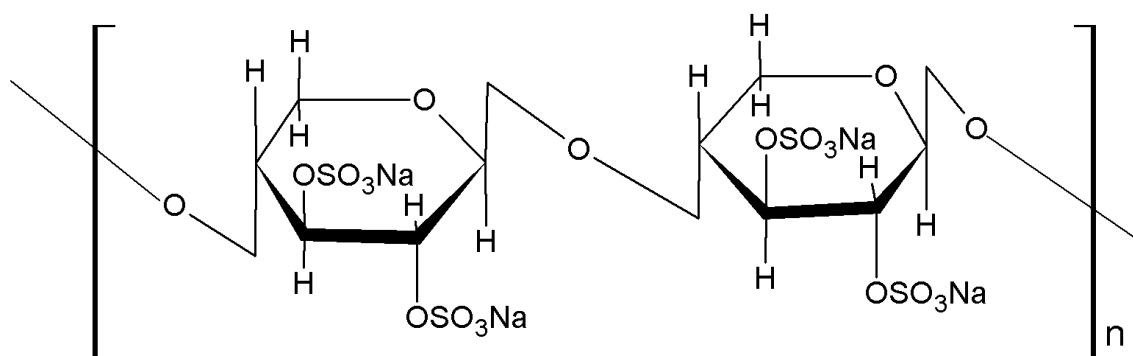
Figure 33   Molecular Structure of Pentosan Polysulphate SP54. Taken from Balaji *et al* 2012 [181]

Maximum inhibition with SP54 was achieved at a concentration of 5mg/ml, reducing activity to 24.5% (±11.2 SD) of control pepsin activity Figure 34, an inhibition of just over 75%.
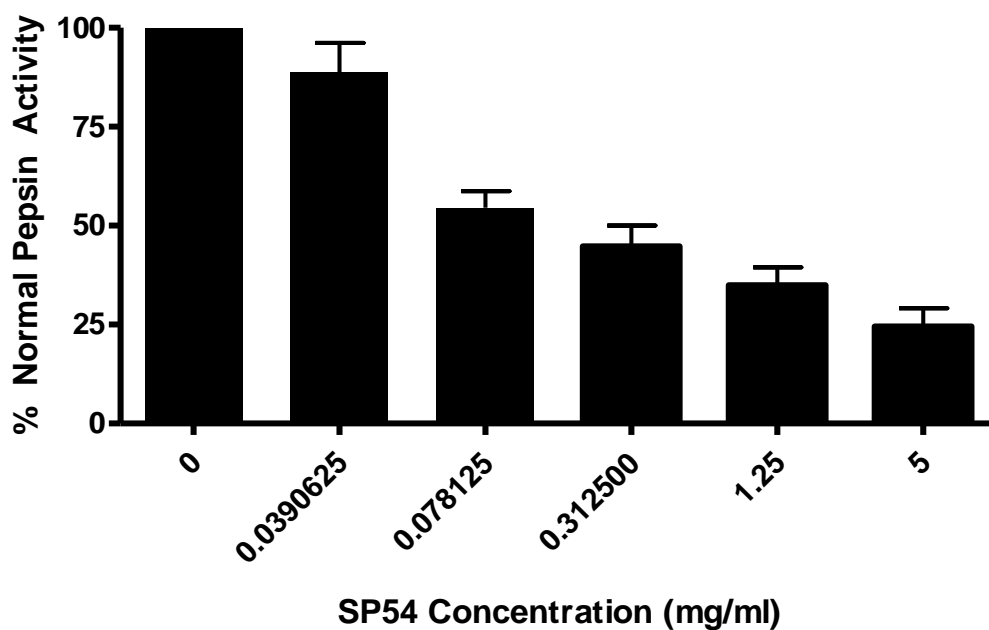
Figure 34 - Concentration dependent inhibition of pepsin in the presence of pentosan polysulphate (SP54). Activity is shown as a percentage of control pepsin activity at a range of concentrations (0-5 mg/ml). All samples were tested in triplicate (n=3) with error bars showing standard deviation.

The catalogue of eighteen alginates provided by Technostics Ltd and FMC biopolymer was tested in the pepsin activity assay. All alginate samples were tested at three concentrations; 5, 2.5 and 1.25mg/ml. This gave concentrations in the reaction mixture of 1.36, 0.68 and 0.34mg/ml respectively. All alginates tested showed the ability to inhibit pepsin activity at the highest concentration (5mg/ml).

In Figure 35 the results for all eighteen alginates have been collated. Taken together, a clear and significant dose response effect can be seen. Average pepsin activity was reduced by 6.8% $\pm$ 6.1 at 1.25mg/ml, by 18.3% $\pm$ 7.5 at 2.5mg/ml and by 31.9% $\pm$ 6.1 at 5mg/ml.
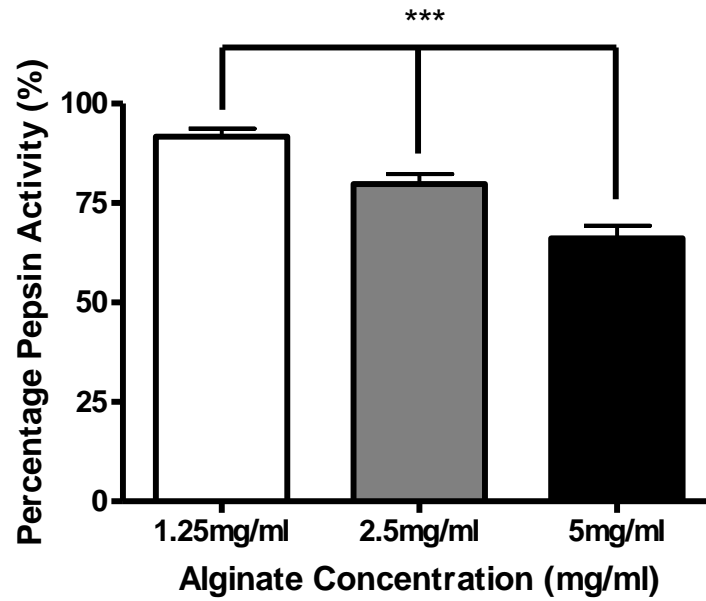
Figure 35- Concentration dependent inhibition of pepsin in the presence of sample alginates. Activity is shown as a percentage of control pepsin activity at three concentrations, ☐ 1.25mg/ml ▨ 2.5mg/ml, ■5mg/ml. All samples were tested in triplicate (n=3) with error bars showing standard deviation.

Figure 35 demonstrates that alginate per se shows a dose dependent inhibition effect on pepsin activity. However, alginates have a high degree of structural and functional variation depending on their guluronic:mannuronic acid content and as such levels of pepsin inhibition varied between alginate biopolymer samples. As will be discussed later, this is related directly to the structure of the alginates.
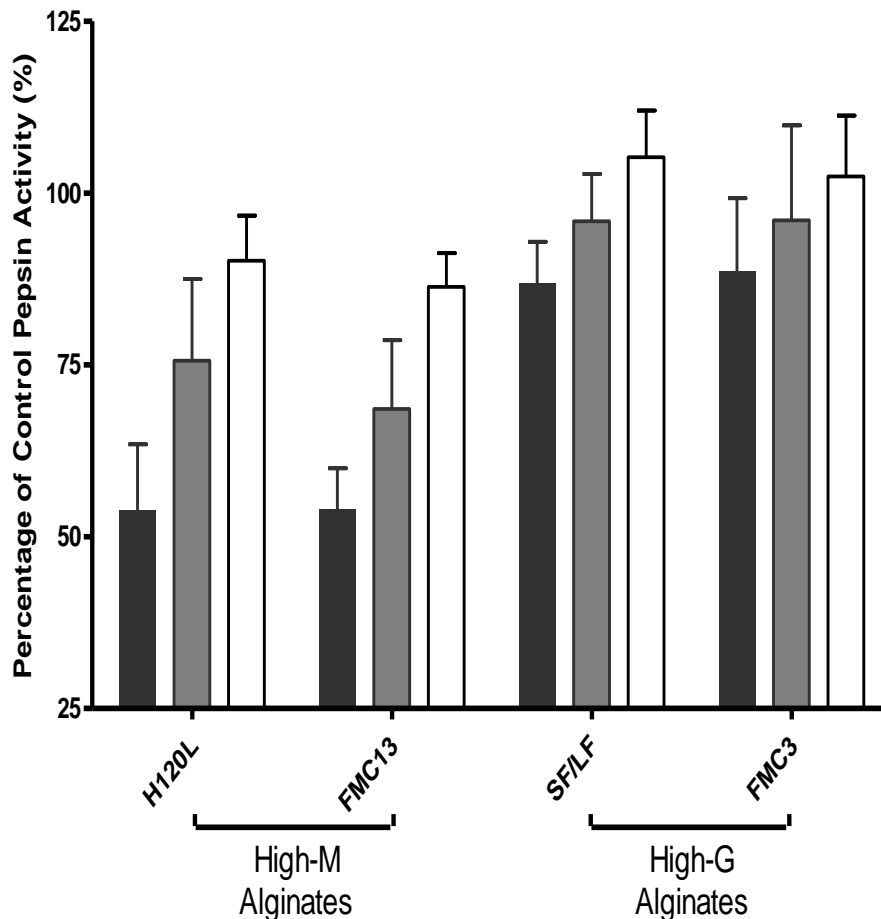
Figure 36- Concentration dependent inhibition of pepsin in the presence of 4 examplar sample alginates. Activity is shown as a percentage of control pepsin activity at three concentrations, ☐ 1.25mg/ml ▨ 2.5mg/ml, ■ 5mg/ml. All samples were tested in triplicate (n=3) with error bars showing standard deviation.

Figure 36 shows the data from 4 examplar alginates. A dose response effect can be seen in the inhibition of pepsin activity with the degree of inhibition of pepsin activity increasing with alginate concentration. H120L and FMC13 are alginates low in G-residues (F[G]= 0.45 and 0.34 respectively) and high in M residues and show a higher degree of inhibition than SF/LF and FMC 3 which are high in G residues (F[G]= 0.66 and 0.68 respectively) and low in M-residues.

The distinct difference in level of pepsin inhibition and the relation to alginate structure is further demonstrated by comparing the 8 alginates provided by Technostics Ltd. These 8 brown seaweed alginates were extracted from two separate species of seaweed; four from High-G Lamanaria, and four from High-M Lessonia (Fig 5). Alginates from Low-G, High-M lessonia inhibited to a significantly higher degree than Low-M High G Lamanaria (Two-Way Anova, p<0.0001). The full catalogue of alginates was tested to

see if this was just a species effect, or if the negative correlation between F[G] and pepsin inhibition was present across the range of F[G].
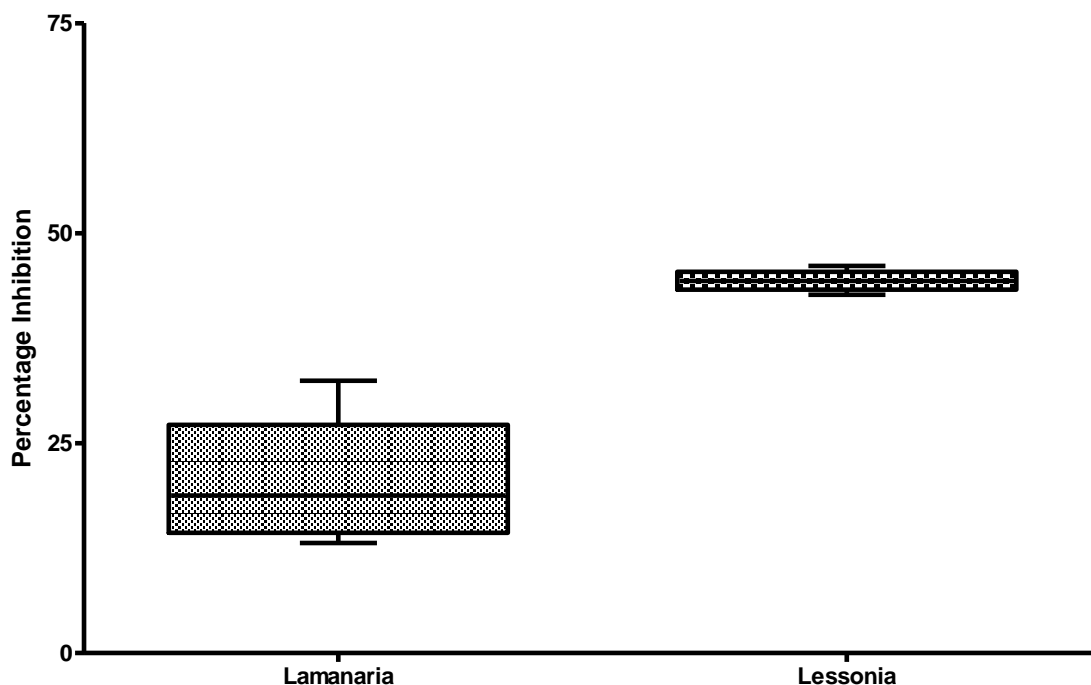
Figure 37 – Comparison of pepsin inhibition levels between high-G Lamanaria alginate and high-M Lessonia Alginate. The boxplots show four High-G alginate samples from Lamanaria and four High-M from lessonia. All samples were done with 6 repeats. The plot shows significantly higher inhibition levels with the Lessonia alginates.

The full results for the eighteen alginate samples tested can be seen in Figure 38, full structural data for all samples can be found in Table 9. The strongest inhibitor at 5mg/ml was H120L which has an F[G] of 0.45 and reduced pepsin activity to 53.9% (±9.5SD) of control activity. The weakest inhibitor at 5mg/ml was FMC3 which has an FG of 0.68 and reduced pepsin activity to 88.6% (±10.6%SD) of control activity.
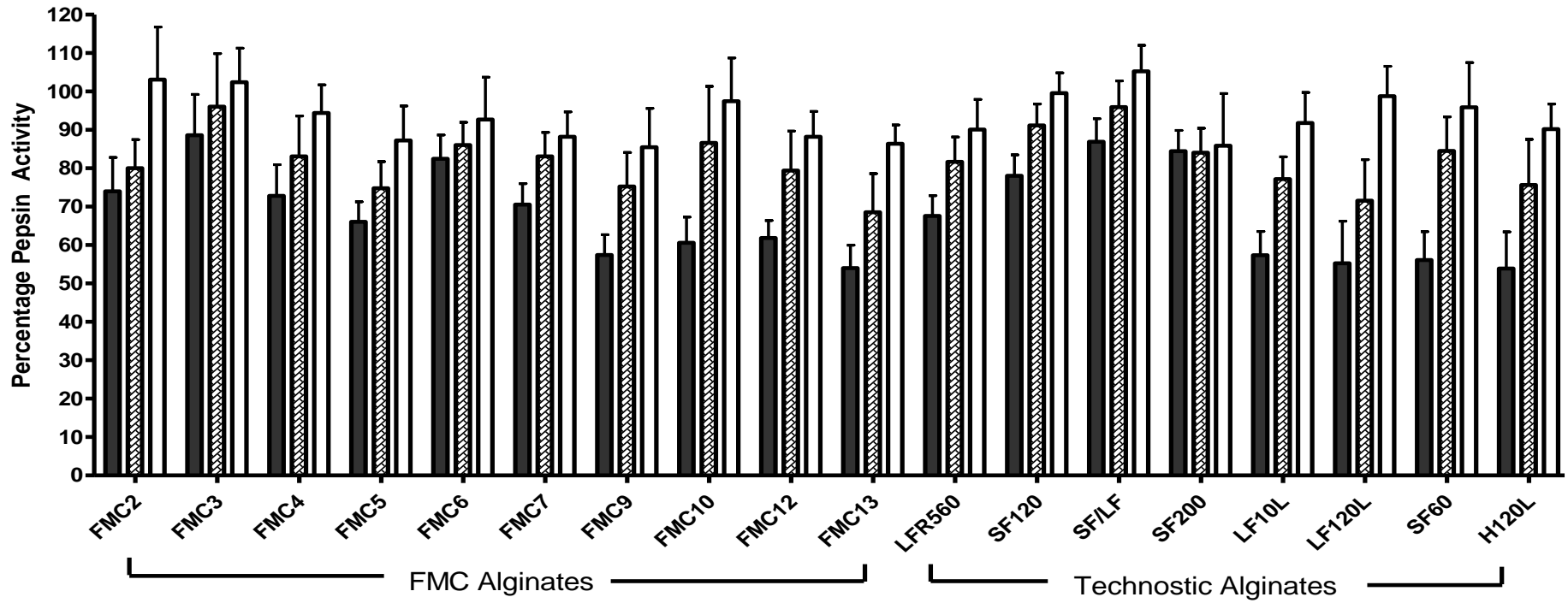
Figure 38- Concentration dependent inhibition of pepsin in the presence of sample alginates. Activity is shown as a percentage of control pepsin activity at three concentrations of alginate, ☐ 1.25mg/ml ▨ 2.5mg/ml, ■ 5mg/ml.. All samples were tested in triplicate (n=3) with error bars showing standard deviation.

All alginates showed significant inhibitory activity against pepsin at the highest concentration (5mg/ml), and all samples apart from FMC3 and FMC6 showed significant dose response effects. The effects were most apparent when comparing inhibition at 5 and 1.25mg/ml.

Using the data from Figure 38 it was therefore possible to correlate percentage inhibition of pepsin activity against alginate F[G] and test the statistical significance using Spearman's Rank Correlation.
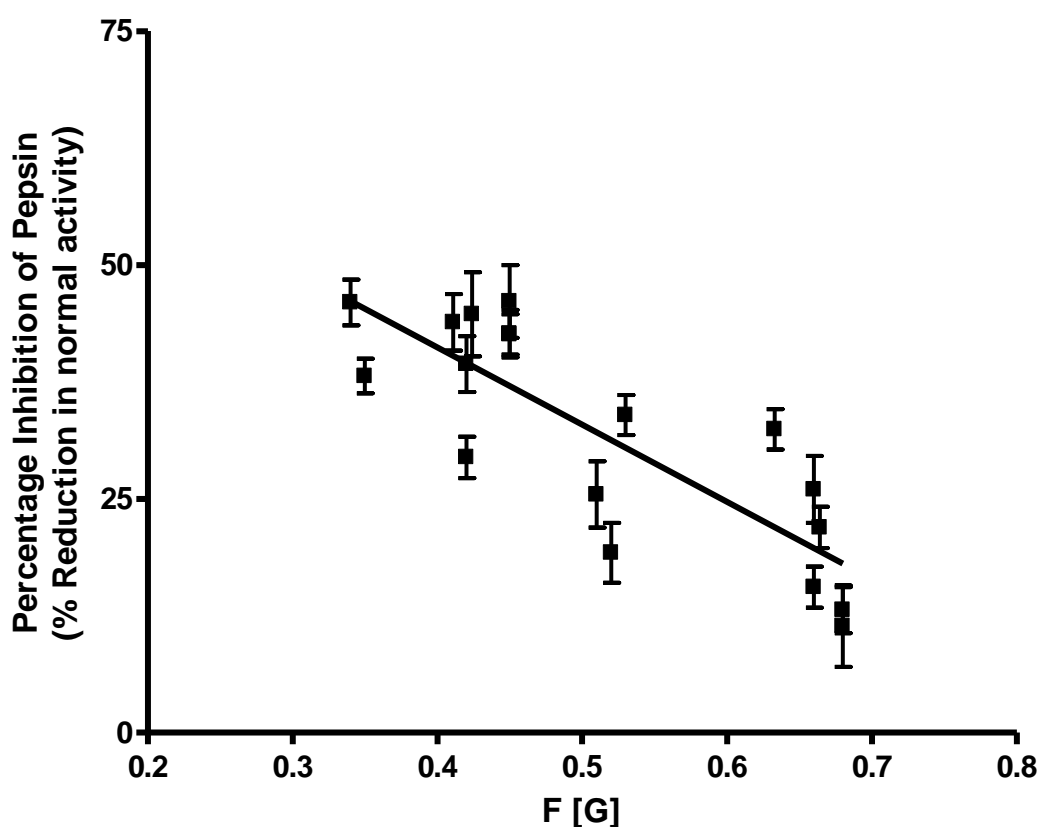
Figure 39 – Correlation of alginate G-residue frequency (F[G]) and level of pepsin inhibition with 5mg/ml alginate. Pepsin activity is shown as a percentage of control pepsin activity. The error bars show the standard deviation of 6 replicates (n=6). The line of best fit indicates a negative correlation which is significant with a Spearman r value of -0.7789 and a p value of 0.0001.

A significant negative correlation between pepsin inhibition and alginate F[G] was found at both 5mg/ml and 2.5mg/ml (Figure 39 & Figure 40). No significant correlation was found at 1.25mg/ml (Figure 41). This indicates that at both 5 and 2.5mg/ml, an increasing proportion of mannuronic acid residues, and decreasing proportion of guluronic acid residues yielded higher levels of pepsin inhibition. No significant outliers were observed and all eighteen samples generally followed this trend.

The significant negative correlation between alginate mediated pepsin inhibition and F[G] was also observed at 2.5mg/ml alginate, with a Spearman correlation coefficient of -0.4878 with a p-value of 0.04 (Figure 40). Levels of pepsin inhibition were significantly lower at 2.5mg/ml alginate than at 5mg/ml, with the highest level of pepsin inhibition at 2.5mg/ml being just a 31.4% ±10.03 reduction in pepsin activity and the correlation between structure and inhibition was not as strong as at the higher concentration, but still significant (p=0.040).
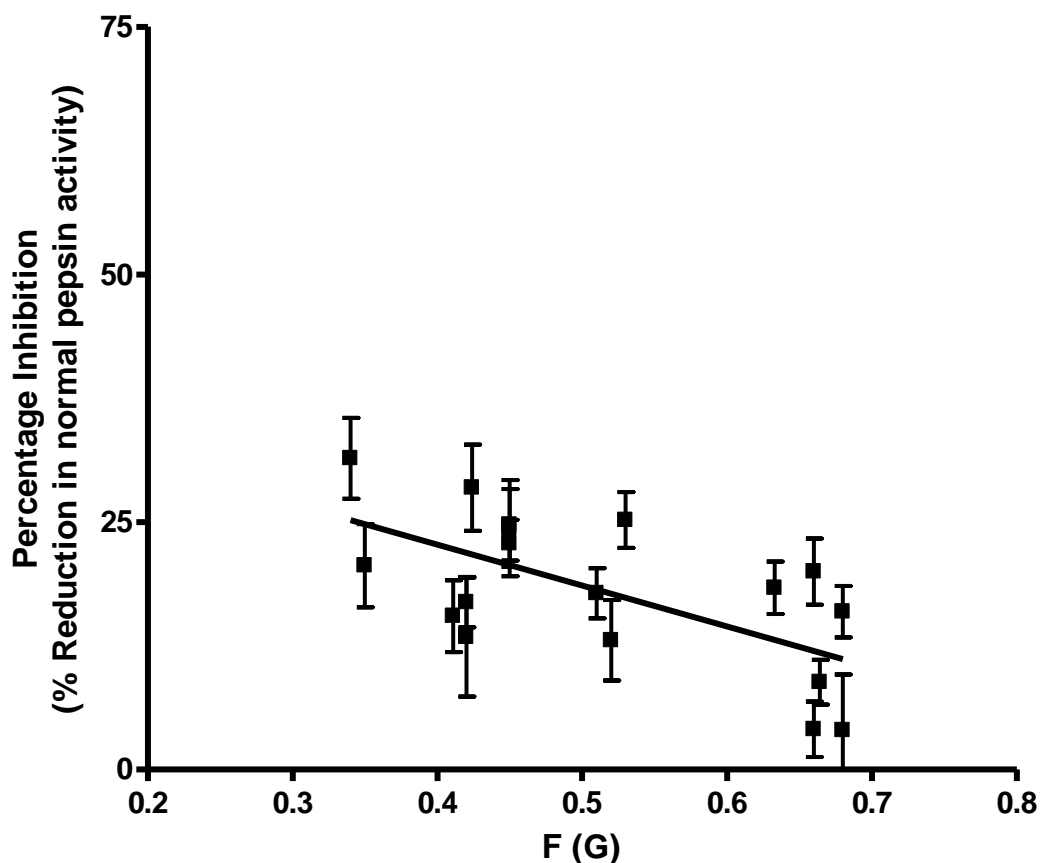
Figure 40– Correlation of alginate G-residue frequency (F[G]) and level of pepsin inhibition with 2.5mg/ml alginate. Pepsin activity is shown as a percentage of control pepsin activity. The error bars show the standard deviation of 6 replicates (n=6). The line of best fit indicates a negative correlation which is significant with a Spearman r value of -0.4878 and a p value of 0.04.

At a 1.25mg/ml concentration of alginate, pepsin activity levels varied from a 14.5% (±10.2%) inhibition of pepsin activity to a 5.3% (±6.8%) increase in activity as shown in Figure 41. Furthermore, no significant correlation was observed at 1.25mg/ml of alginate between frequency of G-residues and pepsin inhibition (Figure 41).
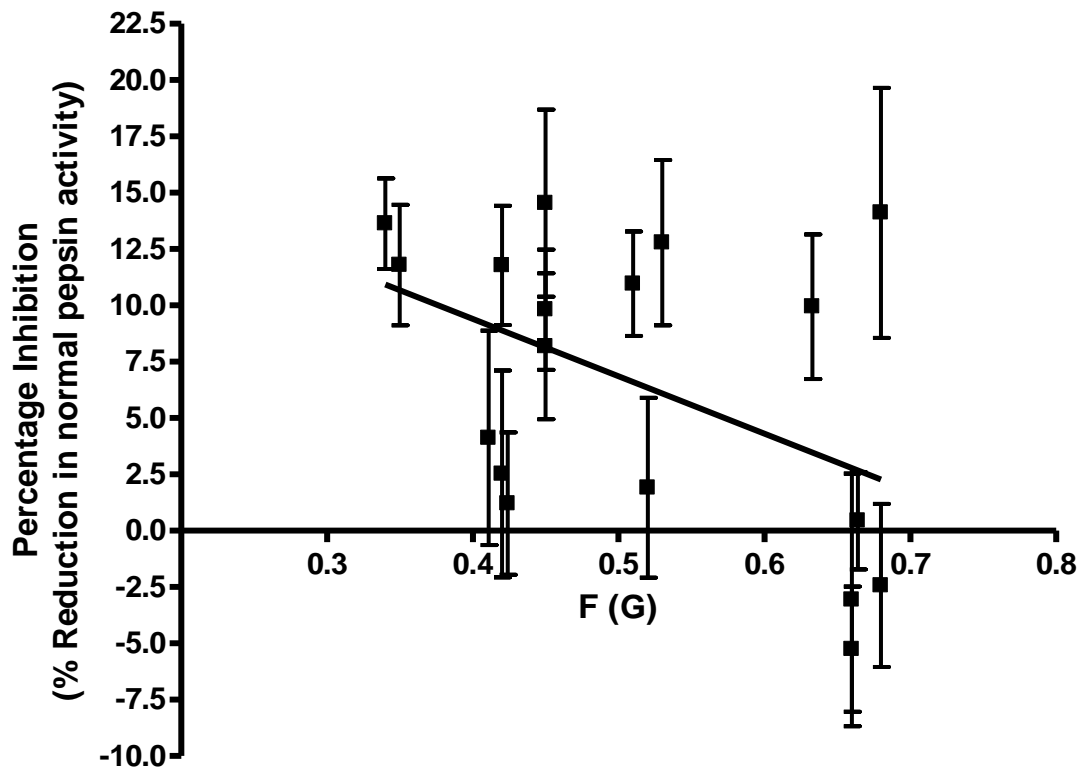
Figure 41 – Correlation of alginate G-residue frequency (F[G]) and level of pepsin inhibition with 1.25mg/ml alginate. Pepsin activity is shown as a percentage of control pepsin activity. The error bars show the standard deviation of 6 replicates (n=6). The line of best fit indicates a non significant negative trend with a Spearman r value of -0.3604 and a p value of 0.1417.

Figure 42 shows the plot for the Frequency of mannuronic acid residues against levels of pepsin inhibition at 5mg/ml alginate. Mannuronic and guluronic acid frequencies are inversely related to each other; as one increases, the other necessarily decreases and visa versa. There is a significant positive correlation between inhibition of pepsin and alginate F[M].
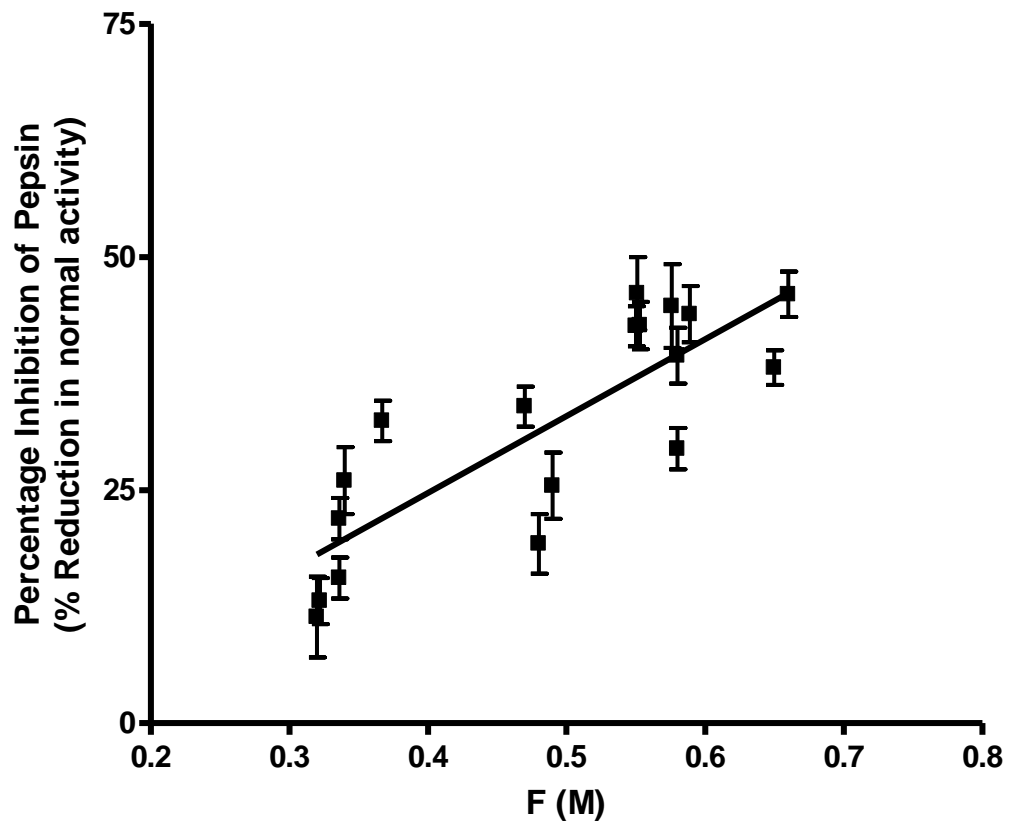
Figure 42 – Correlation of alginate M-residue frequency (F[M]) and level of pepsin inhibition with 5mg/ml alginate. Pepsin activity is shown as a percentage of control pepsin activity. The error bars show the standard deviation of 6 replicates (n=6). The line of best fit indicates a positive correlation which is significant with a Spearman r value of 0.7862 and a p value of 0.0001.

The structure and biophysical properties of alginates are not just dictated by F[G] and F[M] frequency, but also by the arrangement of contiguous blocks of M and G residues as discussed in the introduction. The full characteristics of the alginates are shown in Table 9, Section 2.5.

All alginates tested have been well-characterised using ^{13}C-NMR and therefore other biophysical properties could be correlated with pepsin inhibition. Levels of pepsin inhibition were compared against the frequency of the structural patterns; F[M], F[GG], F[MM], F[GGG], F[MGM] and F[GM/MG] and also against n(g>1), the G-Block length. Similar significant relationships between structure and inhibition were observed, where higher levels of mannuronic acid brought about significantly higher levels of pepsin inhibition.
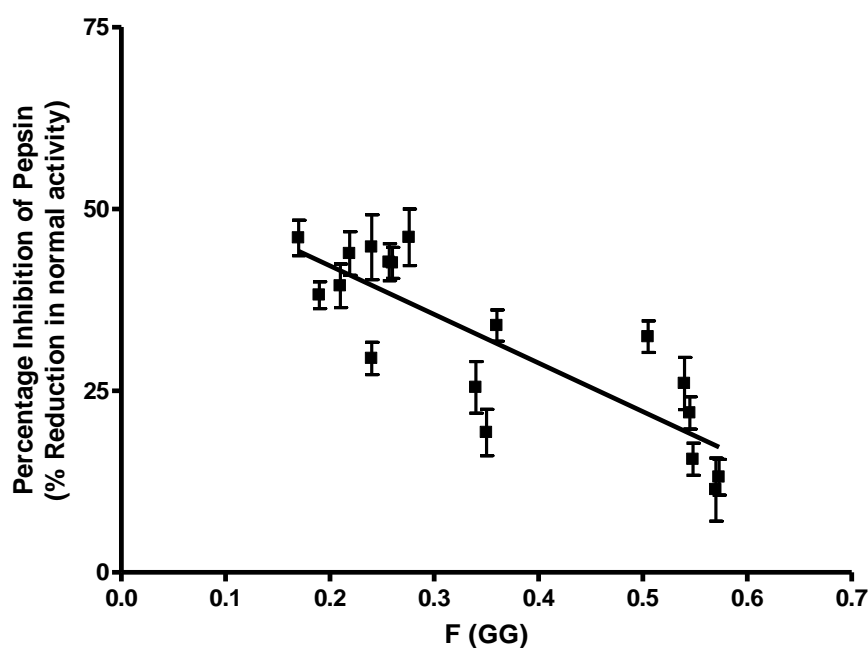
Figure 43 – Correlation of alginate G-residue frequency (F[GG]) and level of pepsin inhibition with 5mg/ml alginate. Pepsin activity is shown as a percentage of control pepsin activity. The error bars show the standard deviation of 6 replicates (n=6). The line of best fit indicates a negative correlation which is significant with a Spearman r value of -0.7816 and a p value of 0.0001.

Figure 43 shows the correlation between pepsin inhibition and the frequency of adjacent guluronic acid residues in a diad. As can be seen contiguous GG blocks are significantly associated with a reduced capacity to inhibit pepsin. This relationship holds true also for GGG-Blocks, that is three adjacent guluronic acid residues. Again there is a negative

correlation between the presence of GGG blocks and inhibition of pepsin, as shown in Figure 44.
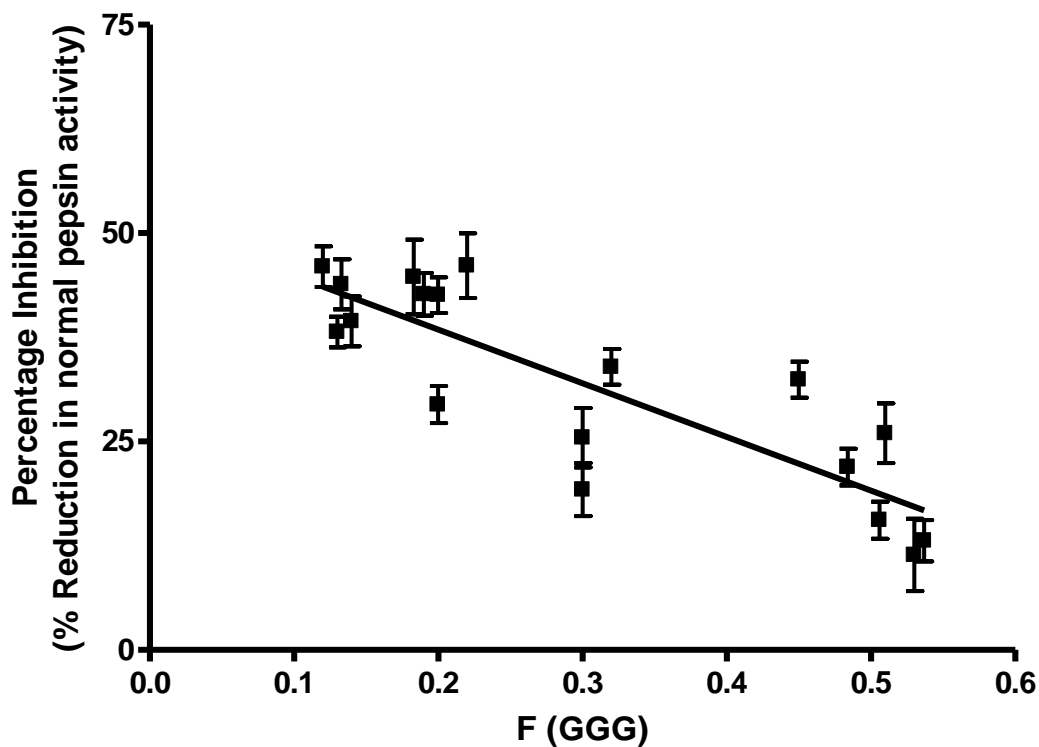
Figure 44 – Correlation of alginate GGG-residue frequency (F[GGG]) and level of pepsin inhibition with 5mg/ml alginate. Pepsin activity is shown as a percentage of control pepsin activity. The error bars show the standard deviation of 6 replicates (n=6). The line of best fit indicates a negative correlation which is significant with a Spearman r value of -0.7996 and a p value of 0.0001.

In fact, across all samples as the G-block length increases, there is a significant reduction in the inhibition of pepsin, showing a negative correlation between inhibition and $n(g>1)$.
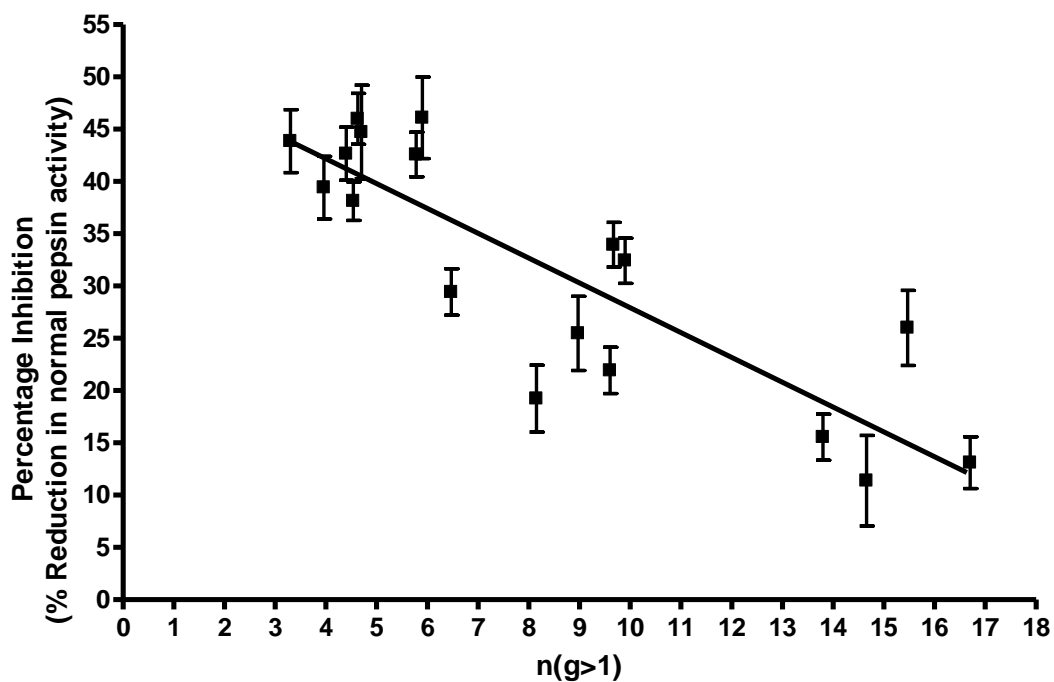
Figure 45 – Correlation of alginate N(G>1) and level of pepsin inhibition with 5mg/ml alginate. Pepsin activity is shown as a percentage of control pepsin activity. The error bars show the standard deviation of 6 replicates (n=6). The line of best fit indicates a negative correlation which is significant with a Spearman r value of -0.7709 and a p value of 0.0002.

Levels of pepsin inhibition were inversely correlated with a frequency of guluronic acid residues, therefore as might be expected, the fraction of MM blocks was positively correlated with levels of pepsin inhibition.
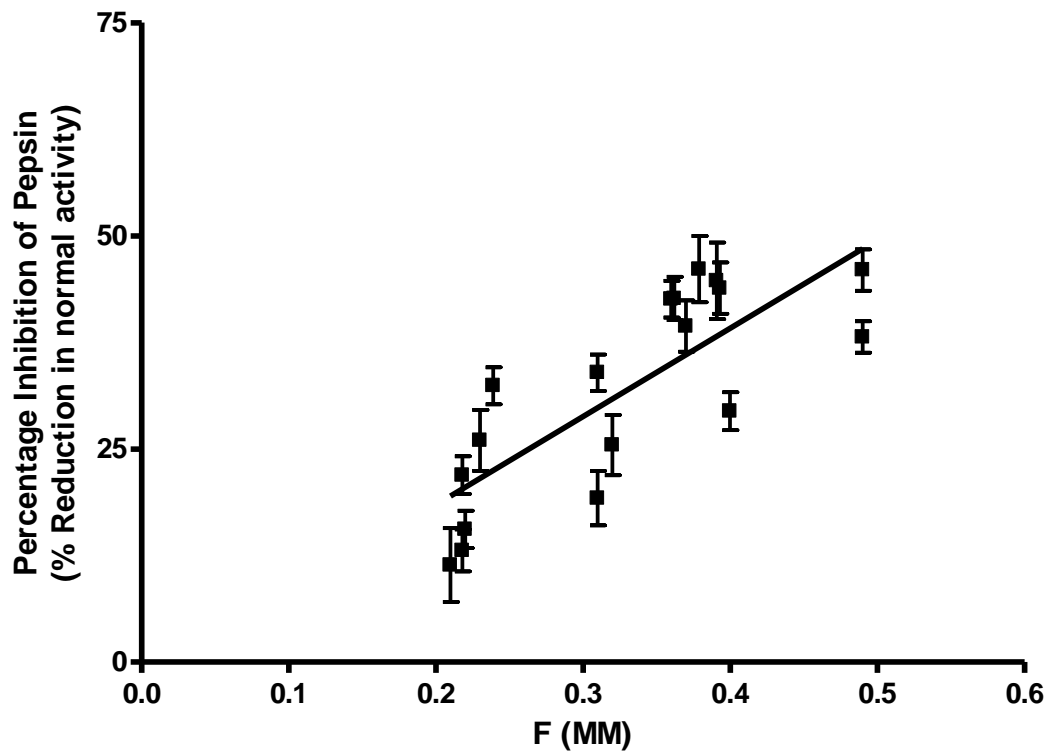
Figure 46 – Correlation of alginate MM-block frequency (F[MM]) and level of pepsin inhibition with 5mg/ml alginate. Pepsin activity is shown as a percentage of control pepsin activity. The error bars show the standard deviation of 6 replicates (n=6). The line of best fit indicates a negative correlation which is significant with a Spearman r value of 0.7917 and a p value of 0.0001.

However, the relationship is not so simple as to say a high M:G ratio is the sole determinant of inhibition levels, as shown in Figure 47 there is a strong positive correlation between the frequency of MGM blocks and pepsin inhibition levels. There is also a strong correlation between the frequency of MG/GM blocks with pepsin inhibition as shown in Figure 48.

However when (F[MGG/GMM]) was correlated against levels of pepsin inhibition there was still a significant positive correlation, however the correlation was weaker. This suggests that as well as depending on an increasing frequency of M-residues being associated with pepsin inhibition, the distribution of the M-residues is important and that their positioning in disrupting continuous G-Blocks may be important to the inhibitory effect. This shall be considered further in the discussion.
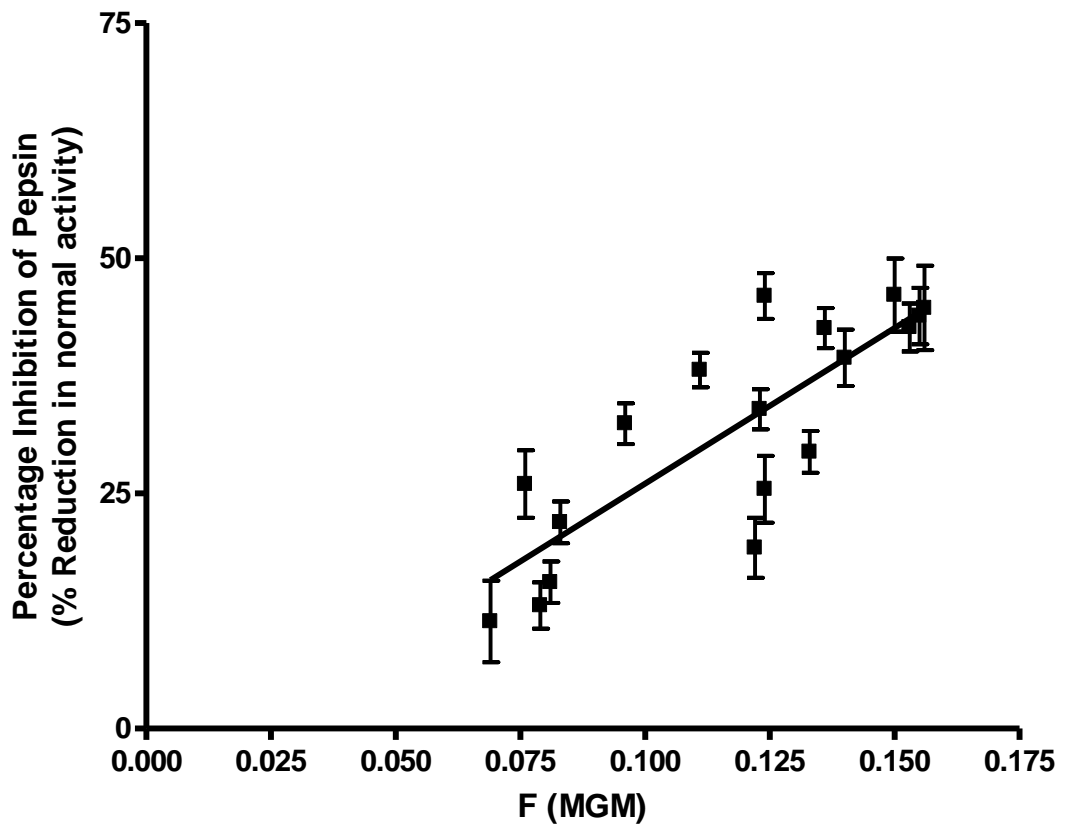
Figure 47   – Correlation of alginate MGM-Block frequency (F[MGM]) and level of pepsin inhibition with 5mg/ml alginate. Pepsin activity is shown as a percentage of control pepsin activity. The error bars show the standard deviation of 6 replicates (n=6). The line of best fit indicates a negative correlation which is significant with a Spearman r value of 0.8219 and a p value of 0.0001.
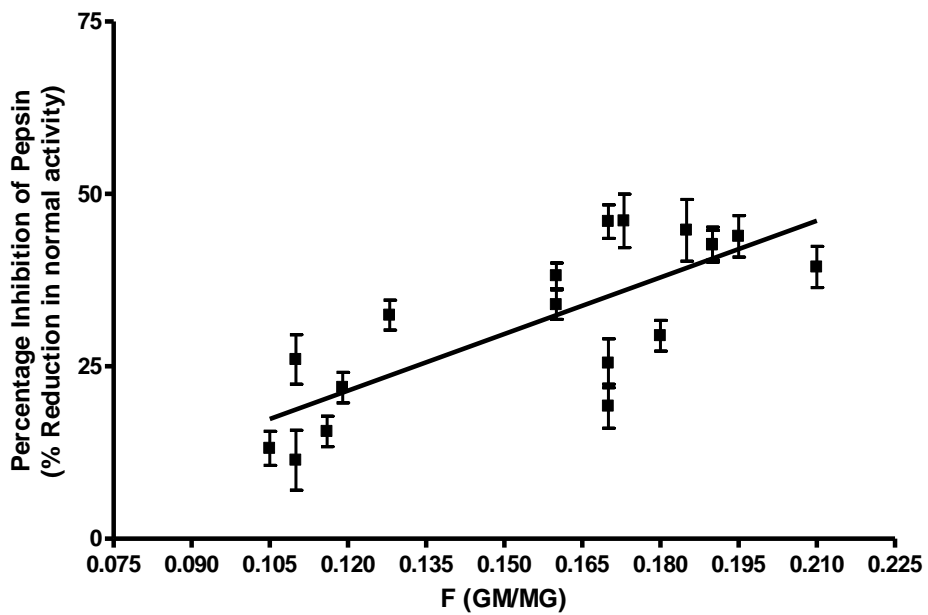
Figure 48 — Correlation of alginate GM/MG-block frequency (F[GM/MG]) and level of pepsin inhibition with 5mg/ml alginate. Pepsin activity is shown as a percentage of control pepsin activity. The error bars show the standard deviation of 6 replicates (n=6). The line of best fit indicates a negative correlation which is significant with a Spearman r value of 0.7240 and a p value of 0.0007.
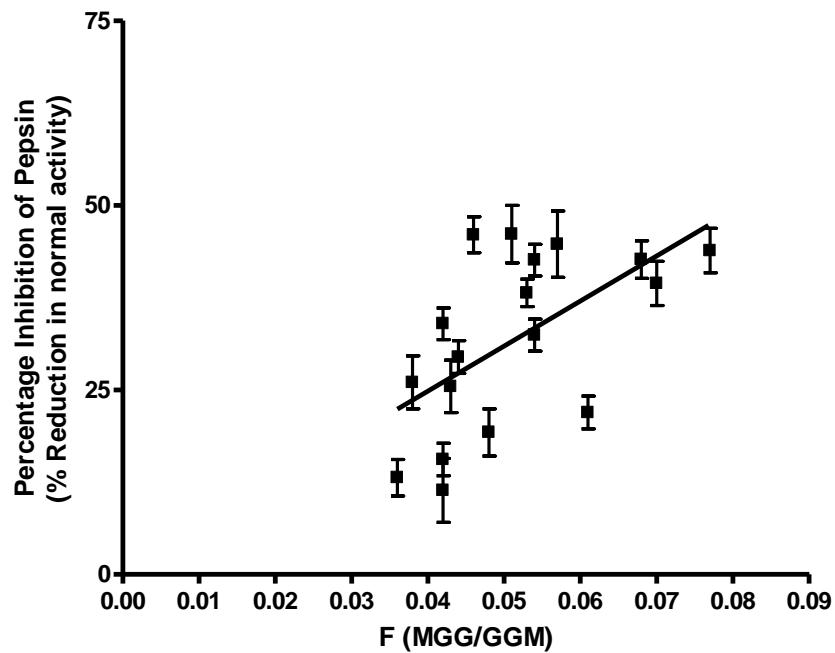
Figure 49 — Correlation of alginate MGG/GMM-residue frequency (F[MGG/GMM]) and level of pepsin inhibition with 5mg/ml alginate. Pepsin activity is shown as a percentage of control pepsin

activity. The error bars show the standard deviation of 6 replicates (n=6). The line of best fit indicates a negative correlation which is significant with a Spearman r value of 0.59 and a p value of 0.01.

Significant but weaker correlations were shown between alginate and certain structural characteristics of alginate at 2.5mg/ml as summarised in Table 11. None of the characteristics showed significant correlation with pepsin inhibition at 1.25mg/ml alginate.

Structural Characteristic	5mg/ml		2.5mg/ml		1.25mg/ml	
	Spearmans value	P-value	Spearmans value	P-value	Spearmans value	P-value
F(G)	-0.779	0.0001	-0.488	0.0400	*-0.360*	*0.1417*
F(M)	0.786	0.0001	0.499	0.0350	0.360	0.1428
F(GG)	-0.782	0.0001	-0.494	0.0374	-0.334	0.1762
F(MG/GM)	0.724	0.0007	0.314	0.2047	0.191	0.4488
F(MM)	0.792	0.0001	0.561	0.0154	0.398	0.1020
F(MGG/GGM)	0.589	0.0102	*0.0807*	*0.7502*	-0.060	0.8130
F(MGM)	0.822	0.0001	0.481	0.0432	0.220	0.3805
F(GGG)	-0.800	0.0001	-0.482	0.0426	-0.320	0.1951
N (G>1)	-0.771	0.0002	-0.327	0.1851	-0.195	0.4380

Table 11   Summary of Correlations between alginate structural characteristics and alginate inhibition at three concentrations 5mg/ml, 2.5mg/ml and 1.25mg/ml. ▮▮▮▮ Significant Negative Correlation, ▭▭▭ Significant Positive Correlation, ▭▭▭ No Correlation.

Molecular weight data was only available for the eight alginates supplied by Technostics Ltd. Alginates can vary greatly in molecular weight and the Technostics alginates used in this study ranged from 34,700 – 387,000 Da. However no significant correlation between molecular weight and pepsin inhibition could be demonstrated as shown in Figure 50.
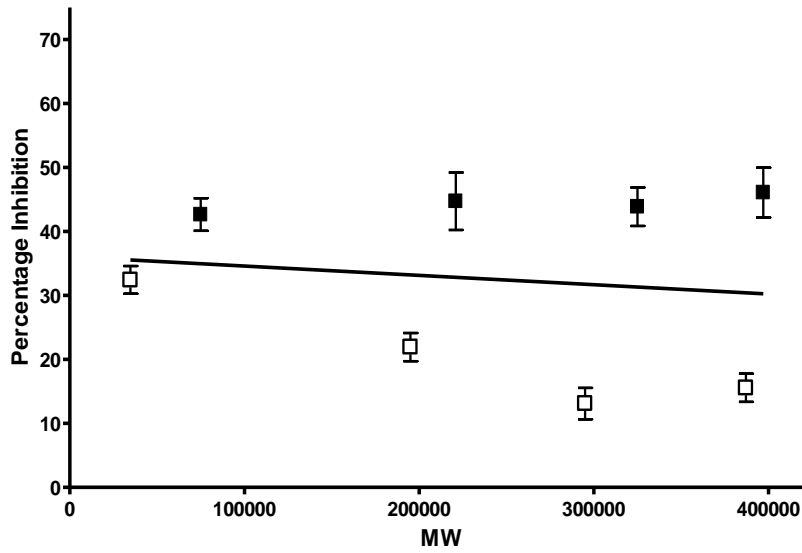
Figure 50 — Correlation of alginate molecular weight (MW) and level of pepsin inhibition with 5mg/ml alginate. Pepsin activity is shown as a percentage of control pepsin activity. The error bars show the standard deviation of 6 replicates (n=6). No significant correlation was found with a Spearman r value of 0.19 and a p value of 0.66. Lamanaria alginates are represented as □ and Lessonia alginate as ■.

3.6.2   Enzyme kinetics

As well as testing the absolute regulatory effects of biopolymers on pepsin, the kinetics of enzyme substrate reactions in the presence of dietary fibres were also analysed. Samples were tested using a modified version of the 96-well plate N-terminal protocol as described in the methodology section. All biopolymers were tested a minimum of 5 times. Kinetic constants were calculated from GraphPad Prism 4 software using substrate-velocity data.

Enzyme kinetics can help provide an understanding of enzyme catalysed reactions and can provide important insights into the mechanisms of enzyme inhibition. The kinetics of an enzyme-substrate interaction alters with substrate concentration (or ratio of substrate to enzyme) and how extrinsic compounds interfere with this can give insight into their mechanism of action. This can be graphically represented by a Michaelis-Menten plot. Velocity of reaction, measured as percentage change in absorbance per minute is plotted on the y-axis against substrate concentration on the x-axis.

This plot can also provide useful information about the kinetics of an enzyme catalysed reaction. The maximum velocity of the reaction (V_{max}), is the theoretical concentration of substrate at which all enzyme active sites are saturated with substrate and functioning at a maximal rate. This value can be determined from where the Michaelis-Menten curve plateaus, this levelling of reaction rate occurs due to substrate saturation.

 The constant V_{max} can be used to calculate the Michaelis Constant (K_m), which is the substrate concentration required for half of maximal enzyme activity. As such the K_m provides an important measure of the affinity of an enzyme for its substrate. A low K_m means that less substrate is required to reach $V_{max}/2$, substrate/enzyme affinity must therefore be higher as less substrate is required to fill active sites. Inversely a higher K_m would indicate a lower affinity.

K_m and V_{max} are therefore important and useful measures of enzyme activity.

Figure 51 below shows a typical Michaelis Menten plot for alginate inhibition of pepsin. In the control digestion, from 0-2.5mg/ml substrate, reaction velocity increases in a linear fashion, however as substrate concentration increases beyond 2.5mg/ml the plot begins to plateaux as the enzyme active site becomes saturated. As can be seen in Figure 51, when the alginate 'FMC2' is added to the reaction, the velocity of the reaction is reduced at all substrate concentrations, and the addition of FMC2 alginate causes a similar plateauxing effect, but at a lower velocity.
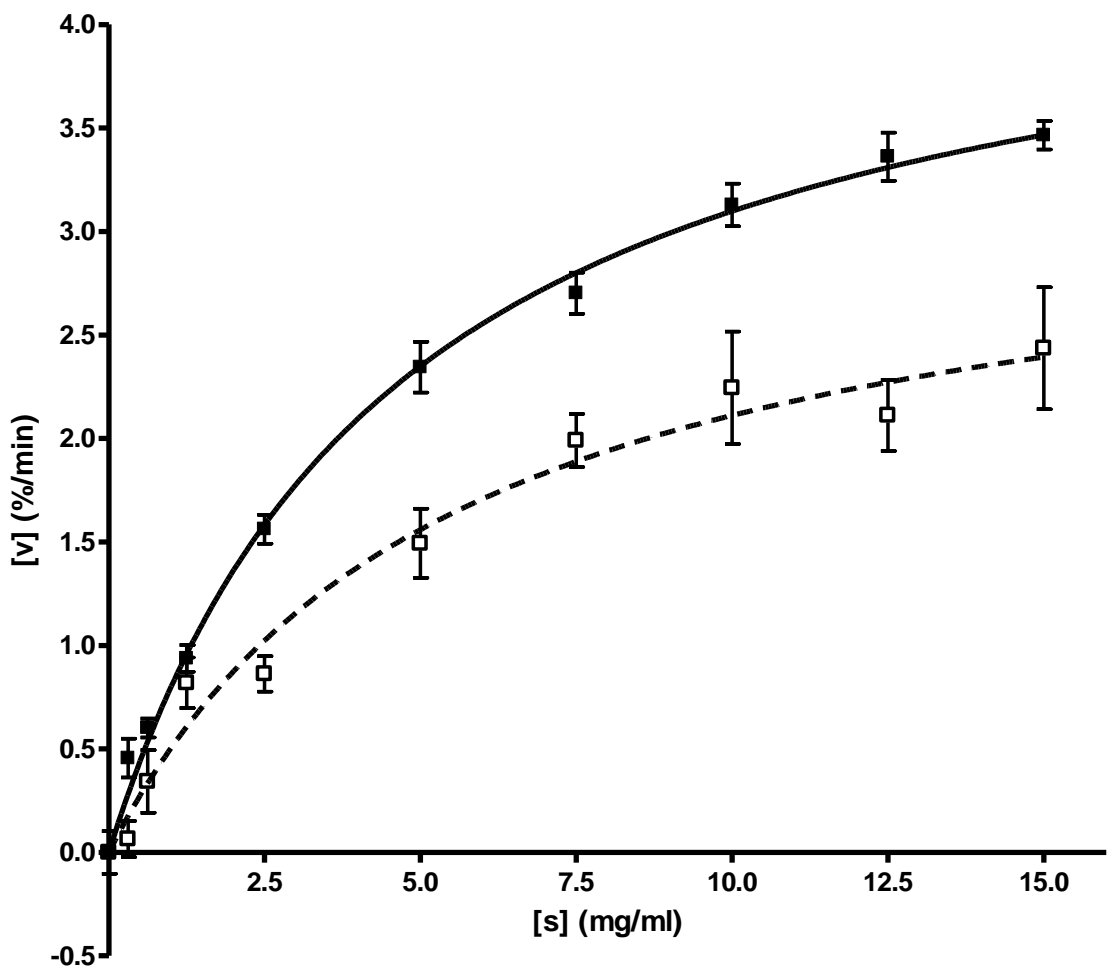
Figure 51   Michaelis-Menten plot for alginate sample FMC2 at 5mg/ml (□) as compared to a pepsin control (■). Substrate concentration [s] is given in mg/ml and the velocity is given as the rate of change in percentage absorbance per minute. The error bars show the standard deviation of at least 5 replicates (n=5)

The kinetic data from the Michaelis Menten plots was transformed in to the double reciprocal plot shown in Figure 52. From this data the K_m and V_{max} of a control pepsin digestion were calculated using Graphpad Prism 4.0, and the apparent K_m and V_{max} of all biopolymer samples were calculated.

Figure 52   - Lineweaver-Burk plot for alginate sample FMC2 at 5mg/ml (☐) as compared to a pepsin control (■). Substrate concentration [s] is given in mg/ml and the velocity is given as the rate of change in percentage absorbance per minute. The error bars show the standard deviation of at least 5 replicates (n=5)

It is important to note that while the kinetic data was calculated using statistical software, lines of best fit were done using linear regression.

With FMC2 alginate in the reaction mixture, pepsin has a V_{max} of 3.267%/min, a K_m of 5.47mg/ml. This is compared to a control pepsin digestion where the K_m is 4.67mg/ml and the V_{max} is 4.55%/min. So as can be seen both the maximum velocity of reaction at a theoretical infinite substrate concentration and the apparent K_m, the affinity of enzyme for substrate are reduced by the addition of FMC2 biopolymer to the reaction mixture.

The kinetic data for all alginate samples analysed is collated below in Table 12, biopolymers have been listed in descending order of potency of pepsin inhibition based on K_i.

From the V_{max} and K_m the inhibition constant K_i was calculated. The kinetic constants K_m and V_{max} provide useful indicators of the type of inhibition or activation. Using V_{max} and K_m it is possible to calculate the K_i or inhibition constant using the formula below. The gradient of the line on the double-reciprocal Lineweaver Burk plot can be calculated as the Michaelis Constant (K_m) divided by the Maximum Velocity (V_{max}).

The relationship between these two slopes is determined by the Inhibitor Concentration [I] and Inhibitor Constant K_i as shown below:

$$Gradient\ of\ New\ Slope = Gradient\ of\ Old\ Slope \times \left(1 + \frac{[I]}{K_i}\right)$$

$$\frac{K_{m1}}{V_{max1}} = \left(\frac{K_{m2}}{V_{max2}}\right)\left(1 + \frac{[I]}{K_i}\right)$$

$$\left(\frac{\left(\frac{K_{m1}}{V_{max1}}\right)}{\left(\frac{K_{m2}}{V_{max2}}\right)}\right) = \left(1 + \frac{[I]}{K_i}\right)$$

$$K_i = \frac{[I]}{\left(\left(\frac{\left(\frac{K_{m1}}{V_{max1}}\right)}{\left(\frac{K_{m2}}{V_{max2}}\right)}\right) - 1\right)}$$

K_i therefore describes the relationship between the uninhibited and inhibited enzyme. Biopolymer FMC2 shown in Table 12 was ranked as 13th most effective inhibitor according to K_i out of 18 alginate polymers.

Rank	F [G]	V_{max} (%/min)	Apparent K_m (mg/ml)	K_i
PEPSIN		**4.547**	**4.677**	
1	SF60	0.411	8.051	48.02	1.042
2	FMC13	0.32	10.08	57.19	1.1072
3	LF10L	0.45	3.847	12.85	2.2248
4	H120L	0.45	8.335	27.53	2.2613
5	FMC12	0.32	6.097	19.09	2.4462
6	FMC10	0.41	7.195	22.25	2.4919
7	LFR560	0.633	5.185	14.5	2.909
8	FMC6	0.53	5.373	13.69	3.385
9	FMC4	0.49	5.962	12.32	4.9555
10	LF120L	0.424	4.151	7.813	6.025
11	FMC9	0.42	3.396	6.032	6.879
12	FMC2	0.65	3.267	5.474	7.9495
13	FMC5	0.55	3.02	2.949	9.618
14	FMC7	0.69	3.855	5.924	10.12
15	FMC3	0.68	3.227	4.847	10.863
16	SF120	0.664	4.605	6.247	15.681
17	SFLF	0.66	4.68	6.132	18.259
18	SF200	0.68	4.34	5.117	34.186

Table 12   Kinetic data for alginate inhibition of Pepsin.

This kinetic data was correlated against alginate F[G], and is plotted in the figures below. Figure 53 shows the correlation between F[G] and apparent K_m. A significant negative correlation was observed. This correlation suggests that with a decreasing frequency of guluronate the enzyme substrate affinity of pepsin for succinyl albumin substrate is decreased and more substrate is required to reach half of the maximal velocity.
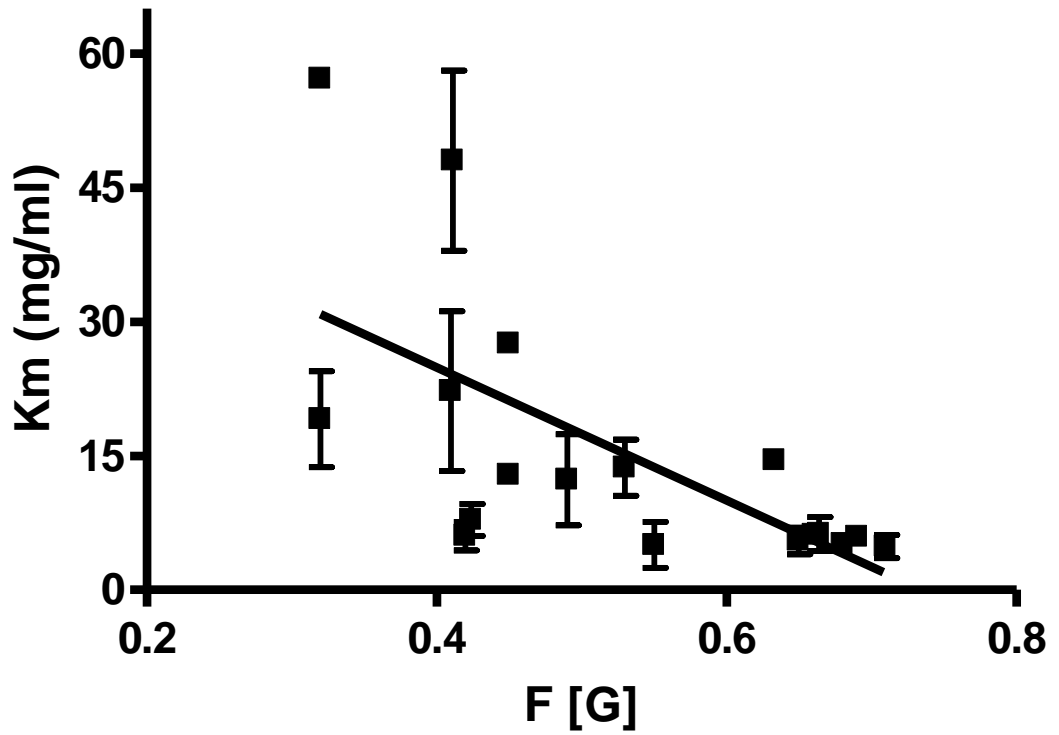
Figure 53   - Correlation between apparent K_m of alginate samples and G-residue frequency (F[G]). Apparent K_m was calculated with Michaelis-Menten Analysis. A negative correlation between apparent K_m and F[G] was shown with a Spearmans r value of -0.7603 with a p-value of 0.0002.

A similar negative correlation was observed between F[G] and Vmax whereby the maximal reaction velocity of the reaction tended to increase in the presence of alginates with decreased guluronic acid residue frequency. A significant negative correlation between alginate F[G] and Vmax was seen.
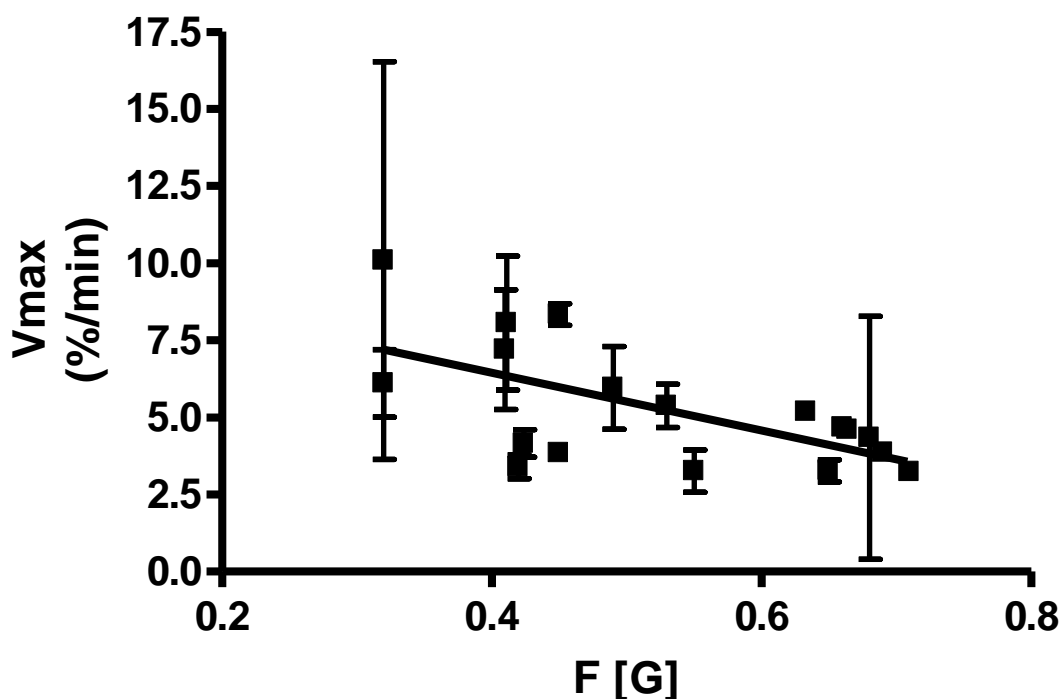
Figure 54   - Correlation between apparent V_{max} of alginate samples and G-residue frequency (F[G]). V_{max} was calculated by Michaelis-Menten analysis. A negative correlation between V_{max} and F[G] was shown with a Spearmans r value of -0.5940 with a p-value of 0.0093.

The implication of this correlation is that an increasing frequency of mannuronate correlates with an increase in theoretical maximum velocity at an infinite substrate concentration. This is counter-intuitive considering that all the other data suggest alginates to have an inhibitory effect on the reaction. This will be considered further in the discussion.

The apparent kinetic constants K_m and V_{max} were used to calculate the inhibitor constant K_i. K_i, is the dissasociation constant of the enzyme-inhibitor complex and therefore the reciprocal of the enzyme-inhibitor binding affinity. In the case of uncompetitive and non-competetive inhibition, the K_i bears a strong relationship to the IC_{50} value, the amount of inhibitor required to cause 50% inhibition. This is not the case for competitive inhibition, however the K_i can be used to indicate how potent an inhibitor is [182].

This data reiterated the correlation between potency of inhibition and F[G] frequency with higher frequency of mannuronic acid and lower frequency of guluronic acid being associated with a lower K_i. This relationship was positive and statistically significant with Spearmans r value of 0.8130 with a p-value of 0.0001.

One value has been starred '*' in Figure 55 below as this appears as though it may be an outlier. However as can be seen from Figure 56, even with this possible outlier removed the correlation holds true with a p value of 0.003 and a Spearmans r value of 0.7951.
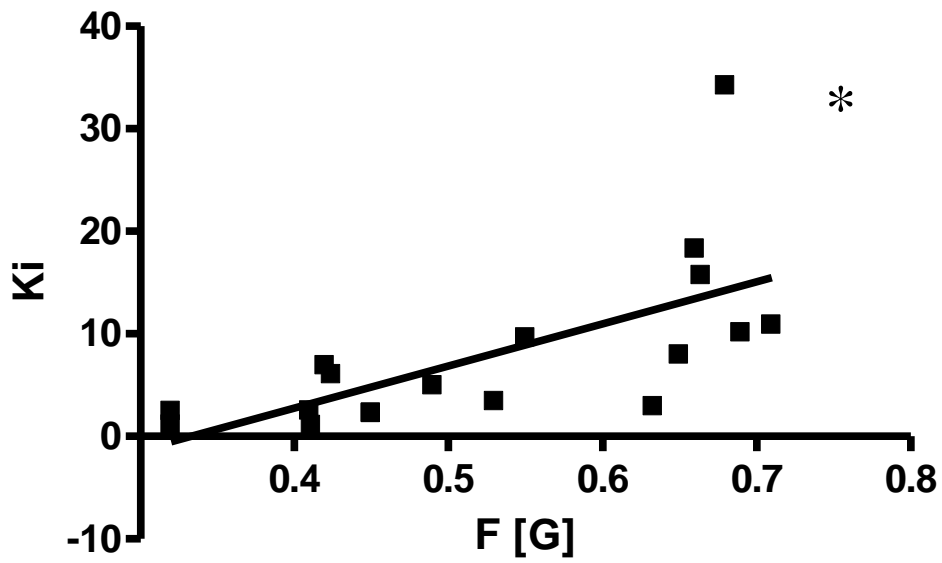
Figure 55   - Correlation between K_i of alginate samples and G-residue frequency (F[G]). V_{max} was calculated by Michaelis-Menten analysis. A positive correlation between K_i and F[G] was shown with a Spearmans r value of 0.8130 with a p-value of 0.0001.
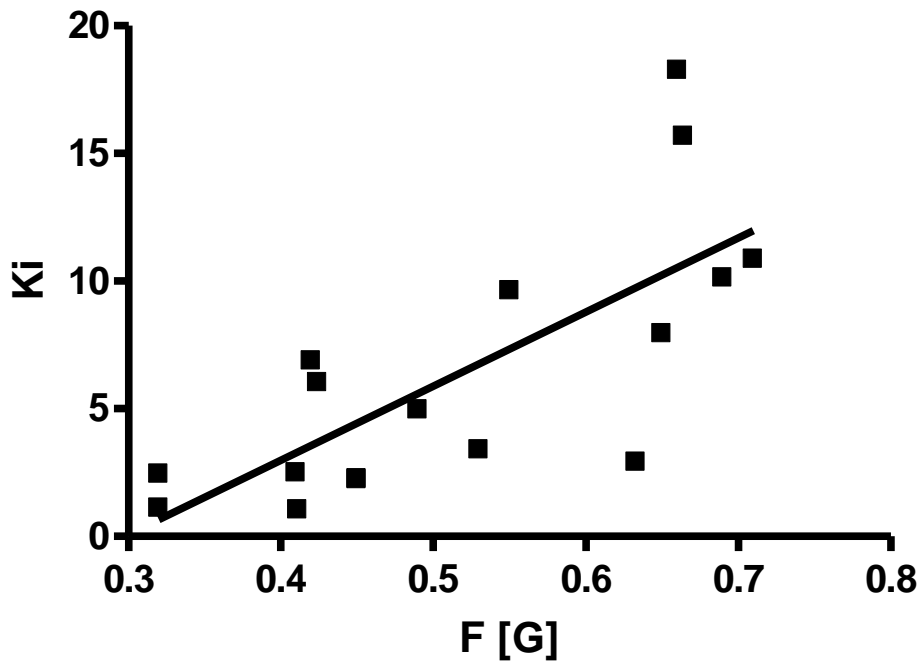
Figure 56   Correlation between K_i of alginate samples and G-residue frequency (F[G]). V_{max} was calculated by Michaelis-Menten analysis. A positive correlation between K_i and F[G] was shown with a Spearmans r value of 0.7951 with a p-value of 0.003.

Lineweaver Burk plots are a useful way of visualising types of enzyme inhibition, and four types of inhibition can be discerned from a Lineweaver Burk plot; competitive, non-competetive, uncompetitive and mixed inhibition. By comparing the derived apparent kinetic constants to the control substrate digestion, the biopolymer samples were fitted to different models of inhibition. The 95% Confidence intervals of the derived values were used and compared to the kinetic constraints of pepsin in an control reaction.

The modelled data is shown in Table 13 below. The substrate control kinetic constants were compared to the apparent K_m and V_{max} values derived for each biopolymer. If these values lay without the 95% confidence interval, they were said to be different, and were fitted to an inhibition model.

Sample	Inhibition Model	Apparent Kinetic Constants		95% Confidence Intervals	
		V_{max} (%/min)	K_m (mg/ml)	V_{max} (%/min)	K_m (mg/ml)
PEPSIN		*4.547*	*4.677*	*4.233 to 4.862*	*3.811 to 5.543*
FMC 2	Non-competitive reversible inhibition	3.267	5.474	2.548 to 3.985	2.467 to 8.481
FMC3		3.227	4.847	2.561 to 3.894	2.258 to 7.436
FMC9		3.396	6.032	2.606 to 4.185	2.813 to 9.251
FMC6	Reversible competetive inhibition	5.373	13.69	3.951 to 6.794	7.384 to 20.00
FMC12		6.097	19.09	3.890 to 8.304	8.281 to 29.90
FMC13		10.08	57.19	-2.921 to 23.09	-31.44 to 145.8
LF10L		3.847	12.85	3.201 to 4.493	9.004 to 16.70
H120L		8.335	27.53	3.946 to 12.72	7.165 to 47.89
SF60		8.051	48.02	-0.002672 to 16.10	-11.44 to 107.5
LFR560		5.185	14.5	4.406 to 5.964	10.79 to 18.20
FMC10	Does not fit to a model	7.195	22.25	3.272 to 11.12	4.222 to 40.28
LF120L		4.151	7.813	3.245 to 5.057	4.156 to 11.47
SF120		4.605	6.247	3.964 to 5.245	4.180 to 8.313
SF/LF		4.68	6.132	3.962 to 5.398	3.839 to 8.426
SF200		4.34	5.117	3.970 to 4.709	3.968 to 6.266
FMC4		5.962	12.32	3.245 to 8.679	2.026 to 22.62
FMC7		**3.855**	**5.924**	**3.287 to 4.422**	**3.908 to 7.939**

Table 13   Kinetic data of alginate inhibition of pepsin fitted to inhibition models at 5mg/ml.

Biopolymers FMC2, FMC 3 and FMC9 fit with the model of non competitive reversible inhibition. In Non-competitive reversible inhibition, the inhibitor binds the enzyme at a point other than the active site, either when the enzyme is free or in complex with the substrate. While the rate of enzyme-substrate formation and disassociation are affected by the inhibitor, association and disassociation are affected by the same amount, therefore the K_m remains unaltered and the x-intercept of the biopolymer sample will be the same as that of the control. V_{max} is reduced as the presence of inhibitor blocks product formation.

$$
\begin{array}{ccccccc}
E & + & S & \leftrightarrow & ES & \rightarrow & P & + & E \\
+ & & & & + & & & & \\
\end{array}
$$

$$
\begin{array}{c}
I \qquad\qquad I \\
\updownarrow \qquad\qquad \updownarrow \\
EI \;+\; S \;\leftrightarrow\; EIS
\end{array}
$$
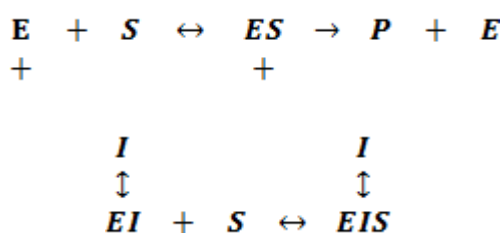
FMC 2 was shown previously in Figure 51 and Figure 52. The Michaelis Menten plot for FMC3 is shown in Figure 57 and the Lineweaver Burk plot in Figure 58.

It is important to note that modelling was done on the basis of the 95% confidence intervals of apparent kinetic values and how they correlated to control values, rather than visually analysing the intercepts. So although in the Lineweaver burke plot for FMC 2, the x-intercepts may appear different, they were not significantly different based on the 95% confidence intervals.
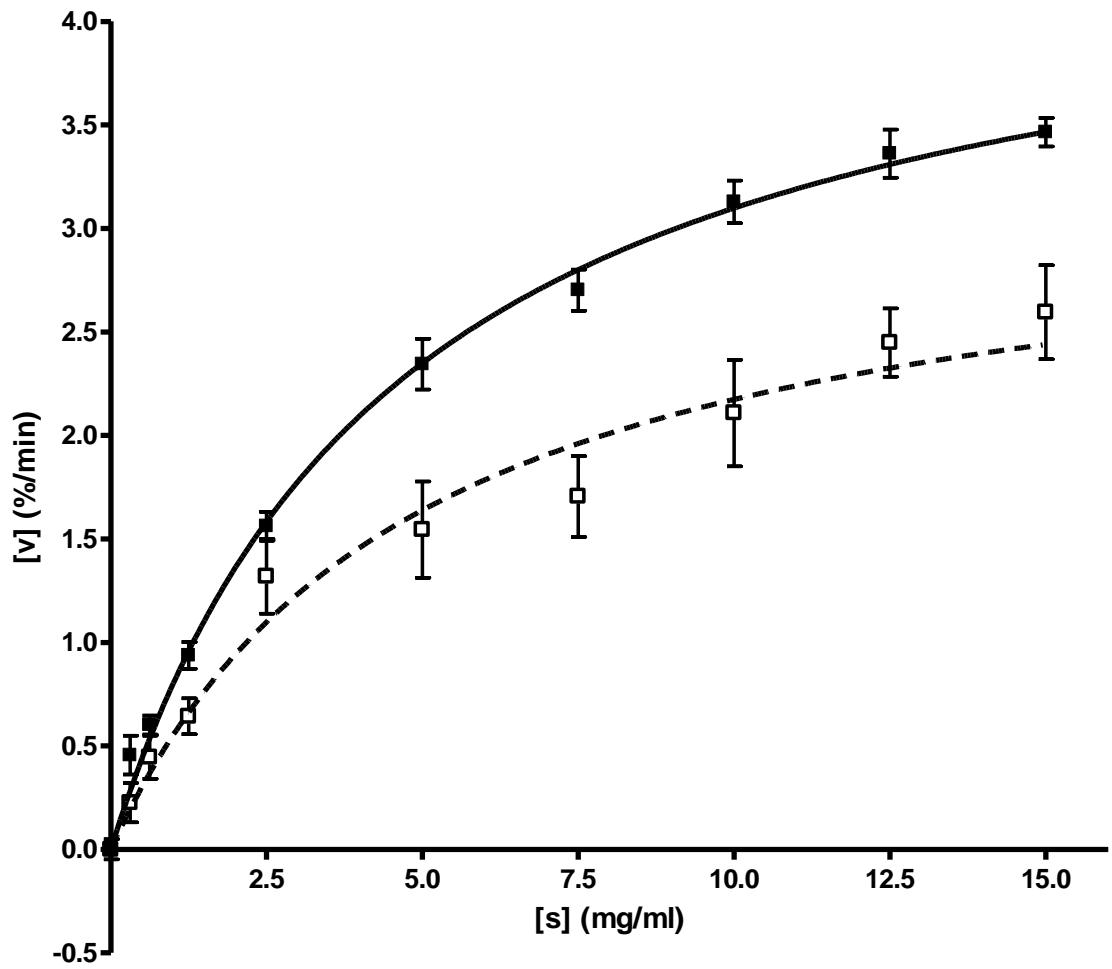
Figure 57   Michaelis-Menten plot for alginate sample FMC3 at 5mg/ml (□) as compared to a pepsin control (■). Substrate concentration [s] is given in mg/ml and the velocity as the rate of change in percentage absorbance per minute. The error bars show the standard deviation of at least 5 replicates (n=5)
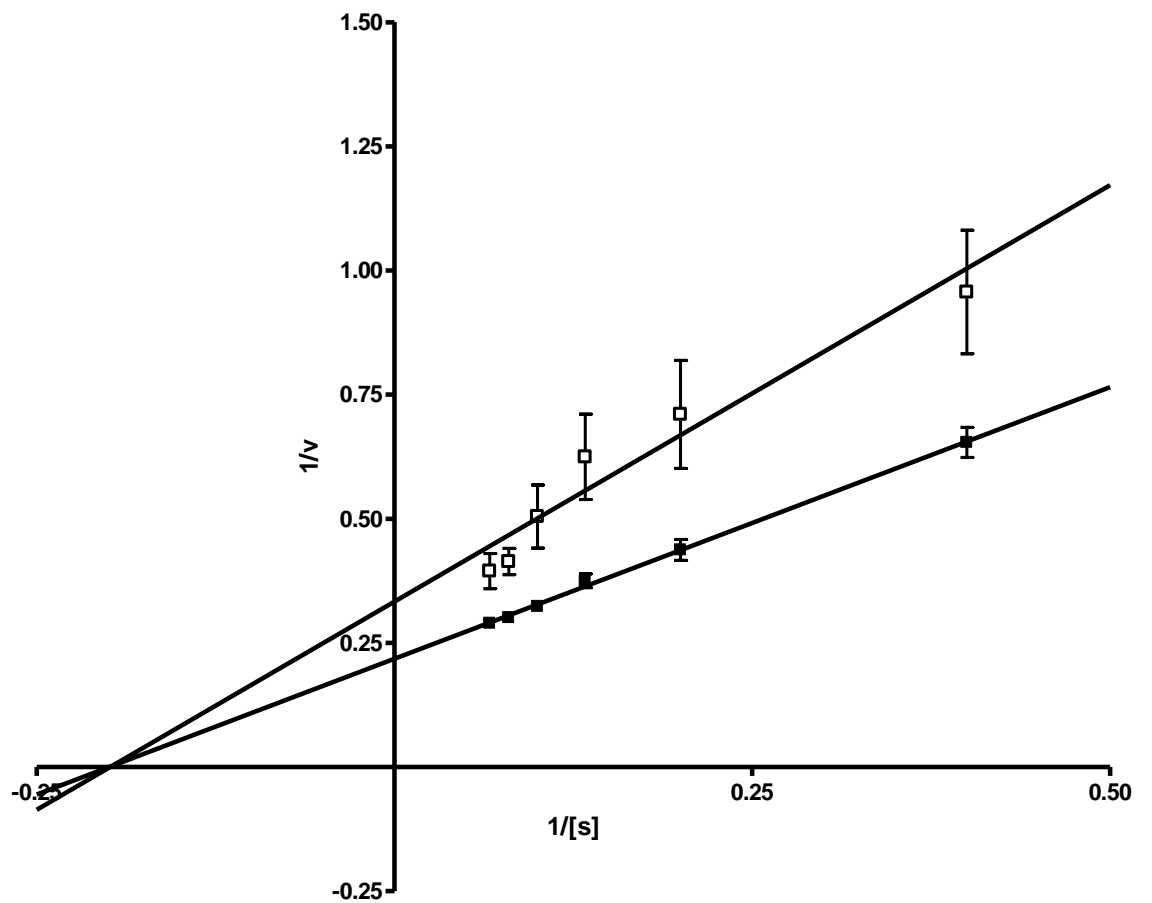
Figure 58 - Lineweaver-Burk plot for alginate sample FMC3 at 5mg/ml (□) as compared to a pepsin control (■). Substrate concentration [s] is given in mg/ml and the velocity as the rate of change in percentage absorbance per minute. The error bars show the standard deviation of at least 5 replicates (n=5)

A number of biopolymers fit with a model of competitive inhibition, these were; FMC6, FMC12, FMC13, LF10L, H120L, SF60, LFR560. Competitive Inhibition occurs when an inhibitor [I] directly competes for the active site and combines with the enzyme, blocking substrate binding to the active site. This causes an increase in K_m, but as the competition can be overcome by increasing substrate concentration, the V_{max} remains unaffected. As V_{max} remains unaffected, the Y-intercept which is equal to $1/V_{max}$ for the biopolymer will be the same as that of the control. This is why this method of inhibition is referred to as competitive, and as the binding is reversible, the inhibitor will dissociate from the enzyme, and all substrate will eventually be converted.

$$E \; + \; S \; \leftrightarrow \; ES \; \leftrightarrow \; P \; + \; E$$
$$+$$

$$I$$
$$\updownarrow$$
$$EI$$
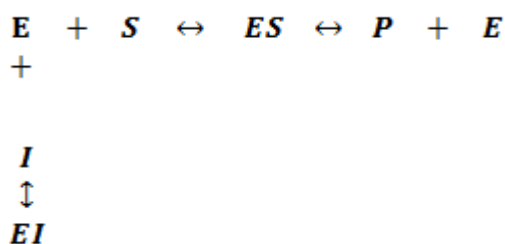
FMC12 is shown in Figure 59 and Figure 60 as a typical example of competitive inhibition. As can be seen the Y-intercepts of both regression lines intersect as the V_{max} is unaffected, but the K_m is increased so the X-intercepts differ.
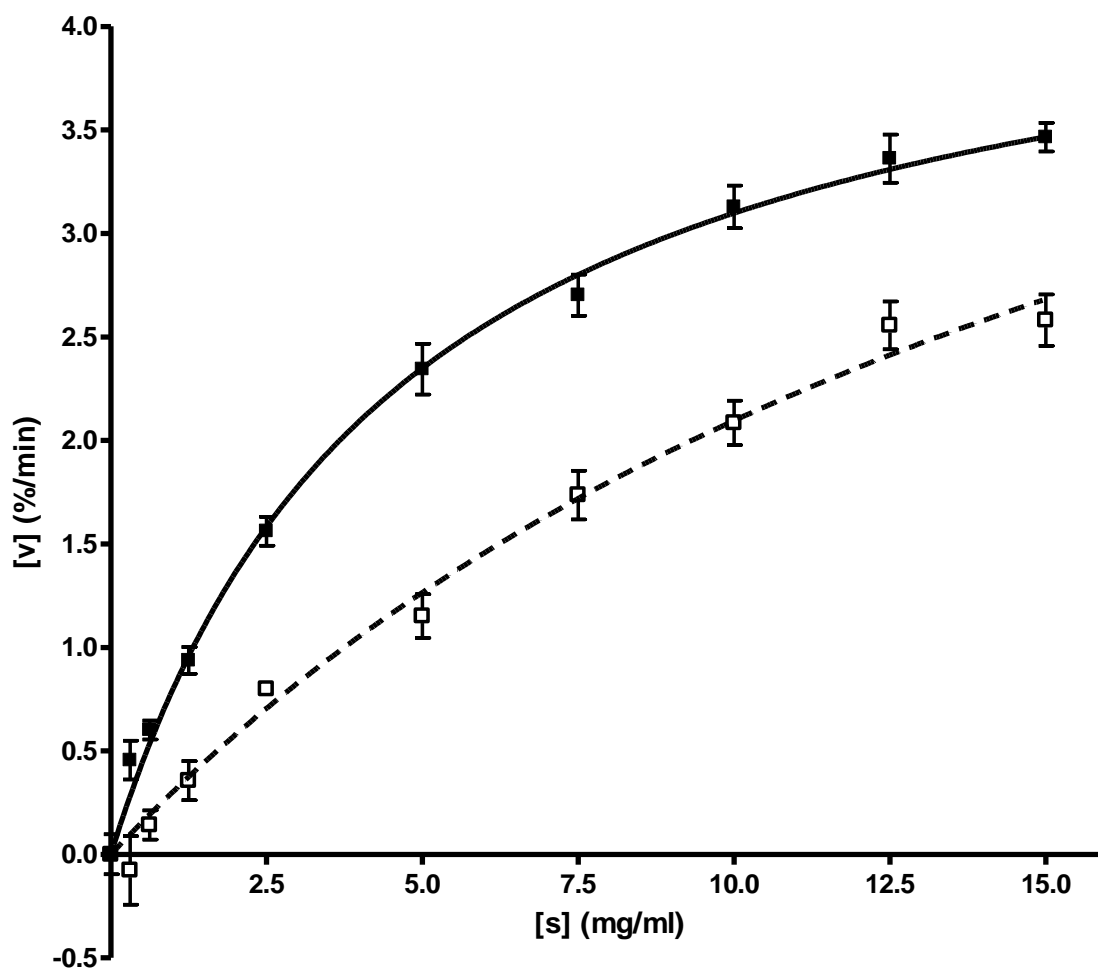
Figure 59   - Michaelis-Menten plot for alginate sample FMC12 at 5mg/ml (☐) as compared to a pepsin control (■). Substrate concentration [s] is given in mg/ml and the velocity as the rate of change in percentage absorbance per minute. The error bars show the standard deviation of at least 5 replicates (n=5)
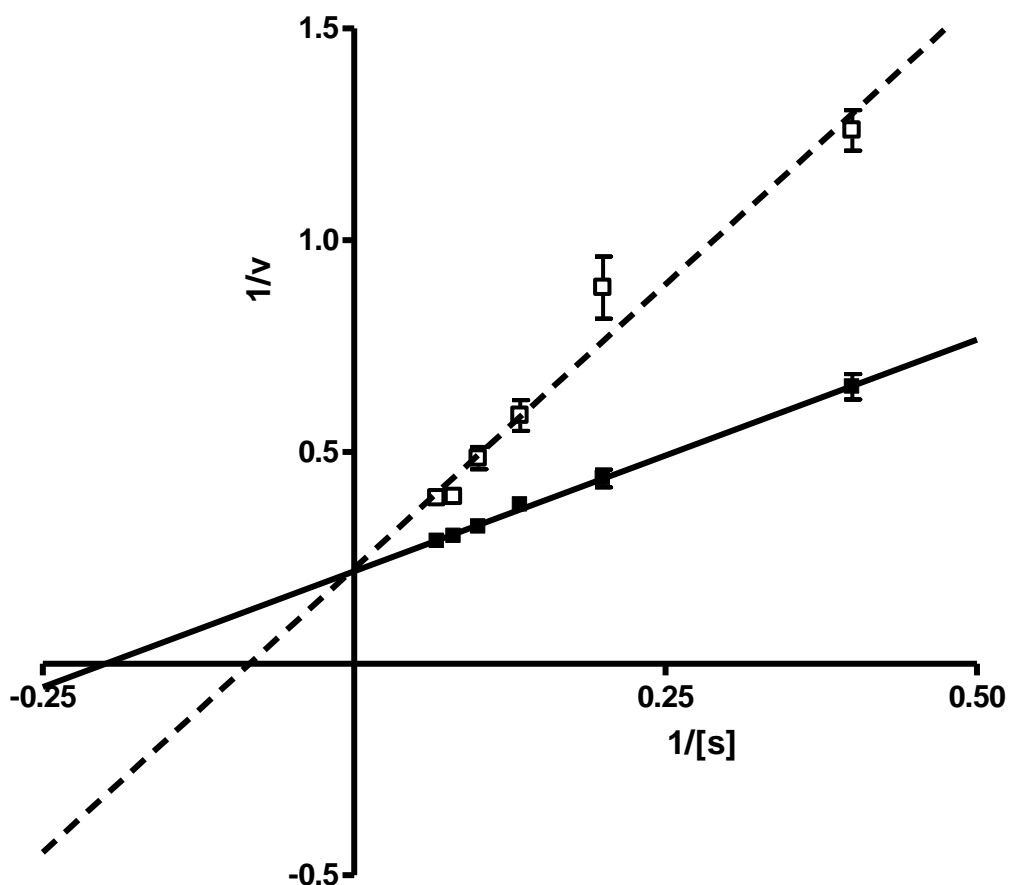
Figure 60   - Lineweaver-Burk plot for alginate sample FMC12 at 5mg/ml (□) as compared to a pepsin control (■). Substrate concentration [s] is given in mg/ml and the velocity as the rate of change in percentage absorbance per minute. The error bars show the standard deviation of at least 5 replicates (n=5)

Alginates FMC10, LF120L, SF120, SF/LF, SF200, FMC4 and FMC7 could not be fitted to any of the inhibition models. While these inhibitory effects do not fit exactly to a model of inhibition, Table 14 below shows the closest-fit models of inhibition based on their lineweaver burke plots.

The michaelis-menten and Lineweaver Burke plots for LF120L are shown in Figure 61 and Figure 62, and as can be seen from Table 14, LF120L is closest to the model of competitive inhibition. As seen in Figure 62, the Y-intercept is unaltered in the presence of the inhibitor, showing that the V_{max} is not affected, however the X-intercept is affected by the presence of inhibitor suggesting that the binding affinity (K_m) is reduced.

Sample	Closest fit Inhibition Model	Apparent Kinetic Constants		95% Confidence Intervals	
		V_{max} (%/min)	K_m (mg/ml)	V_{max} (%/min)	K_m (mg/ml)
PEPSIN		*4.547*	*4.677*	*4.233 to 4.862*	*3.811 to 5.543*
FMC10	Non-competetive reversible inhibition	7.195	22.25	3.272 to 11.12	4.222 to 40.28
LF120L	Reversible Competetive Inhibition	4.151	7.813	3.245 to 5.057	4.156 to 11.47
SF120	Reversible Competetive Inhibition	4.605	6.247	3.964 to 5.245	4.180 to 8.313
SF/LF	Mixed Inhibition	4.68	6.132	3.962 to 5.398	3.839 to 8.426
SF200	Reversible Competetive/Mixed Inhibition	4.34	5.117	3.970 to 4.709	3.968 to 6.266
FMC4	Mixed Inhibition	5.962	12.32	3.245 to 8.679	2.026 to 22.62
FMC7	Non-competetive reversible inhibition	**3.855**	**5.924**	**3.287 to 4.422**	**3.908 to 7.939**

Table 14   Closest fit inhibition models for remaining alginate samples at 5mg/ml.
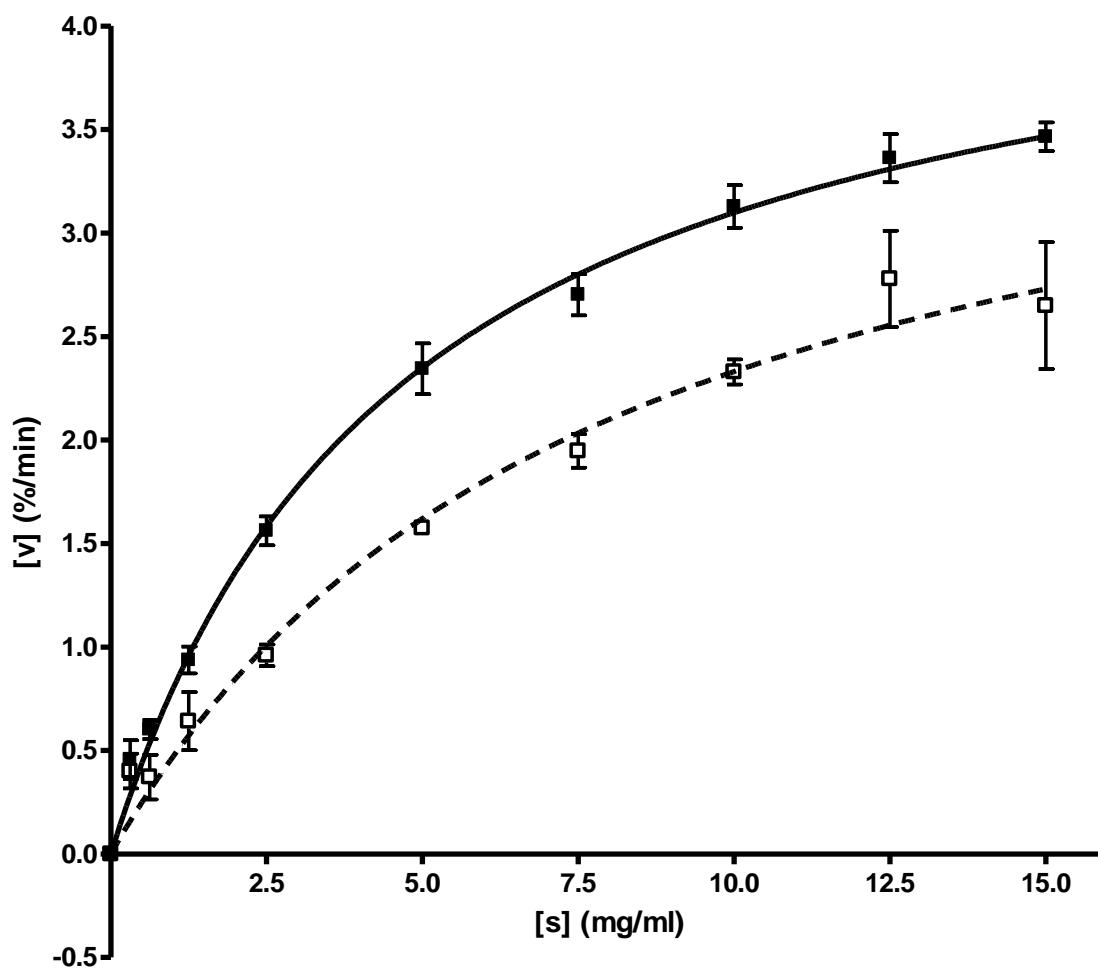
Figure 61 - Michaelis-Menten plot for alginate sample LF120L at 5mg/ml (□) as compared to a pepsin control (■). Substrate concentration [s] is given in mg/ml and the velocity is given as the rate of change in percentage absorbance per minute. The error bars show the standard deviation of at least 5 replicates (n=5)
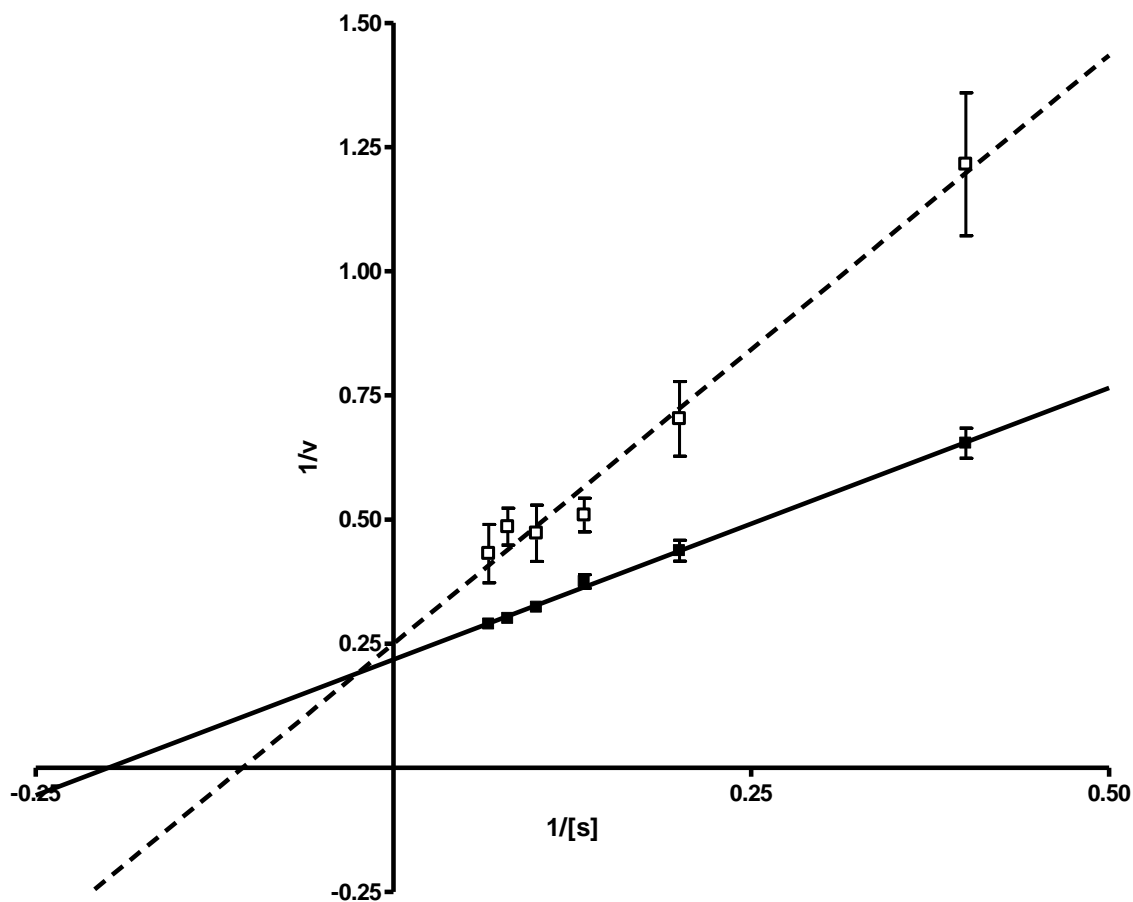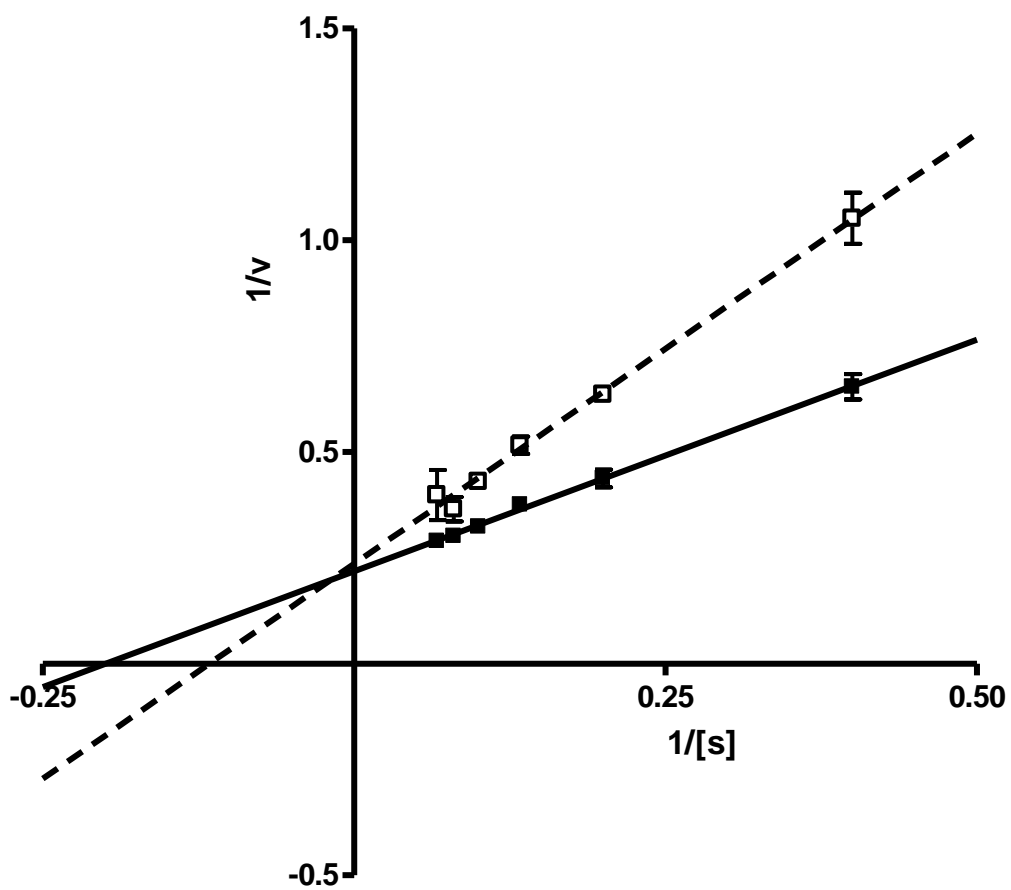
Figure 62 - Lineweaver-Burk plot for alginate sample LF120L at 5mg/ml (□) as compared to a pepsin control (■). Substrate concentration [s] is given in mg/ml and the velocity is given as the rate of change in percentage absorbance per minute. The error bars show the standard deviation of at least 5 replicates (n=5)

3.7 Discussion

A modified N-Terminal (TNBS) assay of proteolytic activity was used to quantify inhibition with alginates. Trinitrophenylated protein turns yellow-orange in colour and can be measured at the wavelength 340nm, the increase in absorbance is directly proportional to the number of N-terminals formed (i.e. peptide bonds cleaved) during proteolysis. This method was used to quantify the modulatory effects of alginates on pepsin activity.

Some modifications had to be made to the original methodology. Alginates are acidic molecules with pK_a's ranging from 3.38 to 3.65 and in aqueous solution will have a pH ranging from 5.75 to 7.25 at 4mg/ml [169]. It was observed that during the testing of aqueous alginates as described by the method of Strugala *et al* 2005, the pH of the reaction mixture is raised by 0.2 units of pH from 2.2 to 2.4 [7]. While only a small change in pH, this shift away from the optimum pH was shown to have a significant effect on the activity of pepsin. The methodology was therefore adapted such that all components of the assay were made up in 0.05M phosphate buffer at pH2.2, to ensure that any inhibitory effects observed were not due merely to a pH effect.

Buffering of the system did result in reduced levels of inhibition detected, this suggests that at least some of the inhibition of pepsin observed by Strugala et al was the result of an alginate induced shift in pH away from the optimum of pepsin. However with all alginates that were tested, significant levels of inhibition were still detected with the buffered system.

The methodology was further adapted by scaling down the assay to run on a 96-well microplate. This was done in order to increase the throughput capability of the assay and reduce any error which may have arisen due to delayed pippeting between wells. The original Lin *et al* 1969, method could not be done using a multi-pipette and required individual spectrophotometric measurements, this introduced slight but potentially significant time delays between samples [168]. Modification of the methodology to a 96 well microplate allowed spectrophotometric measurements to be done in one reading and a multipipette coud be used for adition of substrates.

Each of the catalogue of eighteen alginates was tested in this assay and compared to a Pepsin control which contained buffer only instead of sample, but was in every other

way identical. All alginates tested showed the ability to inhibit pepsin at 5mg/ml (1.36mg/ml in reaction mixture). The strongest inhibitor at 5mg/ml was the High-M alginate H120L.

Using the original Lin et al methodology, Strugala et al had shown that there was a link between alginate structural composition and levels of inhibition [7, 168]. Alginates high in mannuronic acid residues were shown to inhibit pepsin activity more strongly than those high in G-residues. The data presented herein supports this conclusion.

Not all alginates inhibit pepsin activity to the same degree, and as shown in Figure 37 alginates from the Lessonia species of brown seaweed inhibited pepsin activity more potently than Lamanaria alginates. Alginates from Lessonia are high in M-residues with F[M] ranging from 0.411 to 0.45 and Lamanaria alginates are high in G-residues, with F[M] ranging from 0.322 to 0.367. The four alginates from Lessonia seaweed caused significantly higher levels of inhibition than those derived from Lamanaria. This suggested a correlation between alginate structure and inhibition, however to ensure that this was not a species-effect, further alginates across the range of F[G] were tested.

A catalogue of eighteen alginates with a range of structural characteristics from high F[G] to high F[M] were tested in the modified N-terminal assay. The results showed a strong positive correlation between alginate F[M] and levels of pepsin inhibition with alginate at 5mg/ml. These results support the conclusion of Strugala *et al* 2005 that levels of pepsin inhibition are associated with alginates high in M-residues [7].

As the frequency of M-residues increases, the frequency of G-residues decreases and visa-versa. Therefore increasing levels of G-residues correlate with decreased levels of pepsin inhibition. The same pattern of correlation persists with F[GG] and F[GGG]. The frequency of contiguous guluronic-acid diads and triads was negatively correlated with Pepsin inhibition. Furthermore the average length of G-Blocks [n(g>1)] was also negatively correlated with pepsin inhibition. This suggests that an increasing proportion of contiguous G-Blocks is disruptive to the inhibitory effect of the alginates.

The hypothesis that increasing M-residues increases the potency of pepsin inhinition is supported by the data, however the relationship may not be as simple as to say levels of pepsin inhibition are solely determined by the M:G ratio. Patterns of structure-function relationship were apparent when looking at further structural characteristics of the alginates.

While the frequency M residues and contiguous M-Residue diads correlated with inhibition of pepsin, so too did mixed blocks of M and G. Increased F[GM/MG], F[MGM] and F[MGG/GGM] were positively correlated with increased levels of pepsin inhibition. It is therefore possible that while F[M] correlates with increased levels of pepsin inhibition is due to the disruption of gel forming contiguous G-Blocks. Heteropolymeric regions form flexible gels, are not as stable as G-rich gels. The potential importance of flexible gel structure to pepsin inhibition will be discussed further.

From selected kinetic analysis, alginates FMC6, FMC12, FMC13, LF10L, H120L, SF60 and LFR560 fit with a model of competitive inhibition. Competitive inhibition occurs when an inhibitor [I] directly competes for the active site and combines with the enzyme, blocking substrate binding to the active site.

By looking at other competitive inhibitors of pepsin activity, it is possible to get an idea of how alginate may competitively inhibit pepsin activity by binding to the active site. Pepstatin is a linear peptide inhibitor of aspartic proteases including pepsin [183]. It is a competitive pepsin inhibitor which blocks the active site by forming a network of hydrogen bonds and charge-charge interactions with active-site residues. The potential hydrogen bonding between pepsin and the inhibitor pepstatin are shown in Figure 63 below, and a number of charge-charge interactions are formed between the sidechains of the pepstatin residues and the pepsin molecule. The strongly bound inhibitor complexes with the enzyme and prevents substrate binding [184].
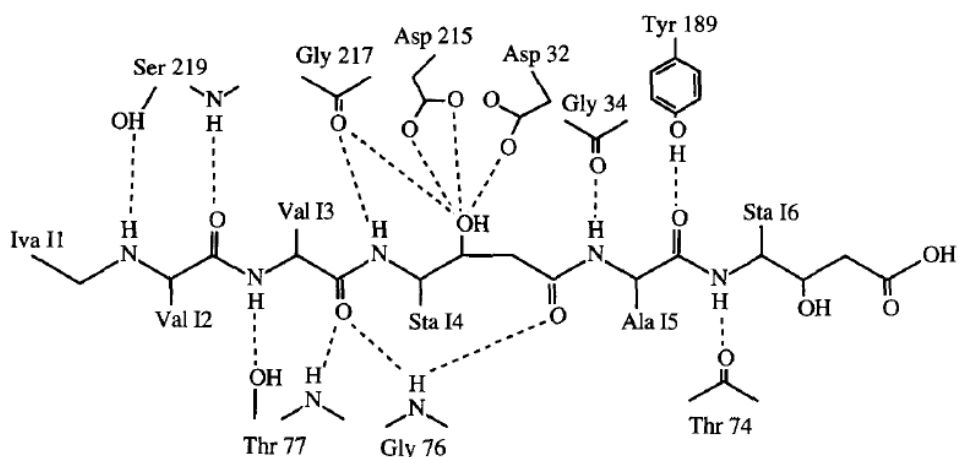
Figure 63   Stylized representation of potential hydrogen bonding between pepsin and pepstatin. Taken from Fujinaga *et al* 1995 [184].

Alginates are composed of mannuronic and guluronic acid residues rich in hydroxyl groups which would be capable of forming hydrogen bond interactions with these same active site residues. Furthermore the C=O group of the carboxyl group of the alginate residue is polarised; the oxygen attracts electrons more strongly than the carbon, making it δ- and the carbon δ+. This polarisation means that the C=O of the carboxyl group is able to participate in hydrogen bonding, and to a lesser extent form charge-charge interactions with positively charged amino acids of the pepsin molecule.

Similarly to pepstatin, alginate may affect pepsin activity by occupying the active site and forming a network of charge-charge interactions and hydrogen bonds to stabilise the interaction and therefore block substrate binding. This may also provide an explanation as to why High-M alginates tend to inhibit to a higher degree than High-G alginates. The increased chain flexibility with High-M alginates will cause the polymer chain to be more supple and able to adapt its shape to fit the active site of pepsin. The freer movement around the glycosydic bonds may therefore mean that High-M alginates are more capable of mirroring the structure of the protein molecules and forming a more stable interaction by bonding throughout the active site, whereas the rigidity of High-G alginates prevents them from doing so.

Other pepsin inhibitors operate by different mechanisms. As discussed, the assay system was validated using pentosan polysulphate (SP54) as a positive inhibition control. Pentosan polysulphate is a highly sulphated oligosaccharide shown to inhibit pepsin activity [179, 181] Sulphated polysaccharides have been shown to have anti-peptic effects, inhibiting the activity of pepsin *in vitro* and reducing peptic ulceration *in vivo* in rats and guinea-pigs [179, 185, 186]. The maximum inhibition with pentosan polysulphate at 5mg/ml was 75.1%.

Interactions between proteins and carbohydrates are common in biology, and are also widely reported *in vitro*, as reviewed in Dickinson et al 1998 [56]. SP54 and other highly sulphated polysaccharides such as heparin are known to inhibit pepsin activity [179, 180]. Heparin sulphate is a ubiquitous glygosaminoglycan well known for regulating proteolytic enzymes. Heparin is composed of repeating disaccharide subunits; composed of either D-glucuronic acid or L-iduronic acid, and D-glucosamine with N- and 6-O-sulphates and N-acetyl substitutions [187]. It is known to bind a wide range of proteins and is implicated as a regulator in hemostasis, inflammation, angiogenesism, cell adhesion and other biological processes. Furthermore heparin is

known to regulate the activity of proteolytic enzymes, both inhibitory and activatory effects have been observed [188, 189]. Heparin is an essential activator for several zymogens involved in the coagulation cascade [190]. It has been suggested that glycosaminoglycans exert their affect on proteolytic enzymes by inducing conformational changes to effect substrate binding, change catalytic activity, protect from pH inactivation or by exposing or masking the active site [191-193].

As well as enzyme-binding, carbohydrates have also been observed to be capable of a more general protein binding, raising the possibility of inhibitor-substrate interactions being involved in enzyme inhibition. Interactions between casein and carrageenans have been observed. This interaction is due to electrostatic interactions forming between the sulphate groups of the carrageenan and positively charged regions of the casein polymer [194, 195]. Hatzmann et al describe how as the pH is lowered and a protein is taken below its iso-electric point, it results in a loss of negative charges and formation of positive charges. The positively charged protein can then form interactions with negative charges on the carbohydrate and carbohydrate-protein complexes form, leading to gelation [196].

Likewise, alginate is a negatively charged polymer, and as such would be capable of forming electrostatic interactions with proteins that have become positively charged after being taken below their pK_a [197]. Alginate may associate with protein through hydrogen bonding at hydroxyl groups; charge-charge interactions with δ- carboxyl groups, and the negatively charged COO- group of the alginate, although this group would become protonated at low pH. As with the carrageenan-casein interactions, these reactions would be sensitive to structure, pH, concentration and levels of counterions. This also provides a clue as to why high-M alginates tend to be better inhibitors of pepsin activity than high-G alginates.

The characteristics of the alginate are dictated by the frequency and arrangement of blocks of guluronic and mannuronic acid. These residues can form G-rich, M rich, or MG rich blocks which determine the gelling properties of alginate in solution. G-rich blocks form relatively stiff blocks as there is limited rotation around the glycosidic bond. The presence of mannuronic acid residues increases chain flexibility with M blocks and MG blocks forming relatively flexible chains because of freer rotation around the glycosidic bonds. As discussed in the introduction, alginates form ionic gels by binding cations and by the formation of interchain associations between fibres.

Homopolymeric regions (M or G blocks) better support the formation of junction zones between adjacent polmers and therefore increase viscosity in solution, with G-Blocks forming the most stable gels. The affinity of an alginate for cations increases with G content as G-blocks have a greatly increased selectivity for divalent cations. Alternating blocks (MG blocks) increase the flexibility of the polysaccharide chain and therefore decrease alginate gel viscosity.

High-G alginates form stiff gels with rigid polymer chains at low pH and strongly bind divalent cations. Cations are strongly bound between adjacent alginate chains in the folded-ribbon "egg-box model" as described in the introduction, forming strong interchain associations. High-M alginates on the other hand form much weaker gels, with more flexible alginate chains. The binding of cations would compete for negatively charged COO- groups on the alginate chain, and the stronger these interactions are, the less likely these COO- groups will be free to interact with free protein substrate. Furthermore with stronger alginate interchain associations, a strong gel will be formed of tightly bound alginate which will not be free to interact with protein substrate. Increased chain flexibility with High-M alginates will also allow the polymer chain to be more supple and have freer movement around its glycosydic bonds, and therefore be more capable of mirroring the structure of the protein molecules it is interacting with.

Sunderland had suggested a link between molecular weight and levels of Pepsin inhibition [57]. The results of Strugala *et al* did not support this finding, and could not show any correlation between MW and levels of inhibition [7]. While data on molecular weight was only available for eight of the eighteen alginates tested, no correlation between molecular weight and inhibition was shown in this study.

The eighteen alginates tested in the higher-throughput micro-plate assays were tested again using a kinetic assay of pepsin activity. The kinetic assay used was a modification of the pepsin N-terminal assay. Alginate at 4mg/ml was tested against pepsin at a range of substrate concentrations (0-15mg/ml). The purpose of enzyme kinetics is to determine the point at which enzyme activity becomes independent of substrate concentration in order to determine enzyme-substrate affinity and the maximum reaction velocity. All tested samples were compared to a pepsin control.

The alginates causing inhibition of pepsin were fitted to theoretical models of pepsin inhibition which were, competitive, non-competitive, uncompetitive or mixed inhibition. Those that could fitted statistically to a model of inhibition fell in to two

categories; Non-competitive inhibition and competitive inhibition (Table 13). Seven of the sample alginates could not be fitted to a model, but were compared to the closest model of inhibition in Table 14.

Alginates FMC6, FMC12, FMC13, LF10L, H120L, SF60 and LFR560 fit with a model of competitive inhibition, and competitive inhibition was the closest fit model for LF120L and SF120. Three of the tested alginates fitted a model of non-competetive inhibition; FMC2, FMC3 and FMC9 and it was the closest fit model for FMC7 and FMC10. Mixed inhibition was the closest fit model for SF/LF, SF200 and FMC4.

As has been discussed already, there are a number of possible inhibition mechanisms by which alginate may reduce pepsin activity, these include; a competitive alginate-pepsin interaction where alginate competes with substrate for the active site; a non-competetive alginate-pepsin interaction where alginate binds to the enzyme somewhere other than the active site and modifies enzyme activity; or by a direct substrate binding. The fact that all of the alginates did not fit to one single model of inhibition suggests that more than one of these single mechanisms of inhibition may be acting in concert to produce the inhibition effects.

Competitive Inhibition occurs when an inhibitor [I] directly competes for the active site and combines with the enzyme, blocking substrate binding to the active site as is the mechanism with Pepstatin. As discussed, alginate may function in a similar way and occupy the binding site, stabilised by hydrogen bonding and charge-charge interactions. However, this is not the only scenario which could produce an inhibition profile for that of competitive binding. If alginate were directly binding the protein substrate, similar to the manner seen with carrageenan and milk-protein, then an inhibition profile would be produced where the V_{max} remained unaltered, but the enzyme-substrate affinity appeared to be reduced. By binding to protein substrate and removing it from the reaction solution, the reaction velocity at low substrate concentration would be reduced. This would occur because although there is an apparent net concentration of substrate in the reaction solution, a certain proportion of this substrate is bound to alginate and therefore not free to interact with the enzyme. However with increasing substrate concentrations, this effect is overcome and as the concentration tends towards an 'infinite' concentration, the binding effect will therefore be diluted into insignificance and the normal maximum velocity will be reached.

Not all of the alginates however fitted the model of competitive inhibition. FMC2, FMC3 and FMC9 fit the model of non-competitive reversible inhibition, and this model was the closest fit model for FMC7 and FMC10. Non-Competitive Reversible inhibition occurs when the inhibitor binds the enzyme at a point other than the active site, either when the enzyme is free or in complex and does not affect substrate binding. As substrate binding and dissociation is unaffected the K_m will be unaltered as [ES] complex formation and dissociation will be unhindered. The inhibitor causes its effect by impeding or blocking substrate formation and V_{max} will therefore be reduced.

The mechanism of non-competitive reversible inhibition may be similar to what can be seen with certain types of heparin sulphate inhibition whereby binding of inhibitor causes conformational changes to the enzyme which impedes or blocks product formation. With non-competitive reversible inhibition, the Km is unchanged, as ES association and disassociation are affected in equal proportions, V_{max} however is reduced, because the inhibitory effect cannot be out competed by increasing substrate concentration.

The idea of a direct inhibitory interaction between alginate and pepsin was also argued by Sunderland et al who showed in an alginate-pepsin centrifugation experiment that pepsin was pulled out of the supernatent by alginate upon centrifugation [57]. This suggested direct binding of pepsin as a possible mechanism of inhibition.

The inhibition of lipase with pectin provides an example of how alginate may inhibit pepsin activity directly. Carboxyl groups have been shown to be important in enzyme inhibition, as in the case of pectin and lipase. The carboxyl groups of pectin are believed to be involved in the protanation of active site serine residue of the lipase enzyme. The catalytic mechanism of lipase is based on a charge relay system between the residues of the catalytic serine-histidine-apartic-acid triad, and protonation of the hydroxyl group of serine blocks the initiation of this charge relay system, thereby inactivating the enzyme [5]. The importance of carboxyl groups to pectin inhibition of lipase has been shown as increasing levels of methyl esterification are correlated with reduced lipase inhibition. As it is the carboxyl group that becomes esterified, an increase in methyl esterification necessarily means a decrease in the number of carboxyl groups.

Similar to pectins, alginates are rich in carboxylic acid groups. As seen in Figure 6, each monosaccharide residue of alginate contains a carboxyl groups which would become

protonated at low pH forming carboxylic acid. These carboxylic acid groups are involved in the hydrogen bonding network which forms as alginate interact to form an acid gel at low pH. It is therefore possible that a similar interaction occurs between the carboxylic acid groups of alginate and active site residues of pepsin as occurs with pectin and lipase. It is possible that similar interactions may form with the active site Asp32 residue of pepsin, disrupting the acid-base pair of Asp32-Asp215, and thereby preventing nucleophilic attack on the peptide bond. As the pH is taken below the pK_a of the alginate, COO- groups will become increasingly protonated, however there will still be a mix of COO- and COOH groups, with the proportion of COOH increasing at lower pH. The COOH groups may participate in hydrogen bonding with the negatively charged active site Asp residues. Aalternatively the COO- groups would disrupt the charge relay system of the catalytic mechanism by the presence of a large negative charge which could disrupt nucleophilic attack by attracting the nucleophillic H+, or attracting H_2O preventing regeneration of the catalytic nucleophile.

While direct interactions between alginate and pepsin may be a possible mechanism of inhibition, data presented in the next chapter supports the theory that there is a more general protein binding interaction which may affect enzyme activity through substrate binding as well binding directly to the enzyme.

The interaction of these two mechanisms; substrate binding and enzyme binding, may explain why the kinetic data fit to more than one model of inhibition, and that in some cases, mixed inhibition was the closest model.

A significant negative correlation between K_m and alginate F[G] was observed. This correlation suggests that with an increasing frequency of Mannuronate the enzyme substrate affinity of pepsin for succinyl albumin substrate is decreased and more substrate is required to reach half of the maximal velocity than with the uninhibited enzyme.

A similar negative correlation was observed between F[G] and V_{max} whereby the maximal reaction velocity of the reaction tended to increase the presence of alginates with increased mannuronic acid residue frequency.

This may seem counter intuitive, that the trend is for the better inhibitors to be associated with a higher V_{max}. However a possible explanation for this is that there are two mechanisms at work, firstly an inhibitory mechanism that reduces enzyme activity

at lower substrate concentrations which can be overcome by increasing substrate concentration. At higher substrate concentrations, the inhibitor is out competed and does not inhibit enzyme activity. This provides an explanation of how the inhibitory effect is lost at high substrate concentrations, but there is necessarily a second mechanism resulting in an increase in V_{max} at high substrate concentrations. This could be a number of mechanisms including the presence of alginate reducing the volume of the reaction mixture causing it to occur at a faster rate.

The apparent kinetic constants K_m and V_{max} were used to calculate the inhibitor constant K_i. K_i, the inhibition constant is the amount of inhibitor theoretically required to halve the V_{max} and therefore indicates how potent an inhibitor is. Despite this unexpected relationship between the structural characteristics and V_{max}, there was astill a strong positive correlation between alginate F[M] and K_i. Reiterating the correlation between potency of inhibition and the presence of mannuronic acid residues.

The current data confirmed the observations of Strugala et al that lengths of G-Blocks (F[G], F[GG], F[GGG] and]N(G>1)]) were associated with reduced inhibition. Higher mannuronic acid F[M], and alternating alginate structure F[GM/MG] and F[MGM] were all positively correlated with pepsin inhibition. Strugala et al suggested that the increased inhibition levels observed with these alginates may either be due to a specific interaction between alternating sequences of alginate and pepsin, or due to the physical properties of these alginates favouring acid solubility. It was shown by Smidsrod and Draget that alternating seguences of M and G residues conferred on alginates good acid solubility and chain flexibility [198]. It was suggested by Strugala *et al* that these physical properties may lead to a prolonged exposure of pepsin to these alginates and increase the probability of inhibitory interactions occurring.

Chapter 4
Modulation of Trypsin Activity

4.1 Introduction

After gastric digestion, the digesta is passed into the small intestine. In the duodenum the acidic chyme is neutralised upon mixing with the pancreatic juices which are rich in bicarbonate (secreted by duct cells). The pancreas secretes a range of proteolytic, amylolytic and lipolytic digestive enzymes as shown in Table 3 in Section 1.7. Although digestion is well underway by the time food reaches the small intestine, the majority of food is digested by pancreatic enzymes which are secreted into the pancreatic duct by acinar cells of the exocrine pancreas [85]. Before the pancreatic juices are released into the duodenum through the sphincter of Oddi, they are mixed with bile in the ampulla of Vater, where the pancreatic duct and common bile duct merge [86].

As discussed in Section 1.7.3, protein digestion is completed in the small intestine in three phases; 1) luminal protein digestion 2) brush border membrane digestion and 3) Cytoplasmic assimilation of polypeptides. Proteolytic enzymes (Table 15) are secreted from the pancreas into the small intestine as zymogens and activated during the proteolytic enzyme cascade which also causes the activation of pancreatic lipase and colipase.

4.2 Pancreatic Proteolysis

A reported 2% of the human genome codes for proteolytic enzymes or protease inhibitors. This fraction of the genome is collectively referred to as the degradome and is comprised of '561 protease and protease-related genes and more than 156 protease inhibitor genes' [199].

The pancreatic proteases can be divided into two groups; the endopeptidases and the exopeptidases (Table 15). The endopeptidases trypsin, elastase and chymotrypsin are serine proteases that cleave interior peptide bonds. The carboxypeptidases are zinc-containing metallopeptidases with exopeptidase activity and cleave single amino acids from the carboxyl terminal of polypeptides [200].

Proteases are a broad category of enzymes which cleave peptides via a range of mechanisms by which they are categorised; proteases are classified as aspartic-, cysteine-, serine-, threonine-proteases and metallo-proteases [199]. Of these, serine proteases are the most abundant, making up over one third of all known proteases [200, 201]

Enzyme Family	Enzyme	Favoured Site of Activity
Serine proteases (endopeptidases)	Trypsin	cleaves on the carboxyl side of basic amino acids (Arg, Lys)
	chymotrypsin	aromatic carbonyl group (Tyr, Phe, Trp)
	Elastase	aliphatic carboxyl group (Ala, Leu, Gly, Val, Ile)
Zinc-containing metallopeptidases (exopeptidases)	Carboxypeptidases A and B	single amino acids from the carboxy terminal ends of proteins and oligopeptides

Table 15   The pancreatic proteases, taken from Erickson *et al* 1990 [201].

4.2.1   Trypsin Activation and the Proteolytic Enzyme Cascade

The proteolytic zymogens trypsinogen, proelastase, chymotrypsinogen, the procarboxypeptidases and kallikreinogen are secreted from the pancreas in response to a meal. This array of proteolytic enzymes are secreted into the small intestine from the pancreas as zymogens which are activated during the proteolytic enzyme cascade (**Error! Reference source not found.**) which also causes the activation of pancreatic lipase and colipase.

The mucosal enzyme enterokinase catalyses the activation of trypsinogen to trypsin. Enterokinase is a 316kDa glycosylated protein synthesised by small intestinal enterocytes. While trypsinogen is capable of autocatalytic activation, activation by enterokinase is reported to be 2000 times more efficient [202]. Activated trypsin then mediates the activation of pancreatic zymogens to their active forms.

4.3   Serine Proteases

Trypsin is part of the serine protease family of proteolytic enzymes. Serine proteases make up over a third of the known proteases and are named as such due to the catlytic mechanism depending upon a nuclephillic serine residue at the active site [200, 203].

Serine proteases are usually endopeptidases and preferentially cleave within the poplypeptide chain.

Commonly the serine residue is as part of the Asp-His-Ser catalytic triad by which Serine proteases were first thought to be characterised. However a range of serine dependent catalytic mechanisms have been identified in other families of serine proteases as described in Table 16.

Clan	Families	Representative member	Catalytic residues	Primary specificity
PA	12	Trypsin	His, Asp, Ser	A, E, F, G, K, Q, R, W, Y
SB	2	Subtilisin	Asp, His, Ser	F, W, Y
SC	2	Prolyl oligopeptidase	Ser, Asp, His	G, P
SE	6	D-A, D-A carboxypeptidase	Ser, Lys	D-A
SF	3	LexA peptidase	Ser, Lys/His	A
SH	2	Cytomegalovirus assemblin	His, Ser, His	A
SJ	1	Lon peptidase	Ser, Lys	K, L, M, R, S
SK	2	Clp peptidase	Ser, His, Asp	A
SP	3	Nucleoporin	His, Ser	F
SQ	1	Aminopeptidase DmpA	Ser	A, G, K, R
SR	1	Lactoferrin	Lys, Ser	K, R
SS	1	L,D-carboxypeptidase	Ser, Glu, His	K
ST	5	Rhomboid	His, Ser	D, E

Multiple members of each clan may give rise to a wide variety of primary specificities, as documented by the PA, SJ, and SQ clans.

Table 16   General properties of serine proteases. Taken from De Cera et al 2009 [200]

Serine proteases are found in prokaryotes, eukaryotes, archae and viruses. In the human they are critical to a range of physiological processes including immune response, blood coagulation, reproduction, signal transduction, and as discussed herein digestion [204].

4.4   Trypsin

In humans, trypsin is synthesised as the proenzyme trypsinogen by acinar cells of the pancreas and stored in secretory granules for release in response to a meal and subsequent activation by enterokinase [205]. As well as its importance as a digestive protease, trypsin is also key for its role in downstream activation of other zymogens in to their active forms.

Trypsin has a strong preference for cleavage after Arg or Lys residues at P1, with relative values of catalytic efficiency 10^5 times higher for basic amino acids than others [205]. The pH optimum of trypsin is generally reported at pH 7-9, although this varies with species [206]. Trypsin is inactive at low pH, although can remain stable in solution

down to pH3 [205]. It was after the discovery of pancreatic trypsin that the German physiologist Willhelm Kuhne fist coined the term enzyme [207].

4.4.1 Categorisation

Trypsin is part of the serine protease family of enzymes (EC 3.4.21.4) and belongs to the PA clan of serine proteases which depend upon the His, Asp, Ser catalytic triad. Trypsin is the major proteolytic enzyme of the small intestine, and along with the other small intestinal proteases is responsible for completing the digestion of dietary protein after passage from the stomach to small-intestine. Trypsin is an endopeptidase which prefererentially cleaves on the carboxyl side of lysine and arginine.

Duodenal trypsin digestion is thought to be important in breaking down large proteins for further digestion by the small-intestinal proteases.

4.4.2 Structure of Trypsin

Active trypsin has a reported molecular weight of roughly 25kDa, *Leon et al* report the MW as specifically 23,800 daltons [205, 208]. Trypsin shares a tertiary structure which is highly conserved throughout the serine protease family. The 3d structure of bovine trypsin was first solved in 1974, trypsin has become the proteotypic structural model for serine proteases [209].

Trypsin is a globular protein molecule whose tertiary structure is comprised primarily of β-sheet. In terms of primary structure, active trypsin is composed of a single polypeptide chain. Trypsin has a two domain structure with the active site domain contained in between the two β –Barrel containing domains.
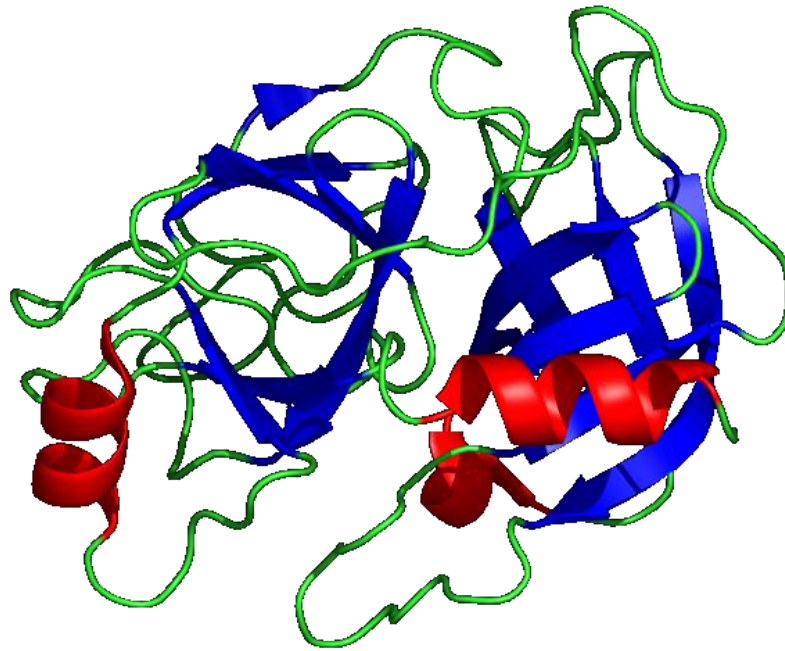
Figure 64   Crystal structure of Bovine Trypsin. Taken from Leiros et al 2004 [210].

Trypsin has a calcium binding site formed by a loop from Glu70-Glu80. Calcium binding is known to be important to trypsin structure and function and autodegredation of trypsin is shown to occur in its absence [209, 211].

4.4.3   Activation of Trypsin

All trypsins are synthesised as pro-enzymes. An N-terminal propeptide which varies between species normally contains hexapeptide consensus sequence of $(Asp)_4$–Lys-Ile16-Val17-Gly-18Gly19 for cleavage by enteropeptidase with clevage occurring between the Lys and Ile16 residues.

Cleavage of the N-terminal propeptide disrupts a His40, Asp194 hydrogen bond which allows a rotation of Asp194 so it is able to interact with the new Ile16 N-terminal.This rotation allows formation of the catalytically critical Oxyanion Hole comprised of the amide groups of Gly193 and Ser195. This new conformation is stabilised by hydrophobic interactions of the Ile16 sidechain [205].

4.4.4   Substrate Binding

Active trypsin binds substrate by forming an anti-parallel beta-sheet across the protein binding site. Asp189 has been shown to be critical to substrate specificity, substitution with Ser results in a 10^5 fold decrease in catalytic efficiency for substrates with Arg and

Lys at P1 position [212]. A direct interaction between Asp189 and the guanidinium side chain of Arg has been shown. In the case of Lys, a water molecule is required to mediate the Asp189-Lys interaction [213].

4.4.5   Catalytic Mechanism

Serine proteases are characterised by the nucleophillic serine residue which is part of the catalytic triad of Asp-His-Ser [205, 214]. The residues of the catalytic triad are spread across the active site cleft. With Ser195 on one side and Asp102 and His57 on the other [214].

The proximity of Asp102 and His57 is important to the reaction mechanism. The carboxylate group of Asp102 forms hydrogen bonds with the imidizole functional group of His57 and polarises it to enhance its function as a proton shuttle [215].   Another important structural feature of the serine protease is the oxyanion hole formed by the amine groups of Gly193 and Ser195 which form a positively charged pocket that is important for stabilising the negatively charged intermediary of the reaction which shall be discussed later [203].

4.4.6   Reaction Mechanism

With the substrate co-ordinated in place, the electronegatively charged base His57 can act to accept the hydrogen from the hydroxyl group of Ser195. This allows Ser195 to act as a nucleophile, attacking the carbonyl carbon of the peptide bond, forming an acyl-enzyme intermediate with the substrate [204]. The carbonyl carbon is $\delta+$ as a dipole is formed over the C=O bond with the electrons pulled towards the electronegative oxygen, leaving the carbon susceptible to nucleophillic attack from serine.

In the newly formed tetrahedral acyl-enzyme intermediate, the carbonyl carbon is bound to the serine oxygen, the carbonyl oxygen, the scissile amino group as well as being bound to the α-carbon of it's own amino acid. Each of these bonds is a single bond, and the electron from C=O double bond moves to the carbonyl oxygen which becomes negatively ionised. The positively charged pocket of the previously described oxyanion hole is important for stabilising this negatively charged intermediate [214].

The His57 bound hydrogen is then donated to the scissile nitrogen and the peptide bond is broken as the double bond is reformed between the carbonyl carbon and the carbonyl

oxygen [204]. The formation of the NH group releases the N-terminal product from the active site and leaves His57 electronegatively charged. With release of product, a water molecule can enter and attack the electron dense nitrogen (δ-) of His57 with a hydrogen and the carbonyl carbon with the resulting hydroxyl group thus deacylating the acyl-enzyme intermediate and freeing the carboxyl component of the substrate from Ser195 [203]. The hydrogen newly bound to the His57 nitrogen then moves across to Ser195 to reform a hydroxyl group and regenerate the active site (Figure 65).
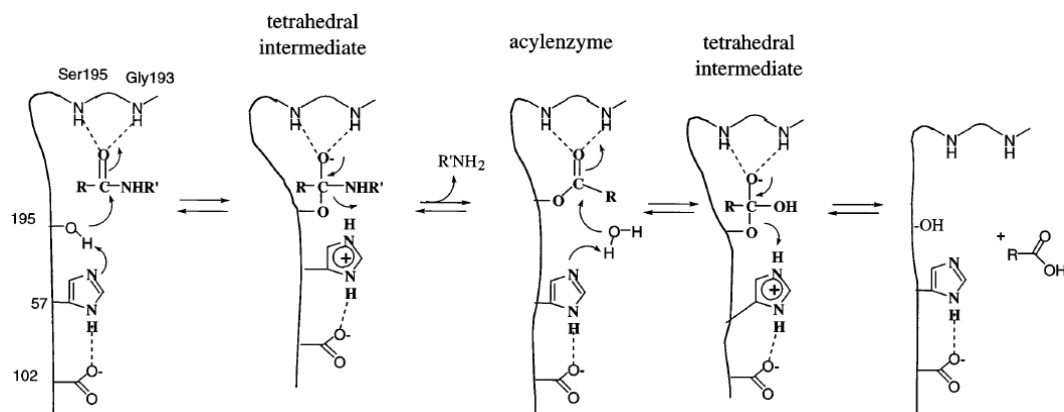
Figure 65   The generally accepted mechanism for serine proteases. Taken from Hedstrom *et al* 2002 [203].

4.4.7   pH optima and inactivation

Ph optimum of trypsin is generally reported at pH 7-9, although this varies with species. Trypsin activity rapidly decreases below pH7 and is relatively inactive at low pH, although can remain stable in solution down to pH3 . Trypsin activity is highest at pH7 and above, however, pH inactivation is also most rapid at above neutral pH [206]. Figure 66 shows the inactivation profile of trypsin after 15 minutes at 0°C and 24 hours at 30°C. As can be seen, at 0°C after 15 minutes, trypsin is stable at pH 1-12, at a pH higher than 12, trypsin is rapidly inactivated. After 24 hours at 30°C trypsin is denatured at low pH and will precipitate, at pH~2.5 the enzyme is stable but inactive, at pH approaching neutral, trypsin becomes active and therefore will autocatalytically digest over the course of 24 hours (Figure 66) [216].
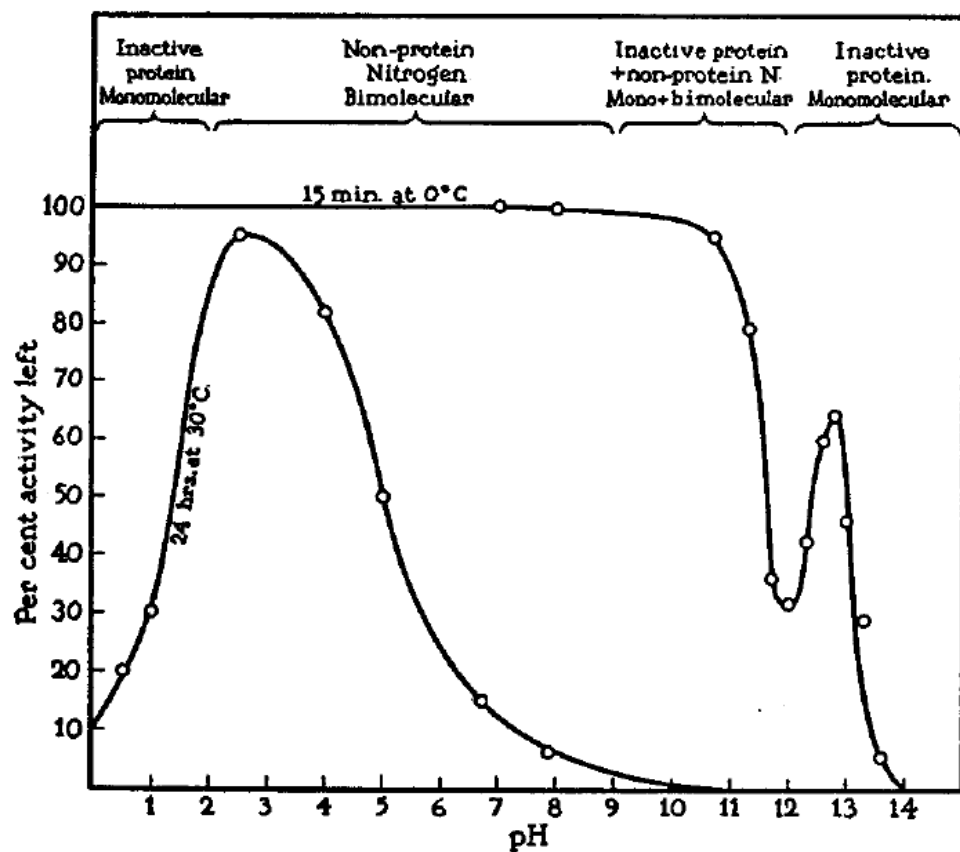
Figure 66   Loss of trypsin activity after 15 minutes at 0°C and 24 hours at 30°C Taken from Kunitz *et al* 1934 [216]

4.5   Aims

Previous literature, and the data generated in Chapter 3 showed that alginates are capable of inhibiting the action of pepsin, and that the levels of inhibition are related to structure.

Protein digestion occurs throughout the upper digestive tract through the combined physical, chemical processes of digestion and the actions of proteolytic enzymes. The aim of this chapter therefore was to investigate the effects of bioactive alginates on the action of the enzyme trypsin. A library of bioactive alginates was tested in high throughput assays to screen for regulatory effects, and structure-function relationships were investigated. Selected enzyme kinetics were carried out to attempt to elucidate the nature of any regulatory effects.

Selected viscometric and rheological investigations were carried out to look at the way in which alginates interact with protein substrates.

4.5.1 Introduction to gel rheology

Rheology is the study of the flow and deformation of materials - liquids and soft-solids - under external stresses.

When alginate gels, it forms a polymeric gel composed of a network of cross-linked biopolymers and as such can have properties like that of a visco-elastic solid [217]. The properties of a polymeric gel are determined by the structure of the polymer, the composition of the surrounding liquid (the sol), and the manner in which the polymers interact. Strong gels may form when polymers are chemically cross linked which if broken will not reform. Weak gels form from the formation of cross-links between polymers and these may break and reform under stress. Pseudo gels may also form, these are entangled polymer systems that mimic some of the properties of gels [217].

Polymeric interactions between proteins and polysaccharides have been shown previously. In solution proteins and polysaccharides may attract and complex, or repel and segregate [218]. A segregation and phase separation occurs when the gain of entropy which would occur on mixing is outweighed by the thermodynamic energy disadvantage, meaning it is energetically favourable to resist mixing. If polymer mixing is energetically favourable a heteropolymeric mixture will occur and lead to polymeric interactions. Such interactions give rise to synergistic changes in rheological properties which are greater than that expected from the individual components.

Alginates form viscoelastic gels which has previously been shown to interact with other biopolymers, including proteins and mucins. Such interactions are likely to modify the rheological properties of the alginate gel

4.6 Plate-Plate Rheology

In plate-plate rheology, the test sample is held between two parallel plates at a fixed distance apart (h) (Figure 67). The bottom plate is fixed in place, and the top plate (moved plate) with a surface area A (m^2) is rotated by a force F [$N=kgm/s^2$] at a speed v [m/s] and the test material is displaced by distance (s) with a deformation angle (α). From this, the shear reate, shear stress, viscosity and strain can be calculated using the formulae shown in Figure 67 below.
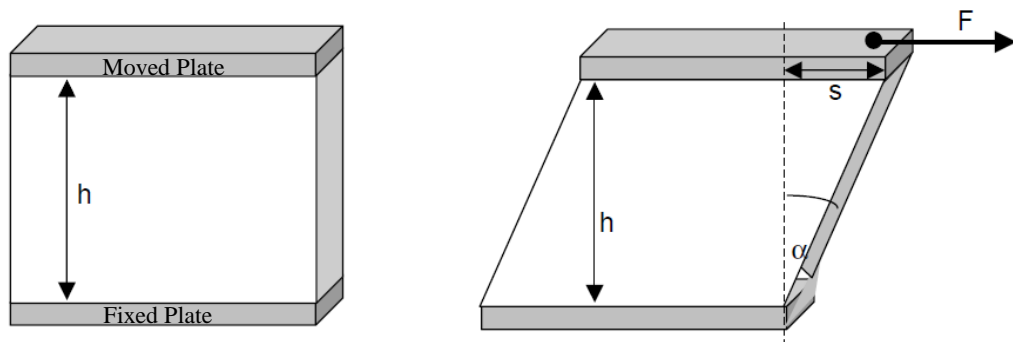
Shear rate	$\dot{\gamma} = v / h$	in s^{-1}
Shear stress	$\tau = F / A$	in Pa
Viscosity	$\eta = \tau / \dot{\gamma}$	in Pas
Strain	$\gamma = ds / h$	dimensionless

Figure 67 Diagram of Plate-Plate rheometer and formulas for calculating shear rate, shear stress, viscosity and strain. Taken from Rheotec: Introduction to Rheology [219]

Plate-plate oscillatory rheology is based on applying a rotational stress to a material and measuring the induced strain. This rotation of the upper plate applies a shear stress to the sample. The shear stress τ is the force (F) applied over the given area (A). Strain is the resulting displacement of particles within the sample, it is a dimensionless unit which can be calculated from the deformation angle (α) and distance of displacement (s).

Pure solids can be referred to as Hookean, as they are non-yielding and follow Hookes law that the force required to produce a displacement is directly proportional to the displacement. This linear-elasticity means that the stress and strain waves are in perfect phase and maximum strain occurs at the point of maximum stress. Hookean solids therefore have a phase angle of 0°.

Hookean Solid:
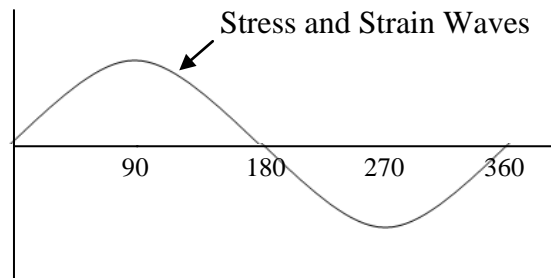
In a newtonian fluid, stress and strain are 90° out of phase as the maximum strain occurs at the point of maximum change in the rate of stress and at the point of maximum stress the strain is zero. However, many materials are neither perfect Hookean solids or perfect Newtonian liquids and therefore under stress the stress-strain wave phase angle will lie somewhere between 0 and 90°.

Newtonian Fluid:
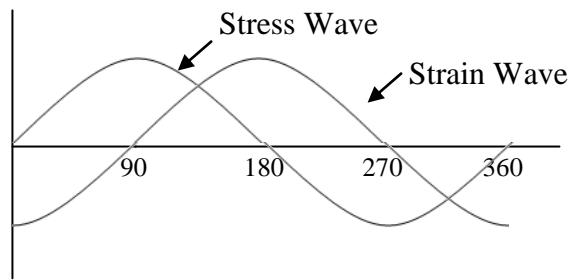
Materials with a phase angle of 0- 45° exhibit more solid-like behaviour and are considered gels. Materials with a phase angle of 45-90° exhibit more fluid-like behaviour and are considered liquid. The solid like behaviour with a phase angle of 0-45° corresponds to a higher elastic modulus (G') than viscous modulus (G"). In liquid like behaviour with a phase angle of 45-90° the viscous modulus is higher than the elastic modulous and G" >G'.

Solid-like Viscoelasctic Fluid
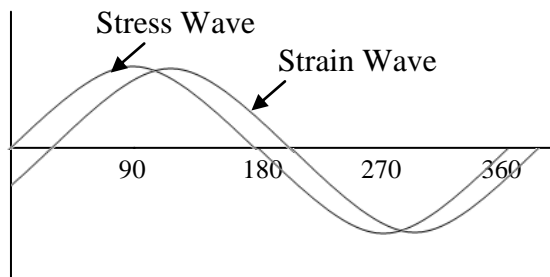
Liquid-like Behaviour:
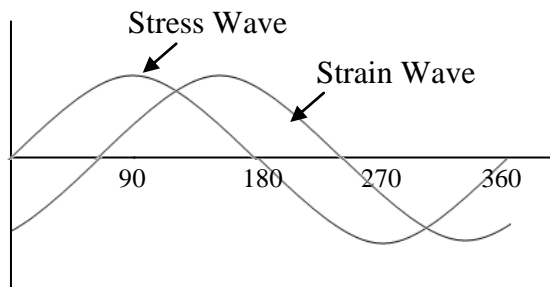
The viscous and elastic moduli are derived from the Shear Modulus, which is a measure of the stress/strain ratio.

$$\text{Shear modulus } G = \frac{\text{Shear stress } \tau}{\text{Strain } \gamma} = \frac{Pa}{1} = Pa$$

The elastic modulus (G') and viscous modulus (G") are derived using the formulae below. The elastic phase is the component of the shear modulus which is in-phase with the deformation, and the viscous component the part which is out-of-phase [217].

$$\text{Elastic modulus} \qquad G' = G*Cos\delta$$

$$\text{Viscous modulus} \qquad G" = G*Sin\delta$$

Oscillatory frequency testing provides an important tool for understanding the rheological properties of a material. The way a material responds to deformation gives information about its physical properties. After a deformation, the material will relax through Brownian motion to its energetically favourable state. At low frequencies both viscoelastic gels and viscoelastic liquids can dissipate energy and return to an energetically favourable state. However as relaxation time is proportionate to molecular weight, gel network relaxation times can increase with the size of the network to an infinite value, at which point they will never relax to their original state. As the frequency of oscillation increases, the polymers do not have time to rearrange and the way in which the polymers are entangled will contribute to the response of the material to stress [217].

4.7   Experimental Section

4.7.1   Materials

All dietary fibre samples were supplied by FMC Biopolymer and Technostics (Hull, UK). Bovine serum albumin was purchased from VWR Jencons. Unless otherwise stated, all other chemicals and reagents were purchased from Sigma Aldrich (Poole, UK).

4.7.2   Equipment

A Biotek 96 well plate reader set at 340nm was used for spectrophotometric measurements (Elx808 Biotek, Bedfordshire, UK). An Autoblot microhybridization oven was used for temperature incubations at 37°C and 55°C (Bellco Glass Inc, Vineland, NJ). A Martini Mi150 pH meter was used for all pH measurements. (Milwaukee Instruments, Inc. NC, 96-Well Plate N-Terminal Method U.S.A.).

4.7.3   Devlopment of High Throughput Trypsin N-Terminal Assay

The trypsin N-terminal assay works on the same basis as the pepsin N-terminal assay as both assays use the generation of new N-terminals during peptide cleavage as a direct measure of proteolysis. The trypsin assay requires a modification of the methodology as trypsin has a pH optimum of around pH7. A 0.066 M Sorensens Phosphate pH 6.85 was used to buffer the alginate samples, as can be seen from Figure 68.
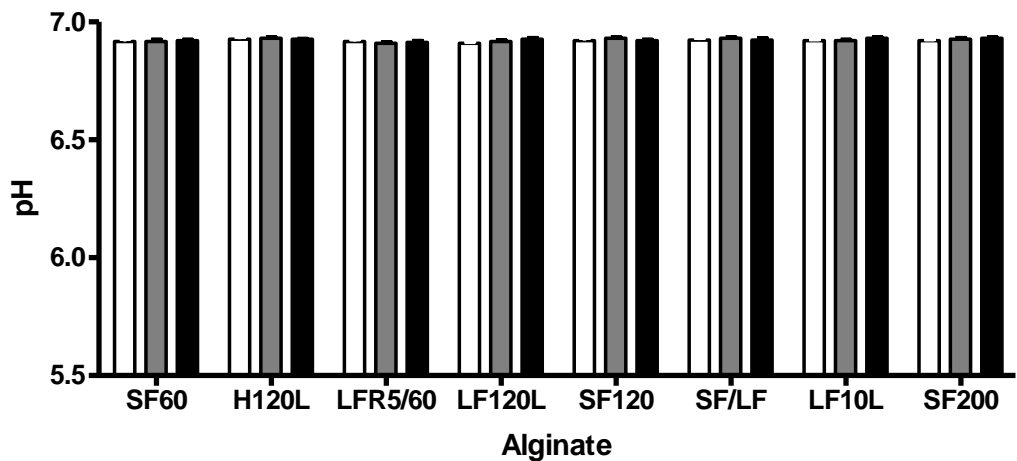
Figure 68   pH variation of reaction solution with addition of alginates made up in 0.066 M Sorensen's phosphate buffer, □ 0.25mg/ml ▨ 1mg/ml, ■ 4mg/ml.

4.8   Preperation of Solutions

Figure 69 shows the assay tested at a range of trypsin and TNBS concentrations in order to work out optimum reaction conditions.
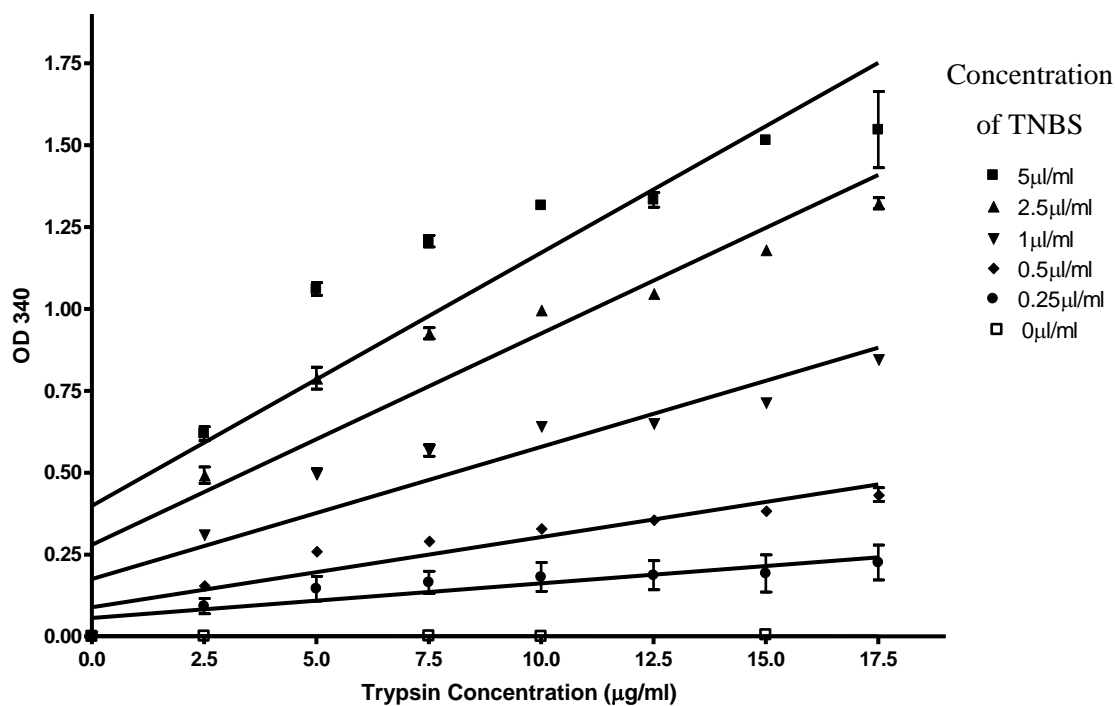
Figure 69   Colour development with Trypsin N-Terminal assay at varying trypsin and TNBS concentrations.

For high-throughput analysis, biopolymer samples were prepared at 10mg/ml in 0.066˙ M Sorenren's Phosphate buffer. It was decided that Tri-nitro benzo sulfonic acid (TNBS) would be prepared at 2µl/ml in deionised water and trypsin at 5µg/ml.

In order to raise the pH for trinitrophenylation, only 4% w/v Sodium Bicarbonate was required.

4.9 Method

30ul alginate sample was pre-incubated with 50μl succinyl albumin substrate for 30 minutes on shaker. At T_0 30μl of trypsin solution or buffer blank was added as appropriate and the plate was incubated for 30min at 37°C. After 30 minutes, 50μl sodium bicarbonate and 50μl TNBS were added and the plate was incubated for 15 minutes in the Autoblot Microhybridisation oven at 55°C. At T_{45}, 50μl SDS and 50μl 1M Hydrochloric Acid were added and the plate was left to stant until all wells had stopped effervescing, and samples were read at 340nm.

To calculate percentage pepsin inhibition the following formula was used:

$$\text{Percentage trypsin inhibition} = \frac{Polymer\ Sample - Sample\ Control}{Trypsin\ Control - Background\ Control} \times 100$$

4.9.1 Plating

4.9.2 Plating – HTP Assay

| | Blank | Trypsin Control | Sample A | | | Sample B | | | Sample C | | | Blank |
| | | | 5 mg/ml | 2.5 mg/ml | 1.25 mg/ml | 5 mg/ml | 2.5 mg/ml | 1.25 mg/ml | 5 mg/ml | 2.5 mg/ml | 1.25 mg/ml | |
	1	2	3	4	5	3	4	5	3	4	5	12
A	60µl Buffer	30µl Buffer 30µl Trypsin	30µl Trypsin 30µl Sample	30µl Trypsin 30µl Sample	30µl Trypsin 30µl Sample	30µl Trypsin 30µl Sample	30µl Trypsin 30µl Sample	30µl Trypsin 30µl Sample	30µl Trypsin 30µl Sample	30µl Trypsin 30µl Sample	30µl Trypsin 30µl Sample	60µl Buffer
B	60µl Buffer	30µl Buffer 30µl Trypsin	30µl Trypsin 30µl Sample	30µl Trypsin 30µl Sample	30µl Trypsin 30µl Sample	30µl Trypsin 30µl Sample	30µl Trypsin 30µl Sample	30µl Trypsin 30µl Sample	30µl Trypsin 30µl Sample	30µl Trypsin 30µl Sample	30µl Trypsin 30µl Sample	60µl Buffer
C	60µl Buffer	30µl Buffer 30µl Trypsin	30µl Trypsin 30µl Sample	30µl Trypsin 30µl Sample	30µl Trypsin 30µl Sample	30µl Trypsin 30µl Sample	30µl Trypsin 30µl Sample	30µl Trypsin 30µl Sample	30µl Trypsin 30µl Sample	30µl Trypsin 30µl Sample	30µl Trypsin 30µl Sample	60µl Buffer
D	60µl Buffer	60µl Buffer	30µl Buffer 30µl Sample	30µl Buffer 30µl Sample	30µl Buffer 30µl Sample	30µl Buffer 30µl Sample	30µl Buffer 30µl Sample	30µl Buffer 30µl Sample	30µl Buffer 30µl Sample	30µl Buffer 30µl Sample	30µl Buffer 30µl Sample	60µl Buffer
E	60µl Buffer	60µl Buffer	30µl Buffer 30µl Sample	30µl Buffer 30µl Sample	30µl Buffer 30µl Sample	30µl Buffer 30µl Sample	30µl Buffer 30µl Sample	30µl Buffer 30µl Sample	30µl Buffer 30µl Sample	30µl Buffer 30µl Sample	30µl Buffer 30µl Sample	60µl Buffer
F												
G												
H												

Figure 70   Plating layout for the trypsin N-Terminal microplate assay.

4.9.3   Kinetic assay of Trypsin Activity

The kinetics of dietary fibre interactions with trypsin were measured, as with pepsin using a modification of the 96 well-plate N-Terminal method previously described.

Substrate dilutions were prepared from a stock of 25mg/ml succinyl albumin and plated out as below, including a control and blank lane both at 10mg/ml succinyl albumin. 200µl was plated into each well so that there would be sufficient substrate for 3 plates to be run in triplicate.

Blank Lane	Control Lane	Substrate Dilutions (mg/ml)									
10	10	25	20	15	10	5	2.5	1.25	0.625	0.3125	0
10	10	25	20	15	10	5	2.5	1.25	0.625	0.3125	0
10	10	25	20	15	10	5	2.5	1.25	0.625	0.3125	0

Table 17 Substrate dilutions for Trypsin N-Terminal Kinetic assay.

In sample plates 30µl of DF sample (4mg/ml) was pre-incubated with 30µl trypsin (5µg/ml) for 15 minutes at 37˚C to give sample concentrations of 2mg/ml and 5µg/ml respectively. At T_0 50µl of of substrate was added into the appropriate wells and incubated for 30 minutes. After 30 minutes 50µl $NaHCO_3$ and 50µl of TNBS was added and the temperature raised to 55°C for colour development. After 15 minutes at 55˚C. 50µl SDS and 50µl HCl was then added and the plate was left to stand until effervescence had stopped. Samples were then read at 340nm.

4.9.4 Plating Kinetic assay

	Blank Lane	Control Lane	Substrate Dilutions 25mg/ml	Substrate Dilutions 20mg/ml	Substrate Dilutions 15mg/ml	Substrate Dilutions 10mg/ml	Substrate Dilutions 5mg/ml	Substrate Dilutions 2.5mg/ml	Substrate Dilutions 1.25mg/ml	Substrate Dilutions 0.625mg/ml	Substrate Dilutions 0.3125mg/ml	Substrate Dilutions 0mg/ml
A												
B	60ul Buffer	30ul Sample 30ul Trypsin	30ul Sample 30ul Trypsin	30ul Sample 30ul Trypsin	30ul Sample 30ul Trypsin	30ul Sample 30ul Trypsin	30ul Sample 30ul Trypsin	30ul Sample 30ul Trypsin	30ul Sample 30ul Trypsin	30ul Sample 30ul Trypsin	30ul Sample 30ul Trypsin	30ul Sample 30ul Trypsin
C	60ul Buffer	30ul Sample 30ul Trypsin	30ul Sample 30ul Trypsin	30ul Sample 30ul Trypsin	30ul Sample 30ul Trypsin	30ul Sample 30ul Trypsin	30ul Sample 30ul Trypsin	30ul Sample 30ul Trypsin	30ul Sample 30ul Trypsin	30ul Sample 30ul Trypsin	30ul Sample 30ul Trypsin	30ul Sample 30ul Trypsin
D	60ul Buffer	60ul Sample	30ul Sample 30ul Buffer	30ul Sample 30ul Buffer	30ul Sample 30ul Buffer	30ul Sample 30ul Buffer	30ul Sample 30ul Buffer	30ul Sample 30ul Buffer	30ul Sample 30ul Buffer	30ul Sample 30ul Buffer	30ul Sample 30ul Buffer	30ul Sample 30ul Buffer
E												
F												
G												
H												

Figure 71   Substrate dilutions for the trypsin N-Terminal Kinetic assay.

4.9.5 pH dependent alginate-protein Viscosity interactions

Alginates were made up at 2.5mg/ml with casein or BSA at 10mg/ml in deionised water. Aliquots of 5ml were taken and titrated across the pH range using HCl and NaOH to pH 1.5, 2, 2.5, 3, 3.5, 4, 4.5, 5, 6, 7, 8 and 9. Samples were incubated at room temperature for 30min and then left to stand for a further 30min to allow any precipitate to settle. 2ml of the sample supernatent was pipetted off the top of the sample and viscosity was measured.

Sample viscosity was measured using a cup and bob viscometer (Contraves, Switzerland) which plots percentage deflection against shear rate. All samples were tested in triplicate and specific viscosity and relative viscosity were calculated from percentage deflection, as recorded, using equations 1 and 2.

Equation 1: Relative Viscosity

$$\eta rel = \frac{Percentage\ Deflection\ of\ Sample}{Percentage\ Deflection\ of\ Solvent}$$

Equation 1: Relative Viscosity

$$\eta sp = \eta rel - 1$$

4.9.6 Rheology Methodology

Rheological measurements were taken with a Kinexus pro+ rotational rheometer (Malvern Instruments Ltd., Malvern, UK) with controlled shear strain, with a parallel plate geometry (CP1/60 60mm diameter with a 1mm gap). All measurements were carried out at 22° C. Data was analysed using rSpace software.

The linear visco-elastic region (LVER) of all samples was determined by carrying out an amplitude sweep at 1 Hz. A value which represented this range was calculated using rSpace software and an oscillation frequency sweep was conducted over a frequency range 0.1-100Hz from which rheological data including G*,G′ ,G″ and phase angle δ (deg) was collected.

All rheological data is typical data from a single sample.

4.10   Results

Trypsin activity in the presence of dietary biopolymers was measured using a 96 well microplate adaptation of the N-terminal proteolysis assay as described in the experimental section.

As with the pepsin activity assay, succinylated bovine serum albumin was used as the substrate.

As with the pepsin analysis, colour development was measured in the presence of dietary bioplolymers and trypsin inhibition was calculated as a percentage change in optical density as compared to uninhibited trypsin. The assay system was validated using three known serine-dependent protease inhibitors; Soya bean trypsin inhibitor, benzamidine hydrochloride and α-amino-n-caproic acid as positive inhibition controls.

Soya bean trypsin inhibitor (SBTI) is a monomeric protein with a molecular weight of 21,500 which binds to and inhibits trypsin by blocking the active site [220, 221]. SBTI is a potent inhibitor of trypsin activity with a K_i reported in the range 10^{-9}-10^{-14}. SBTI inhibits trypsin activity by strongly binding across the active site and blocking substrate binding as is shown in Figure 72 [222]. SBTI binding is thought to mimic the binding seen in a normal productive peptide hydrolysis reaction. Arg63'-Ile64' mimics the 'scissile' peptide bond which occupies the active site with the positively charged Arg63' occupying the primary specificity pocket of trypsin. An equilibrium is reached between SBTI and the cleaved form held in place by covalent interactions between SBTI and Trypsin.
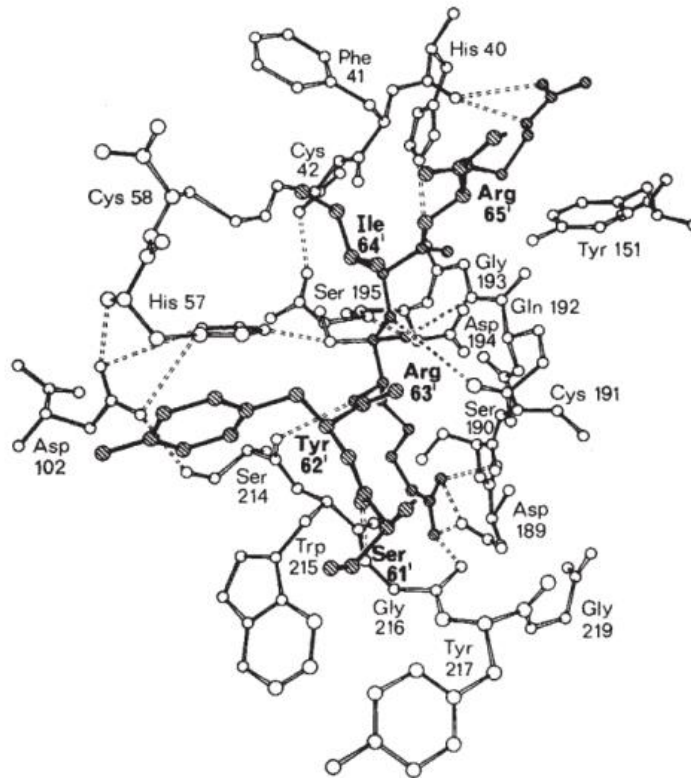
Figure 72   Residues 61'-65' of the Soybean Trypsin Inhibitor, and the residues of the trypsin molecule involved in binding. Atoms of the Trypsin molecule are clear, and of the inhibitor are shaded.Taken from Blow *et al* 1974 [222].

The concentration dependent inhibition of trypsin with SBTI is shown in Figure 73. SBTI was found to be the more potent than the other two inhibitors tested (Figure 75-Benzamidine HCl, and Figure 76-α-amino-n-caproic acid). With SBTI there was a near complete inhibition of the activity of 5µg/ml of trypsin at a concentration of 12.5µg/ml SBTI; trypsin activity was reduced to 1.4±3.1% of normal. A clear dose effect can be seen with 52%±16.4% inhibition at 1.56µg/mlmg/ml SBTI. At concentrations of SBTI higher than 12.5µg/ml, no trypsin activity was observed.
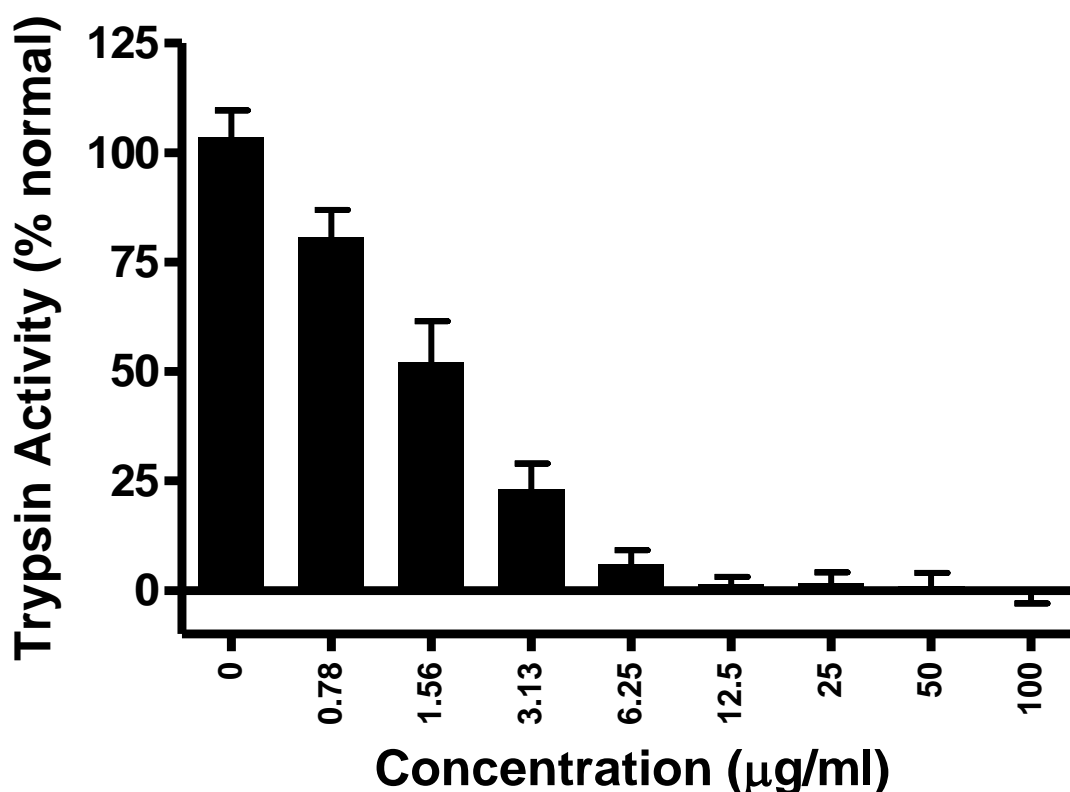
Figure 73 - Concentration dependent inhibition of trypsin (5μg/ml) in the presence of Soya Bean Trypsin Inhibitor. Activity is shown as a percentage of normal pepsin activity at a range of concentrations (0-0.1 mg/ml). All samples were tested in triplicate (n=3) with error bars showing standard deviation.

The concentration dependent inhibition of trypsin with Benzamidine Hydrochlride is shown in Figure 75. Benzamidine Hydrochloride is an amine derivative of benzene known to competitively inhibit trypsin, it does this by occupying the substrate binding cleft of trypsin, competing for substrate binding (See Figure 74) [223, 224]. At 5 and 10mg/ml benzamidine hydrochloride, activity of 5μg/ml trypsin was reduced to 1.7±2.1% and -1.36±2.4% of normal activity respectively. As can be seen benzamidine hydrochloride completely abolished trypsin activity at 5mg/ml compared to SBTI which completely inhibited activity at 12.5μg/ml, meaning SBTI is approximately 400 times more effective at inhibition.
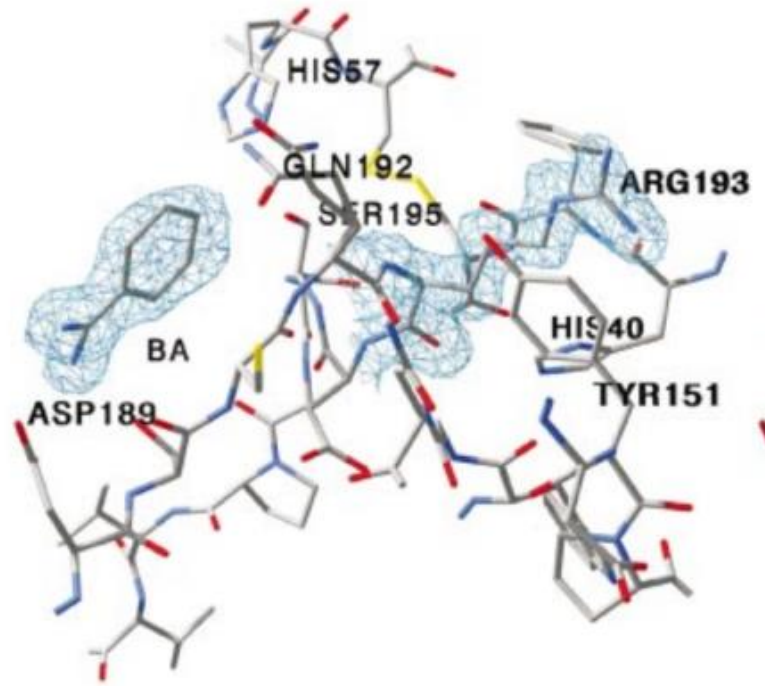
Figure 74   Structural view of Benzamidine occupying the substrate binding cleft of Human Brain Trypsin. Critical substrate binding and catalytic residues are also shown. However in human pancreatic trypsin Arg193 is substituted with Gly193. Taken from Katona et al 2002 [224]
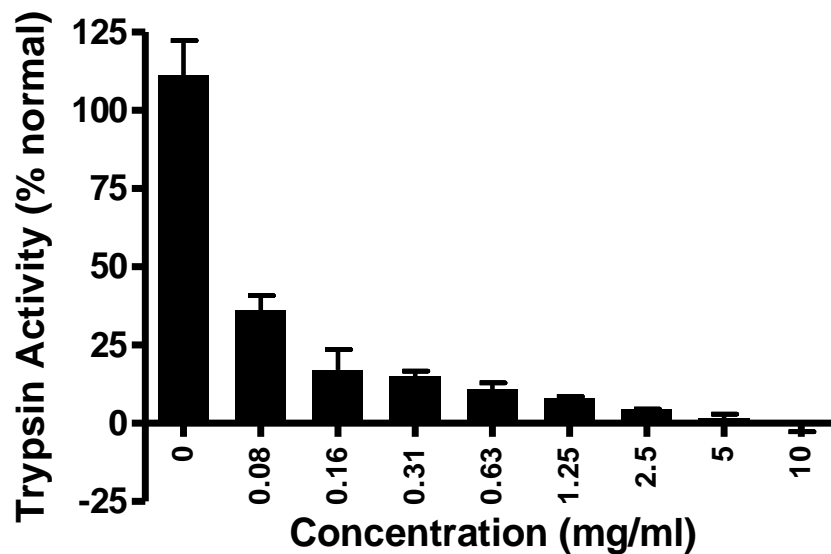
Figure 75 - Concentration dependent inhibition of trypsin in the presence of benzamidine Hydrochloride. Activity is shown as a percentage of normal pepsin activity at a range of concentrations (0-10 mg/ml). All samples were tested in triplicate (n=3) with error bars showing standard deviation.
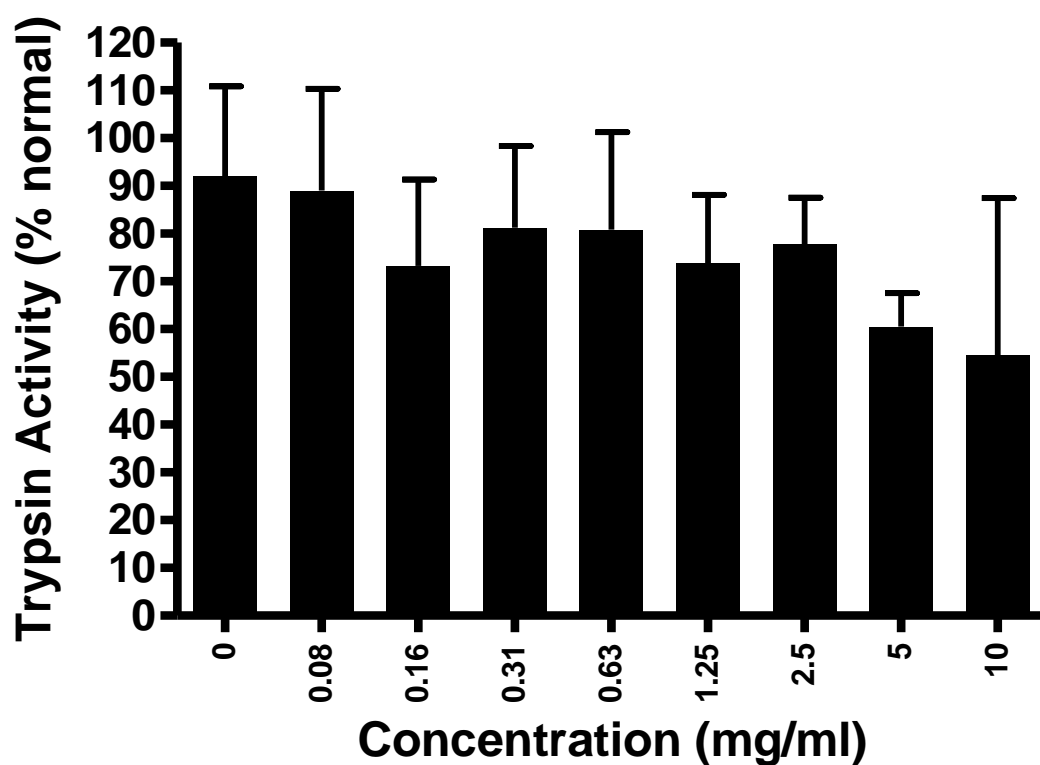
Figure 76- Concentration dependent inhibition of trypsin in the presence of α-amino-n-caproic acid. Activity is shown as a percentage of normal pepsin activity at a range of concentrations (0-10mg/ml). All samples were tested in triplicate (n=3) with error bars showing standard deviation.

α-amino-n-caproic acid, a known protease inhibitor was also tested [225]. As shown in Figure 76, trypsin inhibition was shown to be limited and variable, with a statistically significant correlation between α-amino-n-caproic acid concentration and trypsin inhibition with an r^2 value of 0.7505 and a p-value of 0.0025.

Again, the catalogue of eighteen alginates provided by Technostics Ltd and FMC biopolymer were tested in the trypsin activity assay. All alginate samples were tested at three concentrations; 5, 2.5 and 1.25mg/ml. This gave concentrations in the reaction mixture of 1.36, 0.68 and 0.34mg/ml respectively. These results are shown in Figure 77.

Figure 77 shows the complete catalogue of alginates across the entire range of M:G structural composition. Control trypsin activity is represented by the dotted line running horizontally at 100%, as can be seen there is little deviation from this control trypsin activity with the addition of any of the alginates.
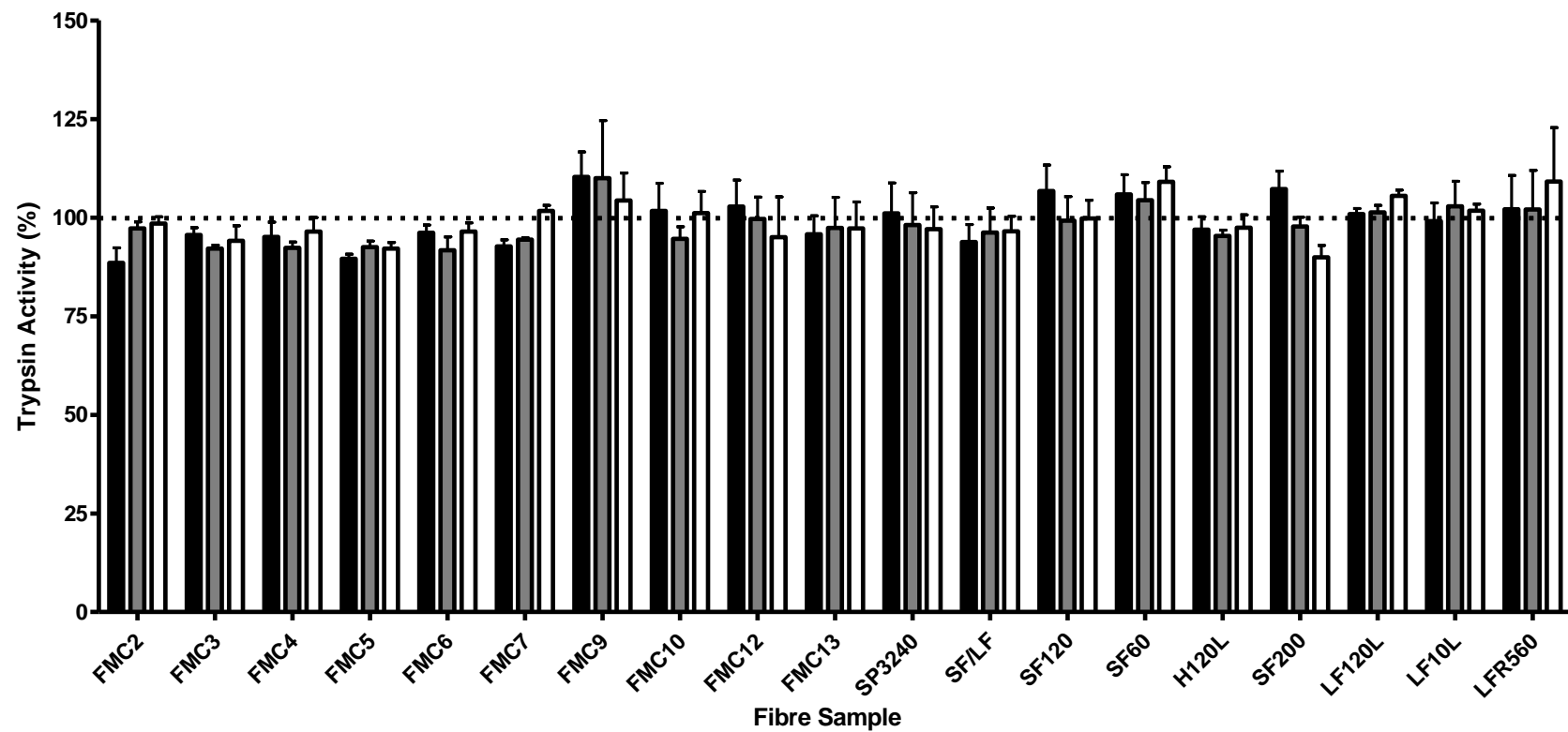
Figure 77 - Concentration dependent regulation of trypsin in the presence of sample alginates. Activity is shown as a percentage of control pepsin activity at three concentrations of alginate, ☐ 1.25mg/ml ▨ 2.5mg/ml, ■ 5mg/ml.. All samples were tested in triplicate (n=3) with error bars showing standard deviation.

While the vast majority of alginate samples had no significant effect on trypsin activity. a small number of biopolymers were observed to have had a statistically significant effect. These are shown in Figure 78, the significant effects have been indicated.

FMC 5 was the only alginate sample to show a significant inhibition of trypsin activity at all three concentrations. 10.4±2% at 5mg/ml, 7.5±2.5% at 2.5 mg/ml and 7.9±2.7% at 1.25mg/ml. FMC3 and FMC4 showed a decrease of 7.8±1.5% and 7.7±2.6% respectively at 2.5mg/ml. However neither alginate showed a significant effect at the other concentrations tested. FMC 7 showed significant inhibition at 5 and 2.5mg/ml of 7.3±2.9% and 5.6±0.8% respectively, however showed no significant affect at 1.25mg/ml.
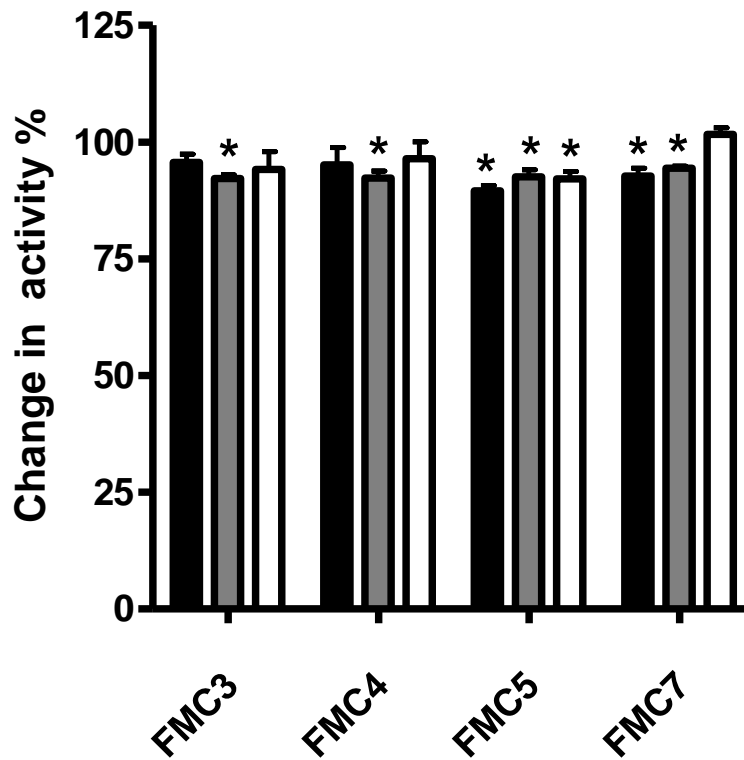
Figure 78 - Concentration dependent regulation of trypsin in the presence of sample alginates. Activity is shown as a percentage of normal pepsin activity at three concentrations of alginate, , ☐ 1.25mg/ml ▨ 2.5mg/ml, ■ 5mg/ml. All samples were tested in triplicate (n=3) with error bars showing standard deviation. Samples which were shown to be significantly different to control are shown with (*) (p=0.05).

Given the limited effects seen in the high throughput assays, all samples were further tested using kinetic methods to see if inhibitory effects varied as the enzyme:substrate ratio was changed.

The kinetics of an enzyme-substrate interaction alters with substrate concentration (or ratio of substrate to enzyme) and extrinsic compounds may have effects at across this range that were not observed in the high throughput assays at a fixed enzyme:substrate ratio.

The kinetics of enzyme substrate reactions in the presence of dietary fibres were analysed using an adapted 96 well microplate assay as described in the methods section. All biopolymers were tested a minimum of 5 times. Kinetic constants were calculated from GraphPad Prism 4 software using substrate-velocity data. Velocity of reaction, measured as percentage change in absorbance per minute is plotted on the y-axis against substrate concentration on the x-axis.

Figure 79 below shows a Michaelis Menten plot for a control trypsin digestion of succinylated BSA. The control digestion begins to reach enzyme saturation at the higher substrate concentration and the plot begins to plateaux.
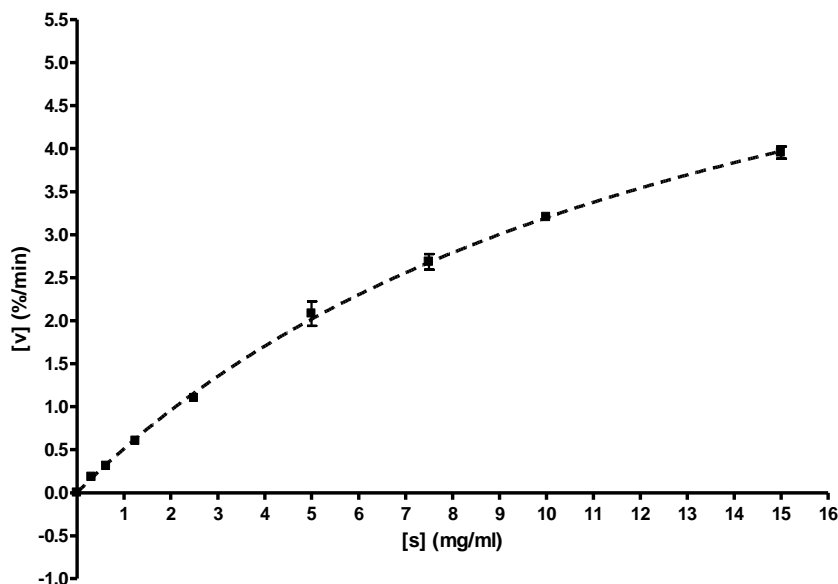
Figure 79 Michaelis-Menten plot for control digestion of trypsin. Substrate concentration [s] is given in mg/ml and the velocity is given as the rate of change in percentage absorbance per minute. The error bars show the standard deviation of 5 replicates (n=5)

Across most of the samples, no effects were seen, confirming what was seen in the highthroughput microplate assays. Some small but statistically significant effects were observed. Interpolated kinetic constants were compared to those of the trypsin control and where there were statistically significant differences to normals, these have been highlighted in Table 18. LF10L, FMC3 and FMC 4 had a significantly different V_{max}, and FMC3 and FMC7 were statistically different for both V_{max} and K_m.

	P-Values of Kinetic Data which are significantly different from control		
	V_{max}	K_m	**Conclusion**
LF10L	0.04		Reject null hypothesis
FMC3	0.04	P<0.0001	Reject null hypothesis
FMC2	P<0.0001		Reject null hypothesis
FMC4	0.04		Reject null hypothesis
FMC7	0.0004	0.002	Reject null hypothesis
FMC5	*0.12*	*0.17*	*Do not reject null hypothesis*

Table 18   Showing alginate samples where kinetic data was significantly different from control values for trypsin. ▨▨▨▨▨ Represents where no significant difference was observed. FMC5 has been included in the table, as significant inhibition was shown in microplate assays (Figure 78).

Figure 80 shows the Michaelis-Menten plot for FMC2, as a representation of the alginate samples that caused a significantly different V_{max} to normals. With FMC3 a significant change in both V_{max} and K_m to be reported. While these effects are statistically significant, with FMC2 and FMC3 the sample lines deviate only slightly from the control line. While statistically significant, the changes in the kinetics of the reaction are marginal and suggest that alginates do not inhibit trypsin activity.
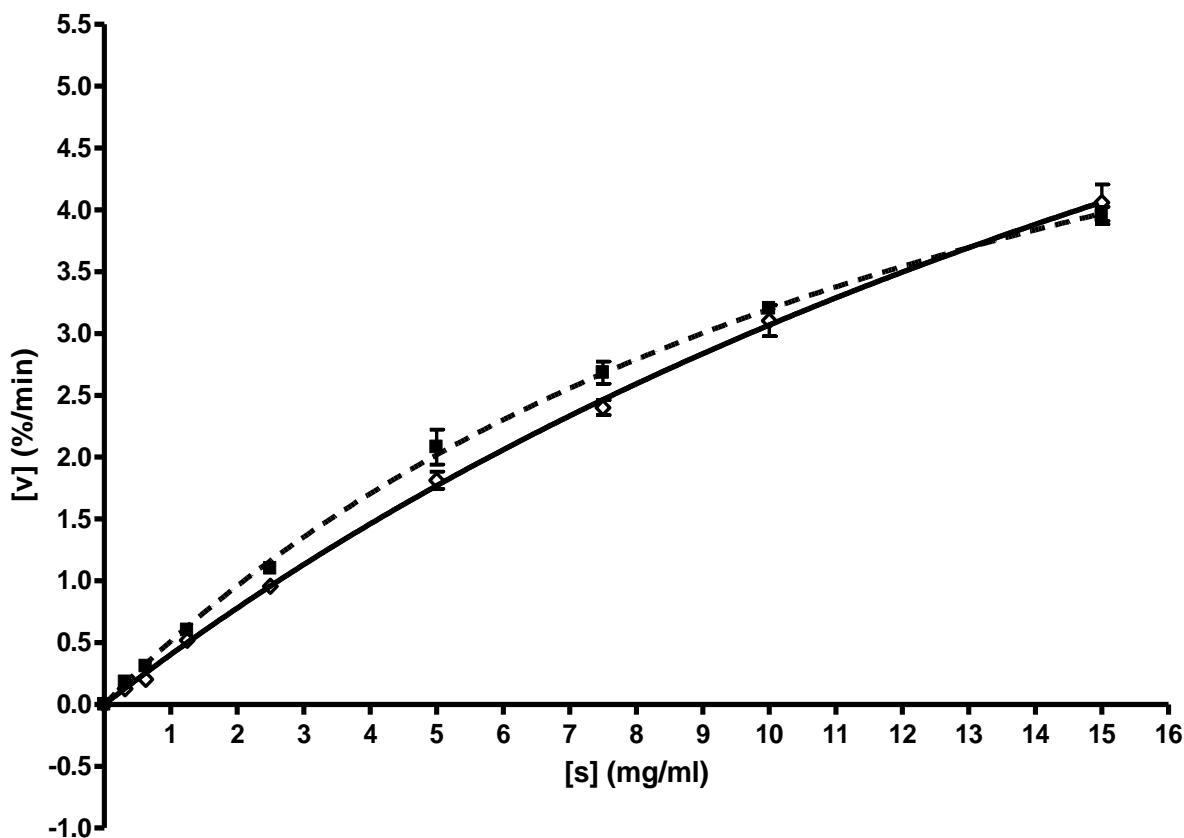
Figure 80   Michaelis-Menten plot for alginate FMC2 at 5mg/ml as compared to a trypsin control . Substrate concentration [s] is given in mg/ml and the velocity is given as the rate of change in percentage absorbance per minute. The error bars show the standard deviation of 5 replicates (n=5).

4.10.1 pH dependent alginate-protein Viscosity interactions

Only marginal changes in trypsin activity with a small number of alginates were observed in microplate high-throughput and kinetic assays. These results contrast with the strong inhibitory effects of alginate on pepsin shown in Chapter 3.

In order to investigate the different inhibition profiles of pepsin and trypsin, the pH dependency of alginate-protein interactions were investigated. As pH dependent gels, the behaviour and bioactivity of alginates can vary dramatically across the pH range, including the way alginate interacts with other molecules and polymers.

In the control alginate solution the samples showed behaviour typical of a pH dependent gel with specific viscosity increasing at lower pH's as an acid gel is formed. Addition of BSA or Casein to the mixture caused a visible precipitate to form in samples titrated to acidic pH, but not in samples at neutral pH. After the precipitate had been allowed to settle for 30 minutes, the viscosity of the remaining supernatant was measured. As can be seen from the pH dependent specific viscosity plot of H120L and BSA/Casein in Figure 81 below, at a pH around neutral there is little or no difference in viscosity of supernatant with the addition of BSA or casein. However as the pH is lowered, the specific viscosity of the H120L alginate control increases as an acid gel is formed. However in the samples with BSA and Casein present, at lower pHs the viscosity of the supernatant approaches zero as a precipitate has formed between alginate and the protein which has settled to the bottom of the tube, bringing the viscous alginate component out of solution.

Four alginates were tested in this way H120L; (Figure 81), SF120 (Figure 82), LFR560 (Figure 83) and SF200 (Figure 84). As can be seen from Figure 83, LFR560 has a maximum specific viscosity of between 3-4 as compared to the other alginates with maximum specific viscosities in the range 15-45. This is due to LFR560 being a low molecular weight alginate (34,700Da) as compared to alginates H120L, SF120 and SF200 with molecular weights up to an order of magnitude larger (195,000- 397,000). These larger alginates have higher specific viscosities as predicted by the Mark-Houwink equation which describes the positive relationship between molecular weight and viscosity – although it is important to note that this relationship is affected by many other factors including structure, pH, and ion chelation.

In all samples the same formation of precipitate and lower supernatant viscosity was seen. In the case of SF200, at neutral pH the addition of BSA and Casein to the mixture caused an approximate doubling of supernatant viscosity suggesting a synergistic interaction between alginate SF200 and protein at neutral pH. The interaction between SF200 and BSA/Casein at lower pH was consistent with the other tested samples, with a precipitate forming and lowering the viscosity of the supernatant.

LFR560 was the only sample in which some viscosity remained at low pH after the addition of BSA, this suggests that there is an interaction by which some alginate remains able to form a gel. This result may indicate a size-dependent interaction between BSA and alginate, although LFR560 was the only low molecular weight available for testing.
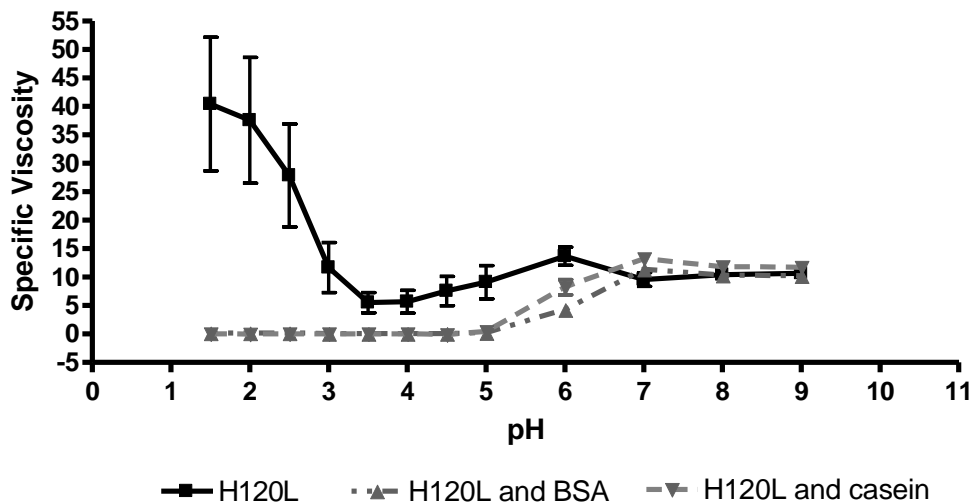
Figure 81– pH dependent viscosity interaction of alginate H120L (2.5mg/ml) with BSA (10mg/ml) and casein (10mg/ml) across the pH range (n=3). H120L molecular weight = 397,000.
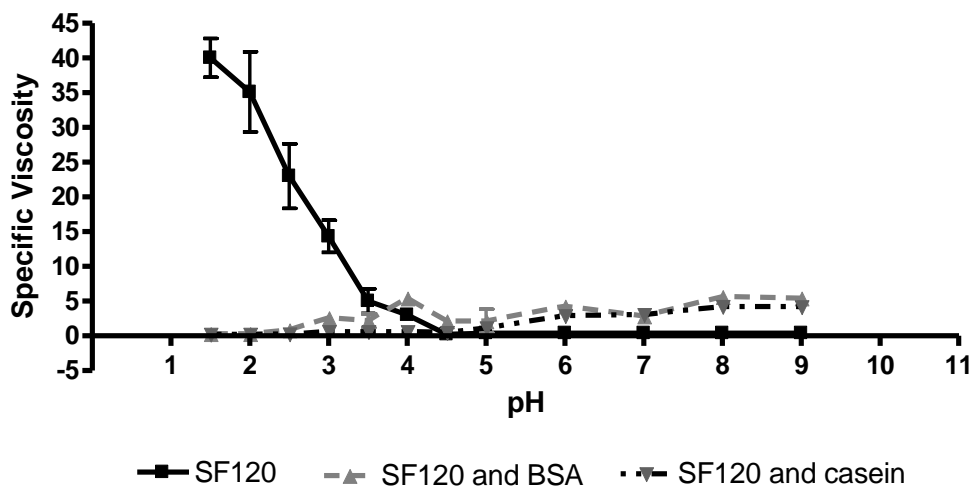
Figure 82 – pH dependent viscosity interaction of alginate SF120 (2.5mg/ml) with BSA (10mg/ml) and casein (10mg/ml) across the pH range (n=3). SF120 molecular weight = 195,000.
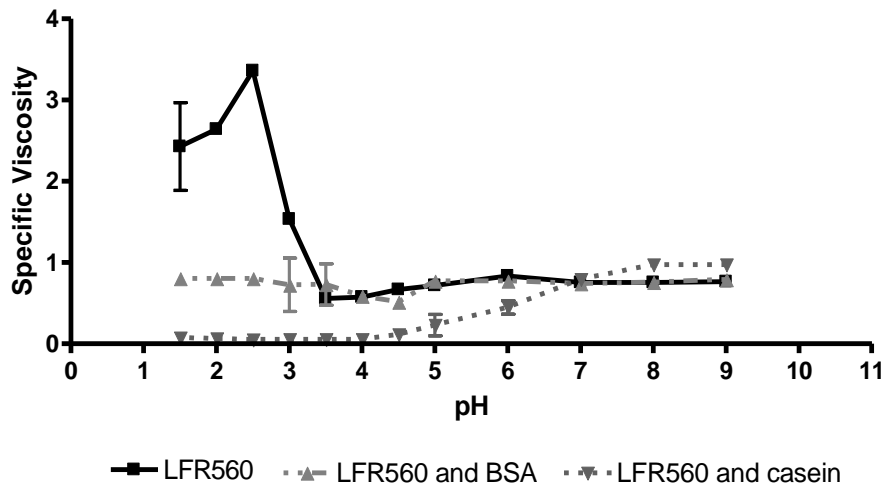
Figure 83– pH dependent viscosity interaction of alginate LFR560 (2.5mg/ml) with BSA (10mg/ml) and Casein (10mg/ml) across the pH range (n=3). LFR560 molecular weight = 34,700
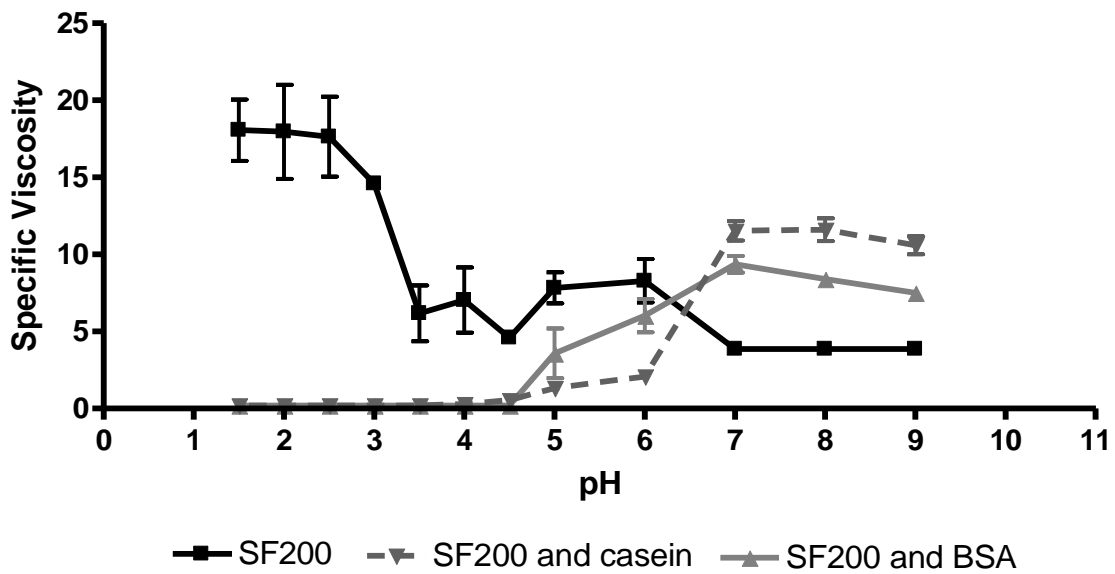
Figure 84 – pH dependent viscosity interaction of alginate SF200 (2.5mg/ml) with BSA (10mg/ml) and casein (10mg/ml) across the pH range (n=3). SF200 molecular weight = 387,000.

The formation of pH dependent precipitate between alginate and protein suggests a possible mechanism by which alginate may prevent the action of pepsin without affecting trypsin in a similar way. Having said this, complex interactions between alginate gels and other polymers such as proteins cannot properly be characterised by viscometry. Viscosity is a fluid property and a measure of how liquids flow and respond to stress. Alginates at low pH are not true liquids, but viscoelastic gels and therefore must be characterised using rheology.

The interaction of alginate samples with BSA, casein and milk protein were compared rheologically nder controlled stress conditions at pH 2 and pH 7 to simulate the pH conditions at which pepsin and trypsin would be active. Casein refers to a group of phosphoproteins which constitute approximately 80% of the total protein in bovine milk including α-s1 Casein, α-s2 Casein, β-Casein, and κ-Casein. Milk powder on the other hand refers to commercially available dried skimmed milk powder, containing all of the other components of dried milk powder, including lactose, fats, and minerals.

Alginate samples and alginate-protein mixes were all subjected to an initial amplitude sweep to determine the linear viscoelastic region: this is the region where the viscoelastic properties are independent of the deformation force. Frequency sweeps were then conducted over the range 0.1-40Hz using the determined LVER values for controlled stress measurements. G*, G', G" and phase angle were monitored throughout.

In Figure 85 the complex modulus G*, which gives a measure of rigidity and stiffness, of the alginate H120L is compared at pH2 and pH7. As can be seen, at lower frequencies the dynamic modulus in the pH2 acid alginate gel is higher than pH7 H120L alginate by an order of magnitude, indicating a much greater gel strength and stiffness at pH2 [226]. In both the pH2 and pH7 samples the alginate shows frequency dependence typical of a viscoelastic gel.

As can be seen from Figure 85, at frequencies above 10Hz, the gradient of the complex modulus curve increases rapidly as the frequency increases. This occurs with H120L alginate at both pH2 and pH7, and is expected due to the way biopolymer gels arre known to respond to deformation. At low frequencies there are longer relaxation times, and the polymer network can respond to stress without rupturing. However, at higher frequencies a process called strain-hardening occurs, whereby the frequency does not allow for a relaxation of the polymer network, and the material cannot accommodate any more stretching or deformation.

This causes an increasing stiffness as the polymer network resists any further deformation, until the junction points cannot accommodate any more stretching and the network ruptures. It would be expected that after the polymer has been taken through the strain-hardening phase and the rupture point has been passed, the polymer would display flow behaviour [227].
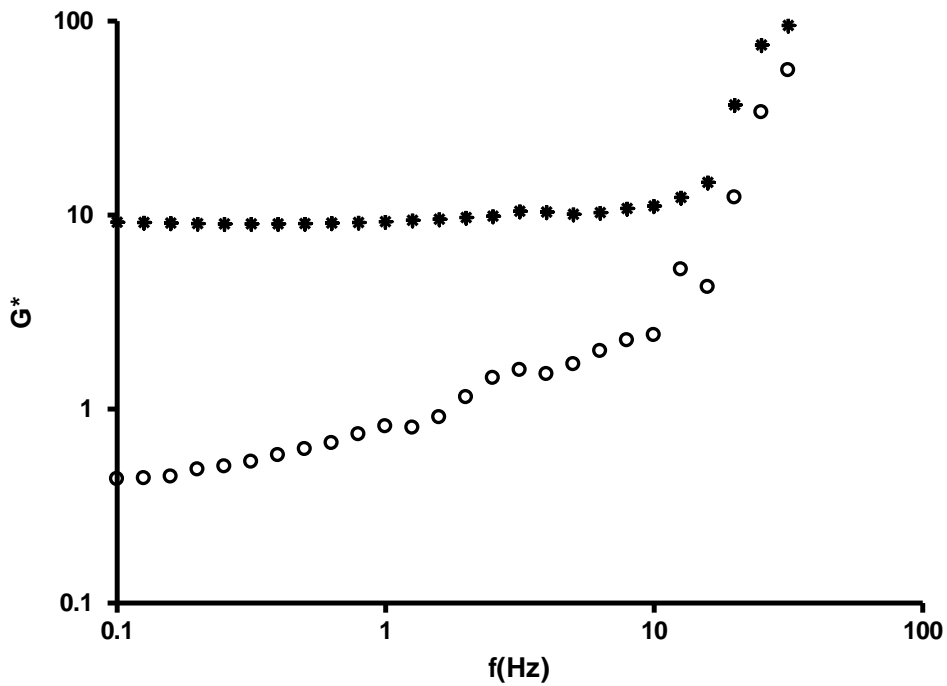
Figure 85 - Typical plot of complex modulus (G*) of alginate H120L at pH2 (O) and pH7 (*) across frequency range 0.1-40Hz. (n=1). $G^* = \sqrt{G'^2 + G''^2}$.

At pH2, alginate H120L shows gel-dominated solid-like behaviour. Comparing the elastic modulus G' at pH2 and pH7 in Figure 86, it can be seen that elastic modulus is an order of magnitude larger in the pH2 alginate gel than the pH7 alginate solution at lower frequencies, as you would expect when comparing a gel to a viscous liquid. Again a frequency dependence is shown with the moduli increasing at higher frequencies such that in both pH2 and pH7 alginate solutions at high frequencies the solid like properties are increased.
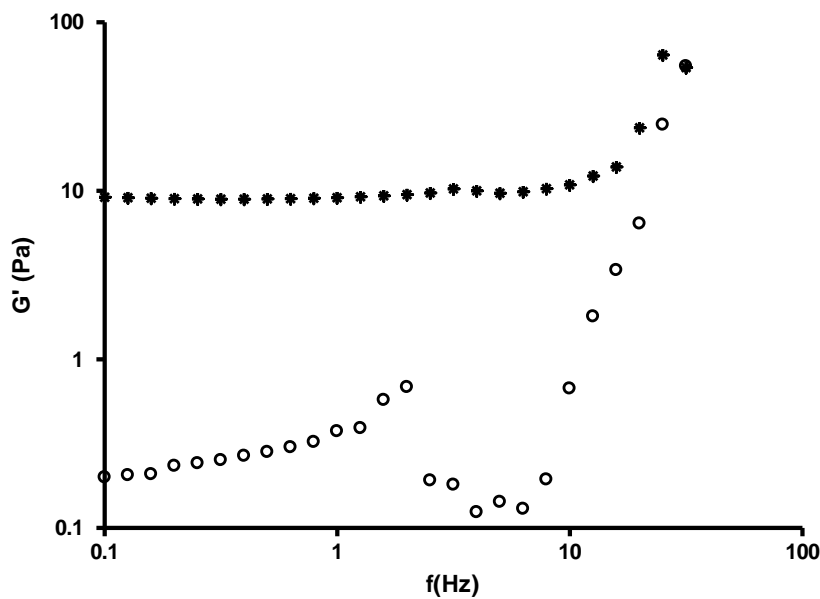
Figure 86   Typical plot of a frequency sweep of elastic modulus (G') of H120L at pH2 (o) and pH7 (*). (n=1) Across frequency range 0.1-40Hz

Again the phenomenom of strain-hardening can be seen at higher frequencies, as the biopolymer network cannot accommodate further deformation. At both pH7 and pH2, the elastic modulus of the alginate solution approaches the same value, as the strain-hardening becomes the dominant factor, above pH and gelling effects.

From Figure 87 it can be seen that the viscous modulus is similar between the pH2 and pH7 solutions, although slightly lower in the pH2 solution, again strain-hardening is apparent at higher frequencies.
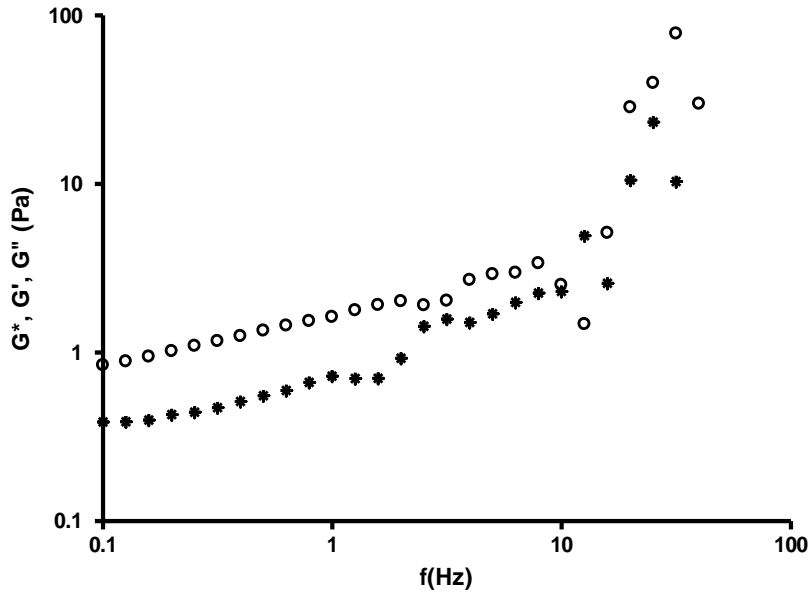
Figure 87   Typical plot of a fFrequency sweep of viscous modulus (G") of H120L at pH2 and pH7. (n=1) Across frequency range 0.1-40Hz

From Figure 88 it can be seen that there is a marked difference in phase angles at frequencies 0.1-10Hz, with pH2-H120L showing strong solid-like behaviour δ=0-45 and pH7 showing viscous, liquid like properties δ=45-90.
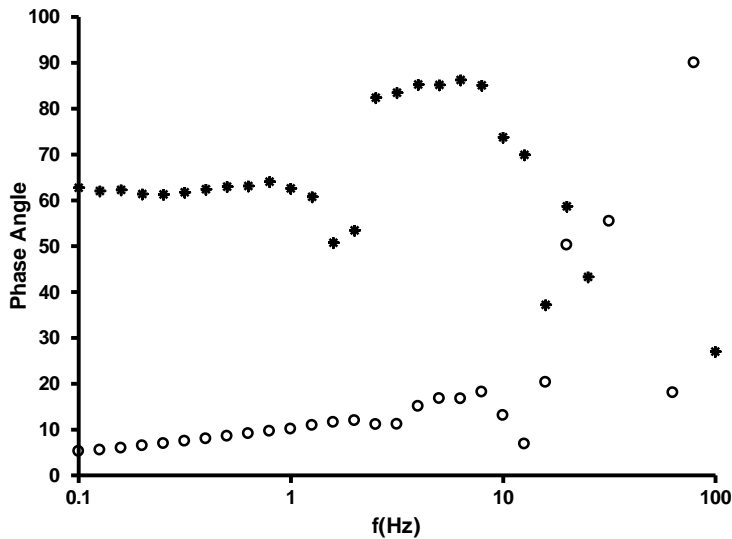
Figure 88   Typical plot of a frequency sweep of phase angle (α) of H120L at pH2 and pH7. (n=1) Across frequency range 0.1-40Hz

At frequencies above 10Hz the readings for phase angle become varable, this tallies with the region of increased G*, G' and G". The relationship between phase angle and the elastic and viscous moduli can be explained by the equation - $\tan(\delta) = G''/G'$. Therefore at pH2, as the viscous modulus increases at higher frequencies, while the elastic modulus stays relatively constant, the phase angle will increase. This corresponds with the polymer network passing through a rupture point and demonstrating more flow like behaviour, although the data in Figure 88 above 10Hz is somewhat variable.

Alginate samples FMC3, FMC13 and SF60 were also compared at pH2 and pH7. Similar pH dependent alginate gel formation at pH2 was shown with all alginate samples as would be expected.

Alginate-protein mixtures were made with alginate at 2.5mg/ml and either BSA, Casein or Milk Protein at 5mg/ml. With the addition of protein to the alginate solution the rheological properties were changed at both pH2 and pH7.

The rheological properties of alginate sample H120L at pH2, with the addition of BSA, Casein and Milk Powder are shown in Figure 89.

From Figure 89a it can be seen that with the addition of protein, the Dynamic Modulus of the mixture was decreased as compared to H120L alginate to varying degrees. These results indicate that there is an interaction between H120L alginate and each of the proteins BSA, Casein and Milk Protein. This interaction is such that the alginate gel is disrupted and the gel strength decreases and becomes less rigid. With H120L, Milk Powder causes the largest decrease in G*, followed by BSA, and casein has the weakest effect. As shown in Figure 89b, at pH2 the addition of the protein substrate results in a lowered G' elastic modulus suggesting the gel strength is weakening with the addition of each of the three protein substrates, these effects again had the same order of magnitude milk powder > BSA > casein. The G" viscous modulus is also lowered at low frequency by the addition of the three proteins in the same order Figure 89c suggesting that the viscous portion of the solutions are too getting weaker. Figure 89d shows that the addition of protein to the H120L sample results in an increased phase angle. Although with the addition of each protein, at all frequencies the phase angle remains less than 45° and gel-like behaviour still dominates, the addition of protein causes an increase in phase angle in all cases and a shift towards more liquid like behaviour.

Figure 89 - Typical plots of rheological properties of H120L at pH2 in the presence of BSA, Casein and Milk Protein. (a) Complex modulus - G*, (b) Elastic Modulus - G', (c) Viscous modulus - G" (d) Phase angle – α. Control H120L is shown as – o, with 2.5mg/ml BSA as -*-, with 2.5mg/ml Casein as -▼-, and with 2.5mg/ml Milk Powder as - Δ.

At pH7 there are less pronounced disruptions to the rheological behaviour of H120L as can be seen in Figure 90a-d, although some frequency dependent variation is apparent. There is a lowering of G* of H120L at pH7 with the addition of BSA and casein, with the addition of milk powder there is a slight increase Figure 90a. With the addition of BSA and Casein there is a decrease in both the elastic modulus G' and viscous modulus G" of H120L, indicating a weakening of the polymer interactions Figure 90b&c. With the addition of BSA and Casein the phase angle remains relatively similar Figure 90d.

However, with the case of milk powder there is an increase in the dynamic modulus and elastic modulus, a decrease in viscous modulus and a pronounced lowering of the phase angle. This suggests that the addition of milk powder is interacting with the alginate to form a heteropolymeric gel. The increase in G* and G' shows that the gel is formed by the addition of milk protein and the shift in phase angle from liquid-dominant behaviour (45-90°) to solid-dominant-behaviour (0-45°) shows the stabilising effect milk protein has at pH7.

Figure 90   Typical plots of rheological properties of H120L at pH7 in the presence of BSA, Casein and Milk Protein. (a) Shear modulus - G*, (b) Elastic Modulus - G', (c) Viscous modulus - G" (d) Phase angle – α. Control H120L is shown as – o, with 2.5mg/ml BSA as -*-, with 2.5mg/ml Casein as -▼-, and with 2.5mg/ml Milk Powder as - Δ.

The change in rheological properties of alginate H120L with the addition of protein substrate suggests alginate-protein interactions. The fact that changes in rheological properties occur with casein, BSA and milk protein suggests that these interactions are non-specific protein-alginate interaction, but that the nature of the interaction is both alginate and protein dependent as shall be discussed.

Although changes in rheological properties were apparent at both pH2 and pH7, it is evident from Figure 91 that in absolute terms, the change in properties is much more apparent at pH2. The addition of BSA to H120L alginate has been used as an example, as bovine serum albumin was the substrate used in the pepsin and trypsin activity assays. At pH2 there is a 91% decrease in G* with the addition of BSA, compared to a 49% reduction respectively at pH7.
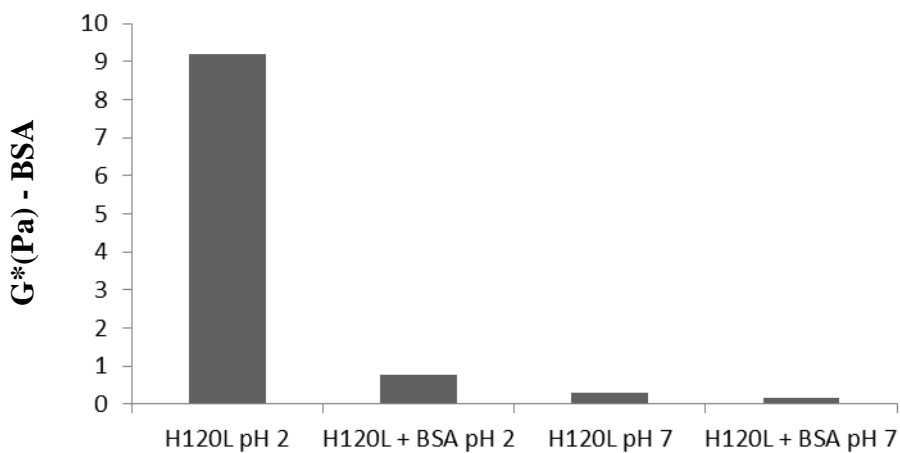
Figure 91   Dynamic modulus of H120L at 1Hz frequency with and without the addition of BSA at pH2 and pH7

4.10.2 FMC3

FMC3 shows the behaviour of a classic weak viscoelastic gel system as defined by JD Ferry [228]. The interactions between alginate and protein appear to be dependent upon both the type of proteins and alginate involved. With alginate FMC3 at pH2 the rheological properties change with the addition of protein, and the magnitude of the change in rheological properties is different for each of the three protein substrates. When protein was added to H120L alginate solution at pH2, the gel structure was disrupted and the alginate gel weakened. However with the addition of protein to FMC3 alginate there is an increase in dynamic modulus, elastic modulus and viscous modulus Figure 92a-c. There is however no change in phase angles at lower frequencies (Figure 92d), so the addition of protein to FMC3 alginate gel acts to stabilise the alginate gel and biopolymer interactions but does not affect phase angle and cause the solution to become more solid-like or more liquid like, although with a

phase angle already under 10, the solution is displaying very strong solid-dominant behaviour. FMC3 alginate does not show the same frequency dependence across the range 0.1-10Hz that was seen with H120L. Following the model of JD Ferry the increase in G" and increased tanδ indicate that the proteins seem to be acting as filler between the gum network.
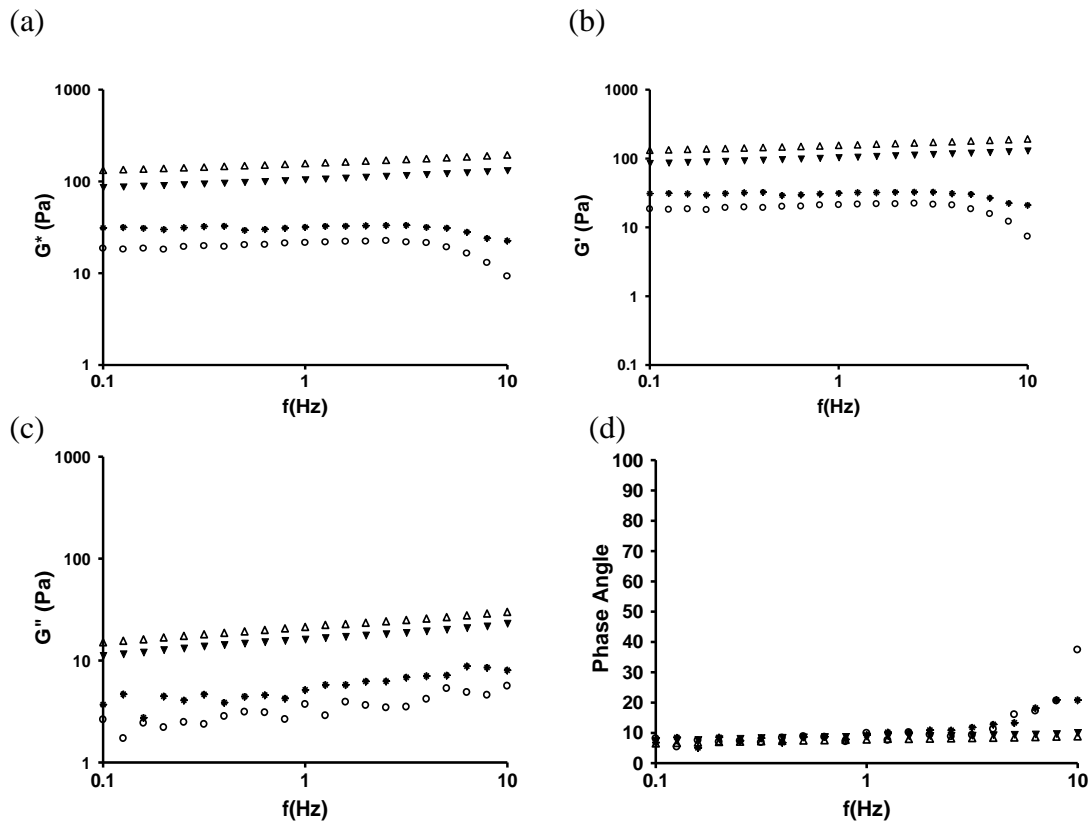
Figure 92 Typical plots of rheological properties of FMC3 at pH2 in the presence of BSA, casein and milk powder with change in frequency across the range 1-10Hz. (a) Shear modulus - G*, (b) Elastic Modulus - G', (c) Viscous modulus - G" (d) Phase angle – α. Control H120L is shown as – o, with 2.5mg/ml BSA as -*-, with 2.5mg/ml casein as -▼-, and with 2.5mg/ml milk powder as - Δ.

The rheological properties of alginate FMC3 are largely unaffected with the addition of protein substrate at pH7 (Figure 93a-d), suggesting no interaction between the two polymers. Across all frequencies, G*,G' and G" remain largely similar to control FMC3. Although there is more variation with phase angle at lower frequencies, the alginate-protein mixtures display largely the same behaviour to FMC3 alone at pH7.
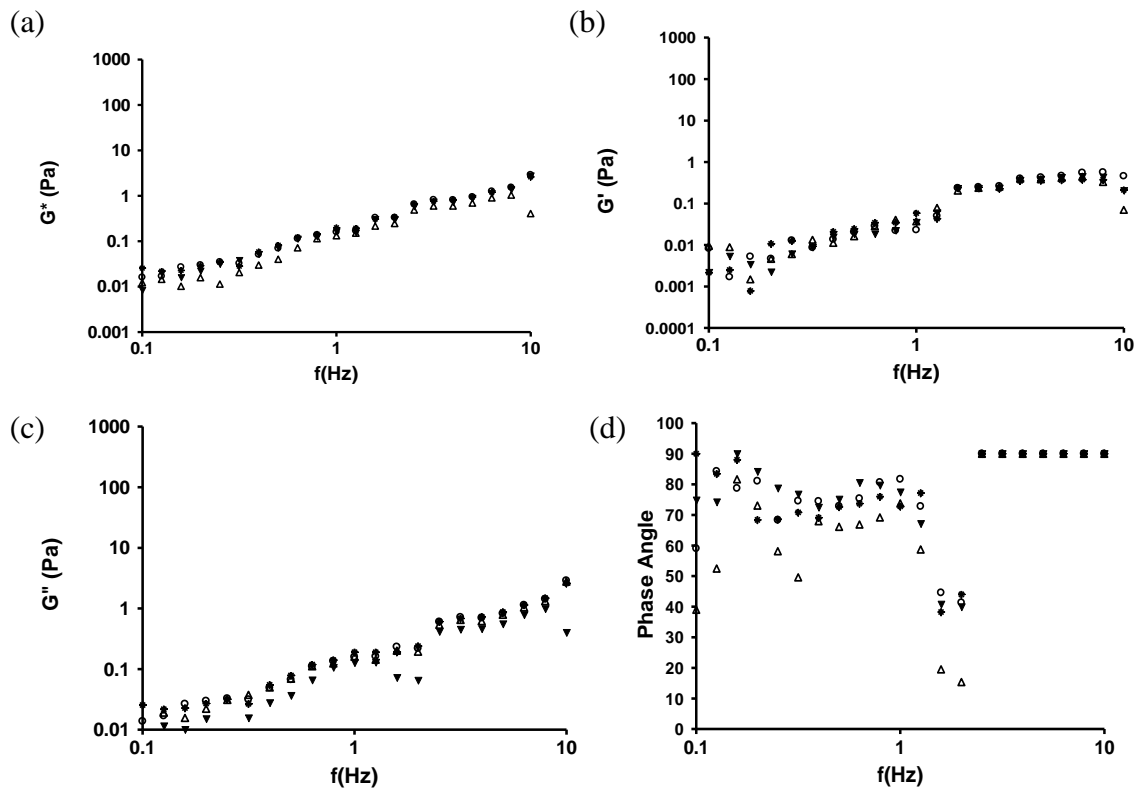
Figure 93   Typical plots of rheological properties of FMC3 at pH7 in the presence of BSA, casein and milk powderwith change in frequency across the range 1-10Hz. (a) Shear modulus - G*, (b) Elastic Modulus - G', (c) Viscous modulus - G" (d) Phase angle – α. Control H120L is shown as – o, with 2.5mg/ml BSA as -*-, with   2.5mg/ml   Casein   as   -▼-,   and   with   2.5mg/ml   Milk   Powder   as   -   Δ.

4.10.3 SF60

Alginates SF60 (Figure 94a-d & Figure 95a-d) and FMC13 (Figure 96a-d & Figure 97a-d) were also tested for pH dependent rheological interactions with protein substrates.

At pH7, SF60 alginate behaved like a viscous liquid across most of the frequency range tested, as is indicated by the phase angle, which for most of the frequency range is between δ=80-90. However, at frequencies above 1Hz, there is a shear hardening effect, as both the elastic and viscous components of the complex modulus plateaux, but the phase angle rapidly drops. This indicates that the molecular interactions are strengthening as the frequency is increasing and resisting the deformation, and as the phase angle indicates, the polymer network becomes more solid-like. This phenomenom carries on as the frequency increases up to a point where the polymer network ruptures, and while the gel strength continues to increase, the phase angle returns to the range 80-90 as the polymer behaves like a viscous liquid again. At this pH, with SF60 there was no significant change in this rheological behaviour at with the addition of BSA, casein or milk powder (Figure 95a-d).

However at pH2, BSA and Casein acted to change the rheological properties of the alginate gel, causing a decrease in both the dynamic and elastic modulus Figure 94a&b. The viscous modulus at pH2 was also decreased by the addition of BSA and Casein, although the phase angle was relatively unaffected Figure 94c&d. The fact that both the viscous and elastic components of the complex module increase with the addition of all three proteins suggests that interactions between the polymer network are strengthened by the inclusion of protein. There is little change in the phase angle with the inclusion of protein, indicating that the flow properties of the material are not greatly changed. This suggests that the interactions of the alginate polymer chains are strengthened with the inclusion of protein, but that under deformation they can be broken and reformed such that the flow properties are not changed.

With FMC13, BSA and Casein addition acted to stabilise the polymeric interactions and cause an increase in gel strength. Complex modulus, elastic modulus and viscous modulus of FMC13 at pH2 were all increased by the addition of BSA and Casein, without causing significant change to the phase angle Figure 96a-d.

Milk powder had no significant rheological affects on either SF60 or FMC13. This is unusual as casein forms a major constituent of milk powder, it would therefore be expected that if

casein alone interacts with alginate, that the casein component of milk powder would also interact with alginate. As discussed previously, milk powder also contains the other components of dried milk powder, including lactose, fats, and minerals, which may interact with either the alginate or casein, to disrupt interactions, although further investigations would be required in order to determine this.

The low-G alginate FMC13 is a weaker system at pH2 than was seen with the high G FMC3, the tanδ value is 10 times higher and with the G' and G" tending to close tofether there is a more liquid like behaviour. This suggests theat as with FMC3 there is a weak viscoelastic gel system, but with liss interactions between the polmer chains. At pH7 FMC13 shows the behaviour of a frequency dependent liquid system rather than a network. In the case of pH2, the addition of BSA to this system appears to produce an interactive structure approximately three orders of magnitude stronger in terms of G' and G" and is indicative of cooperative interaction between the polymers as opposed to infill.
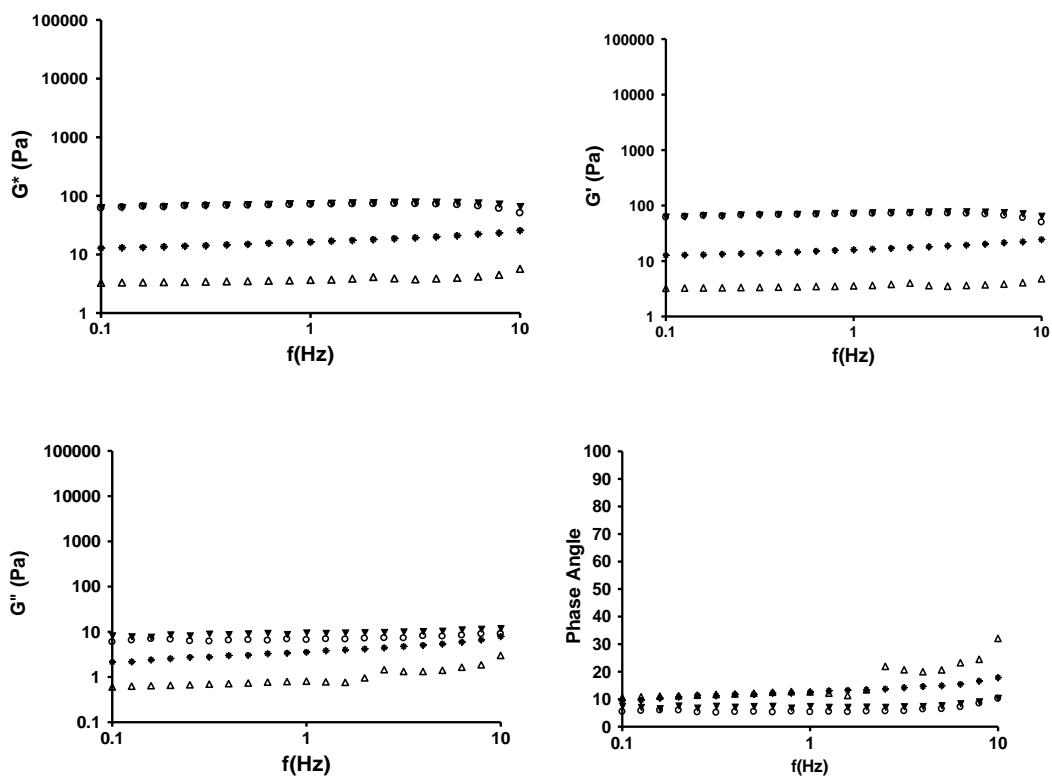
Figure 94   Typical plots of rheological properties of SF60 at pH2 in the presence of BSA, casein and milk powder. (a) Shear modulus - G*, (b) Elastic Modulus - G', (c) Viscous modulus - G" (d) Phase angle – α. Control SF60 is shown as – o, with 2.5mg/ml BSA as -*-, with 2.5mg/ml Casein as -▼-, and with 2.5mg/ml Milk Powder as - Δ.
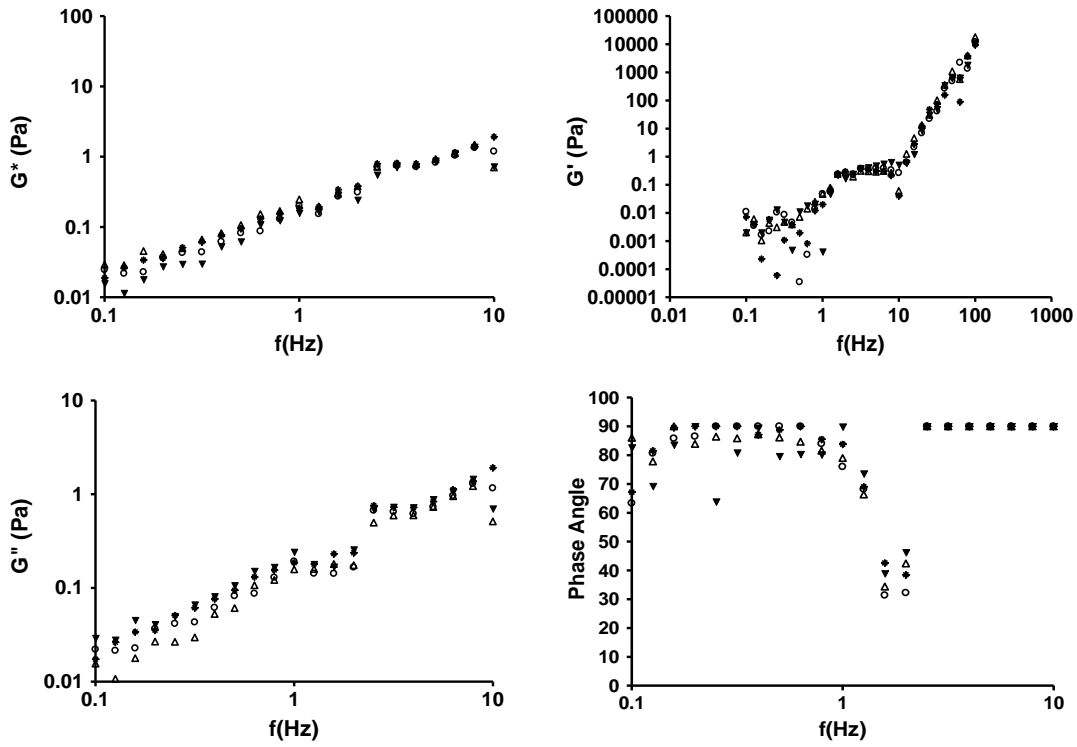
Figure 95   Typical plots of rheological properties of SF60 at pH**7** in the presence of BSA, casein and milk powder. (a) Shear modulus - G*, (b) Elastic Modulus - G', (c) Viscous modulus - G" (d) Phase angle – α. Control SF60 is shown as – o, with 2.5mg/ml BSA as -*-, with 2.5mg/ml Casein as -▼-, and with 2.5mg/ml Milk Powder as - Δ.
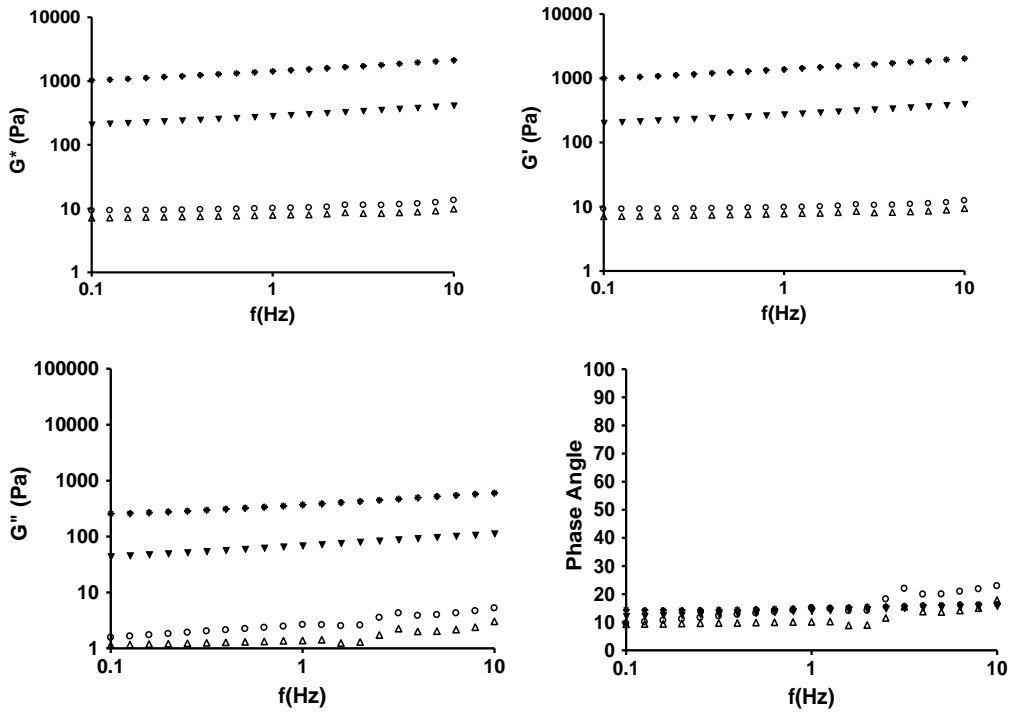
Figure 96   Typical plots of rheological properties of FMC13 at pH2 in the presence of BSA, casein and milk powder. (a) Shear modulus - G*, (b) Elastic Modulus - G', (c) Viscous modulus - G" (d) Phase angle – α. Control FMC13 is shown as – o, with 2.5mg/ml BSA as -*-, with 2.5mg/ml Casein as -▼-, and with 2.5mg/ml Milk Powder as - Δ.
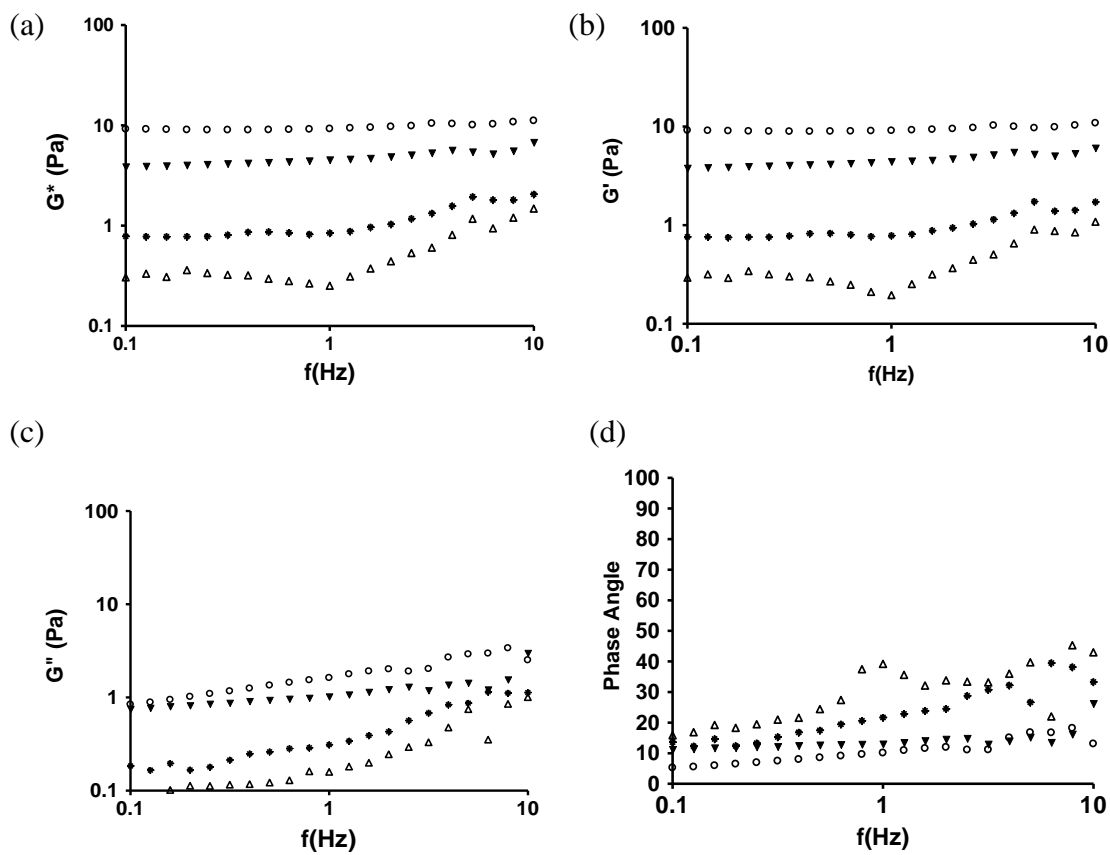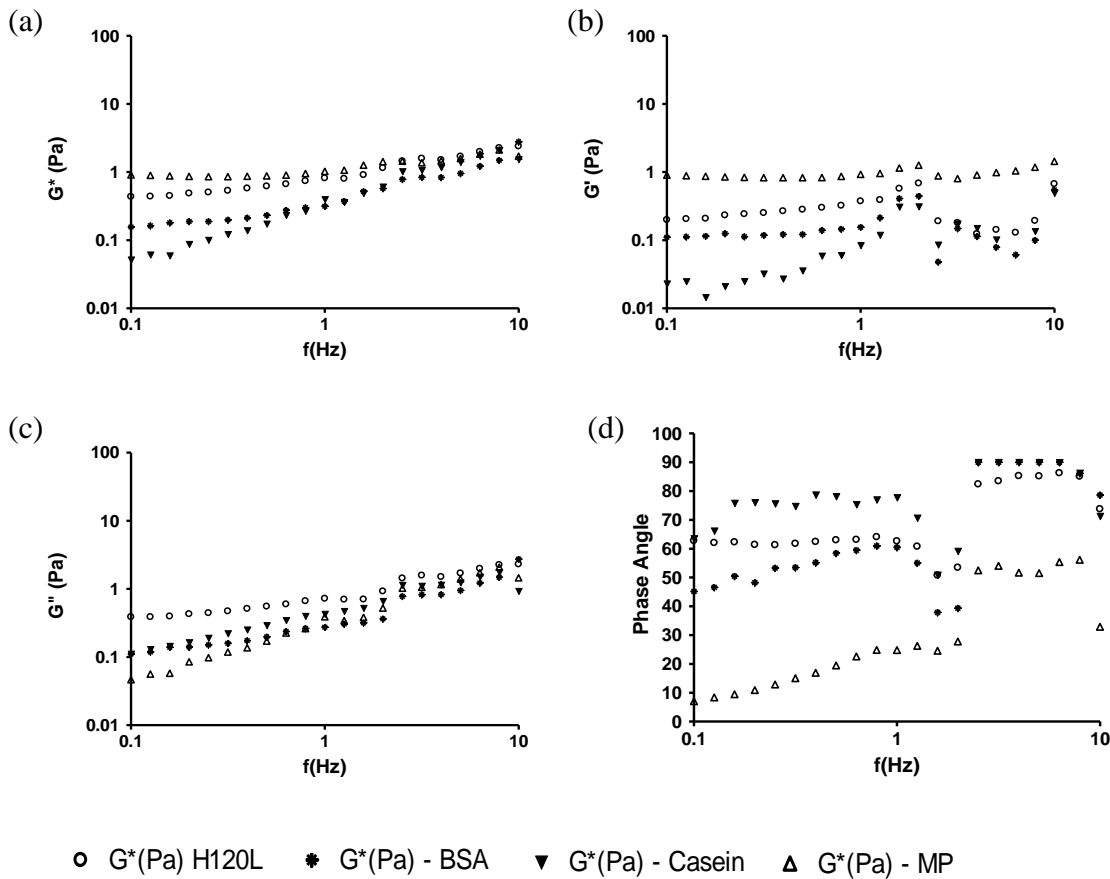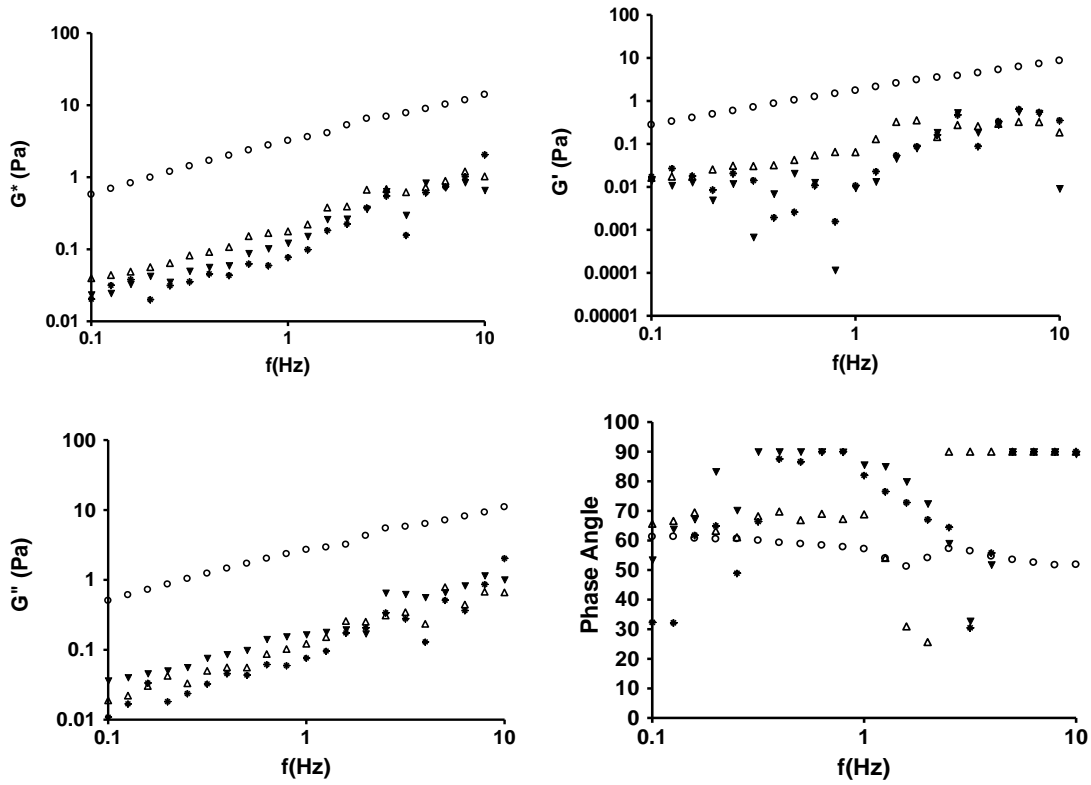
Figure 97   Typical plots of rheological properties of FMC13 at pH7 in the presence of BSA, casein and milk powder. (a) Shear modulus - G*, (b) Elastic Modulus - G', (c) Viscous modulus - G" (d) Phase angle – α. Control FMC13 is shown as – o, with 2.5mg/ml BSA as -*-, with 2.5mg/ml Casein as -▼-, and with 2.5mg/ml Milk Powder as - Δ.

4.11 Discussion

As with the pepsin methodology, the trypsin N-terminal assay was scaled down to a 96 well microplate in order to increase the throughput capability of the assay and reduce error. While alginates are basic molecules and so were unlikely to have a profound effect on pH, all samples and reagents were buffered in a Sorensen's Phosphate buffer. As shown from Figure 68, the 0.066 M Sorensens phosphate buffer was effective at buffering the alginates so that there was no significant variation in pH.

The assay system was validated using three known serine protease inhibitors; Soya bean trypsin inhibitor, benzamidine hydrochloride and α-amino-n-caproic acid as positive inhibition controls. SBTI was the most potent of the three inhibitors, completely inhibiting the activity of 5µg/ml of trypsin at 0.0125mg/ml SBTI. Benzamidine Hydrochloride at 5mg/ml reduced 5µg/ml trypsin to 1.72±2.14% of normal activity. Inhibition of trypsin with α-amino-n-caproic acid was shown to be limited and variable.

The same catalogue of eighteen alginates provided by Technostics Ltd and FMC biopolymer were tested in the trypsin activity assay. The vast majority of alginate samples had no significant effect on trypsin activity, however a small number of biopolymers were observed to have had a statistically significant effect. Despite these few examples of statistically significant inhibition, the effects are inconsistent between alginates, do not show a dose response and the levels of inhibition were not to the same extent as was observed with alginates and pepsin. Given these limited effects in the high throughput assays, the samples were further tested using kinetic methods to see if inhibitory effects varied as the enzyme:substrate ratio was changed.

Again, as with the higher-throughput assays, across most of the samples no significant effects were seen, however, some small but statistically significant effects were observed. Again, while statistically significant, the changes in the kinetics of the reactions were marginal, and not of as great a magnitude as those observed with alginate inhibition of pepsin. These data therefore suggests that alginates do not inhibit trypsin activity.

In the previous chapter a number of potential mechanisms of alginate inhibition of pepsin were discussed, including both alginate interaction with substrate and alginate interaction

with enzyme. It must therefore be considered what mechanism of enzyme inhibition would allow for the observations that alginate can inhibit activity of pepsin at acidic pH, but have no effect on the activity of trypsin at neutral pH.

It was discussed in Chapter 3 that Lipase is inhibited by pectin. The mechanism for this inhibition is that the carboxyl group of pectin protonates key active site residues, disrupting the charge relay mechanism of the catalytic triad thereby blocking enzyme activity [229]. It was discussed how a similar mechanism may be responsible for the inhibition of pepsin by alginate, with the carboxyl groups of alginate protonating key active site residues and inactivating the enzyme, for example protonation of the active site Asp32 of the acid-base pair would prevent nucleophillic attack on the scissile peptide bond.

At the assay pH which was used for the experiments described herein, and at the physiological pH at which trypsin is active, the carboxyl groups of alginate would not be protonated, and therefore would be unable to act as proton donors. It is therefore unlikely that a similar mechanism of inhibition is possible with trypsin, whereby the carboxylic acid groups of alginate would interact with catalytic residues of trypsin.

However, as was shown in Figure 72-Figure 74, trypsin activity can be inhibited by a range of serine-dependent protease inhibitors. SBTI inhibits trypsin activity by strongly binding across the active site and blocking substrate binding. As discussed previously, SBTI binding mimics a normal productive peptide hydrolysis reaction with Arg63'-Ile64' of SBTI mimicking the scissile peptide bond which occupies the active site with the positively charged Arg63' occupying the primary specificity pocket of trypsin [222]. Evidently, as a polysaccharide, an alginate molecule would not be able to mimic binding of a protein substrate in.

Substrate binding by trypsin has been shown to be highly specific, with the Asp189 residue being critical to protein substrate binding and a strong preference for cleaving on the carboxyl side of basic amino acids (Arg, Lys). Active trypsin binds to protein substrate by forming an anti-parallel beta-sheet across the protein binding site. Not only therefore is trypsin highly specific to the binding of protein, but also shows strong preference for cleavage sites, it is therefore unlikely that an alginate molecule could form a stable interaction and mimic substrate binding in the same way that SBTI does. Furthermore the active site of trypsin is enclosed within the centre of the two domains of the globular trypsin protein, which would further reduce alginate accessibility to those key active site residues [224].

179

Likewise, benzamidine hydrochloride is a small molecule serine-dependent protease inhibitor known to completely inhibit trypsin by occupying the substrate binding cleft of trypsin and competing for substrate binding (See Figure 74) [223, 224]. Benzamidine hydrochloride is held in place in the substrate binding pocket by electrostatic interactions. All trypsin enzymes have a negatively charged substrate binding pocket, and as alginates are large negatively charged polymers, they would be repelled from the trypsin substrate binding site due to charge:charge repulsion and have poor accessibility to the active site binding pocket due to size [224].

Due to the distinctly different inhibition profiles for pepsin and trypsin, the manner in which alginates and protein substrates interact across the pH range was investigated. Pepsin is an acid protease with a pH optima of 2.2; this is the pH that was used for analysis of pepsin inhibition in Chapter 3. Trypsin on the other hand is a serine protease and has a pH optimum of 7-9. A pH as high as 9 will not be reached in the small intestine, and the pH of the duodenum is in the range of 6-.65, therefore the current experiments were undertaken at at pH 6.85 so as to be more physiologically relevant to the small intestine.

As pH dependent gels, the behaviour and bioactivity of alginates can vary dramatically across the pH range, including the way alginate interacts with other molecules and polymers [230-232]. A series of alginate-protein binding experiments were carried out across the pH range where an alginate-protein solution was made and any precipitate formed from molecular interactions was allowed to settle. The viscosity of the remaining supernatant was then measured as a means of comparing and quantifying the interactions of alginate and protein at the different pH values.

With all alginates, there was typical pH dependent acid gel behaviour, with specific viscosity increasing at lower pH's as an acid gel is formed. With all of the alginate samples tested, at the lower end of the pH range there was a visible precipitate formed when BSA or Casein was added to the mixture. After 30 minutes the precipitate was allowed to settle and there was a measurable drop in the viscosity of the remaining supernatant. This precipitation and interaction between alginate and protein was not however evident at higher pH values at and above neutral.

The observation of a pH dependent interaction between alginate and protein suggests a possible mechanism by which alginate may prevent the action of pepsin without affecting trypsin in a similar way. By binding to protein and pulling it out of solution by the formation

of a precipitate the alginate may make the protein substrate unavailable to pepsin. However, this precipitation interaction did not occur at higher pH's and substrate remains available for trypsin digestion. As was discussed in Chapter 3, carbohydrates have been shown to be capable of a general protein binding, and it was discussed that the mechanism of inhibition of pepsin may be due to a direct inhibitor-substrate interaction.

At low pH interactions occur between positively charged protein molecules and negative charges on carbohydrate polymers leading to the formation of carbohydrate-protein complexes and gelation [196]. Electrostatic interactions have also been demonstrated to form between negatively charged sulphate groups of carrageenan and positively charged regions of casein [194, 195]. However the formation of positive charge on the protein only occurs as it the pH is lowered and the protein is taken below its iso-electric point. At the pH at which trypsin is active, both in the current experiments, and physiologically, protein would be above its iso-electric point and carry negative charges therefore making it unable to interact with carbohydrate polymers.

The interaction of alginate samples with BSA, Casein and Milk Protein were therefore compared rheologically at pH2 and pH7 to simulate the pH conditions at which pepsin and trypsin would be active.

In general, across all samples, changes in rheological preoperties were observed with the addition of protein to alginate solutions, as would be expected with the combination of any two polymer solutions. The nature of the change in rheological properties was shown to vary with the type of protein, type of alginate, and the pH. In some cases addition of protein to the alginate solution caused an increase in gel strength, and in some cases a weakening of the gel. But in all cases the synergistic effects were more pronounced at pH2, suggesting that interactions between alginate and protein are pH dependent, and occur more strongly at low pH.

With alginate H120L at pH2, the addition of all three protein types (BSA, Casein and MP) caused a weakening of gel strength with the both the viscous and elastic component of the dynamic modulus decreasing, and an increase in phase angle indicating a shift to more liquid like behaviour. At pH7, the addition of protein also caused changes to rheological properties, although as is demonstrated in Figure 91, in terms of the magnitude, the effects are much greater on the alginate gel at pH2, than at pH7. G*, G' and G" the dynamic, elastic and viscous moduli are directly related to gel strength, and as can be seen alginate forms a much

stronger gel at low pH, with the dynamic modulus of H120L alginate at pH2 being approximately an order of magnitude larger than at pH7 (~1Pa at pH7, ~ 10Pa at pH2). So the addition of protein has a more disruptive effect on the physical properties of alginate at a lower pH in terms of magnitude.

Similarly with alginate SF60, there was a weakening of gel strength at pH2 with the addition of BSA and Casein, with a decrease in both viscous and elastic modulus. There was however no change with the addition of milk powder, and no interactions were observed at pH7 between SF60 and any of the proteins. With FMC3 and FMC13 alginates, at pH2 the addition of protein to the mixture served to strengthen the gel, causing an increase in both the viscous and elastic component of the dynamic modulus, without changing the phase angle.

In each of the alginates tested, at pH2 the elastic modulus G' is higher than the viscous modulus G", this indicates that elastic solid-like properties dominate and the material has formed a strongly cross-linked gel as opposed to a physically entangled gel network. This occurs because in a physically entangled network, upon relaxation the material can untangle and reform, behaving like a viscous liquid, but in a cross-linked gel network interactions between polymers are broken at high frequency and do not have time to reform.

This oscillation profile is indicative of a gel that is formed by both molecular entanglement and hydrogen bonds forming between polymers. Alginate by itself is known to form strongly cross-linked gels, the data presented here shows that alginate will non-specifically interact with proteins to form a heteroplolymeric cross-linked gel and that this synergism can either have a strengthening or weakening effect on gel strength as compared to alginate by itself, but in both cases the effect is caused by the crosslinking of alginate-protein molecules and not just by physical entanglement [233].

Furthermore, the pH sensitivity of the synergism indicates that ionisation plays a role in the formation of electrostatic interactions. This further supports the argument that at low pH, interactions occur between positively charged protein molecules and negative charges on carbohydrate polymers leading to the formation of non-specific carbohydrate-protein complexes and gelation [196]. This would explain why interactions between alginate and protein are much stronger at low pH, as the formation of positive charge on the protein occurs as the protein is taken below its iso-electric point.

There is evidence *in vivo* of interactions between carbohydrates and protein affecting the digestion kinetics of protein. It was shown by Lambers et al 2013, that casein forms a protein network in the acidic gastric environment which caused casein coagulation and elevated viscosity, and with whey protein, a precipitate has been shown to form that causes a lowering of solute viscosity [175]. Lambers et al suggested that these intramolecular interactions slowed the digestion kinetics of casein as compared to whey protein which did not coagulate in the same way. It was shown that by mixing casein with low molecular weight carbohydrates such as lactose and dextran the intramolecular casein network could be disrupted and reaction kinetics enhanced. What has been observed in the previous chapter is that when interacting with the high molecular weight polysaccharide alginate, inter-molecular interactions occur which increase coagulation and elevate the viscosity profile beyond what is seen with casein alone and further slow the kinetics of casein digested. This coagulation was also observed when alginate was mixed with whey protein and milk powder, suggesting alginate would be an effective additive to attenuate and retard the digestion kinetics of these and perhaps other proteins such as BSA in the acid environment of the stomach. It further raises the prospect that carefully chosen carbohydrate additives can be used to modulate and manipulate the digestion kinetics of protein in the acid environment of the stomach as desired.

The speed at which protein digestion occurs and the rate of amino acid absorption from the gut has been shown to affect whole body post prandial protein synthesis and anabolism [174]. Dangin *et al* 2001 argue that 'slow and fast' protein digestion can be important in health and disease, with slow digested proteins having applications in cases of protein-energy malnutrition and slow digested proteins in cases such as renal diseases where high protein intakes have to be avoided. Carefully selected carbohydrates which interact with proteins may present a way of modulating protein digestion.

Alginates are used in the treatment of gastro-oesophogeal reflux. The major mechanism of protection is the raft of acid-gel which forms when alginate enters the stomach which creates a protective barrier to reflux. It is well established that non-acid components of refluxate cause damage to the oesophagus in reflux, it had been thought that a possible mechanism of the protective effect of alginate could be inhibition of pepsin. The data presented here suggests that the major mechanism of alginate inhibition of pepsin is through binding and making substrate unavailable. However these results do not conflict with the findings of Sunderland et al that alginate directly binds to pepsin; alginate likely non-specifically binds

to gastric pepsin and removes it from solution [57, 172]. Inhibition of pepsin activity may occur by two mechanisms; direct enzyme binding, and substrate binding. Furthermore, the *in vivo* gastric environment is not buffered as in the *in vitro* assays, therefore alginate will also affect the activity of pepsin also by raising the pH of the gastric environment.

Alginate protein interactions have previously been utilised in cold gelling matrices. Alginate-protein microbeads have been used as a gastric resistant delivery system to protect nutrients such as retinol and riboflavin through the stomach for release in the small intestine, where they are absorbed [234]. These delivery methods work by keeping the protein separate from the enzyme and therefore protecting it from proteolytic degredation.

The observations that alginates are capable of inhibiting pepsin digestion of a protein environment in the stomach, but not capable of inhibiting trypsin digestion in a pH neutral environment such as the small intestine suggests that alginates may not affect total protein digestion, but alter the kinetics and timecourse of protein digestion. Alginate may retard protein digestion in the stomach, with little effect in the small intenstine to the rate and kinetics of protein digestion. However, the gastric phase of digestion is important for the breakdown of large polypeptides into smaller oligopeptides and some amino acids, therefore a lower level of gastric protein digestion means that protein passed from the stomach will reach the small intestine at a slower rate or in a more complex form. This will mean that while the total yield of protein digestion may remain unaltered, the release and absorption of amino acids from protein will be slowed.

Furthermore it has been shown that exocrine pancreatic secretion of trypsin and chymotrypsin in to the duodenum is upregulated in response to proteinase inhibition in the small intestine [235]. These feedback mechanisms may overcome small intestinal trypsin inhibition, therefore inhibition in the gastric phase may be a better therapeutic target, and be less susceptible to treatment resistance.

While distinctly different profiles of alginate interaction with pepsin and trypsin were shown in *in vitro* microplate assays, the way in which alginate may interact with gastro-intestinal and dietary components in a physiologically relevant system is much more complex. In Chapter 6 the way in which alginate interacts with proteins in a model gut system is studied.

Chapter 5
Modulation of α-amylase Activity

5.1 Amylase

5.1.1 Categorisation

The α-amylases belong to glycosyl-hydrolase family 13. Glycosyl hydrolases are the super-family of enzymes that catalyse the cleavage of glycosidic bonds between sugar residues. This family also includes pullulunases, glucanotransferase, cyclomaltodextrinase, trehalose-6-phosphate hydrolase, malto-oligosyltrehalose trehalohydrolase [110]

The α-amylases are a class of glycosyl hydrolases that catalyse the cleavage of α-(1-4) glycosidic bonds in polysaccharides, α-amylase will cleave at multiple sites in linear polysaccharides to generate primarily maltose and maltotriose product. Enzymes which cleave α-D-(1-4) glycosidic bonds are also referred to as amylolytic enzymes or α-glucanases [236]. Of these α-glucanases, α-amylases are the pre-eminent starch hydrolysing enzymes in humans. The α-amylases are endohydrolytic α-glucanases, cleaving within the polysaccharide chain.

5.2 Structure of α-amylase

α-amylase is monomeric, consisting of a single polypeptide chain. The molecular weights of microbial α-amylases have been reported to vary from between 10,000 and 139,000 Da but are usually between 50 and 60,000 Da [237]. Porcine pancreatic amylase is reported as 45-50,000 Da in molecular weight and in man between 55,000 and 65,000 Da [85]. The porcine pancreatic α-amylase enzyme consists of approximately 470 amino acids [238].

All mammalian and bacterial α-amylases have been shown to have three domains, A,B and C as can be seen from (Figure 98) and contain an alpha-beta barrel structure (αβ)8 in the B domain. Domain A is composed mainly of an eight stranded β-barrel structrure which contains the active site [239]. Domain A constitutes residues 1-99 and 169-404, containing residues involved in the active site and a Cl⁻ binding site. The binding of a Cl⁻ ion has been shown to activate α-amylase [240]. All a-amylases bind an essential Ca+ ion which is required for structure and catalytic activity, this Ca+ binding site is located in Domain B.

Domain C is the N-terminal portion of the enzyme, and is thought not to be important to the catalytic mechanism [240].
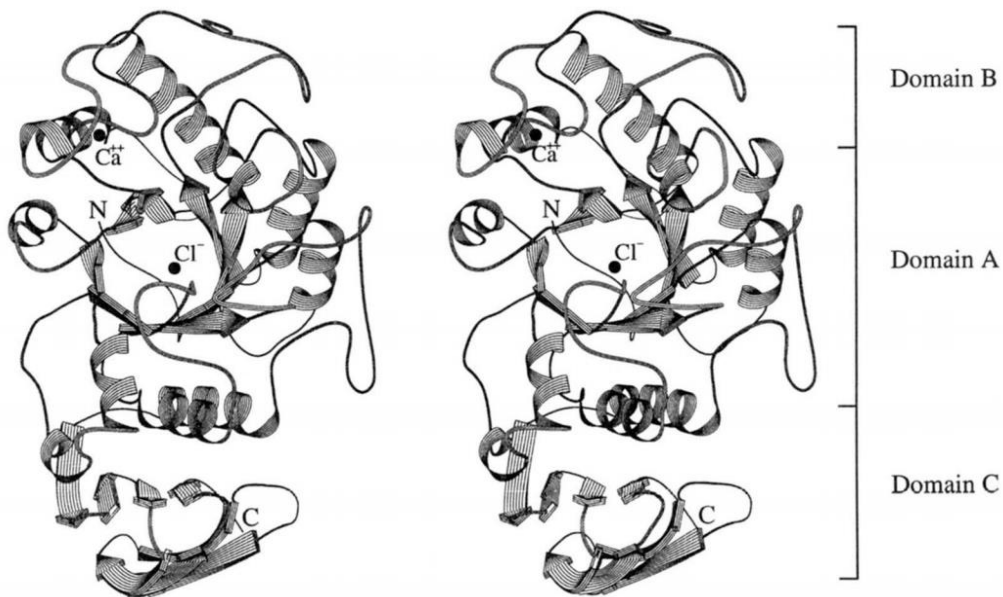
Figure 98 Schematic representation of the polypeptide chain fold of human pancreatic α-amylase and the positionings of the three structural domains (Domain A, residues 1-99, 169-404; Domain B, residues 100-168; Domain C, residues 405-496) Calcium and chloride binding sites, N- and C-terminal ends of the polypeptide chain have also been shown. Taken from Brayer et al 1995 [239]

5.3 Catalytic Mechanism

The active site is contained within Domain A and contains three perfectly conserved residues throughout the α-amylase family, corresponding to Asp180, Glu205, and Asp291 in barley and Asp176, Glu208, and Asp269 in *Bacillus subtilis* α-amylase. Mutation of these results in total loss of activity [240-242].

The α-amylase active site can hold five sugar residues and holds the substrate between the conserved catalytic residues. Amylase will cleave the polysaccharide chain at the glycosidic bond between residues 3 and 4 (Figure 99).
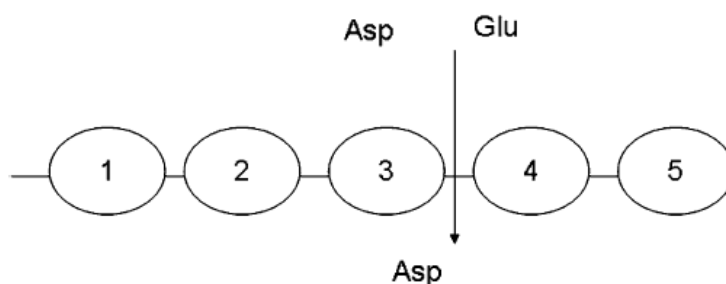
Figure 99   Active site centre of α-amylase. Cleavage occurs between residues 3 and 4. Taken from Butterworth *et al* 2011 [240].

Glycosyl hydrolases cleave in different ways and at different sites, but operate with the same essential mechanism which depends on two residues; a catalytic proton donor (glutamate) and a nucleophile/base (aspartate) [110]. The cleavage can result in either a 'retention or an inversion, of the anomeric configuration' which depends upon the distance between the proton donor and nuceophilic base [243]. α-amylase is a retaining glycosyl hydrolase and so the sugar residue conserves it's anomeric configuration after cleavage [244, 245].

In stereochemical retention, the reaction mechanism is two-step; first the acid/base catalysis, then nucleophillic attack. Both are mediated by carboxylic acid groups on the conserved active site residues. The first step is proton donation; the glycosydic oxygen at C6 is protonated by the acid-catalyst residue. i.e. the hydrogen of the carboxyl OH group forms a hydrogen bond with the glycosidic oxygen. Secondly, the nucleophilic base attacks the δ+ C6 of the sugar residue, releasing the glycosidic product from the active site and forming a glycosyl-enzyme intermediate. Release of substrate from the glycosyl-enzyme intermediate requires nucleophillic attack by a water molecule; the water molecule is split into H+ which attacks the negatively charged acid/base residue, regenerating the acid/base hydroxyl group and the remaining OH- group of the water molecule attacks the C6 carbon of the sugar residue, releasing it from the enzyme and reforming the nucleophillic O- group.
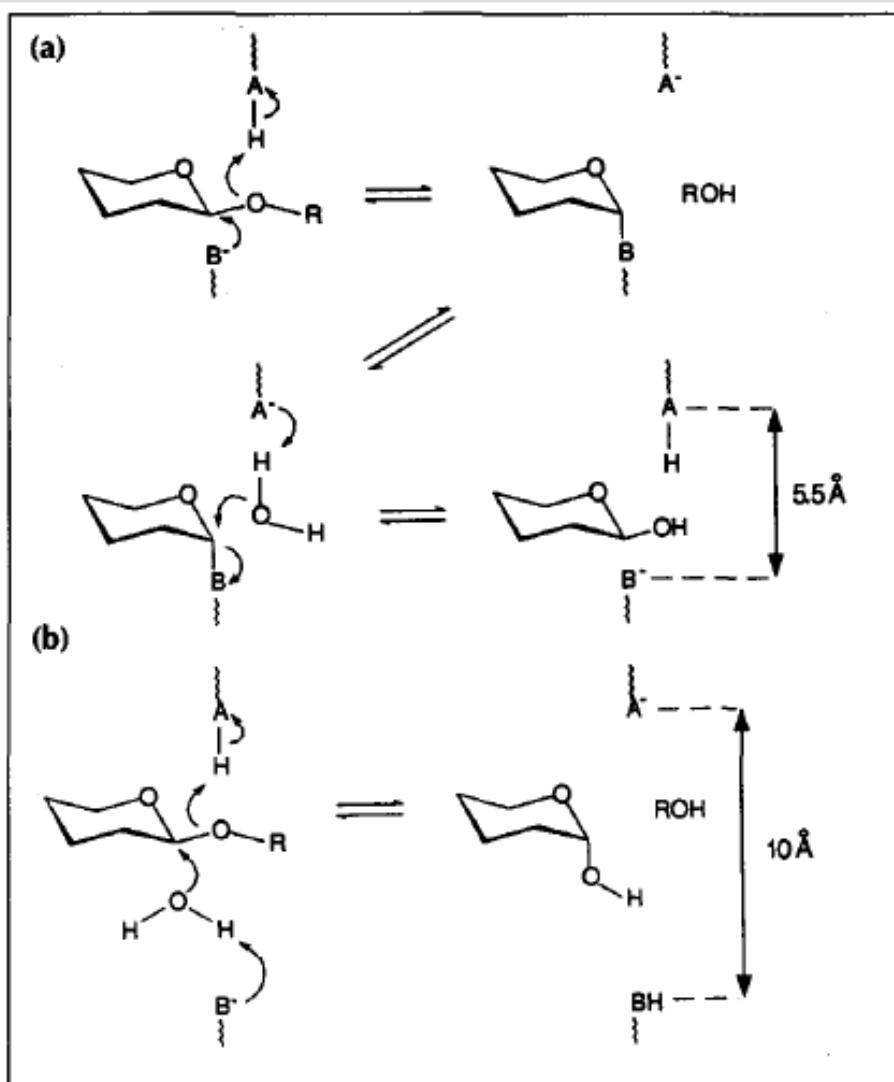
Figure 100 Glycosidic bond hydrolysis, 2 mechanisms: (a) The retaining mechanism (b) The inverting mechanism . Taken from Davies and Henrisatt 1995 [243]

The diference in stereochemical inversion is that the catalytic bases are further apart and protanation and nucleophilic attack are believed to occur simultaneously. The distance of the nucleophilic base from the aglycon C6, results in an inversion of stereochemistry [243].

5.4 Amylase pH optimum and activity

Porcine pancreatic α-amylase has been shown to have a substrate dependent pH-optimum. With starch and amylose substrates, the pH optimum of α-amylase is 6.9. However with p-nitrophenyl, α-D-maltoside, ϒ-cyclodextyrin and maltopentitol (low molecular weight oligosaccharides), the pH optimum was shifted down to 5.2.

Ishikawa et al showed this substrate dependent shift in pH optimum to be dependent on the occupation of subsite 5 of the enzyme active site. With subsite 5 occupied in the case of saccharides of 5 residues or more in length the pH optimum is 6.9. When subsite 5 is not productively occupied, the pH optimum is shifted down to pH5.2 (Figure 101).
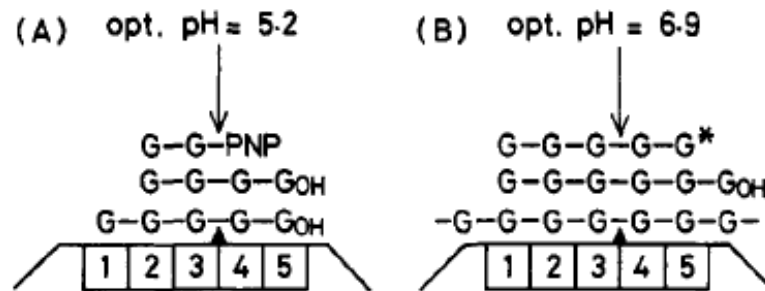
Figure 101   Active site of porcine pancreatic amylase binding substrates. The catalytic residue is located between subsites 3 and 4. Taken from Ishikawa et al 1990 [246].

This substrate dependent pH optimum has been shown to occur in human pancreatic α-amylase as well as in porcine α-amylase [246].

5.5   Dietary Fibre and Amylase Activity

As discussed in the introduction, the α-glucosidase inhibitor acarbose (Figure 3) has been shown to significantly attenuate development of Type 2 Diabetes in patients with glucose intolerance and promote a return to normal glucose tolerance [31]. Acarbose is a pseudo-oligosaccharide and is similar in structure to the substrate maltotetraose (Figure 3). Acarbose can be effectively transported through the maltose-maltodextrin transport system, but is a poor substrate for α-glucosidases and can not be metabolised and therefore occupies and blocks α-glucosidase capacity [33]. By slowing carbohydrate digestion, acarbose reduces the glycaemic-hit of a meal and reduces post-prandial insulin secretion. [32]. In the 2002 STOP-NIDDM randomised control trial, 682 patients with impaired glucose tolerance were treated with acarbose and 686 with placebo, there was a significant reduction in diabetes development in the treatment group, with 32% of patients on acarbose developing diabetes compared to 42% in the control group [31]. In a 5-year study of nearly 2000 individuals with Type II diabetes, 4.7% showed adverse effects believed to be linked to acarbose. Side effects included; flatulance, diarrhoea, nausea, abdominal pain, loss of appetite and heart burn [35].

Dietary fibres have also been investigated as potential treatments of diabetes and metabolic disease. The dietary fibre guar gum was shown to have anti-hyperlipidaemic and anti-hyperglycaemic effects when given as a dietary supplement to diabetic rats [139]. Guar gum is composed of 80-85% galactomannan, with 1.5-2.0 mannose residues for every galactose. It is structurally composed of a (1-4) β-D-mannopyranosyl backbone with single β-D-galactopyranosyl branching residues and can form thick gels [247]. Forty two male rats with Streptozotocin induced diabetes were split in to groups and were fed diets with 0%, 5%, 10% and 20% guar gum. Blood and glucose levels were measured at 0, 7, 14 and 28 days. It was shown that after 28 days there was a significant hypoglycaemic effect in the rats that had been fed 20% glucose with a 52% decrease in blood glucose. It was also shown that rats fed 5, 10 and 20% guar gum had significantly lower circulating cholesterol and triglyceride levels.

Partially Hydrolysed Guar Gum (PGHH) has been investigated as a human intervention in a randomised clinical trialo. 63 patients with type-2 diabetes were split into a control group and an intervention group fed 5g PHGG twice a day for 6 weeks. The PHGG diet was shown to have beneficial effects towards markers of metabolic syndrome with a significant reduction in

waist circumferance in the intervention group (average 1.2cm) and a significant hypoglycaemic affect. The PGHH was shown to blunt the post-prandial increases in blood glucose and insulin [140].

Dietary fibre including pectin, alginate, xantham gum and guar gum have been shown to attenuate post-prandial blood glucose response and to be an effective treatment of diabetes [141, 248-251]. It has been argued that this is due to the soluble dietary fibres increasing the viscosity of the meal which slows digestion and delays gastric emptying. Alginate has been investigated as a dietary additive to be used in diabetes management. Seven patients with type 2 diabetes were fed test meals with control or 5g alginate added and blood glucose and gastric emptying were compared. Addition of alginate to the meal resulted in reduced post-prandial blood glucuse (31% lower) and serum insulin (42% lower). Radiolabelled chromium was used to monitor the rate of gastric emptying, at 75 minutes after feeding 29% less of the meal was emptied with alginate supplementation and by 105 minutes 19% less had emptied. Furthermore the reduced blood glucose rise correlated with slowed gastric emptying. This study suggests that like other soluble dietary fibres, alginate may be a potential treatment for diabetes and that through delayed gastric emptying can reduce the glycaeminc hit of a meal and attenuate the ensuing glucose and insulin response.

Kimura *et al* 1996 looked at the effects of alginates supplementation in rats groups of 5-6 rats were fed a range of alginates and it was found that two low molecular weight alginates attenuated glucose response 30min and 60min after feeding [252].

The importance of viscosity in blunting the glycaemic response was shown by Jenkins et al. Six types of dietary fibre were compared for their ability to reduce post-prandial blood glucose. Guar, pectin, tragacanth gum, methylcellulose, wheat bran and cholestyramine were compared and Guar Gum was shown to be most effective at flattening the glucose response, however when hydrolysed non-viscous guar gum was administered, the effect was abolished. This adds weight to the argument that it is the viscosity of guar and other fibres which is important to the blunting of post-prandial hyperglycaemia [249].

Interest in bioactive compounds and carbohydrate digestion has not just been on garstric emptying and GI transit time, but also into direct effects exogenous compounds may have on amyolytic enzymes. Research into fibres as inhibitors of digestive enzymes began in the late 70s and early 80s. Rats fed a high fibre diet containing 20% cellulose have shown a

significant decrease in intestinal proteolytic, lipolytic and amylolytic enzyme activity upon analysis of intestinal contents [50]. Dilution of stomach contents with DF has been suggested as a possible factor during *in vivo* studies of enzyme activity [50]. However, the same investigators were also able to demonstrate *in vitro* inhibiton of pancreatic enzymes in samples of human pancreatic juice. Activity of lipase, amylase, trypsin and chymotrypsin was compared in samples of human pancreatic juice incubated with or without a range of DFs. With the exception of pectin, the fibres examined (alfalfa fibre, oat bran, hemicellulose, wheat bran and cellulose) all brought about a reduction in activity of trypsin, chymotrypsin, lipase and α-amylase, with cellulose and hemicellulose producing the largest effect. However, incubation with pectin was shown to bring about a 48% increase in α-amylase activity and a 23% increasse in lipase activity [51].

In the 1980s starch blockers became a popular area of research in the treatment of obesity and other 'carbohydrate-dependent' diseases such as diabetes and insulin resistance as researchers sought to find ways of inhibitting α-amylase in order to block carbohydrate digestion. Although starch blocker tablets are still widely marketed, their efficacy is the subject of dispute [24-26]. The active agents in starch blockers are proteins extracted from a number of plants; *Phaseolus vulgaris* (Common bean) extract [27], *Triticum aestivum* (wheat flour) extract [28] and Ttype 1 α-amylase Iinhibitor (α-AI) from *Amaranthus hypochondriacus* seeds [29]. It is thought that these natural amylase inhibitors evolved as a defense mechanism to protect the plant against predation [30]. Relatively recent work has again supported the use of *Phaseolus vulgaris* extract. In a small human trial weight-loss with *Phaseolus vulgaris* extract was shown to be higher than placebo when 25 healthy individuals were fed *Phaseolus vulgaris* extract or placebo with meals [25].

5.6 Methods

5.6.1 Dinitrosalycylic assay of a-amylase activity

The DNSA α-amylase assay, first developed by Sumner in 1921, works on the principle of measuring the amount of reducing sugar produced by α-amylase cleavage of substrate starch [253].

Reducing sugars are generated by the α-amylase cleavage of the starch substrate. When 3,5-dinitrosalycylic acid is heated to 100°C in the presence of reducing sugars, a red colour is formed proportionate to the amount of reducing sugar. At 100°C these reducing sugars reduce 3,5-Dinitrosalycylic acid to 3-amino, 5-nitrosalycylic acid and the aldehyde group of the sugar is oxidised to carbonyl. Change in absorption can be detected at 550nm in a 96-well plate spectrophotometer.

5.6.2 Scaling Down to 96 well microplate

30µl of amylase solution was incubated with 30µl of biopolymer sample and incubated for 30 minutes. At T0 60µ of starch substrate was added and incubated at 37°C for 30 minutes. At T_{30} 120µl of DNS reagent solution was added to all wells and the plate was heated to 100°C for 15 minutes. Colour absorption was then measured at 550nm.

As with the N-terminal assay, in an unbuffered system there is a large degree of pH variation in the reaction solution with the addition of alginate, as can be seen in Figure 102.
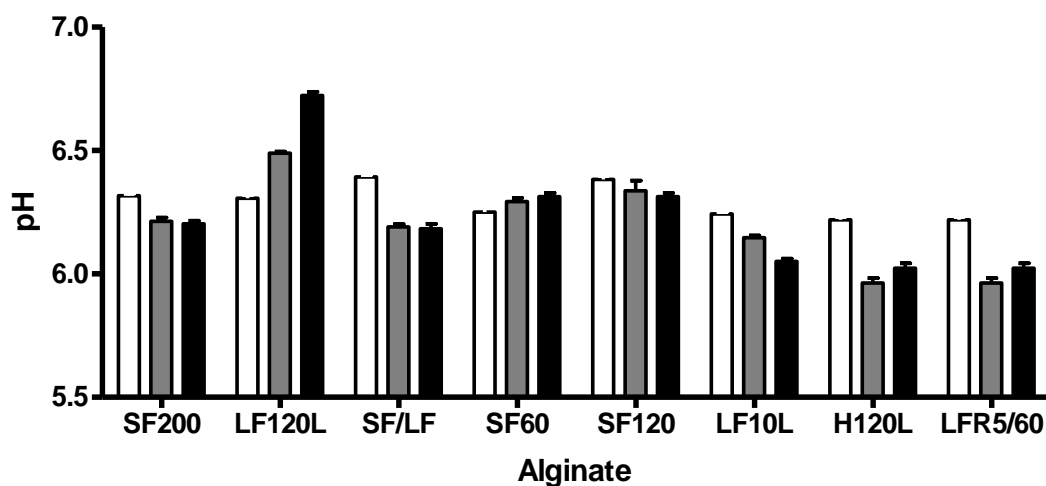
Figure 102   pH variation of Dinitrosalycylic acid reaction solution with the addition of alginate . □0.25mg/ml, ▨1mg/ml, ■4mg/ml.

The assay was therefore set up to run in a 30mM Sorensen's phosphate buffer. As can be seen from Figure 103 this effectively buffers the alginates, and keeps the reaction pH consistent.
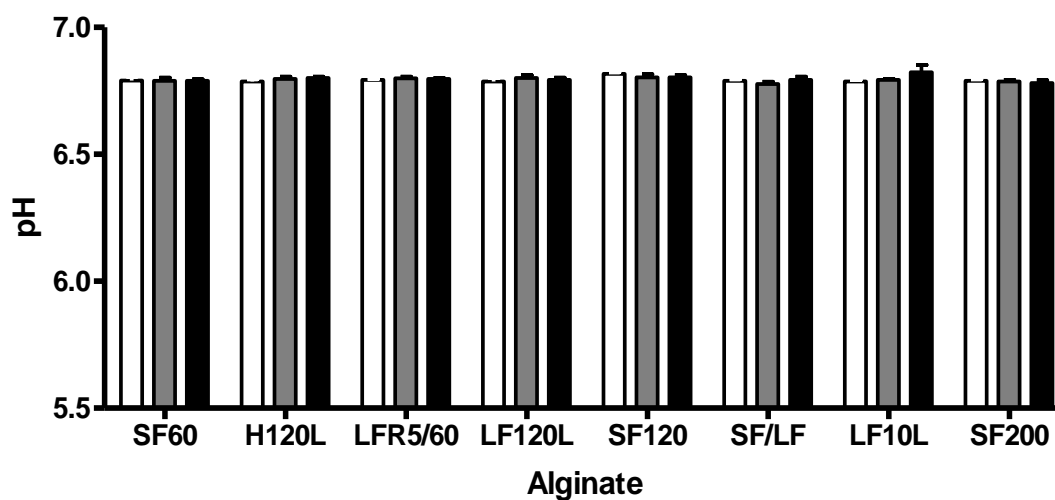
Figure 103   pH variation of Dinitrosalycylic acid reaction solution with the addition of alginates buffered in 30mM sorensen's phosphate.. □0.25mg/ml, ▨1mg/ml, ■4mg/ml.

A range of starch and amylase concentrations were tested. As can be seen from Figure 104 at 0.5 and 1mg/ml amylase there was a non-linear relationship between colour development and substrate concentration. At 0.25mg/ml the relation between substrate concentration and activity was linear as shown in Figure 104.

Iit was therefore decided that dietary fibre activity would be tested against 0.25mg/ml amylase with 5mg/ml Starch substrate concentration.
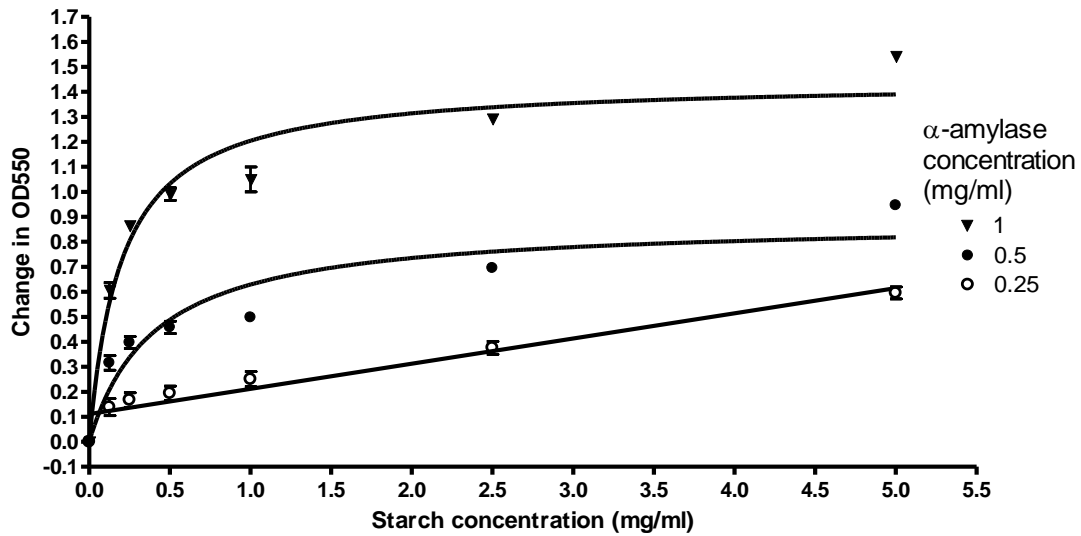
Figure 104   Colour development in DNS assay with varying starch and α-amylase concentrations.

5.7 α-Amylase HTP Assay

5.7.1 96-Well Plate N-Terminal Method

5.7.2 Preperation of Solutions

For high-throughput analysis, biopolymer samples were prepared at 10mg/ml in 30mM Sorensen's Phosphate buffer. Starch substrate was prepared by heating 5mg/ml potato starch to 80°C while stirring and then left to cool and kept at 27°C. α-amylase was prepared at 0.25mg/ml in buffer.

The dinitrosalycylic acid reagent was prepared by dissolving 0.25g DNS in 5ml 2N NaOH and making up to 12ml. 7.5g Sodium Tartrate was then added and the solution was made up to 25ml.

A 0.2% (w/v) Maltose Standard was also prepared in buffer.

5.7.3 Method

30µl Fibre Sample was pre-incubated with 30µl α-amylase for 30 minutes on a shaker. At T0 60µl of Starch substrate solution or buffer blank was added as appropriate and the plate was incubated for 30min at 37˚C.

After 30 minutes, 120µl of DNS reagent was added and mixed and the plate was incubated for 15 minutes in an Autoblot Microhybridisation oven at 100˚C.

At T_{45}, the plate was removed from the microhybridisation oven and left to cool to room temperature and read at 550nm.

For each dietary fibre sample an adjacent control sample was run on the opposite side of the plate. This was to ensure that any affect on the rate of the dinitrosalyclic acid reaction due to uneven heating of the plate as the temperature is raised to 100°C was controlled for.

5.7.4 Plating

| | Blank | Sample A | | | Sample B | | | Sample C | | | Blank |
| | | 5 mg/ml | 2.5 mg/ml | 1.25 mg/ml | 5 mg/ml | 2.5 mg/ml | 1.25 mg/ml | 5 mg/ml | 2.5 mg/ml | 1.25 mg/ml | |
	1	3	4	5	3	4	5	3	4	5	12
A	60ul Buffer	30ul Buffer 30ul Sample	30ul Buffer 30ul Sample	30ul Buffer 30ul Sample	30ul Buffer 30ul Sample	30ul Buffer 30ul Sample	30ul Buffer 30ul Sample	30ul Buffer 30ul Sample	30ul Buffer 30ul Sample	30ul Buffer 30ul Sample	60ul Buffer
B	60ul Buffer	30ul Buffer 30ul Sample	30ul Buffer 30ul Sample	30ul Buffer 30ul Sample	30ul Buffer 30ul Sample	30ul Buffer 30ul Sample	30ul Buffer 30ul Sample	30ul Buffer 30ul Sample	30ul Buffer 30ul Sample	30ul Buffer 30ul Sample	60ul Buffer
C	60ul Buffer	30ul Amylase 30ul Sample	30ul Amylase 30ul Sample	30ul Amylase 30ul Sample	30ul Amylase 30ul Sample	30ul Amylase 30ul Sample	30ul Amylase 30ul Sample	30ul Amylase 30ul Sample	30ul Amylase 30ul Sample	30ul Amylase 30ul Sample	60ul Buffer
D	60ul Buffer	30ul Amylase 30ul Sample	30ul Amylase 30ul Sample	30ul Amylase 30ul Sample	30ul Amylase 30ul Sample	30ul Amylase 30ul Sample	30ul Amylase 30ul Sample	30ul Amylase 30ul Sample	30ul Amylase 30ul Sample	30ul Amylase 30ul Sample	60ul Buffer
E	60ul Buffer	30ul Amylase 30ul Sample	30ul Amylase 30ul Sample	30ul Amylase 30ul Sample	30ul Amylase 30ul Sample	30ul Amylase 30ul Sample	30ul Amylase 30ul Sample	30ul Amylase 30ul Sample	30ul Amylase 30ul Sample	30ul Amylase 30ul Sample	60ul Buffer
F	60ul Buffer	30ul Amylase 30ul Sample	30ul Amylase 30ul Sample	30ul Amylase 30ul Sample	30ul Amylase 30ul Sample	30ul Amylase 30ul Sample	30ul Amylase 30ul Sample	30ul Amylase 30ul Sample	30ul Amylase 30ul Sample	30ul Amylase 30ul Sample	60ul Buffer
G	60ul Buffer	30ul Buffer 30ul Sample	30ul Buffer 30ul Sample	30ul Buffer 30ul Sample	30ul Buffer 30ul Sample	30ul Buffer 30ul Sample	30ul Buffer 30ul Sample	30ul Buffer 30ul Sample	30ul Buffer 30ul Sample	30ul Buffer 30ul Sample	60ul Buffer
H	60ul Buffer	30ul Buffer 30ul Sample	30ul Buffer 30ul Sample	30ul Buffer 30ul Sample	30ul Buffer 30ul Sample	30ul Buffer 30ul Sample	30ul Buffer 30ul Sample	30ul Buffer 30ul Sample	30ul Buffer 30ul Sample	30ul Buffer 30ul Sample	60ul Buffer

Figure 105   Plating layout for the α-amylase microplate assay.

.

5.7.5 Kinetic Analysis

As with the high-throughput assay α-amylase was made up at 0.25mg/ml in 30mM Sorensens Phosphate. All biopolymer samples were made up at 4 mg/ml in 30mM Sorensen's Phospate buffer.

Substrate starch solution was prepared by heating 5% (w/v) sigma starch from potato in 30mM Sorensen's Phosphate to 80°C while stirring.

DNSA colour reagent was prepared by dissolving 0.25g DNSA in 5ml 2N NaOH. This was then made up to 12ml with water and 7.5g of sodium tartrate was added. The final solution was then made up to 25ml.

A 0.2% (w/v) Maltose Standard was also prepared in buffer.

5.7.6 Procedure

On Plate 1 a range of dilutions of substrate starch was prepared in three lanes ranging from 5% w/v to 0.6125% w/v. These values represent the highest concentration that will go into solution, and the lowest concentration that produces a reliable result.

5.7.1 Plating Kinetic assay

	Substrate Dilutions 5mg/ml	Substrate Dilutions 4mg/ml	Substrate Dilutions 3mg/ml	Substrate Dilutions 2.5mg/ml	Substrate Dilutions 2mg/ml	Substrate Dilutions 1.5mg/ml	Substrate Dilutions 1mg/ml	Substrate Dilutions 0.5mg/ml	Substrate Dilutions 0.25mg/ml	Substrate Dilutions 0.125mg/ml	Substrate Dilutions 0.06125mg/ml	Substrate Dilutions 0mg/ml
A												
B	30µl α-amylase 30µl sample	→										
C	30µl α-amylase 30µl sample	→										
D	30µl buffer 30µl sample	→										
E	60µl of buffer	→										
F	30µl α-amylase 30µl buffer	→										
G	30µl α-amylase 30µl buffer	→										
H												

Figure 106   Plating layout for the α-amylase kinetic microplate assay.

On one plate, substrate dilutions were prepared at appropriate concentrations. On a second plate 30µl of biopolymer at 4mg/ml was added to all wells in the three test rows. 30µl of buffer was added to all wells in the control lane and 30µl of 0.025mg/ml α-amylase was added to all wells in the two test lanes. The plate was then pre-incubated for 30 minutes at 37°C.

At T_0, 60µl of substrate from plate 1 was added to the relevant column on plate 2 and pre-incubated for 30 minutes. At T_{30}, 120µl of DNS reagent was added to all wells and heated at 100°C until T_{50}. After the plate has cooled for 30 minutes samples were read at OD_{540}.

All results were done in duplicate on the plate and standardised to the control. Each plate was run in triplicate with fresh solutions.

5.8 Alginate and Amylase

5.8.1 Microplate Screening

Amylase activity in the presence of dietary biopolymers was measured using a 96-well microplate adaptation of the DNSA α-amylase assay, first developed by Sumner in 1921, as described in the experimental section. The assay system was validated using EDTA, a known α-amylase inhibitor as a positive inhibition control. EDTA is a calcium chelator thought to inhibit amylase activity by chelating the tightly bound calcium of α-amylase [254].
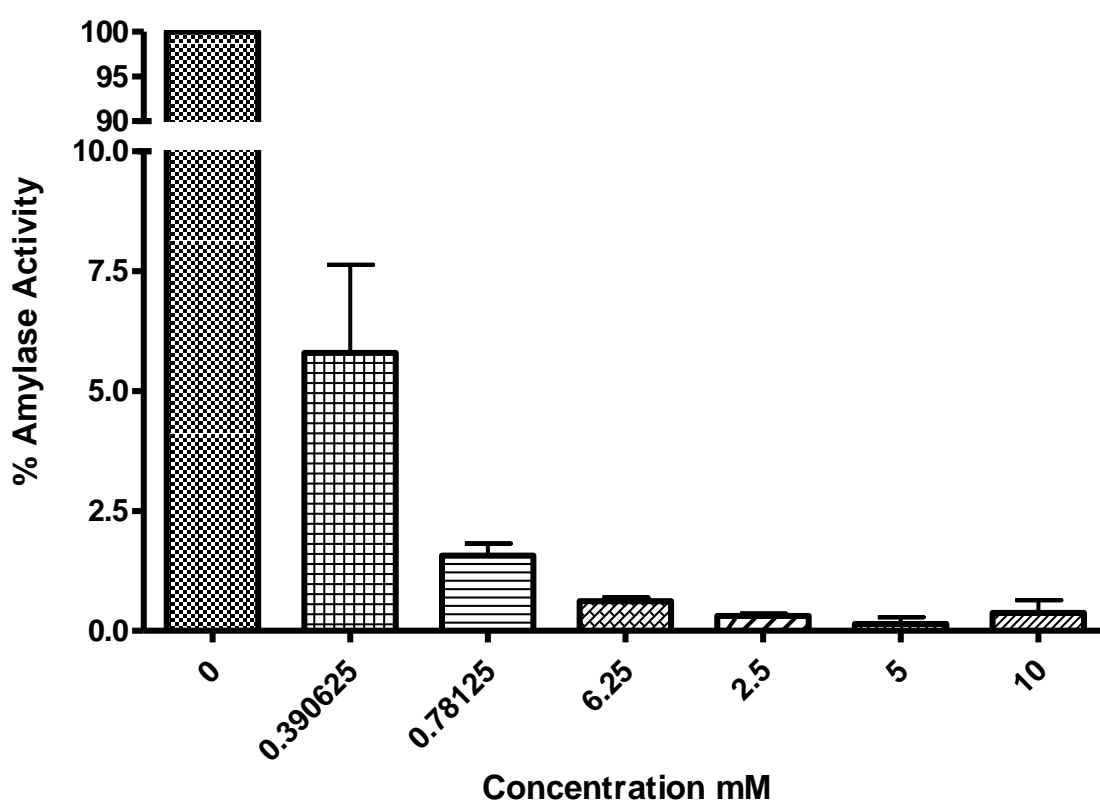
Figure 107 – Amylase Inhibition with EDTA. Amylase activity is plotted against EDTA concentration in mM as a positive inhibition control. (n=3). Uninhibited α-amylase control activity is represented by 100%.

Maximum inhibition with sodium EDTA was achieved at a concentration of 5mg/ml, there is a clear dose response effect, as shown in Figure 107. The strongest inhibition of α-amylase was at 5mg/ml, reducing activity to $0.15\pm0.13\%$ of normal amylase activity.

Again the catalogue of 18 well characterised alginates was tested for their modulatory activity towards α-amylase. All alginate samples were tested at three concentrations; 10, 2.5

and 0.625mg/ml. This gave reaction concentrations of 2.5, 0.625 and 0.156mg/ml, respectively.

In Figure 108 the results for the catalogue of eighteen alginates have been collated. Taken together there is a clear dose effect as can be seen in Figure 108. At a 2.5mg/ml concentration of alginate, there is an average increase in amylase activity of 18.45±6.1%. At a 0.625mg/ml concentration of alginate, there is an average increase in amylase activity of 11.0±4.4%. At a 0.1625mg/ml concentration of alginate, there is an average increase in amylase activity of 5.5±3.3%.
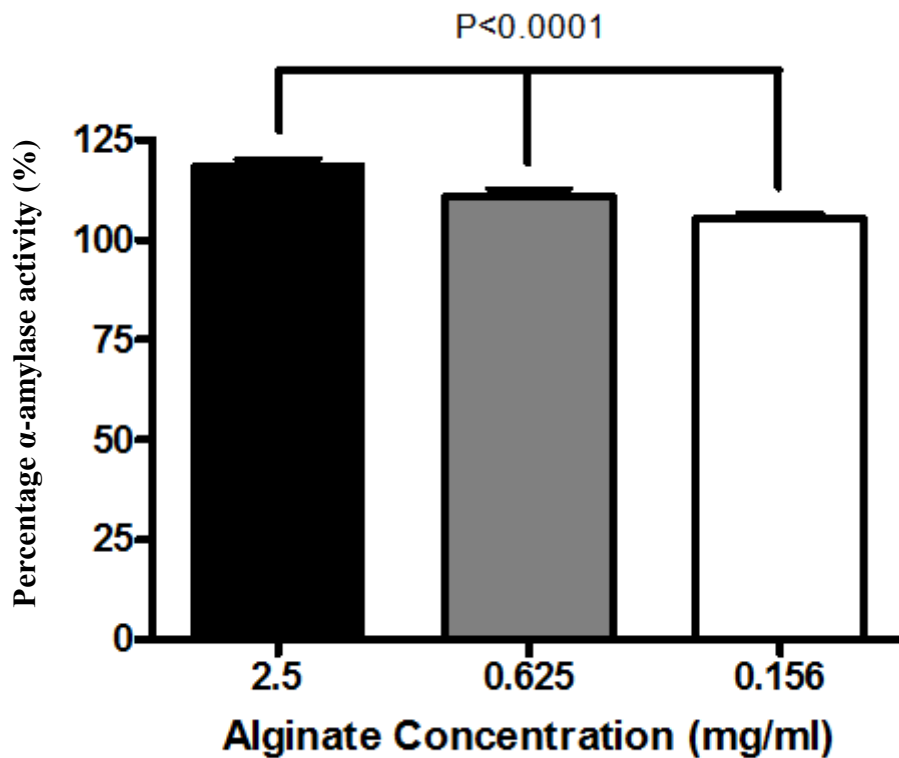
Figure 108   - Concentration dependent activation of amylase in the presence of sample alginates. Activity is shown as a percentage increase from normal amylase activity at three concentrations. ☐ 0.156mg/ml, ▨ 0.625mg/ml, ◼ 2.5mg/ml. All samples were tested in triplicate (n=3) with error bars showing standard deviation.

The complete data for alginate regulation of α-amylase is shown in Figure 109. Tthe highest concentration of 2.5g/ml all alginates bring about an increase in amylase activity. However there is a large degree of variation in the magnitude of activation from alginate to alginate. This variation was investigated in relation to alginate structure.
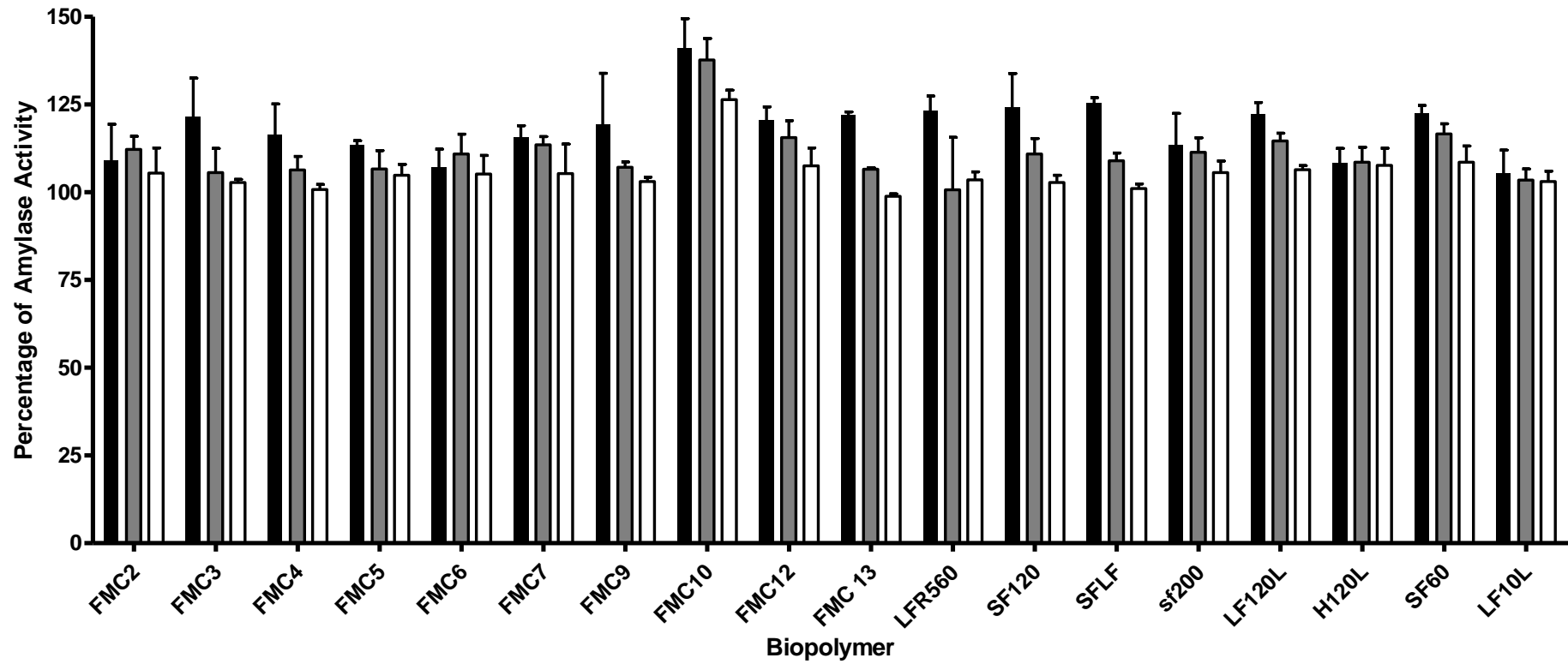
Figure 109 - Concentration dependent activation of amylase in the presence of alginates. Activity is shown as a percentage of normal amylase activity at three concentrations of alginate, ☐ 0.156mg/ml, ▨ 0.625mg/ml, ■ 2.5mg/ml. All samples were tested in triplicate (n=3) with error bars showing standard deviation.

Figure 108 demonstrates that alginates per se can activate α-amylase activity and increase the rate of activity in a dose dependent way. In order to investigate links between this activation and alginate structure, the levels of activation were correlated against alginate F:G content.

As previously stated, the 8 brown seaweed alginates provided by Technostics Ltd were extracted from two separate species; High-G Lamanaria, and High-M Lessonia. These have been compared in the Box-Plots in Figure 110. No statistically significant difference could be shown between these two groupings using an unpaired T-Test (P=0.24), and therefore no species effect was demonstrated.
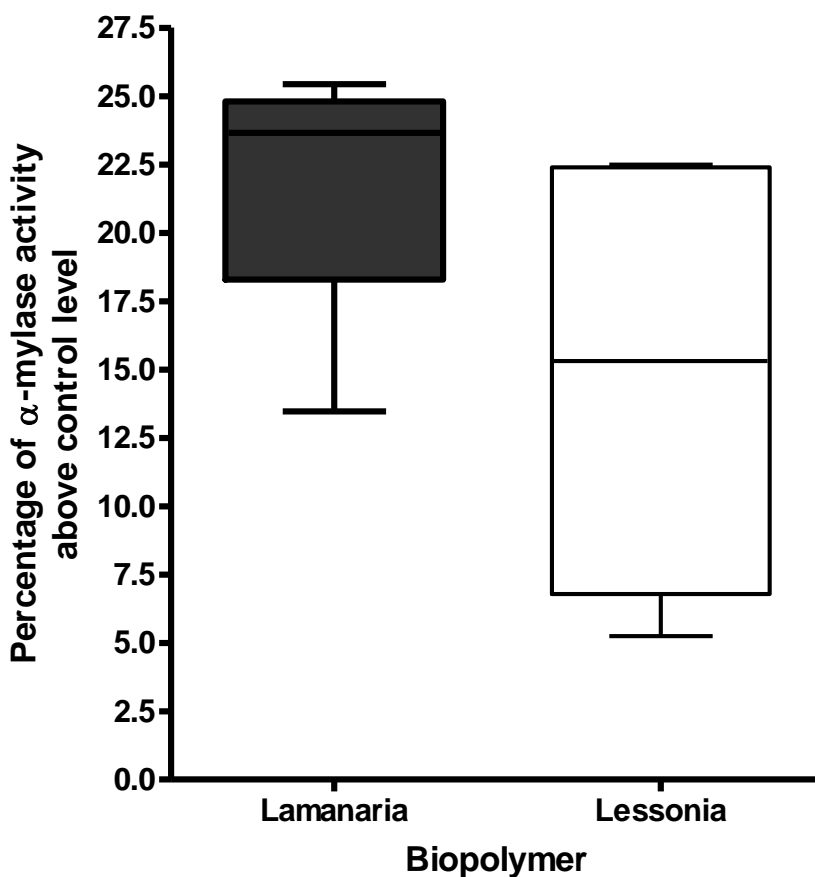
Figure 110 – Comparison of amylase activation levels between high-G Lamanaria alginate and high-M Lessonia Alginate. The boxplots show four High-G alginate samples from Lamanaria and four High-M from lessonia. All samples were done with 6 repeats. The plot shows no significant difference in activation between the two species, P=0.2379 with an unpaired T-Test.

The catalogue of 18 alginates tested cover a full range of structural F[G] content, as shown in Figure 111 it was therefore possible to correlate percentage activation of amylase activity against alginate F[G] and test the statistical significance using Spearman's Rank Correlation.

No significant correlation was found between alginate F[G] and percentage pepsin activation at 2.5mg/ml, 0.625mg/ml or 0.156mg/ml. That is therefore to say that no significant link could be demonstrated between manuronic/guluronic acid residue content and levels of pepsin activation.
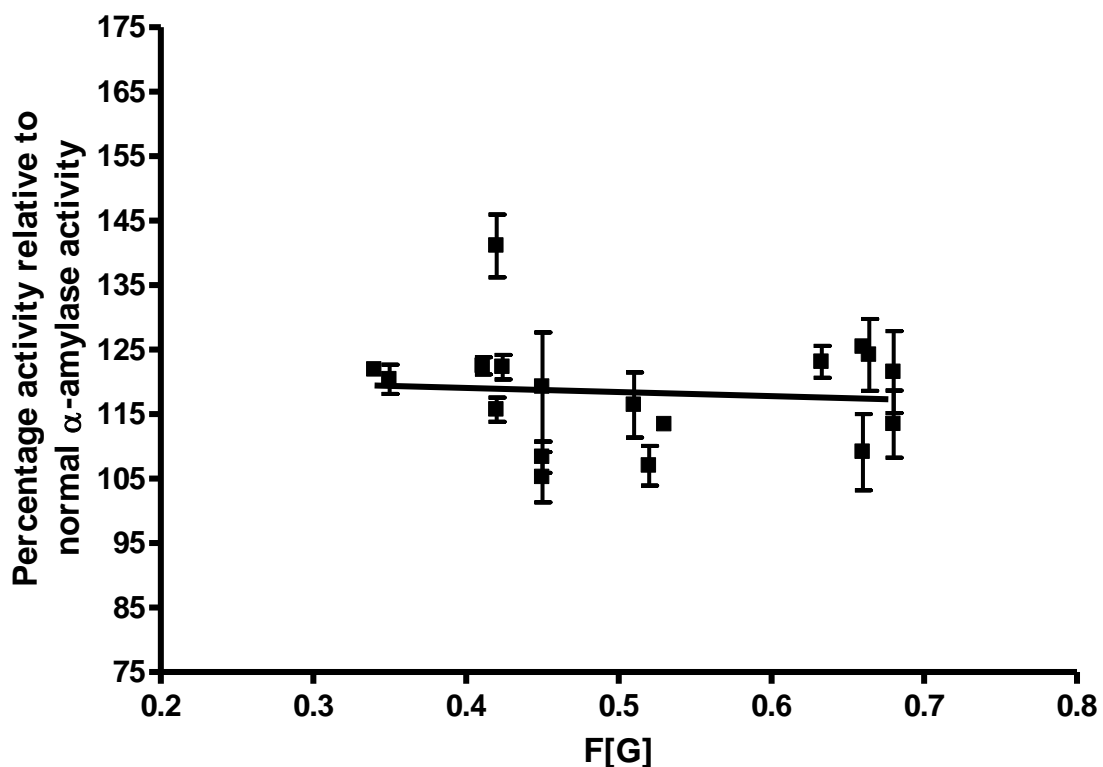
Figure 111 - Correlation of alginate G-residue frequency (F[G]) and level of amylase activation with 2.5mg/ml alginate. Amylase activation is shown as a percentage of normal amylase activity. The error bars show the standard deviation of 3 replicates (n=3). No statistically significant correlation could be shown with a Spearman r value of -0.085 and a p value of 0.74.

At 12.5mg/ml the Spearman rank correlation coefficient, as shown in Figure 111 was -0.085 and a p value of 0.74, showing no statistically significant correlation between α-amylase activation at 10mg/ml and alginate F[G] content. At 0.625mg/ml the Spearman rank correlation coefficient, as shown in Figure 112 was -0.36 and a p value of 0.14, showing no statistically significant correlation between amylase activation at 2.5mg/ml and alginate F[G] content. At 0.156mg/ml the Spearman rank correlation coefficient, as shown in Figure 113 was -0.33 and a p value of 0.18, showing no statistically significant correlation between amylase activation F[G] content.
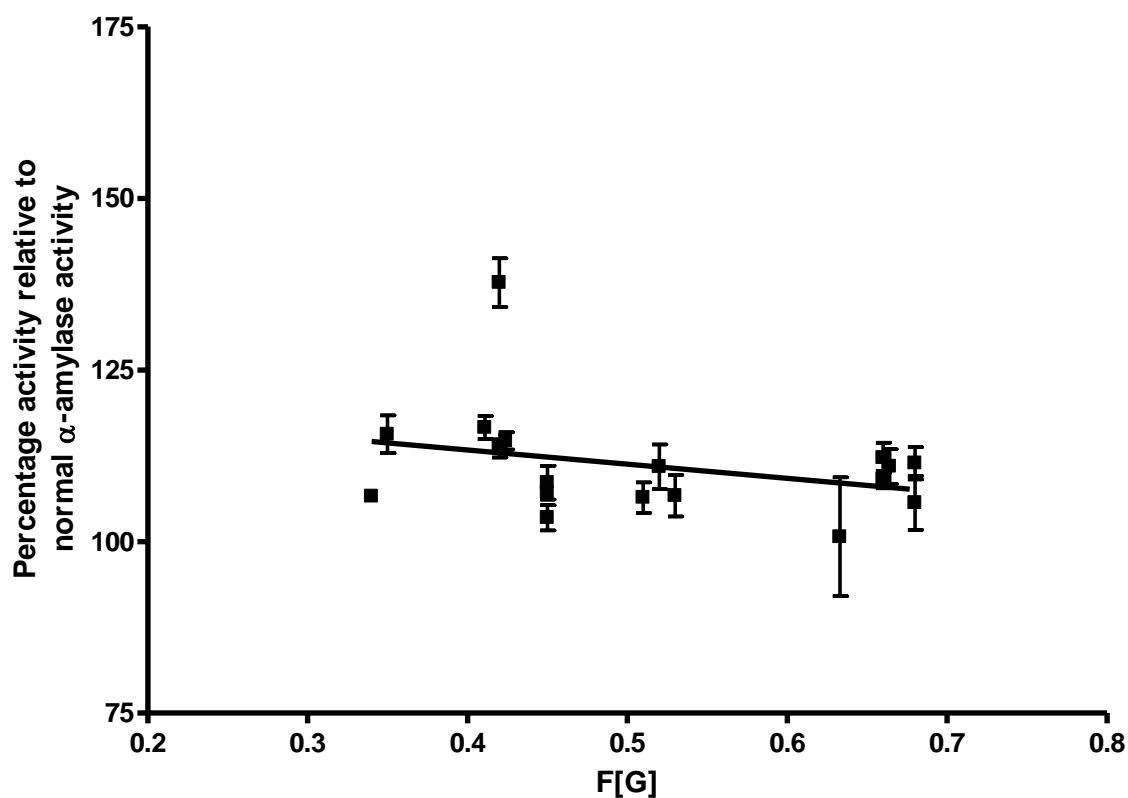
Figure 112- Correlation of alginate G-residue frequency (F[G]) and level of amylase activation with 0.625mg/ml alginate. Amylase activation is shown as a percentage of normal amylase activity. The error bars show the standard deviation of 3 replicates (n=3). No statistically significant correlation could be shown with a Spearman r value of -0.36 and a p value of 0.14.
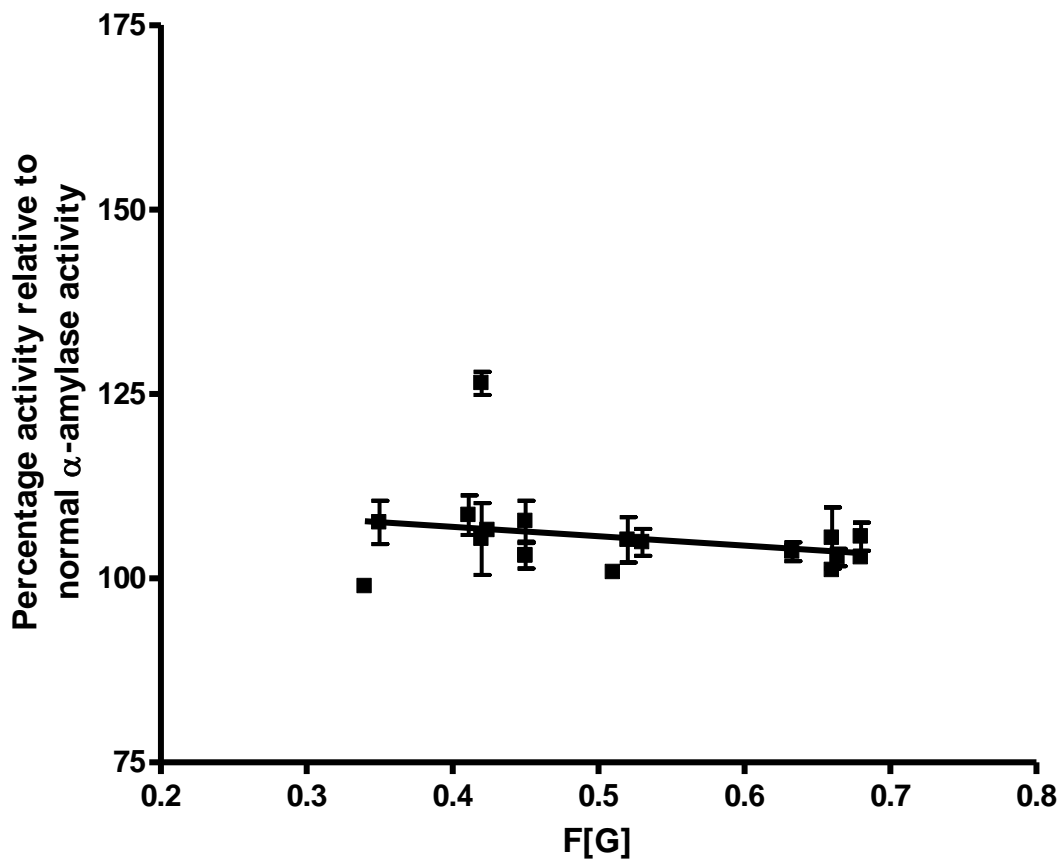
Figure 113 - Correlation of alginate G-residue frequency (F[G]) and level of amylase activation with 0.156mg/ml alginate. Amylase activation is shown as a percentage of normal amylase activity. The error bars show the standard deviation of 3 replicates (n=3). No statistically significant correlation could be shown with a Spearman r value of -0.33 and a p value of 0.18.

The fact that no correlations could be shown with alginate F[G] at any of the tested correlations suggest that the activation effect observed with alginates is a nonspecific activation caused by any alginate and not affected by alginate composition. However, while no correlation was demonstrated between alginate F[G] and amylase activation levels, the structure and biophysical properties of alginates are not just dictated by F[G] frequency, but also by the arrangement of contiguous blocks of M and G residues as was discussed in the introduction. Levels of amylase activation were correlated against the other structural data available for the well characterised alginates (Table 19). No statistically significant correlations could be shown between levels of α-amylase and activation and any of the structural characteristics of the well characterised alginate samples.

Structural Characteristic	2.5mg/ml		0.625mg/ml		0.156mg/ml	
	Spearmans value	P-value	Spearmans value	P-value	Spearmans value	P-value
F[G]	-0.085	0.7376	-0.360	0.1417	-0.329	*0.1820*
F[M]	0.049	0.8483	0.365	0.1368	0.347	0.1582
F[GG]	-0.096	0.7047	-0.353	0.1506	-0.324	0.1893
F[MG/GM]	0.032	0.8994	0.249	0.3199	0.350	0.1544
F[MM]	-0.023	0.9286	0.346	0.1593	0.356	0.1476
F[MGG/GGM]	0.349	0.1562	0.233	0.3526	0.321	0.1944
F[MGM]	-0.046	0.8547	0.207	0.4110	0.366	0.1358
F[GGG]	-0.129	0.6096	-0.314	0.2044	-0.286	0.2497
N [G>1]	-0.127	0.6157	-0.329	0.1822	-0.352	0.1521

Table 19   Correlation between levels of α-amylase activity and structural characteristics of alginate.

Molecular weight data was only available for the eight alginates supplied by Technostics Ltd. Levels of amylase activation were correlated against these eight alginate with molecular weights ranging from 34,700 – 387,000 Da. However no significant correlations could be shown between molecular weight and amylase activity as shown at substrate contractions of either 2.5mg/ml, 0.625mg/ml or 0.156mg/ml as shown in Figure 114, Figure 115 and Figure 116 respectively.
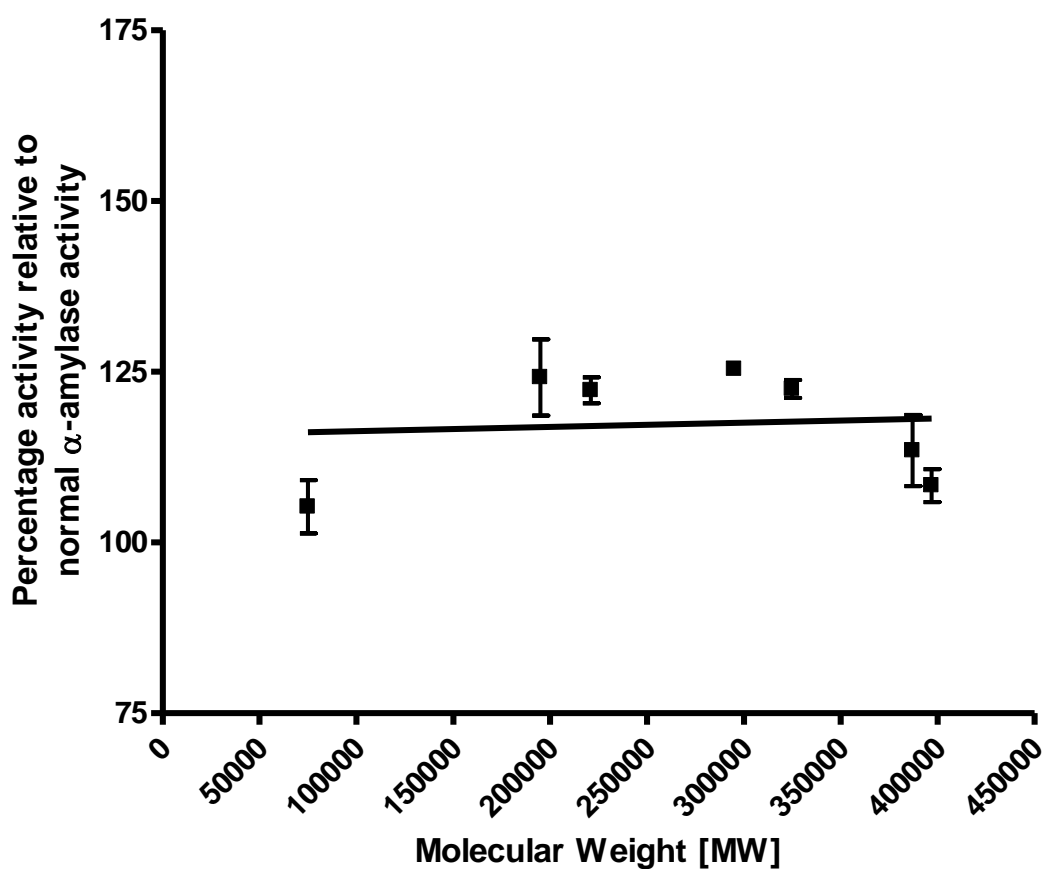
Figure 114 - Correlation of alginate Molecular Weight (MW) and level of amylase activation with 2.5mg/ml alginate. Amylase activation is shown as a percentage of normal amylase activity. The error bars show the standard deviation of at least 3 replicates (n=3). No statistically significant correlation could be shown with a Spearman r value of -0.07143 and a p value of 0.9063.
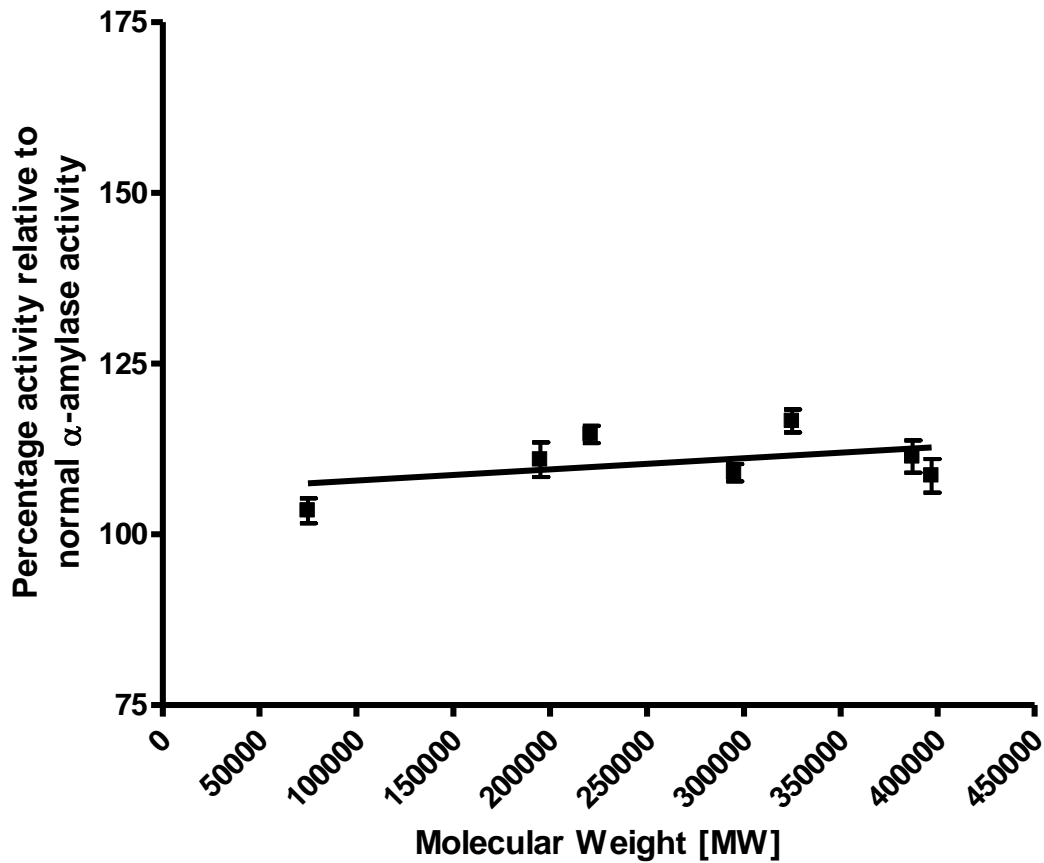
Figure 115 - Correlation of alginate Molecular Weight (MW) and level of amylase activation with 0.625mg/ml alginate. Amylase activation is shown as a percentage of normal amylase activity. The error bars show the standard deviation of at least 3 replicates (n=3). No statistically significant correlation could be shown with a Spearman r value of 0.2143and a p value of 0.6615.
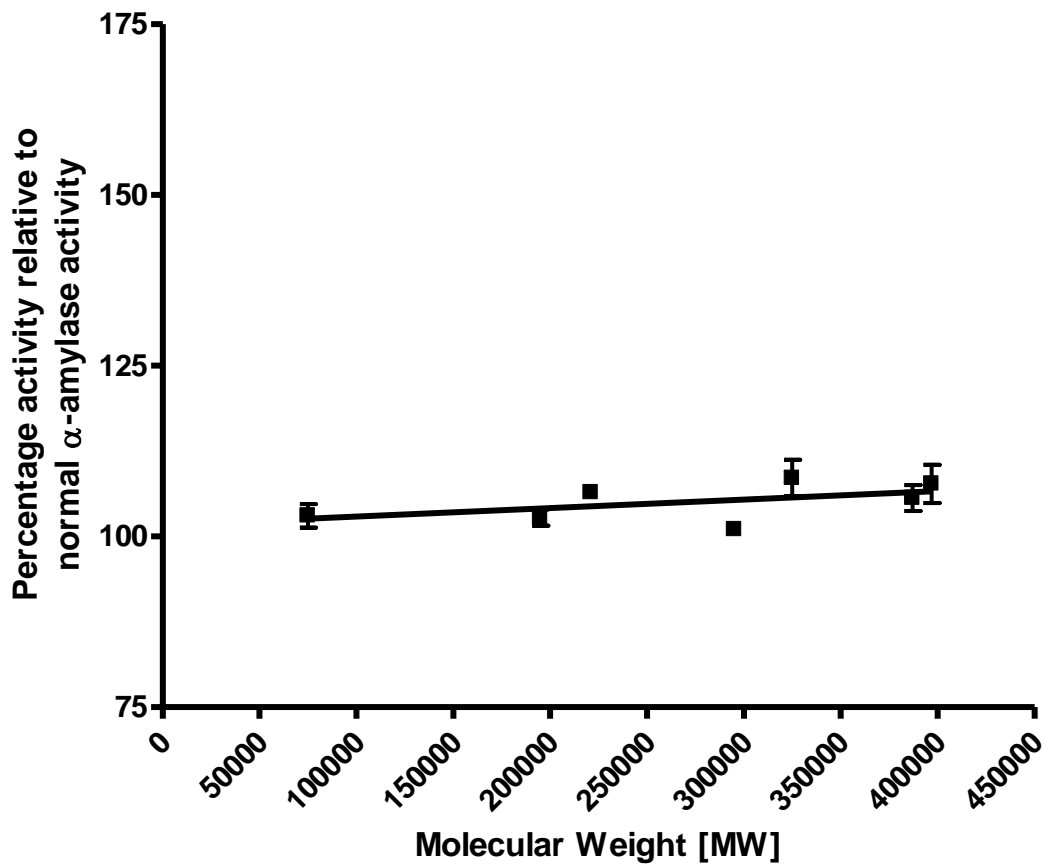
Figure 116 - Correlation of alginate Molecular Weight (MW) and level of amylase activation with 0.156mg/ml alginate. Amylase activation is shown as a percentage of normal amylase activity. The error bars show the standard deviation of at least 3 replicates (n=3). No statistically significant correlation could be shown with a Spearman r value of 0.5357 and a p value of 0.2357.

5.9 Alginate-amylase enzyme kinetics

Selected kinetic analysis was carried out on all well characterised alginate samples using a modified version of the 96 well microplate DNS Acid Assay as described in the methods section. All biopolymer samples were tested a minimum of 5 times and kinetic data was calculated using Graphpad Prism 4 software.

Enzyme kinetics is primarily used for the study of enzyme inhibition, but the principles may also be applied to enzyme activation. Enzyme activation may occur through an increase in the affinity of the enzyme for the substrate. This would cause an increased rate of reaction at low substrate concentrations, but would be saturated out at higher substrate concentrations and therefore the K_m would be lowered, but the V_{max} would remain unchanged.

Alternatively the enzyme becomes more active towards the substrate via a mechanism other than increased enzyme-substrate affinity and the maximum velocity of the reaction is increased, but as there is no change in enzyme-substrate affinity the K_m remains the same.

Figure 117 below shows a typical kinetic plot for alginate activation of α-amylase. In the control digestion the velocity of the reaction increases more or less proportionally with the concentration of the substrate from 0-0.5mg/ml of substrate, after which the reaction velocity begins to plateaux as the enzyme active site becomes saturated. As can be seen from Figure 117 below, when the alginate FMC13 is added to the reaction mixture at 1.25mg/ml the velocity of the reaction is increased at all concentrations, with the increase in reaction velocity slowing and beginning to plateaux at substrate concentrations higher than 1mg/ml.

Figure 117- Michaelis-Menten plot for alginate sample FMC13 at 1.25mg/ml (▲) as compared to a normal α-amylase control (■). Substrate concentration [s] is given in mg/ml and the velocity is given as the rate of change in percentage absorbance per minute. The error bars show the standard deviation of at least 5 replicates (n=5)
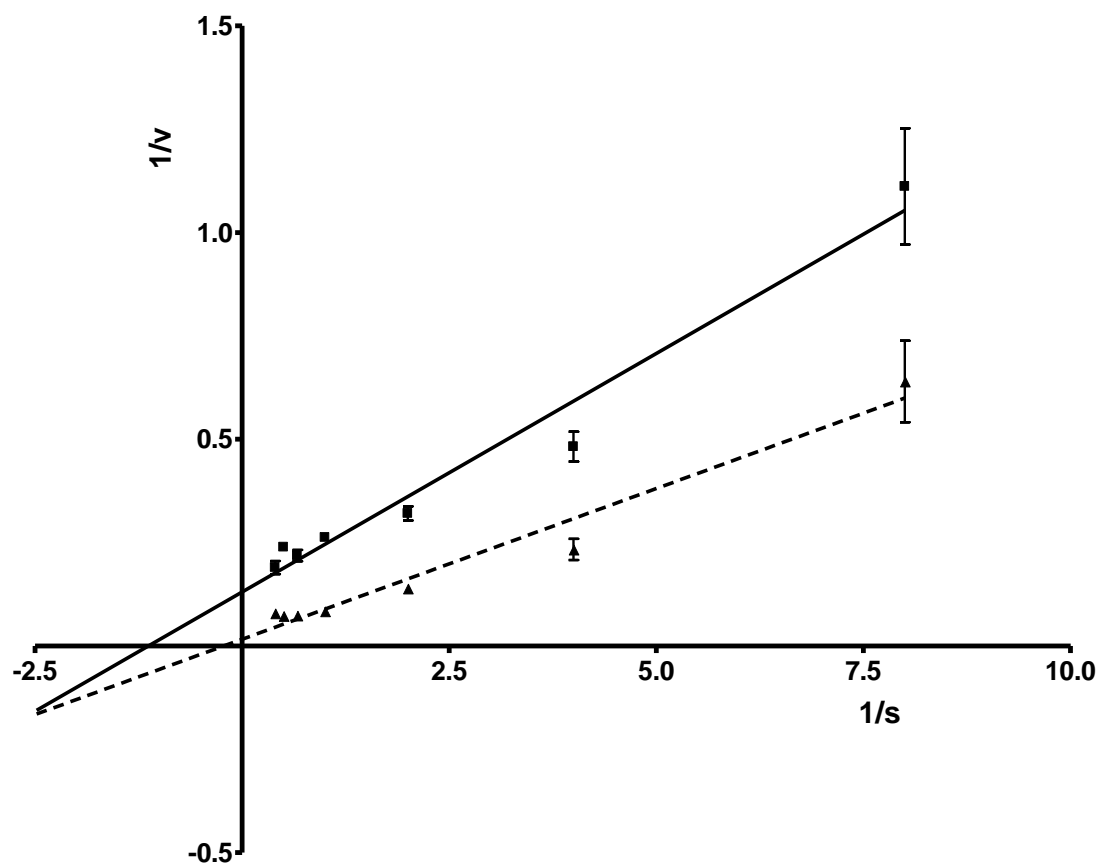
Figure 118- Lineweaver-Burk plot for alginate sample FMC13 at 1.25mg/ml (▲) as compared to a normal α-amylase control (■). Substrate concentration [s] is given in mg/ml and the velocity is given as the rate of change in percentage absorbance per minute. The error bars show the standard deviation of 5 replicates (n=5).

The kinetic data from the Michaelis Menten plot was transformed into the double reciprocal Lineweaver Burke plots shown in Figure 118. From these data the kinetic constants V_{max} and K_m were calculated for a normal α-amylase control and for each of the alginate samples tested.

In a normal α-amylase digestion of potato starch substrate the V_{max} is 6.024 %/min and the K_m is 0.51. In the case of FMC13 shown above in Figure 118, the addition of FMC13 alginate to the reaction mixture resulted in an increase of V_{max} to 18.33, and a K_m increased to 1.29. However, while the V_{max} was significantly different, the K_m was not as the control value lay within the 95% confidence interval of the test sample FMC13.

Although no statistically significant relationships between alginate structure and levels of activation in the high-throughput microplate analysis, the kinetic data was assesed to investigate any correlations, this data is included in Table 20.

Structural Characteristic	V_{max}		K_m		K_A	
	Spearmans value	P-value	Spearmans value	P-value	Spearmans value	P-value
F(G)	-0.601	0.0084	0.000	1.0000	-0.024	0.9252
F(M)	0.599	0.0086	0.030	0.9061	0.020	0.9384
F(GG)	-0.638	0.0044	-0.049	0.8484	-0.030	0.9061
F(MG/GM)	0.377	0.1230	-0.073	0.7750	0.016	0.9512
F(MM)	0.520	0.0270	-0.003	0.9903	-0.007	0.9773
F(MGG/GGM)	0.283	0.2561	-0.383	0.1169	0.099	0.6950
F(MGM)	0.174	0.4912	-0.172	0.4939	-0.050	0.8452
F(GGG)	-0.569	0.0137	0.054	0.8323	-0.018	0.9449
N (G>1)	-0.474	0.0471	0.133	0.5985	-0.042	0.8676

Table 20   Kinetic date for alginate activation of α-amylase.

There is a significant negative correlation between levels of guluronic acid in alginate and the maximum reaction velocity (Figure 119). Therefore increasing levels of guluronic acid tends towards a lower level of α-amylase. Conversely increasing levels of mannuronic acid F[M] correlates with an increased level of α-amylase activation as would be expected with a spearmans coefficient of 0.60 and a p-value of 0.008.
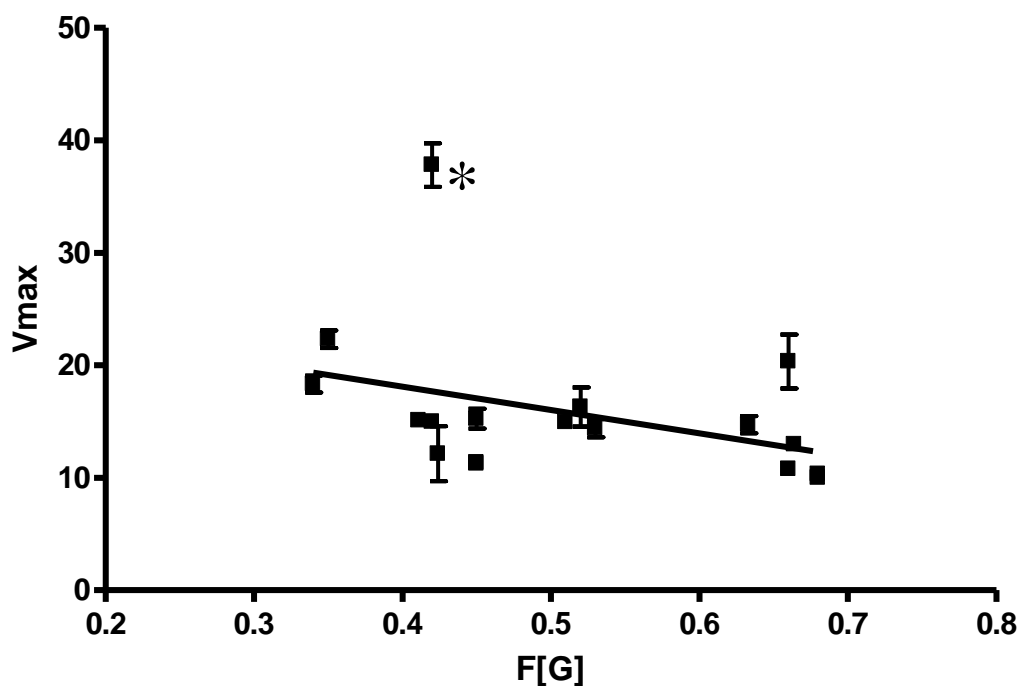
Figure 119- Correlation between apparent Vmax of α-amylase in the presence of alginate samples (1.25g/ml) and alginate G-residue frequency (F[G]). A significant negative correlation was shown between Vmax and F[G] with a spearmans r value of -0.60 and a p-value of 0.008.

As can be seen in Figure 119 there is one starred value which represents alginate sample FMC10 that stands apart from the rest of the data-set. In Figure 120 this outlier has been excluded from the data set, and the correlation still remains significant with a spearman value of -0.5584 and a p-value of 0.0198 between alginate F[G] and V_{max}. Likewise the correlation between F[M] and V_{max} also remains significant with the outlier removed with a spearmans value of 0.5567 and a p-value of 0.0203.
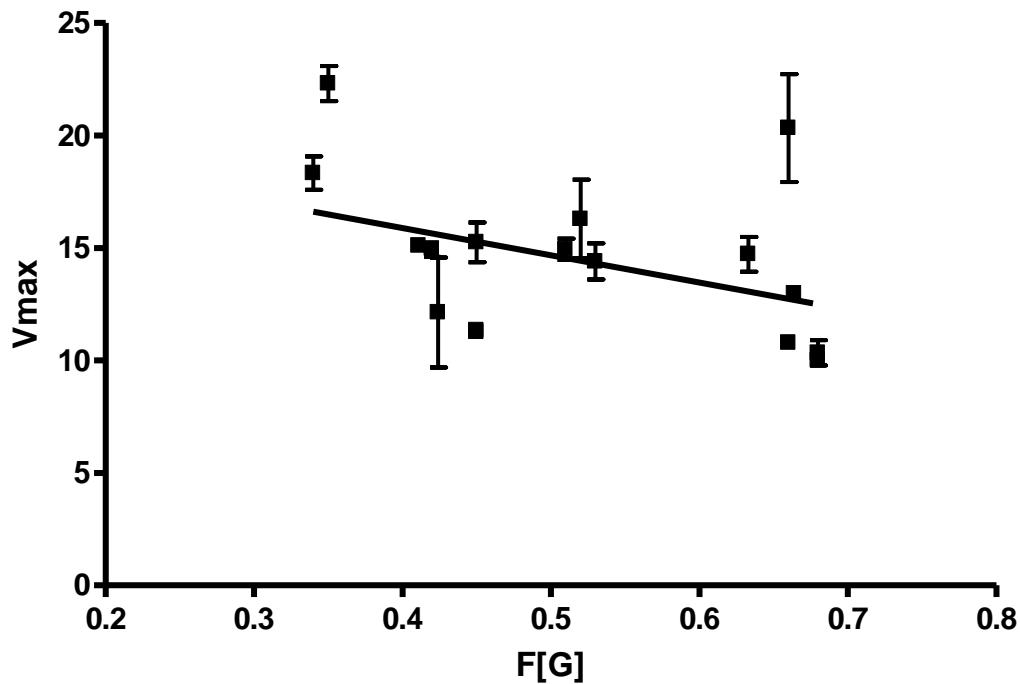
Figure 120- Correlation between apparent Vmax of α-amylase in the presence of alginate (1.25g/ml) samples and alginate G-residue frequency (F[G]). A significant negative correlation was shown between Vmax and F[G] with FMC10 data removed, with a spearmans r value of -0.56and a p-value of 0.020.

Significant negative correlations between structural characteristics of alginate and V_{max} were also present when comparing F(GG), F(GGG) and N (G>1). A significant positive correlation between V_{max} and F(MM) was also shown.

As with overall G-residue frequency (Figure 120), decreasing frequency of GG-block frequency (Figure 121), GGG-block frequency (Figure 122) and overall G-block length (Figure 123) are all associated with increasing levels of apparent V_{max}.

The correlation in Figure 121 between alginate F[GG] and apparent V_{max} is significant and negative with a spearman value of -0.6381 and a p-value of 0.0044. This correlation remained significant with the starred outlier shown in Figure 122 excluded with a spearman value of -0.5800 and a p-value of 0.0147. In Figure 122 there is also a significant negative correlation between F[GGG] and apparent V_{max}, with a spearman value of -0.5692 and a p-value of 0.0137. Again, this correlation remained significant with the starred outlier excluded with a spearman value of -0.5129 and a p-value of 0.0353.
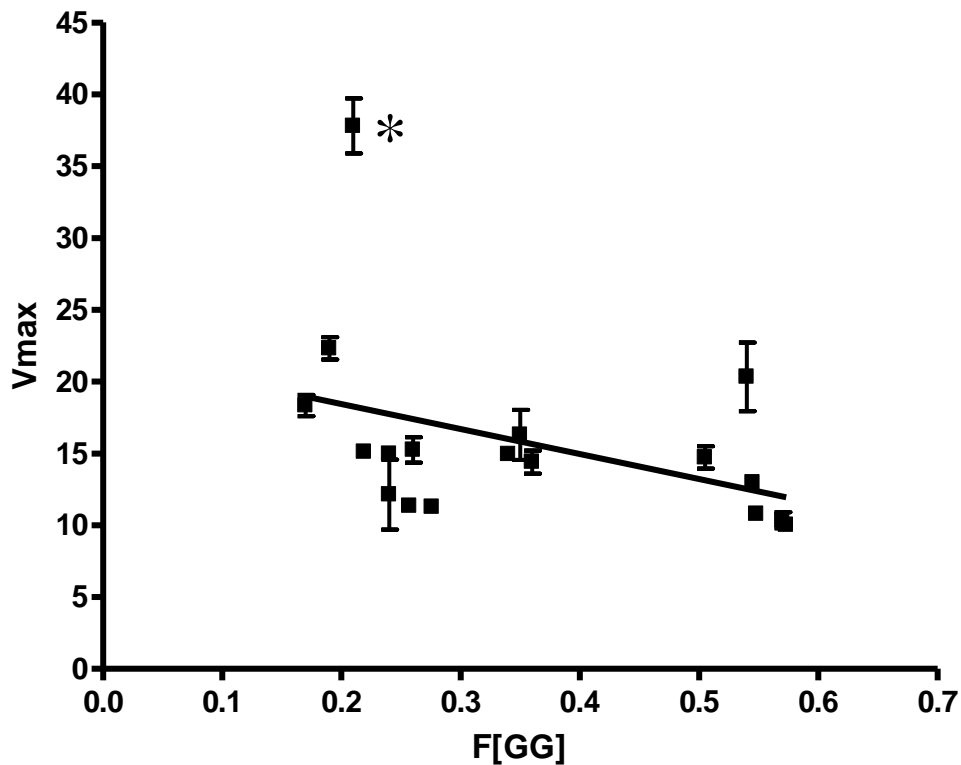
Figure 121- Correlation between apparent Vmax of α-amylase in the presence of alginate samples and alginate G-residue frequency (F[GG]). A significant negative correlation was shown between Vmax and F[G] with a spearmans r value of -0.6381 and a p-value of 0.0044.
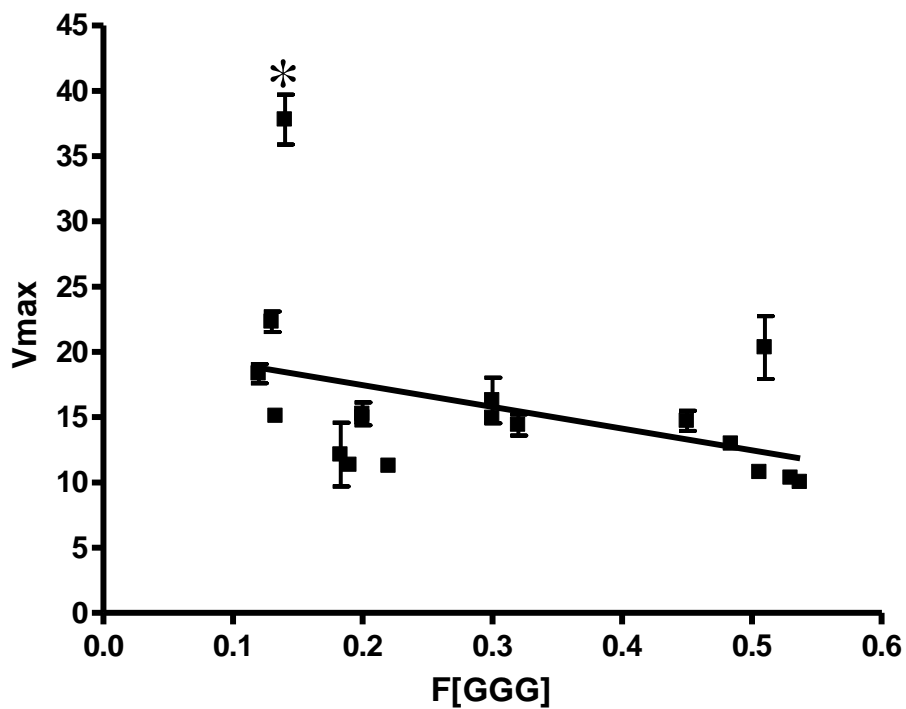
Figure 122- Correlation between apparent V_{max} of α-amylase in the presence of alginate samples and alginate G-residue frequency (F[GGG]). A significant negative correlation was shown between V_{max} and F[G] with a spearmans r value of -0.5692 and a p-value of 0.0137.

There is also a negative correlation between apparent V_{max} of α-amylase in the presence of alginate and the overall size of G-blocks in alginate. As shown in Figure 123 the trend is that the larger the G-Block length, the lower the increase in V_{max}. The spearman r value is -0.4737, with a p-value of 0.0471. However when the starred outlier is removed the correlation between V_{max} and [N(G>1)] is no longer significant and the outlier may be giving the data a false correlation.
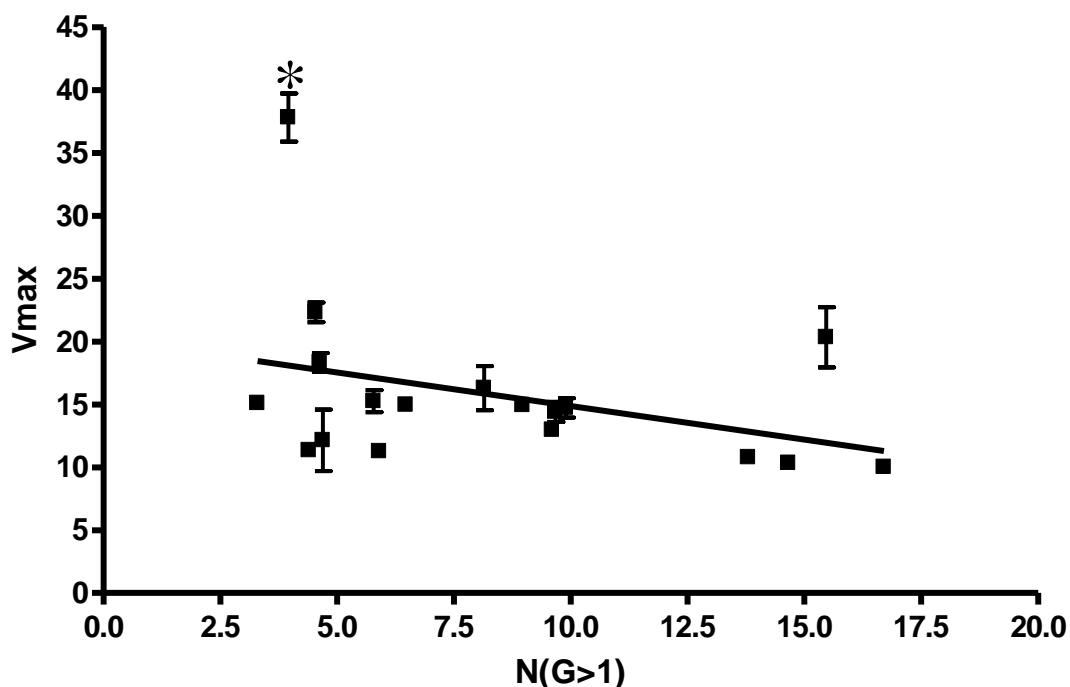
Figure 123- Correlation between apparent V_{max} of α-amylase in the presence of alginate samples and alginate G-residue frequency [N(G>1)]. A significant negative correlation was shown between V_{max} and F[G] with a spearmans r value of -0.4737 and a p-value of 0.0471.

Figure 124 shows the positive correlation between alginate F[MM] and apparent V_{max}. As would be expected from the negative correlation with G-residue frequency, there is a positive correlation between apparent V_{max} and frequency of GG blocks. The spearman r value is 0.5199 with a p-value of 0.0270. When the starred outlier is removed, the relationship remains significant.
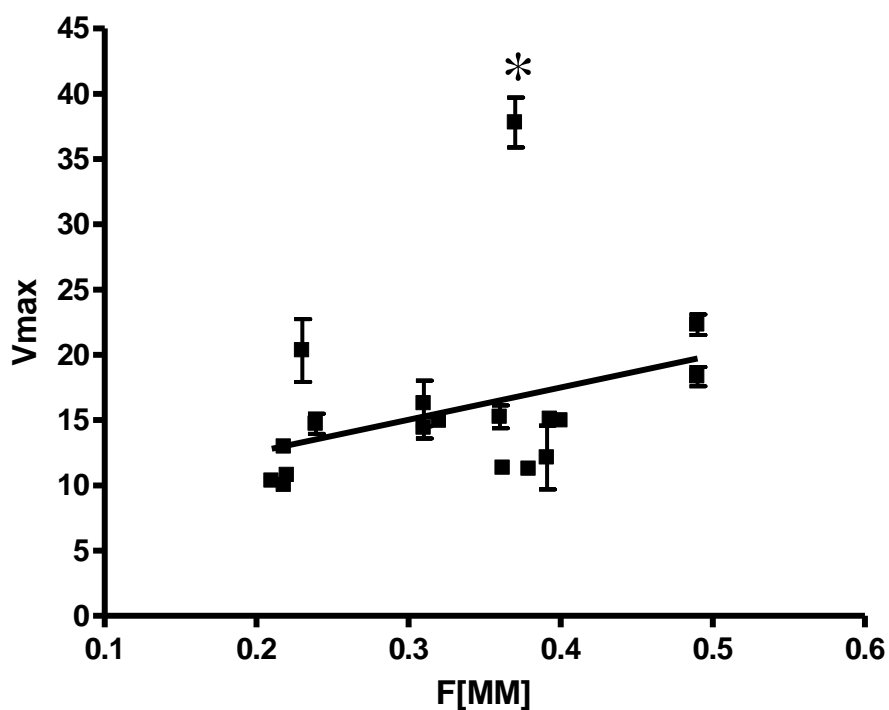
Figure 124- Correlation between apparent Vmax of α-amylase in the presence of alginate samples and alginate G-residue frequency (F[MM]). A significant negative correlation was shown between Vmax and F[G] with a spearmans r value of -0.5199 and a p-value of 0.0270.

Apparent V_{max} was also compared against F(MG/GM), F(MGG/GGM) and F(MGM), however no significant correlations were shown between these structural characteristics. The kinetic constants K_m and K_i were also compared against the structural characteristics of alginate and no significant correlations were shown.

5.9.1 FMC10

The alginate sample FMC10 has been described as an outlier as it causes much higher increases in V_{max} than all of the other alginates. This tallies with the results of the higher throughput microplate assays which showed FMC10 to be the most potent activator of α-amylase. Figure 125 shows the microplate HTP assay results for FMC10 as compared to the overall average of all alginate samples. As can be seen at each of the three tested alginate concentrations, FMC10 is considerably more potent than both the average level of alginate activation and LF120L, which is the next most potent activator of α-amylase after FMC10
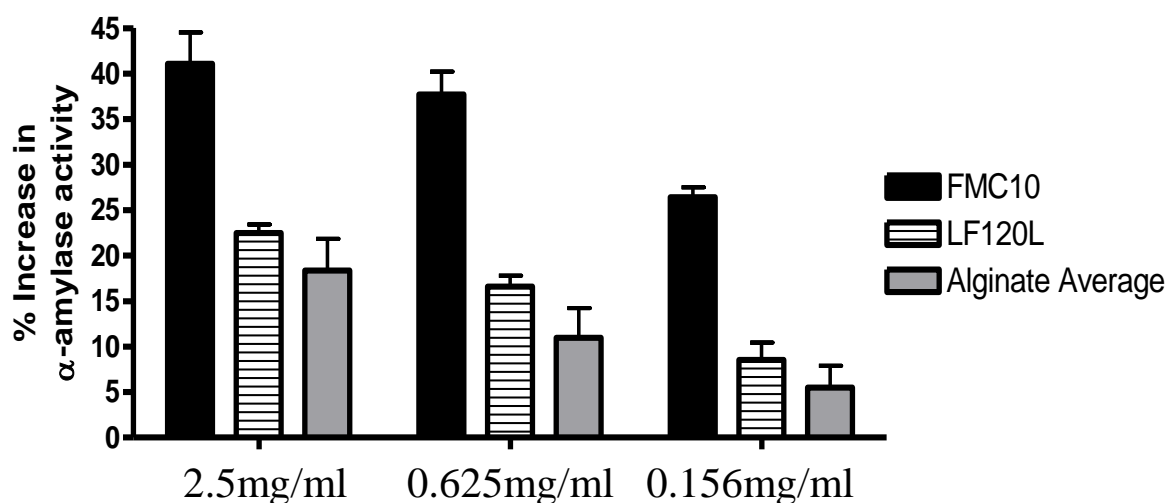
Figure 125 - Comparison of α-amylase inhibition with FMC10 and the next most potent activator LF120L and the average level of α-amylase activation with alginates.

As can be seen from Figure 109 the apparent V_{max} of α-amylase in the presence of FMC10 is significantly higher than the rest of the alginates. However the other two kinetic constants K_m and K_A are not dissimilar to those of other alginates.

When looking at the structural characteristics of FMC10 it does not differ remarkably from the range of the catalogue of well characterised alginates, and the structurally similar alginate SF60 does not show such a level of activation (Full characteristic for all alginates are included in Appendix 8.1).
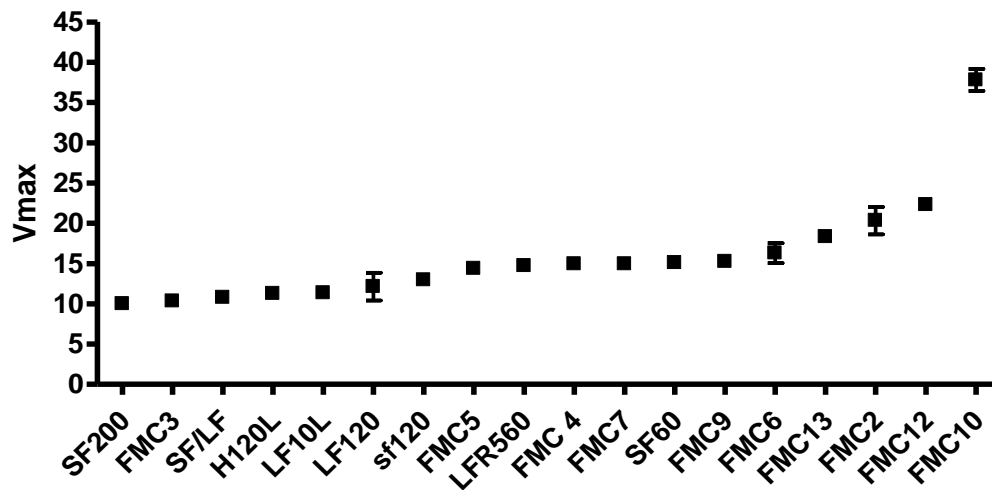
Figure 126 V_{max} of   α-amylase   in   the   presence   of   all   alginate   samples.

From the kinetic analysis, two different modes of activation were seen. The more common case was where the maximum velocity of the reaction was increased, but enzyme-substrate affinity was unaffected, this gave a significantly higher apparent V_{max}, but apparent K_m remained unchanged. This was the case with SF200, LF10L, FMC13, FMC9, LFR560, SF/LF, FMC12, SF120, SF60, FMC10, H120L and FMC2. The Michaelis Menten plot for FMC12 have been included as an example of this kind of activation Figure 127.

In the presence of alginate FMC12, the velocity of the reaction is increased at all substrate concentrations and the maximum reaction velocity is over 3-fold higher in the presence of alginate FMC12 than control. However the K_m of α-amylase is not significantly different in the presence of FMC12 than in control suggesting that the activation of α-amylase occurs without a significant change in enzyme-substrate affinity.
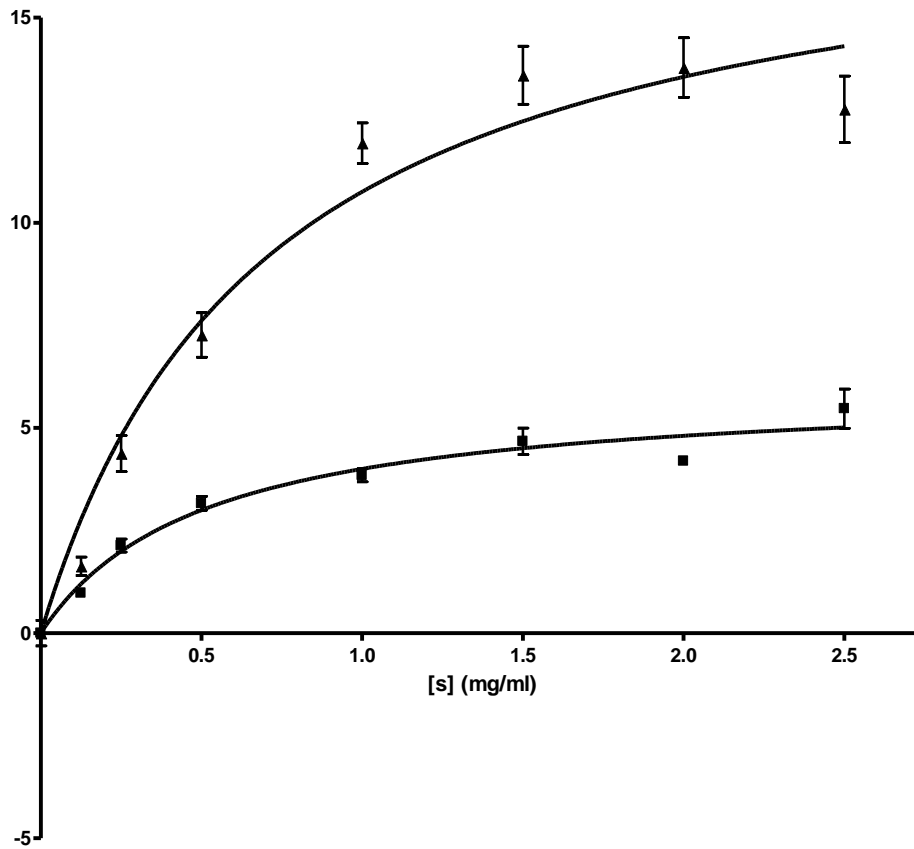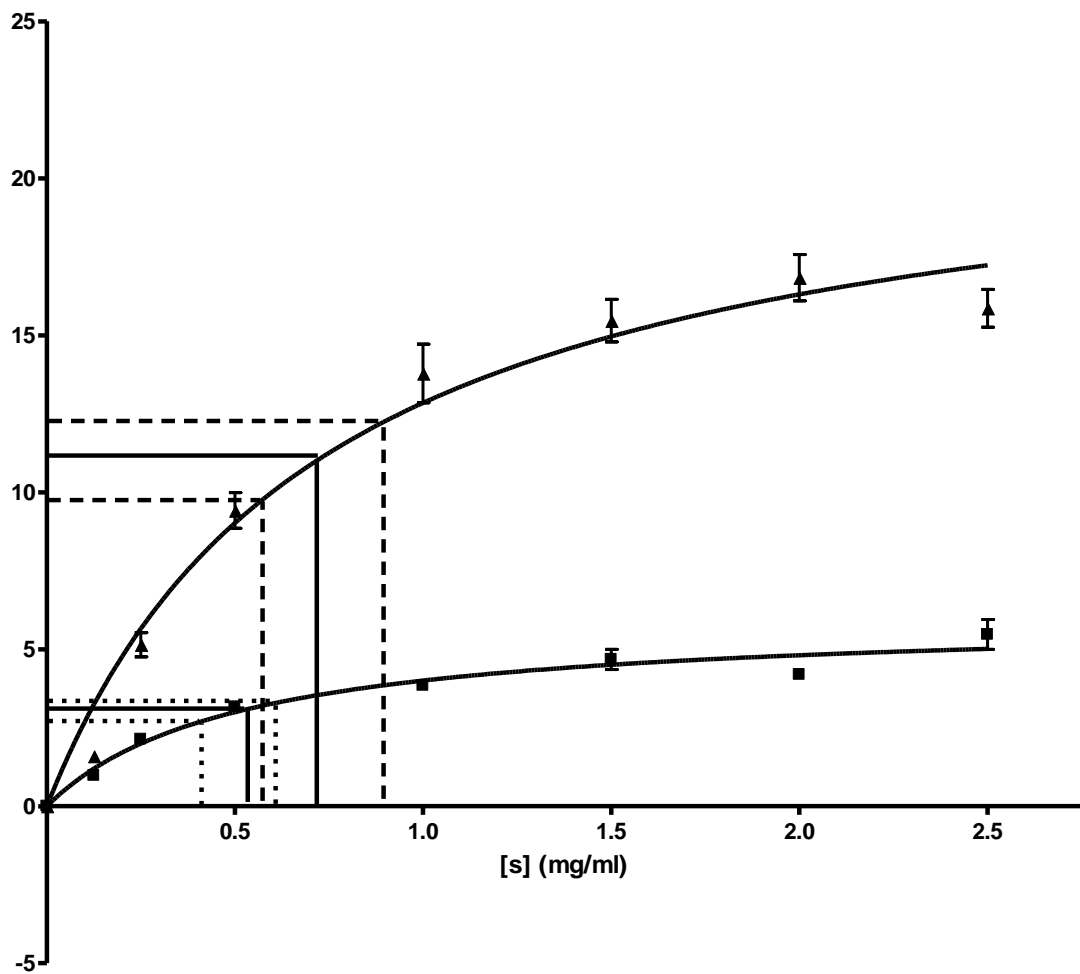
Figure 127- Michaelis-Menten plot for alginate sample FMC12 at 1.25mg/ml (▲) as compared to a normal α-amylase control (■). Substrate concentration [s] is given in mg/ml and the velocity is given as the rate of change in percentage absorbance per minute. The error bars show the standard deviation of 5 replicates (n=5). ▬ Represents K_m and ▬ ▬ ▬ represents the upper and lower 95% confidence limits of K_m.

The samples FMC3, FMC4, FMC5, FMC6 and FMC7 all brought about significant changes to both V_{max} and K_m. The Michaelis Menten plot for FMC5 is included below, and as can be seen there is an increase in both the apparent K_m and apparent V_{max} of α-amylase with the addition of alginate sample FMC5 (Figure 128). This suggests that for these samples that a change in substrate-enzyme affinity may be involved in the activation.
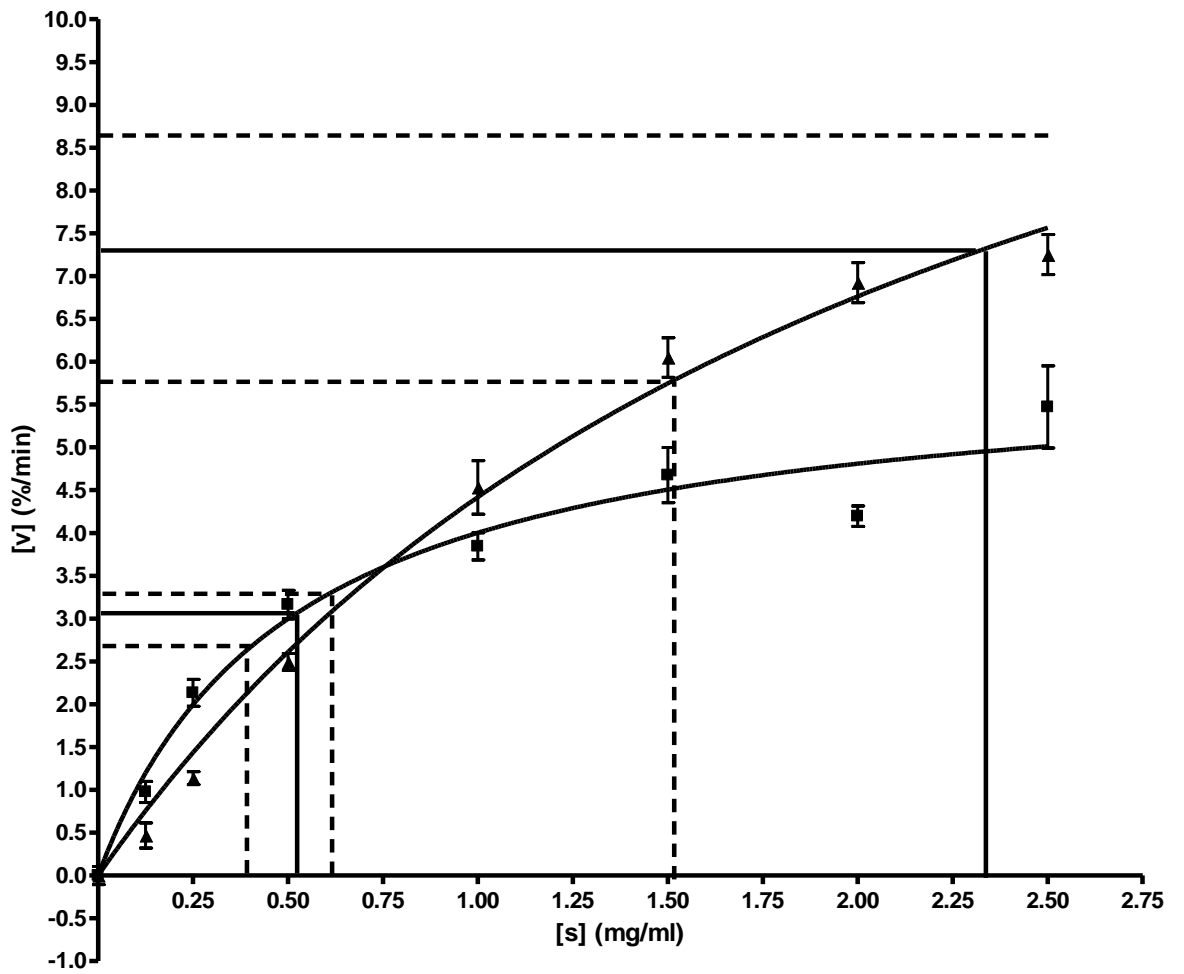
Figure 128- Michaelis-Menten plot for alginate sample FMC5 at 1.25mg/ml (▲) as compared to a normal α-amylase control (■). Substrate concentration [s] is given in mg/ml and the velocity is given as the rate of change in percentage absorbance per minute. The error bars show the standard deviation of 5 replicates (n=5). ▬▬ Represents K_m and ▪▪▪▪ represents the upper and lower 95% confidence limits of K_m.

LF120L was the only alginate sample which did not cause a statistically significant change in either V_{max} or K_m.

5.10 Alginate starch interactions

Figure 129 shows the viscosity of an alginate solution (H120L, 2.5mg/ml, pH7) both alone and with the addition of three starch substrates (5mg/ml; corn, wheat or potato starch). As can be seen from Figure 129, the addition of each of these starches causes a loss of viscosity as compared to alginate by itself. The current experiment was underataken at room temperature, and provides evidence ofstarch disrupting the interactions etween alginate molecules and a possible interaction between starch and alginate.
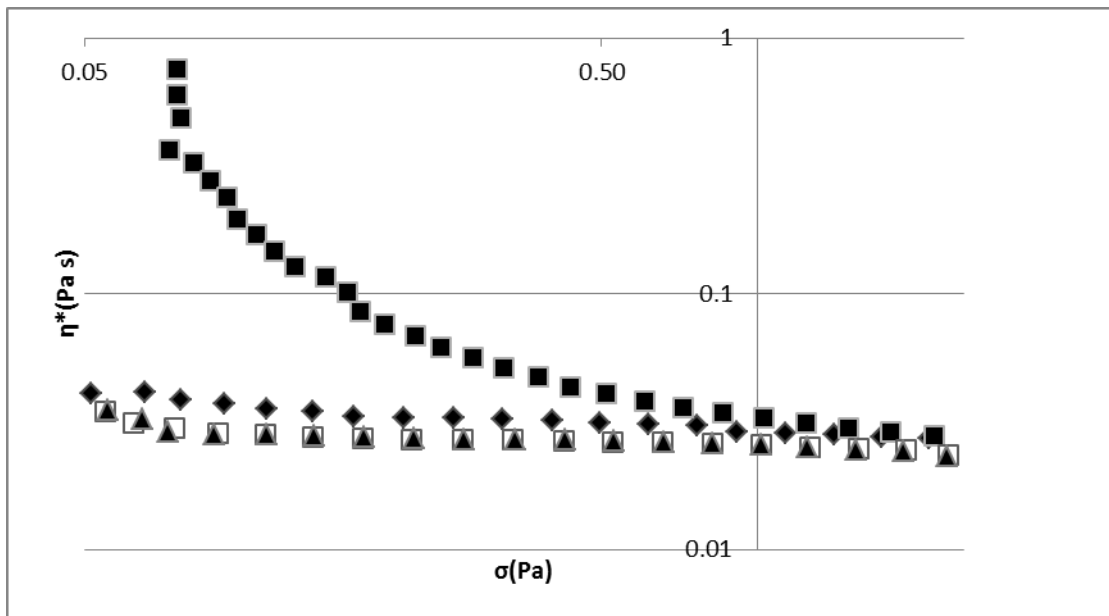
Figure 129   Viscosity vs Shear stress of alginate and starch solutions at pH7. H120L alginate (■), H120L alginate and corn starch (□), H120L and Wheat Starch (▲), H120L and potato starch (◆) 2.5mg/ml aqueous alginate was ade up with 10mg/ml starch and incubated for 30 minutes before viscosity measurement.

5.11 Discussion

Activity of α-amylase was quantified using an adapted version of the Sumner et al Di-nitro salicylic acid assay. The DNSA assay works by detecting the reduction of 3,5-Dinitrosalycylic acid to 3-amino, 5-nitrosalycylic acid in the presence of reducing sugars above 100°C. Reducing sugars are produced by α-amylase cleavage of substrate starch and therefore, quantification of the coloured product is measurable spectrophotometrically at 550nm proportionate to the amount of reducing sugar.

Certain modifications had to be made to the original methodology. All solutions and reagents in the reaction mixture were buffered with Sorensen's phosphate bufferand the volume was scaled down to a 96 well microplate. The assay system was validated using the known α-amylase inhibitor EDTA as a positive inhibition control. Dose response inhibition was shown with EDTA.

The catalogue of eighteen well characterised alginates was tested for modulatory activity against α-amylase. Alginates increased α-amylase activity by an average of 18.35±6.05% at the highest tested concentration. Significant activation of α-amylase was also shown at lower alginate levels.

There was a large degree of variation in the magnitude of the activation, and this variation was investigated in relation to alginate structure.

The effect was shown not to be species dependent, with no significant difference between the four High-G lamanaria alginates and the four High-M lessonia alginates. Furthermore, across the full catalogue of alginate samples tested in the high throughput microplate assays, no significant correlation was found between alginate F[G] and percentage α-amylase activation.

The observation that there is no correlation between alginate F[G] and levels of alginate activation suggests that there is a nonspecific activation of α-amylase which does not relate to the alginate composition. This was further demonstrated by the fact that no statistically significant correlations could be shown between levels of α-amylase and activation and any of the structural characteristics of the well characterised alginate samples; F(G), F(M), F(GG), F(MG/GM), F(MM), F(MGG/GGM), F(MGM), F(GGG) or N (G>1).

Furthermore, for the eight alginates with characterised molecular weights, no correlation could be shown between alginate size and levels of inhibition.

As no structural correlations could be shown in the high throughput assays, selected kinetic assays were carried out on all well characterised alginate samples in order to investigate the mechanisms of the alginate-enzyme interactions, and see if any structural correlations could be shown with kinetic data. While enzyme kinetics is primarily used for the study of enzyme inhibition, the principles may also be applied to enzyme activation.

Although the high-throughput microplate analysis had shown no statistically significant relationships between alginate structure and levels of activation, significant negative correlation was shown between levels of guluronic acid in alginate and the maximumun reaction velocity (V_{max}). That is to say that alginates higher in mannuronic acid residues tended to be better activators of α-amylase.

Significant negative correlations between structural characteristics of alginate and V_{max} were also present when comparing F(GG), F(GGG) and N (G>1). A significant positive correlation between V_{max} and F(MM) was also shown. The kinetic constants K_m and K_A were also compared against the structural characteristics of alginate and no significant correlations were shown.

FMC10 was the strongest activator of α-amylase of the tested alginates. As can be seen in Figure 125, after FMC10, the next strongest activator of α-amylase was LF120, which increased amylase activity by 22.5±2.3%. This was close to the average level of alginate activation of 18.4±8.5%. The activation levels of FMC10 were greatly in excess of that seen with any of the other alginate samples. However no extraordinary structural properties could be identified when comparing the characteristics of FMC10 to other alginates to try identify any stand-out properties which may explain the different activity profile.

While the guluronic and mannuronic acid composition for FMC10 was available, the molecular weight for FMC10 was not charachterised in this current study. It is therefore possible that the molecular weight of FMC10, or some other structural charachteristic is responsible for the elevated activation profile. It must be considered that there is another factor at work, such as contamination of the sample or a fault in the production process.

Enzyme activation can be described as essential or non-essential. Essential activation occurs when the presence of the activator is required for the reaction to take place. With α-amylase activity, binding of a calcium ion is essential to enzyme activity, and the binding of monovalent cations is known to increase enzyme activity, with Chloride being the most potent anionic activator. Non-essential activation occurs when the reaction would take place without the presence of the activator, although at a slower rate, as α-amylase is capable of catalysing the breakdown of starch in the absence of Chloride, but is more potent in its presence.

All α-amylases bind an essential Ca^{++} ion which is required for structure and catalytic activity, this Ca^{++} binding site is located in Domain B of the enzyme. The α-amylase inhibitor EDTA stops amylase activity by chelating the calcium of α-amylase which is necessary for activity [254].

Alginates are also known to chelate divalent cations such as calcium, and it is possible that there is some kind of alginate interaction with the α-amylase enzyme that occurs through this known calcium binding site [255]. However, clearly alginate does not remove the calcium ion from α-amylase otherwise there would be a decrease in α-amylase activity. It is possible that by attempting to chelate this calcium ion that alginate associates with the enzyme and in doing so stabilise the binding of the calcium cation at the enzyme binding site and helps to present Ca^{++} to the α-amylase enzyme.

However, as was seen with protein and alginate, it is possible that there is also an alginate-substrate interaction which affects the activity of the enzyme. Interactions between alginate and starch have been previously reported. When investigating the way alginate affects starch pasting, Richardson et al showed that potato starch in an alginate solution had a much lower viscosity than potato starch in water suspension at high temperatures (at 80–85 °C). While this is a higher temperature than was used in the assays described in this chapter, the data presented by Richardson *et al* shows that under the right circumstances, alginate will interact with starch in such a way to disrupt gellation [256].

However as can be seen in Figure 129, the addition of corn, wheat and potato starch to an H120L alginate solution greatly reduced alginate viscosity. This experiment was undertaken at room temperature and provides evidence of an interaction between alginate and starch. It may be therefore that a mechanism by which alginate increases

the activity of α-amylase is by disrupting the gel network of starch, increasing the surface area of starch substrate that is available for α-amylase to act upon.

The results discussed herein are interesting in that they somewhat go against what has been shown in the literature regarding dietary fibres and their protective affects against diabetes. Dietary fibres have been shown to have anti-hyper-glycaemic effects and high long term intake of dietary fibre is associated with decreased risk of diabetes [44]. There is a well established link between fibre defficient diets and metabolic disease including diabetes. It is therefore somewhat counterintuitive that alginates actually increase α-amylase activity. However, these results are in a pH controlled single-enzyme environment; how alginate affects carbohydrate digestion in a physiologically relevant system will be discussed in Chapter 6.

Guar gum reduced post-prandial hyperglycaemia in diabetic rats [139]. Partially Hydrolysed Guar Gum (PGHH) has been shown to have beneficial effects towards markers of metabolic syndrome with a significant reduction in waist circumferance in and a significant hypoglycaemic affect when fed 5g PHGG twice a day for 6 weeks.

Kimura *et al* 1996, showed that alginate feeding could attenuate the post-prandial blood glucose response in rats. Furthermore post-prandial blood glucose and serum insulin were lowered in a group of seven patients who were fed test meals with alginate [252].

These results contrast with the data presented in this chapter that alginates cause an increase in the activity of α-amylase. It would be expected that an increase in α-amylase activity would be associated with faster carbohydrate digestion kinetics and elevated post-prandial hyperglycaemia and hyperinsulaemia. However the studies cited above have suggested that the opposite is the case.

In the Torsdottir *et al* 1991 study, rates of gastic emptying were measured in the seven test subjects [257]. Radiolabelled chromium was used to monitor gastric emptying, and it was shown that alginate supplementation significantly slowed the rate of gastric emptying, and that this reduced blood glucose rise correlated with slowed gastric emptying. As was discussed in the introduction, the breakdown of starch into maltose, maltotriose and α-limit dextrin is thought to occur very rapidly and within 10 minutes of transit into the duodenum [258]. This rapid digestion of carbohydrate offers an explanation of how despite alginates having been shown to be activators of α-amylase

in vitro, that they have proven to have anti-hyperglycaemic effects *in vivo*. Because the duodenal digestion of carbohydrate is so rapid, an increase in amylolytic activty will have a marginal effect on the speed of carbohydrate digestion. Gastric emptying however will present a rate limiting step. As carbohydrate predominantly occurs in the duodenum, the reate at which carbohydrates are delivered to the duodenum will therefore be the determining factor in the rate of carbohydrate digestion.

In the Torsdottir *et al* 1991 study, Radiolabelled chromium was used to monitor the rate of gastric emptying, and 75 minutes after feeding, 29% less of the meal was emptied with alginate supplementation and by 105 minutes 19% less had emptied. This is likely to be the determining factor which resulted in the anti hyper-glycaemic effect, as reduced blood glucose rise correlated with slowed gastric emptying [257].

This theory is further supported by the observations of Jenkins *et al* 1978 that in human volunteers undergoing glucose tolerance tests after consuming 50g of glucose and a dietary fibre, that the reduction in blood glucose rise correlated with the viscosity of the fibre [249]. The more viscous fibres were more effective at delaying mouth to caecum transit time and attenuating the blood glucose response.

In the study of alginate supplementation in rats, Kimura *et al* 1996 advanced another theory as to why alginate reduces glucose uptake in the small intestine [252]. Alginate has been shown to increase Na+ excretion during digestion, as alginate inhibits sodium absorption in the small intestine [259]. Sodium is essential for intestinal absorption of glucose, as glucose uptake occurs through the sodium glucose co-transporter [260]. Reduced glucose uptake and the hypoglycaemic effect of alginates may be due to in part to alginate making sodium unavailable to the NaGluc Cotransporter.

Kimura *et al* 1996, suggest that the net hypoglycaemic effect of alginate supplementation may be due to a combination of alginate gelling in the stomach and delaying gastric emptying, and reduced sodium uptake in the small intestine inhibiting the action of the sodium-glucose co-transporter [252].

A further mechanism suggested by V Dall'Alba *et al* 2013, in the case of Guar Gum inhibition of carbohydrate digestion, which would also be applicable to alginates, is that the increased viscosity of the gut lumen contents caused by the viscous fibre reduces the accessibility of amylase to it's substrate, and reduces the rate of glucose diffusion through the lumen for uptake [140].

Chapter 6
Model Gut Analysis

6.1 *Introduction*

6.1.1 Overview

A physiologically relevant *in vitro* Model Gut System (MGS) has been developed which simulates the digestive processes of the gastrointestinal tract from mouth to terminal small intestine. This model can be used to study the chemical and enzymatic digestion of the macronutrients; fat, protein and carbohydrate, and to analyse the effects of exogenous compounds on their digestion.

The efficacy of the MGS has been validated by the role it has played in building a case for the novel lipase inhibitor alginate as a weight loss treatment [Unpublished Data].

The digestion and absorption of macronutrients (fat, protein and carbohydrate) is a major factor in health and in metabolic diseases such as obesity and diabetes. For absorption across the intestinal epithelia, dietary macronutrients must be mechanically, chemically and enzymatically broken down as they pass through the upper GI tract. Modulating macronutrient digestion with food additives and pharmaceuticals has been shown to be an effective approach in the management and treatment of health and disease, for example the treatment of obesity with Orlistat and diabetes with Acarbose [4, 261]

Model gut systems provide a physiological simulation of normal human digestion, as such they provide an *in vitro* model that can be used to validate effects seen with bioactive compounds in single enzyme analysis in a more physiologically relevant mixed model. Furthermore model gut analysis provides a well controlled, reproducible and cost-effective alternative to *in vivo* studies. The method presented here describes a synthetic gut system designed to simulate the conditions of the GI tract from mouth to small intestine. Assay systems are described to analyse fat, carbohydrate and protein digestion.

6.1.2 Current Model Gut Systems

As with pharmacological studies, randomised, double blinded control trials in human populations are the gold standard of nutrition studies, however cost and complexity are often prohibitive [262]. Smaller scale acute human studies may look at the processes of digestion by sampling from the stomach and upper small intestine after feeding [263]. Ileostomy studies and faecal sampling allow analysis of the the latter parts of the GI tract.

Animal models have played an important part in nutrition research and greatly contributed to the understanding of nutrition and nutrient metabolism. Animal studies have enabled researchers to solve nutrient-nutrient interactions, look at nutrient bioavailability, tolerances and toxicity and to study diet associated disease [264]. However ethical concerns over the use of animal testing is a source of continual debate and both British and European law ensure strict controls and ethical standards for the use of animal testing [265]. Furthermore the relevance of animal studies to human digestion is a source of debate and because of perceived negative public attitudes towards animal testing, companies will where possible avoid the use of animal testing. This is particularly apparent in an industry as public facing as the nutrition, food and health sector.

Due to cost, ethics and scale a wide range of *in vitro* methods have been developed to model the gastrointestinal tract in the lab. Model gut systems aim to provide a physiological simulation of normal human digestion, and a number of models have been developed to study different aspects of digestion and GI physiology. Models have been developed to study; bioavailability and bioaccessibility of contaminants [266], digestion of allergens [263], study of pre and probiotics, models of gut motility [267], peristaltic motion and physiological mixing and shearing, enzymatic digestion [268], substrate digestion and interaction [268], intestinal microbiota [269], water and nutrient absorption [270] and drug delivery [271].

Wickham *et al* 2012, define a major distinction in model gut systems between static models and dynamic models [272]. Static models are models designed as accurate biochemical and enzymatic simulations, but do not accurately model the physical processes of digestion and there is no absorptive phase. Dynamic models on the other hand aim to replicate the physical forces of shear and mixing and replicate transit times

from *in vivo* data, these dynamic models allow for a fuller simulation of the digestion of structured foods and the effects of physical food breakdown on digestion.

6.1.3 Physical Models

Model gut systems have provided a methodology for examining the physical aspects of digestion; how food is mixed, sheared, propelled and broken down in a model situation. *In vivo,* imaging studies, endoscopy and capsule sensors have been used to model transit time, GI motility and food processing, but these studies can be prohibitive due to cost. Whickham *et al* 2012 have developed the Dynamic Gastric Model, a "physical simulator…paralleled by in silico modelling of gastric flow patterns, mixing and shears [272].
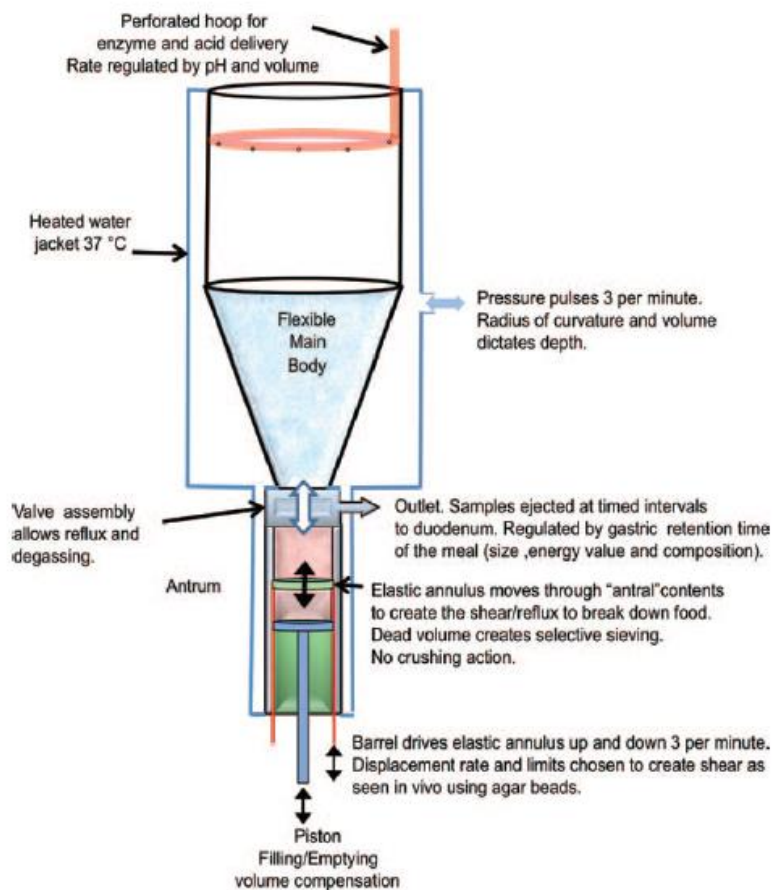
Figure 130   "DGM schematic (not to scale). The unit replicates the internal volumes of the average human stomach, and operates in real time and within physiological references ranges" Taken from Wickham et al 2012 [272]

The Dynamic Gastric Model consists of a Flexible main body representing the gastric chamber which is contained within a heated water jacket at 37°C. Gastric churning and mixing is simulated in the main body by a 0.05Hz pulsing of water in the heated jacket.

Gastric secretions are added through a "perforated hoop" according to *in silico* calculations. Rate of gastric emptying into duodenal compartment is controlled by *in silica* calculations. The process is autonomous and a range of data can be obtained as shown in Table 21. However as has been pointed out even this modelling of physical gastric conditions are not a wholly accurate approximation of the forces food is subjected to in the stomach [268].

Data that can be obtained:
- Emptying profile (mass-v-time) by weighing or analyzing each antral sample.
- Emptying profile (mass-v-time) of components (e.g., pharmaceuticals).
- Antral pH (as each sample is emptied).
- Enzyme digestion of gastric contents over time by analysis.
- Particle size reduction.
- Behavior of gastro-retentive/-resistant formulations.
- Dilution by gastric secretions.
- Solid/dissolved ratios of components.
- Mass transfer of components between phases.
- Rupture time of capsules and delivery profile of active to duodenum.
- Emulsification of lipid in stomach/antrum.
- Phase separation (lipid and low/high density components).
- Gel formation and effects of antral shear.
- Rate of creation of absorbable forms (nutrients, drugs).
- Video footage of stomach contents from the surface.

Table 21   Data that can be obtained from the Dynamic Gastric Model. Taken from Wickham *et al* 2012 [272]

Kong *et al* 2010, also developed an *in vitro* model of the stomach which they named as the Human Gastric Simulator which aims to more accurately replicate a realistic peristaltic action [268]. In this case the peristaltic motion of the stomach is modelled by a system of belt driven rollers which agitate a latex vessel at 'similar amplitude and frequency' to *in vivo* reports. The rollers mimic peristaltic action by a simultaneous movement of the rollers creating a ring shaped contraction. Kong *et al* argue that this mimics the propagation of a peristaltic wave across the stomach, at a physiologically relevant rate of 3 cycles per minute with a propagation speed of 2.5mm per second [273].   The system is temperature controlled and gastic secretions are pumped in through microtubing and an emptying system consisting of a peristaltic pump. The simulation of peristaltic action allow studies into the disintegration kinetics and breakdown of food, although as is pointed out, the true complexity of the system of

physiological controls of digestion and gastric motility such as neurohumoral regulation cannot be accurately simulated in this model.

The TIM (Figure 131) is a multi-compartmental dynamic model of the upper GI tract developed by Minekus *et al* [274]. The TIM model has been used in a range of studies looking at food digestion, enzyme supplementation, drug delivery, nutrient bioavailability, transit time and probiotic delivery. The TIM model is comprised of four compartments progressively representing; the stomach, the duodenum, the jejunum and the ileum. Each compartment is comprised of two chambers with flexible walls around which is a heated glass water jacket. Pumping of water at varied pressure through the water jacket creates movement aiming to simulate peristaltic action. Transit through the system is controlled by 'peristaltic valves' and the pH is monitored and controlled by computer throughout. Samples are collected by pumping through hollow fibre, semi permeable membrane into compartments at two sites; in the jejenum and ileum chambers in which water and small molecule metabolites are collected. The TIM system uses Nitrogen and glucose as markers of protein and carbohydrate digestion respectively. As far as can be seen from the literature, no marker of fat digestion has been developed in the system.

Blanquet *et al* 2004, state that the TIM model meets the following five requirements: "(i) sequential use of enzymes in physiological amounts, (ii) appropriate pH for the enzymes and addition of relevant cofactors such as bile salts and coenzymes, (iii) removal of the products of digestion, (iv) appropriate mixing at each stage of digestion, and (v) physiological transit times for each step of digestion." [271]
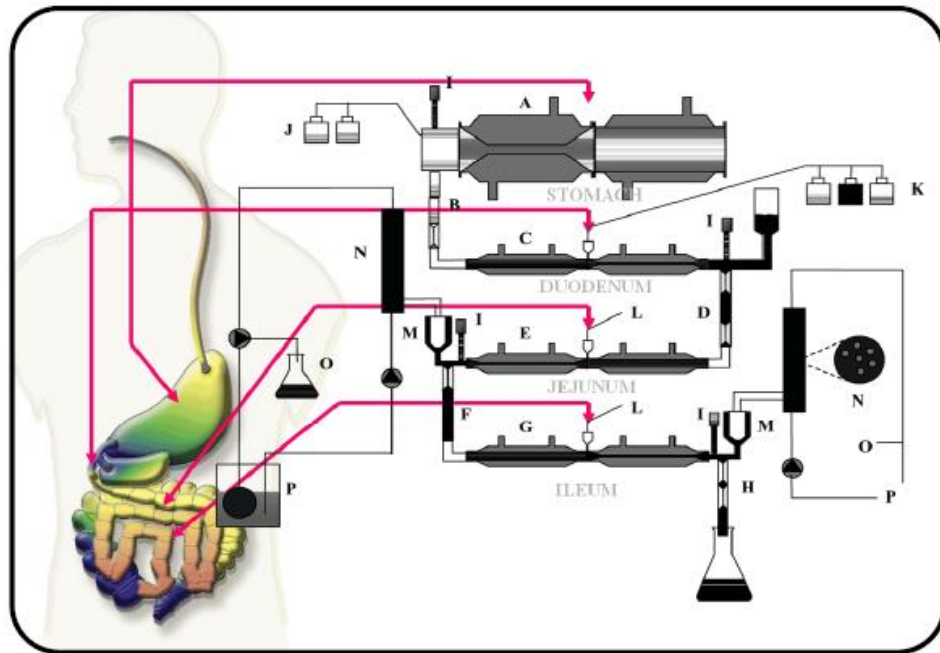
Figure 131   "Schematic diagram of the dynamic, multi-compartmental model of the stomach and small intestine (TIM-1): A. gastric compartment; B. pyloric sphincter; C. duodenal compartment; D. peristaltic valve; E. jejunal compartment; F. peristaltic valve; G. ileal compartment; H. ileo-caecal valve; I. pH electrodes; J. gastric secretion bottles with acid and enzymes; K. duodenal secretion bottles with bile, pancreatin, bicarbonate; L. secretion of bicarbonate to control the intestinal pH; M. pre-filter system; N. hollow fibre semi-permeable membrane system; O. water absorption system; P. closed dialysing system." Taken from National Enzyme Company, 2004 [275]

The patented TMI system developed by Minekus *et al* has also been developed and adapted to model the large intestine (Figure 132). The large intestinal reactor was inoculated with a microflora population by addition of faeces obtained from healthy volunteers and an anaerobic environment was maintained by flushing the system with nitrogen gas. This model has been validated for the study of carbohydrate fermentation by measuring SCFA (short chain fatty acid) release with pectin, lactulose, lactilol and fructo-oligosaccharide substrates [276].
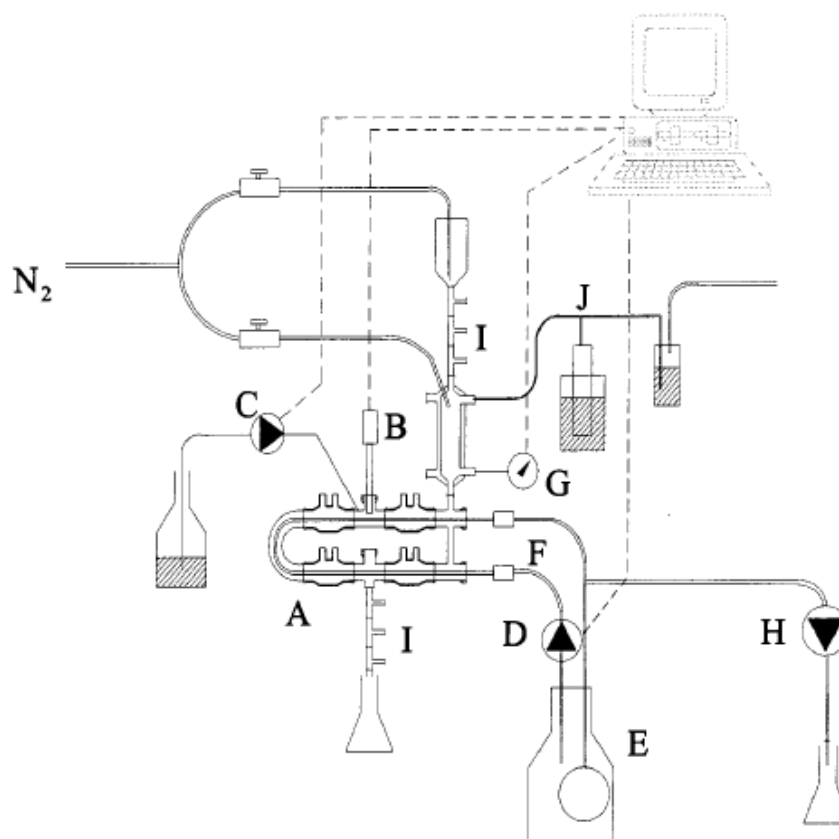
Figure 132   "A±J Schematic presentation of the system to simulate conditions in the large intestine. A mixing units; B pH electrode; C alkali pump; D dialysis pump; E dialysis light; F dialysis circuit with hollow fibres; G level sensor; H water absorption pump; I peristaltic valve pump; J gas outlet with water lock." Taken from Minekus et al 2000 [276]

6.1.4   Static models of nutrient digestion

Wickham *et al* 2009, in a review of the utility of *in vitro* models of digestion define three stages of digestion which model guts must consider; "(i) processing in the mouth, (ii) processing in the stomach (cumulative to the mouth) and (iii) processing in the duodenum (cumulative of the mouth and stomach)" [263].

In vitro gut models of nutrient digestion have been developed before to look at nutrient digestion either in specific sections of the GI tract or from mouth to small intestine, but to my knowledge, no models have been developed to simulate the digestive tract from the buccal cavity to the end of the small intestine in which digestion of the three major macronutrients protein, starch and fat can be measured and modelled.

A simple model of gastric digestion of protein was developed by Savalle *et al* 1989, to model the digestion of milk protein in the calf stomach [277]. This simple model is composed of a vessel in a shaken water bath containing a reservoir of calf rennet (the

somach enzyme complex) in to which further gastric secretions and HCl were peristalticaly pumped. Samples are collected and analysed through TCA-precipitation and SDS-Page. While the authors acknowledge that exact reproduction of the *in vivo* processes is technically impossible the model provided a simulation of proteolytic digestion taking into account progressive acidification, gastric secretions and gastric emptying .

A similar model of porcine gastric digestion was developed by Chiang *et al* 2008 which they claim was developed into a 'dynamic model' by the use of a helical Teflon rod which was used to stir the contents of a temperature controlled glass vessel [278]. Use of this 'dynamic' method was shown to more closely model gastric protein digestion *in vivo* in the initial phases of digestion than the static model, the authors argue that this is due to a more realistic and slower mixing process.

It is acknowledged throughout the literature that completely accurate modelling of the GI tract is impossible. Depending upon the aims of individual studies a range of *in vitro* model systems have been developed to study different aspects of digestion.

The TIM system developed by Mikenus *et al* 1996, aims to provide a comprehensive dynamic modelling of the upper GI tract and has been adapted and validated for use in modelling the large intestine [274]. This is a complex and patented system that aims to simulate peristaltic motion and GI transit time with computer modelling. However this system has its limitations. No modelling or consideration is given to the buccal phase of digestion and the physical effects of mastication, which would affect how food arrives in the stomach, which does not meet the first criteria of Wichham *et al* to model processing in the mouth.

Dynamic models often use computer modelling of *in vivo* data on transit time to model GI movement and motility. However, gut motility is a highly complex system under neurohumoral control in response to a meal. The postprandial hormone response to a meal includes the release of "insulin, neurotensin, cholecystokinin (CCK), gastrin, glucagon-like-peptides (GLP-1 and GLP-2), glucose dependent insulinotropic polypeptide (GIP, previously known as gastric inhibitory peptide)" which affect gut motility in a number of ways. Furthermore a large number of neurohumoral effector molecules have been established which have stimulatory of inhibitory effects on muscle GI smooth muscle control *in vivo* [279].

Therefore, as the physical response to a meal is dictated by a specific postprandial response in reaction to feeding, computer modelling will always be a gross simplification of the controls of gastric motility.

6.2   Methods

6.2.1   Preperation of Synthetic GI Fluids

Synthetic GI fluids are not specifically buffered, but have been designed to simulate the pH changes and ionic content of the GI tract. Fluids were made up as stock solutions, enzymes are added fresh before each run. All chemicals and enzymes were purchased from Sigma-Aldrich unless otherwise stated.

Synthetic Saliva – α-amylase was prepared at 1µl/ml in Salivary Diluent (62mM $NaHCO_3$, 6mM $K_2HPO_4.3H_2O$, 15mM NaCl, 6.43mM KCl, 3mM $CaCl_2.2H_2O$ titrated to pH 7.4) Prior to assay salivary diluents containing 1µl/ml α-amylase was made up 1:1 with deionised water to give Synthetic Saliva.

Synthetic Gastric Juice - 40µg/ml Bacterial Gastric Lipase (Amano Enzyme Inc) and 0.5mg/ml Porcine Pepsin was prepared in Gastric Diluent (49.6 mM NaCl, 9.4mM KCl, 2mM KH_2PO_4, 5mM Urea titrated to pH 2.0).

Synthetic Pancreatic Juice – 70mg/ml Pancreatin was prepared in Pancreatic Diluent (110mM $NaHCO_3$, 2.5mM K_2HPO_4, 54.9mM NaCl, 1mM $CaCl_2.2H_2O$, 1.67mM Urea titrated to pH 8) and filtered through glass wool.

Fresh Porcine Bile – Gall Bladders are collected on ice from the abattoir, bile is pooled (approximately 50 per batch), mixed and frozen in aliquots for storage. 25ml was required for each replicate.

6.2.2 Substrate Preperation

All substrates, samples and controls are tested in triplicate. Protein, triglyceride and carbohydrate substrates can be tested separately, or in a mixed model, but are described here separately. Substrate mixes were made up to 10ml with synthetic saliva as described below and incubated on rollers for 10 minutes before addition to the resting reservoir of gastric diluent.

Fat Digestion - Six triglycerides of varying fatty acid chain lengths have been tested in the model gut system (Table 1). For triglycerides which release FA's with low pK_a (*) *Pancreatic Diluent* is modified to 322.8mM $NaHCO_3$ to counteract a lowering of pH as FAs are released. Glyceryl Trioctanoate has been used as the tryglyceride substrate for all assays of fat digestion reported herein. 2mmoles (0.94136g) of Glyceryl Trioctanoate is added as Synthetic Saliva Preperations at T[-10].

Triglyceride	*Fatty Acid*	*pK_a*
*Triacetin**	*Acetic Acid*	*4.5*
*Glyceryl Tributyrate**	*Butyric Acid*	*4.84*
*Glyceryl Trioctanoate**	*Octanoic Acid (Caprylic acid)*	*4.9*
Glyceryl Tripalmitate	*Palmitic Acid*	*9.7*
Glyceryl Trioleoate	*Oleic Acid*	*9.95*
Glyceryl Tristearate	*Stearic Acid*	*10.15*

Table 1 – Triglyceride substrates and the pK_a *of their constituent fatty acids*

Carbohydrate Digestion - Corn, wheat and potato starch in both native and gelatanised forms have been tested as carbohydrate substrates in the model gut system. Native Corn Starch has been used as the carbohydrate substrate for all assays of carbohydrate digestion reported herein. 1g of Corn Starch was added to synthetic saliva preperation at $T_{[-10]}$.

Protein Digestion- In order to distinguish effects on protein digestion from the gastric and pancreatic phases of digestion, gastric and pancreatic proteolysis assays are described separately. *Gastric Protein Digestion* -Bovine serum albumin (BSA) and casein have both been tested as protein substrates in the model gut system. BSA was purchased from Fisher Scientific and has been used as the protein substrate for all

assays of protein digestion reported herein. In the gastric phase 0.5g BSA was added to the salivary diluents at $T_{[-10]}$ and the assay was run until the end of the gastric phase at $T_{[60]}$.

Small intestinal Protein Digestion - For assays of protein digestion in the small-intestinal phase 1g of BSA was added to Synthetic Saliva at T[-10] and gastric pepsin was omitted from the gastric diluent to prevent any protein digestion in the gastric phase.

Background Control - For background controls 10ml Synthetic Saliva was prepared without substrate.

6.2.3   Samples Preperation

For sample testing substrate was prepared identical to substrate control with a known amount of test sample added. For sample controls 10ml synthetic saliva was prepared with appropriate amount of test sample, but without substrate.

For biopolymer testing 125, 250 and 500mg of biopolymer sample was prepared with synthetic salivary preperations. Acarbose, orlistat, pentosan polysulphate and soybean trypsin inhibitor were used as positive inhibition controls for α-amylase, lipase, pepsin and trypsin respectively. Alginate samples were provided by FMC Biopolymer and Technostics Ltd.

6.2.4 Equipment

Synthetic GI fluids were pre-incubated in a 37°C water bath. Sample beakers (three 500ml glass beakers) were prepared in a 37°C water bath with overhead stirrers to simulate stomach churning. A Watson Marlow Peristaltic pump was set at 0.5ml/min. A BioTek EL808 96 well plate spectrophotometer was used for sample analysis. Equipment was set up as shown in Figure 133.
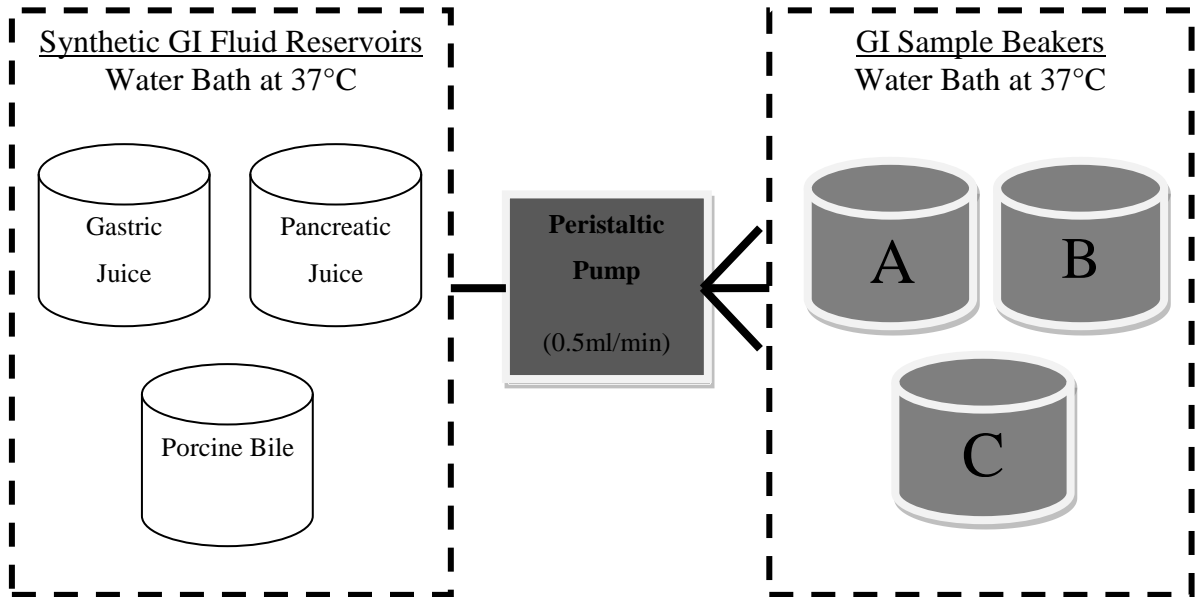
Figure 133   Set up of model gut system.

6.2.5 Procedure

Salivary Phase - At $T_{[-10]}$, salivary preparations containing substrate/sample/controls were prepared as above and incubated for 10 minutes on rollers. *Gastric Phase* – at $T[0]$ salivary preparations were added to a resting reservoir of 50ml Synthetic Gastric Juice (pre-incubated to 37°C in a water bath with overhead stirrer for 20 minutes). Additional gastric juice was added at a rate of 0.5ml/min with a peristaltic pump. Due to pepsin auto-digestion, gastric diluent is prepared immediately prior to addition at $T_{[-20]}$. *Pancreatic Phase* – At $T_{[60]}$ 25ml of Porcine Bile was added, the pumping of synthetic gastric juice was stopped, and filtered synthetic pancreatic juice was pumped in at a rate of 0.5ml/min. In the current examples the small-intestinal phase was continued until $T[180]$ however it can be run for longer. A schematic of the procedure is shown in Figure 135.
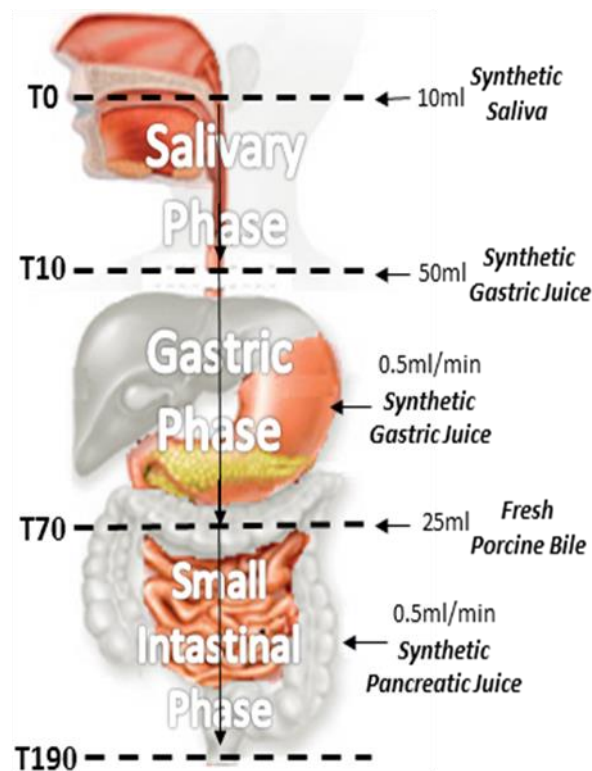
Figure 134   Schematic of Model gut system

6.2.6 Sampling

Samples of 0.5ml were taken at T0, T5, T10, T15, T30, T45, T60, T60^B, T65,T70,T75, T90, T105, T120, T150 and T180. (T60^B) represents a second sample at T60 after the addition of fresh porcine bile). Samples were immediately precipitated 1:1 in 10% TCA (w/v) (Trichloroacetic Acid) to stop enzyme activity and precipitate out undigested protein. Samples were stored at 4°C overnight to allow for precipitation and centrifuged at 10,000 r.p.m. for 10 minutes, the supernatant was then analysed. Dilution of synthetic GI fluid volume and sample dilution in TCA was accounted for in calculations.

6.2.7 Analysis

<u>Glycerol analysis</u> – Triglyceride digestion was measured using ZenBio Glycerol Reagent A to quantify the release of glycerol. 5µl of sample was incubated with 80µl Reagent A for 30 minutes and colour development was measured at 550nm. A standard curve was prepared a from stock 2.5mM glycerol solution.

<u>Starch Analysis</u> – In order to separate maltose products of digestion from undigested starch substrate, 50µl of supernatant was mixed with 950µl of 1%KCl (w/v) 75% methanol solution (v/v) and after 20 minutes samples were centrifuged at 10,000 rpm for 10 minutes. 500µl of the resulting supernatant was then evaporated down to a volume of 100µl. Once cooled to 37°C 50ul of 1mg/ml α-glucosidase (Sorachim) was added and incubated at 37°C for 2 hours. Liberated glucose was then assayed using the Megazyme D-Glucose (glucose oxidase/peroxidase; GOPOD) Assay Kit.

<u>Proteolysis Analysis</u> - Undigested polypeptides were removed from samples by TCA precipitation and centrifugation. Protein digestion was measured by assaying amino acids and short oligopeptides remaining in the supernatant with the Pierce BCA Total Protein assay kit. Working Reagent (WR) was prepared by mixing Reagent A and Reagent B at ratio 50:1. 25µl of samples were incubated with 200µl WR at 37°C for 30minutes and the colour development measured at 575 nm. A standard curve was prepared using a stock solution of BSA at 2mg/ml.

The Pierce BCA assay is known to under-report amino acid and oligo-peptide metabolites of protein digestion [280]. Figure 135 shows that only 37.76% of BSA is reported in the BCA assay after complete proteolysis. This can be corrected for by multiplying results by a factor of 2.65 as discussed below.

Figure 136 shows that in the pancreatic phase, only 60.33% of digested protein is detected due to bile binding of protein metabolites. Therefore when analysing protein digestion in the small intestinal phase data must be multiplied by a factor of 6.68 which corrects for this under-reporting and bile binding.
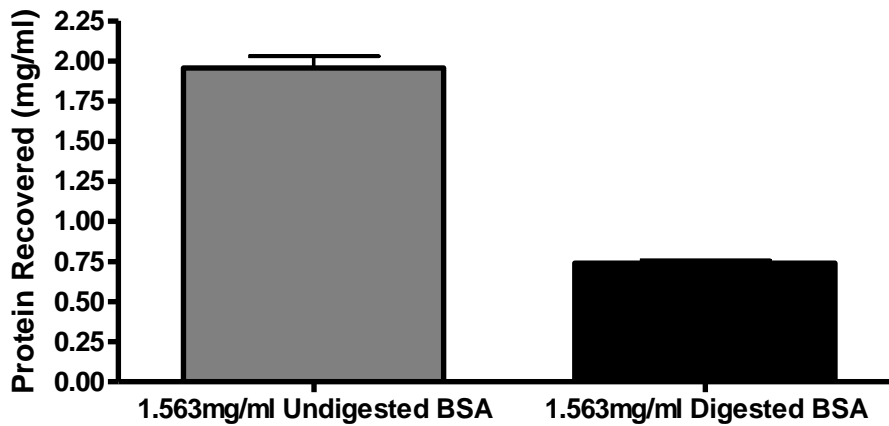
Figure 135   Comparison of BCA reporting of 1.563mg of BSA before and after a 2-step pepsin/trypsin digestion (n=3). A known amount of protein (1.563mg/ml aqueous) was tested in the BCA protein assay, and then after exhaustive overnight digestion with pepsin pH2 (1mg/ml) and then trypsin pH7 (1mg/ml) at 37°C.
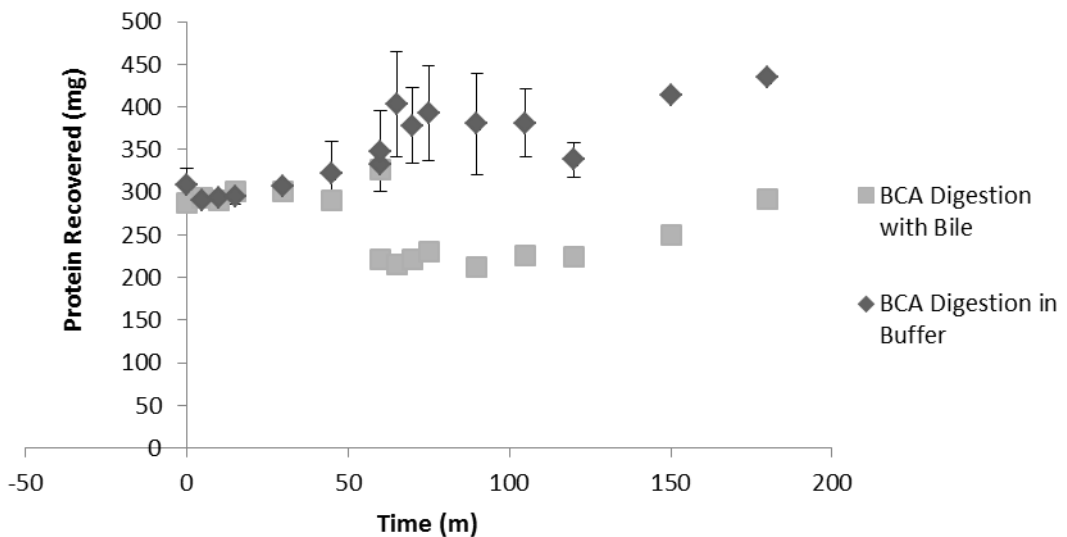
Figure 136   Detection of constant, known amount of digested protein in Model Gut system, with and without bile. 1g of BSA (in 10ml deionieed water) was exhaustively digested as described in Figure 135 and run through the model gut with or without the addition of bile at $T_{[60]}$. (n=3)

6.3 Results

Four alginate polymers were tested in the model gut system for their effects on fat, protein and carbohydrate digestion. Two of these were guluronic acid rich alginates, these were FMC3 and SF120. Two of the alginates tested were rich in mannuronic acid, these were FMC13 and H120L.

A number of other bioactive polymers were tested in the system as will be discussed in Chapter 7. The alginate LFR560 has also been tested for its effects on fat digestion, as it is a High-G alginate that has been used in human trials currently underway in the Pearson Lab.

6.3.1 Fat Digestion in the Model Gut

In vitro assays have shown alginates to reduce fat digestion by up to 75% *in vitro* [6]. Preliminary data has shown that alginate when delivered in a bread vehicle can reduce fat digestion in humans, and reduce post-prandial circulating blood triglyceride levels after supplementation with alginate in a bread vehicle [Unpublished Data].

Figure 137 shows a control digestion of glycryl trioctanoate in the model gut system. The first sample is taken after the salivary phase, and the artificial 'bolus' is passed into the resting gastric reservoir. $T_{[0]}$ therefore represents the start of the gastric phase of digestion, this runs for 60 minutes, during which time further gastric secretions are pumped in to the digestion vessel.

As can be seen from Figure 137, at $T_{[0]}$ no significant release of glycerol has occurred during the salivary phase, prior to addition to the resting gastric reservoir. Throughout the gastric phase between $T_{[0]}$ and $T_{[60]}$, there was similarly no release of glycerol.

At $T_{[60]}$ the system enters the small-intestinal phase. Pig bile was added to the system and synthetic pancreatic juices are pumped into the digestion vessel. As can be seen from the control digestion in Figure 137, for the first 10 minutes of the small-intestinal phase there is little or no change. However, after $T_{[70]}$, there is a gradual release of glycerol, which continues throughout the small intestinal phase. The small intestinal phase was run for two hours until $T_{[180]}$.
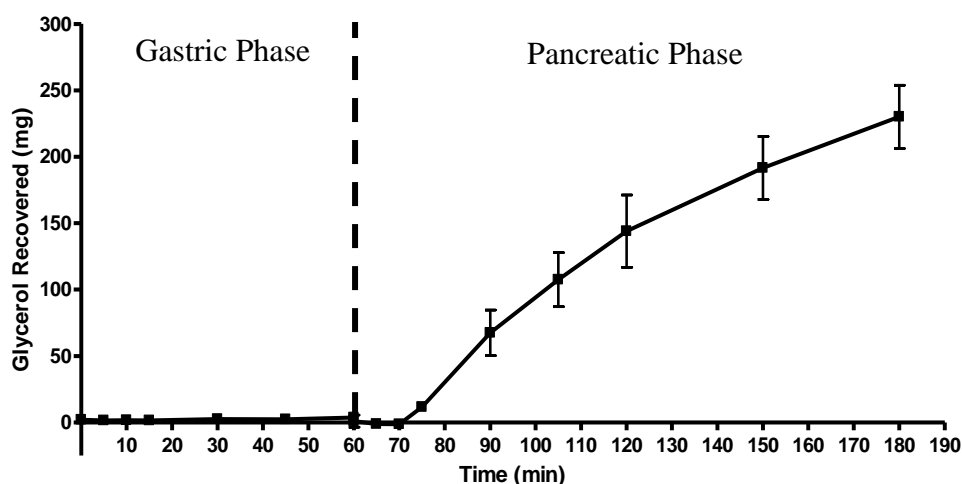
Figure 137 – Glyceryl Trioctanoate digestion in a model gut system. 2mmol of glyceryl trioctanoate was digested (Control Digestion). The graph shows total glycerol recovered from model gut system after TCA (Trichloroacetic Acid) precipitation to stop enzyme activity. Control digestion is represented as (■). All samples were tested in triplicate, errors are shown as standard deviation. The volume of the digestion solution varies throughout the assay, therefore total recoverable glycerol is quantifed using ZenBio Glycerol Kit to calculate the concentration of each sample, this value is used to extrapolate the total free glycerol in the system.

Fat digestion in the model gut system was validated with Orlistat, as can be seen from Figure 138, at all concentrations of Orlistat there was a reduction in fat digestion.

With 2.5mg/ml Orlistat, by the final time-point at $T_{[180]}$, glyceryl trioctanoate digestion was reduced to 54.8±13.6% of control digestion. With a 5mg/ml concentration of Orlistat, glyceryl release was reduced to 37.4±15.7% of control by $T_{[180]}$. With the highest tested concentration of Orlistat, 10mg/ml, total glyceryl trioctanoate digestion was reduced to 0.9±3.9% of control. These results showed clearly that the model gut system is capable of quantifying dose-dependent inhibition of fat digestion.

Figure 138 – Glyceryl Trioctanoate digestion in a model gut system with and without Orlistat. The graph shows total glycerol recovered from model gut system after TCA (Trichloroacetic Acid) precipitation to stop enzyme activity. 2mmol of Glyceryl Trioctanoate was digested alone (Control Digestion) and in the presence of varying concentrations of Orlistat . Control digestion is represented as (■) and digestion with Orlistat at 2.5mg as (▼), 5mg (◆) and 10mg (●). All samples were tested in triplicate, errors are shown as standard deviation.

As stated previously, work in this lab has shown that alginate can inhibit lipase activity by up to 72.2% *in vitro[281]*. Five alginates were tested for their regulatory activity towards lipase in the model gut system.

With the Alginates FMC3 and FMC13, there were no significant changes to the digestion of glyceryl trioctanoate by the addition of alginate at any of the timepoints (Figure 139 & Figure 140 respectively).
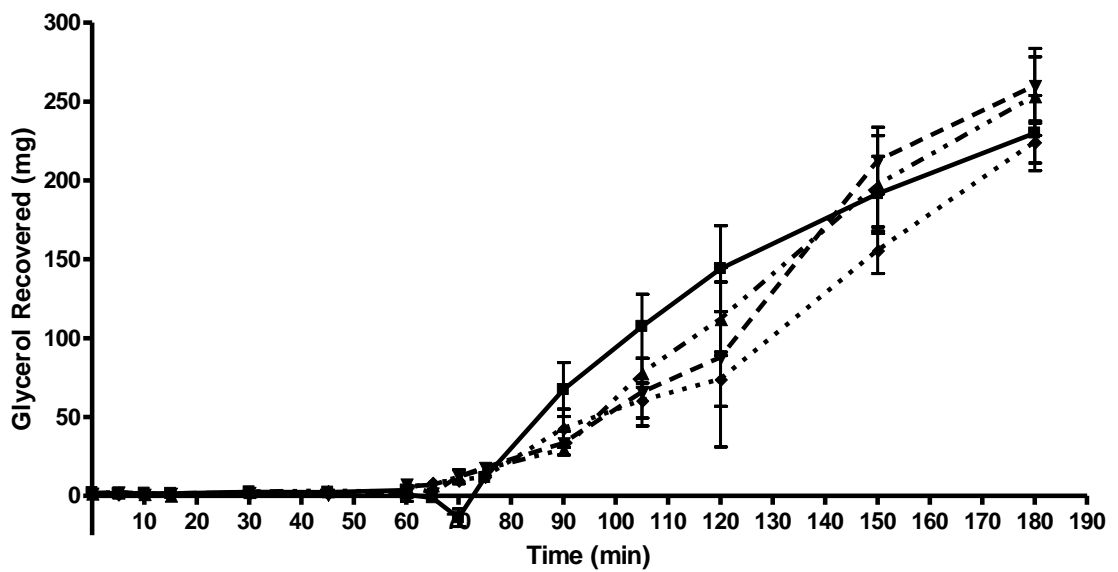
Figure 139 – Glyceryl Trioctanoate digestion in a model gut system with and without FMC3. The graph shows total Glycerol recovered from model gut system after TCA (Trichloroacetic Acid) precipitation to stop enzyme activity. 2mmol of Glyceryl Trioctanoate was digested alone (Control Digestion) and in the presence of varying concentrations of FMC3. Control digestion is represented as (■) and digestion with FMC3 at 125mg as (▲), 250mg (▼) and 500mg (◆). All samples were tested in triplicate, errors are shown as standard deviation.
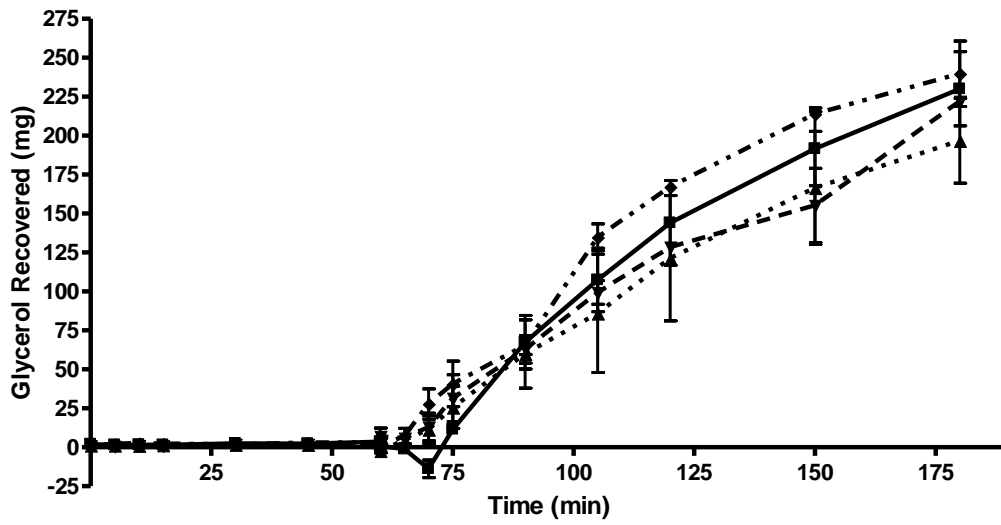
Figure 140   Glyceryl Trioctanoate digestion in a model gut system with and without FMC13. The graph shows total Glycerol recovered from model gut system after TCA (Trichloroacetic Acid) precipitation to stop enzyme activity. 2mmol of Glyceryl Trioctanoate was digested alone (Control Digestion) and in the presence of varying concentrations of FMC13. Control digestion is represented as as (■) and digestion with FMC13 at 125mg as (▲), 250mg (▼) and 500mg (◆). All samples were tested in triplicate, errors are shown as standard deviation.

The alginate LFR560 was the most effective of the alginate inhibitors tested against glyceryl trioctanoate. After 90 minutes, the level of glyceryl release from glyceryl trioctanoate in the modelgut system was significantly reduced at all three doses of alginate (Figure 141).

At $T_{[90]}$ after half an hour in the small intestinal phase, 125mg of alginate LFR560 had reduced the amount of glyceryl trioctanoate digested by 87.7±29.9%, at 250mg LFR560, digestion was reduced 91.1±10.9% and at 500 mg of LFR560 alginate digestion was reduced by 90.9±11.4%. All of these were shown to be statistically significant with a T-Test with P-Values of 0.025, 0.015 and 0.015 respectively.

By $T_{[180]}$ the inhibition was still apparent but had reduced in magnitude. With 125mg LFR560 at $T_{[180]}$ inhibition was 29.0±39.9%, although this was not statistically significant. With 250mg LFR560, inhibition was 40.8±17.4% which was shown to be statistically significant using a T-Test with a p-value of 0.030696. With 500mg LFR560, inhibition was 58.3±22.2% which was shown to be statistically significant using a T-Test with a p-value of 0.018.

With 10mg of Orlistat there was a complete inhibition of fat digestion at each of this timepoints, maximum inhibition at $T_{[180]}$ with LFR560 was a reduction of 58.3±22.1% with 500mg, suggesting that alginate LFR560 is a weaker inhitor of orlistat by between 1 and 2 orders of magnitude.
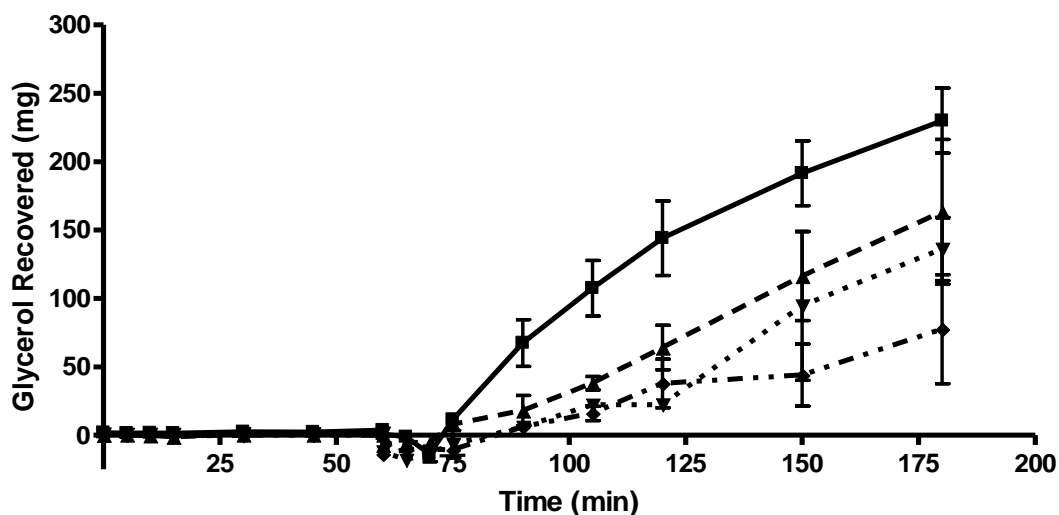
Figure 141 – Glyceryl Trioctanoate digestion in a model gut system with and without LFR560. The graph shows total Glycerol recovered from model gut system after TCA (Trichloroacetic Acid) precipitation to stop enzyme activity. 2mmol of Glyceryl Trioctanoate was digested alone (Control Digestion) and in the presence of varying concentrations of LFR560. Control digestion is represented as as (■) and digestion with LFR560 at 125mg as (▲), 250mg (▼) and 500mg (◆). All samples were tested in triplicate, errors are shown as standard deviation.

With the alginate SF120, a guluronic-acid rich alginate, there was no statistically significant change in the digestion profile of glyceryl trioctanoate up to 120 minutes Figure 142. After 120 minutes, at $T_{[150]}$ and $T_{[180]}$, a plateuaing effect was seen, and at all concentrations of alginate there was a reduction in glyceryl trioctanoate digestion. At $T_{[150]}$, 125mg SF120 reduced glyceryl trioctanoate digestion by 29.3±0.2%, at 250mg digestion was reduced by 32.0±20.0% and at 500mg of SF120 digestion was reduced by 29.0±4.5%. None of these inhibitions were however statistically significant.

At $T_{[180]}$ similar levels of inhibition were observed. With 125mg SF120 at $T_{[180]}$, glycerol release from glyceryl trioctanoate was reduced by 31.9±0.7%, although this was not shown to be statistically significant.

With 250mg and 500mg, there was a reduction in glycerol release from glyceryl trioctanoate of 52.3±18.0% and 38.1±1.6% respectively. Both of these inhibitions were shown to be statistically significant with p-values of 0.013 and 0.014 respectively.

Figure 142 – Glyceryl Trioctanoate digestion in a model gut system with and without SF120. The graph shows total Glycerol recovered from model gut system after TCA (Trichloroacetic Acid) precipitation to stop enzyme activity. 2mmol of Glyceryl Trioctanoate was digested alone (Control Digestion) and in the presence of varying concentrations of SF120. Control digestion is represented as as (■) and digestion with LFR560 at 125mg as (▲), 250mg (▼) and 500mg (◆). All samples were tested in triplicate, errors are shown as standard deviation.

A similar inhibition profile was seen with the alginate H120L as shown in Figure 143, whereby there was little difference in the digestion of glyceryl trioctanoate with/without H120L up until timepoint $T_{[120]}$ after which there was a plateuxing of glycerol release in samples containing alginate H120L.

At $T_{[150]}$, 125mg H120L reduced glyceryl trioctanoate digestion by 29.0±5.3%, at 250mg digestion was reduced by 30.9±10.2% and at 500mg of SF120 digestion was reduced by 42.3±4.3%. However, only the inhibition with 500mg H120L at $T_{[150]}$ was shown to be statistically significant using a T-Test, with a p-value of 0.018.

At $T_{[180]}$ similar levels of inhibition were observed. With 125mg H120L at $T_{[180]}$, glycerol release from glyceryl trioctanoate was reduced by 58.2±10.4%, which was shown to be statistically significant with a p-value of 0.003. With 250mg H120L there was a reduction in glycerol release from glyceryl trioctanoate of 33.4±12.4% which was statistically significant, with a p-value of 0.033. With 500mg H120L, there was a

35.6±7.4% reduciion in glycerol release from glyceryl trioctanoate which was statistically significant 0.018.
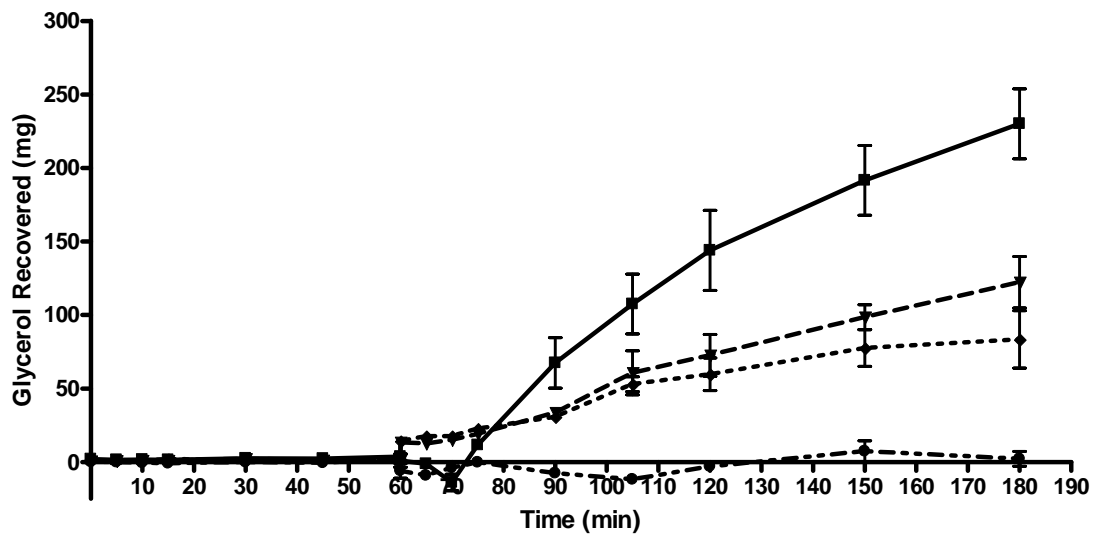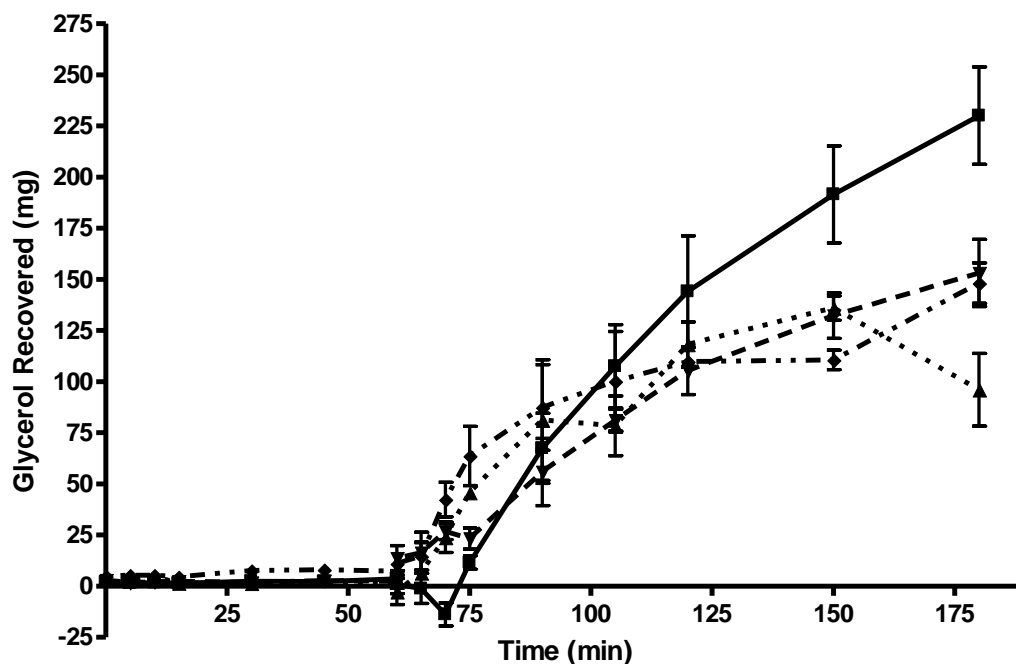

Figure 143 – Glyceryl Trioctanoate digestion in a model gut system with and without H120L. The graph shows total Glycerol recovered from model gut system after TCA (Trichloroacetic Acid) precipitation to stop enzyme activity. 2mmol of Glyceryl Trioctanoate was digested alone (Control Digestion) and in the presence of varying concentrations of H120L. Control digestion is represented as as (■) and digestion with LFR560 at 125mg as (▲), 250mg (▼) and 500mg (◆). All samples were tested in triplicate, errors are shown as standard deviation.

6.3.2 Carbohydrate Digestion in The Model Gut

In the *in vitro* microplate assays of alginate regulation of α-amylase activity in Chapter 5, it was shown that alginate increased the activity of α-amylase by up to 41.1±8.42%. While no clear relationship was shown with alginate structure, alginates high in mannuronic acid tended to result in a greater increase in maximum reaction velocity.

As was discussed in Chapter 5, these results contradict what has been shown in the literature suggesting that alginates have a hypoglycaemic affect *in vivo* and blunt post-prandial blood glucose spikes. From the literature, it is suggested that this may be due to a combination of alginate gelling in the stomach and delaying gastric emptying, and

reduced sodium uptake in the small intestine inhibiting the action of the sodium-glucose co-transporter.

The current model gut system described is a model of the chemical and absorbative phases of digestion, so does not model physiological gastric emptying control, or active nutrient uptake. It does however provide a model of physiologically relevant enzymatic and chemical digestion, which can be used to see if the activation of α-amylase shown in Chapter 5 would occur in a physiologically relevant system.

Figure 144 shows a control digestion of Corn Starch in the Model Gut system.
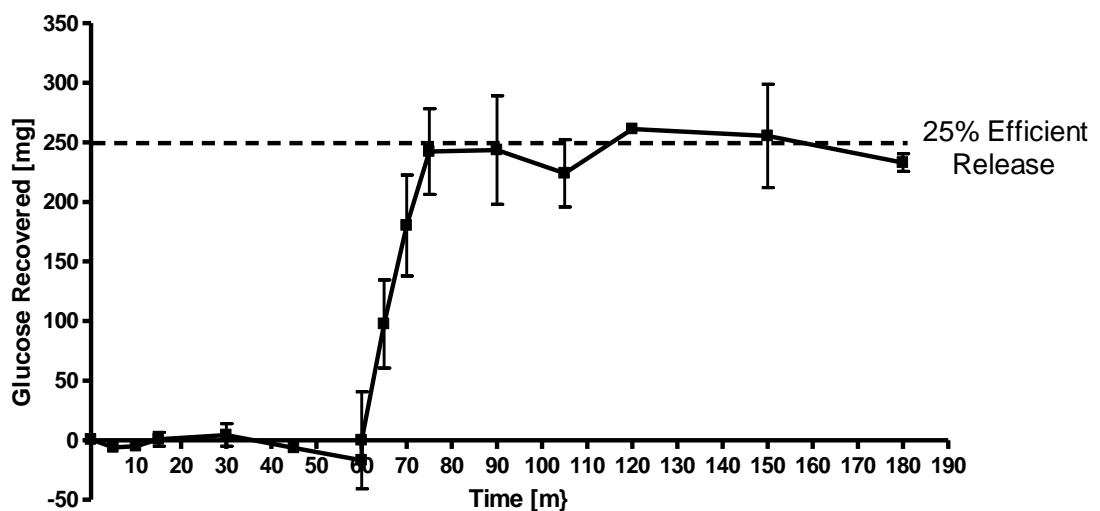
Figure 144 – Corn Starch digestion in a model gut system. 1g of Native Corn Starch was digested (Control Digestion). The graph shows total glucose recovered from model gut system after TCA (Trichloroacetic Acid) precipitation to stop enzyme activity and Methanol-KCl precipitation to remove undigested starch. Control digestion is represented as (■). All samples were tested in triplicate, errors are shown as standard deviation. 1g of native corn starch was added to synthetic saliva; the term 'native' refers to powdered, un-gelatinised corn starch. Native starch was used in order to prevent inconsistencies and the introduction of error in the gelatinisation process.

As can be seen from Figure 144, at $T_{[0]}$ there has been no significant digestion of starch during the salivary phase. Throughout the gastric phase from $T_{[0]}$ to $T_{[60]}$, there is similarly no significant release of glucose detected.

At $T_{[60]}$ as the system enters the small-intestinal phase and synthetic pancreatic secretions and bile are added to the digestion mixture. From $T_{[65]}$ the release of glucose is detected in the small intestinal phase, and this continues at a more or less constant rate until $T_{[75]}$ where digestion levels off and there is no increase in detected glucose. This is consistent with the literature which suggests that starch breakdown into maltose,

maltotriose and α-limit dextrin occurs very rapidly and within 10 minutes of transit into the duodenum [100].

1g of native corn starch was used as the carbohydrate substrate, however, as is indicated on Figure 144, only 25% of this is recovered in the assay, even after the digestion curve has plateaued. This indicates that either not all the starch is getting digested, or the assay system is under-reporting digestion of carbohydrate. This will be commented upon further in the discussion.

The model of corn starch digestion in the model gut system was validated using the inhibitor acarbose (Figure 145).
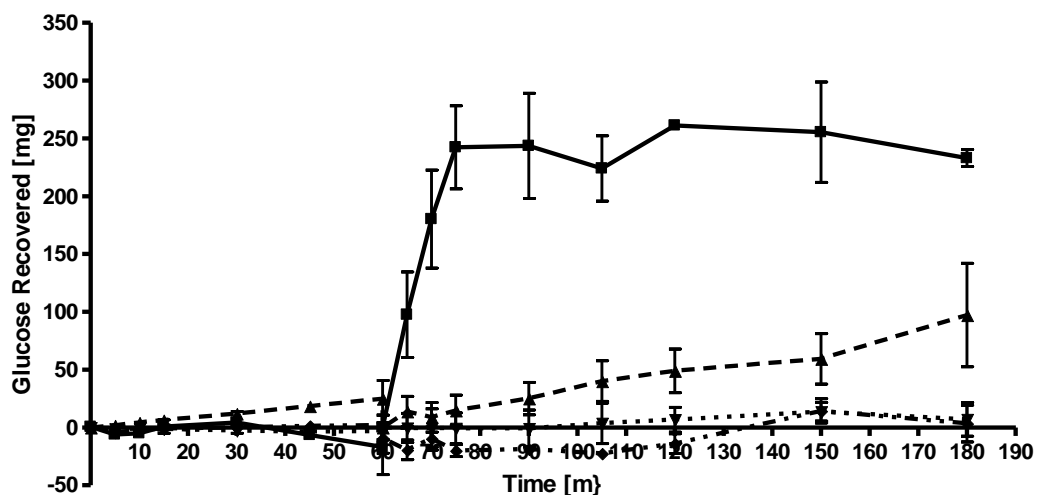
Figure 145 – Corn Starch digestion in a model gut system with and without Acarbose. The graph shows total glucose recovered from model gut system after TCA (Trichloroacetic Acid) precipitation to stop enzyme activity and Methanol-KCl precipitation to remove undigested starch. 1g of Native Corn Starch was digested alone (Control Digestion) and in the presence of varying concentrations of Acarbose . Control digestion is represented as as (■) and digestion with acarbose at 125mg as (▲), 250mg (▼) and 500mg (●). All samples were tested in triplicate, errors are shown as standard deviation.

Although some variation can be seen in the gastric phase in Figure 145 with the addition of acarbose to the model gut system, there was no significant change from the control digestion. In the initial 5 minutes of the small intestinal phase between $T_{[60]}$ and $T_{[65]}$, there is a visible reduction in the amount of carbohydrate digestion at all three tested

concentrations of acarbose, however none of these reductions could be shown to be statistically significant.

From $T_{[65]}$ onwards until $T_{[180]}$, there is a statistically significant reduction in carbohydrate digestion relative to control at all time-points at all three tested concentrations. With 25mg Acarbose, by the final time point of $T_{[180]}$ carbohydrate digestion was reduced to 41.7% of control (P=0.002). With 50mg Acarbose, by $T_{[180]}$ carbohydrate digestion was reduced to 3.01% of control (P=0.0009). With 100mg Acarbose, by $T_{[180]}$ carbohydrate digestion was reduced to 1.45% of control (P=0.0013).

As was discussed in Chapter 5, it had been expected from the literature that alginates would reduce the rate of carbohydrate digestion, as they had been shown to have anti-hyperglycaemic effects *in vivo*. However the results shown in Chapter 5 show a non-specific activation of α-amylase by alginates. In order to investigate if this activatory effect persists in a physiological environment, or if the reaction dynamics are somehow different in the milieu of the physiological conditions, the affects of alginate on carbohydrate digestion were investigated in the model gut system.
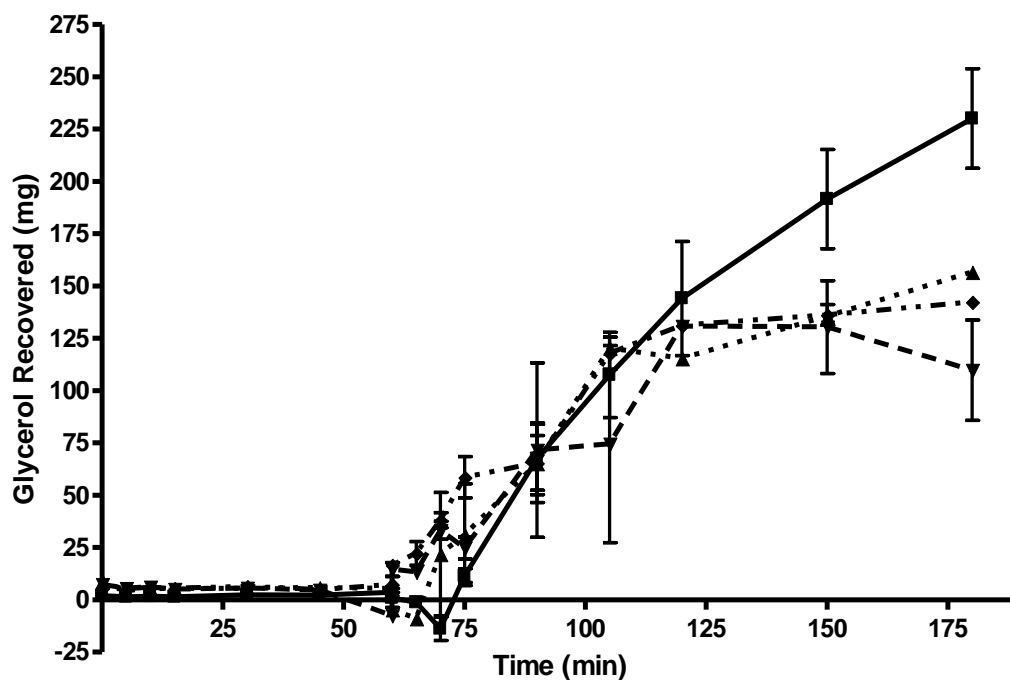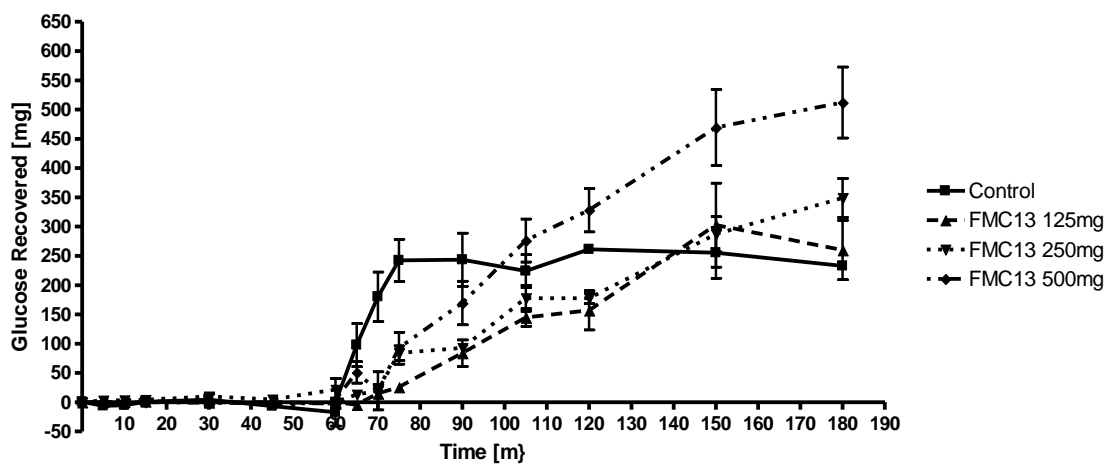

Figure 146 – Corn Starch digestion in a model gut system with and without FMC13 Alginate. The graph shows total glucose recovered from model gut system after TCA (Trichloroacetic Acid) precipitation to stop enzyme activity and Methanol-KCl precipitation to remove undigested starch. 1g of Native Corn Starch was digested alone (Control Digestion) and in the presence of varying concentrations of FMC13 . Control digestion is represented as as (■) and digestion with FMC13 at 125mg as (▲), 250mg (▼) and 500mg (●). All samples were tested in triplicate, errors are shown as standard deviation.

The digestion profile of corn starch was greatly changed in the presence of alginate. With the addition of alginate FMC13, digestion of corn starch was inhibited during the first 15 minutes of the small intestinal phase from $T_{[60]}$-$T_{[75]}$ (Figure 146). At $T_{[75]}$ with

all concentrations of FMC13 alginate there was statistically significant inhibition; at 125mg FMC13 corn starch digestion was reduced by 89.3% (P=0.025), at 250mg FMC13 digestion was reduced by 65.4% (P=0.036) and with 500mg FMC13 digestion was reduced by 61.9% (P=0.032).

By $T_{[105]}$, there is no significant difference between samples containing alginate and control, suggesting that the glucose yield has recovered to normal levels. From $T_{[105]}$ to $T_{[180]}$ there is no significant difference from control with the addition of 125mg or 250mg of FMC13. With 500mg FMC13 there was no significant variation from control digestion between $T_{[105]}$ and $T_{[150]}$, however at $T_{[180]}$ there was a 119.77% increase in glucose yield from corn starch which was shown to be statistically significant (P=0.042).

In the presence of alginate FMC3, corn starch showed a similar digestion profile to that described with FMC13 (Figure 147). Corn starch digestion was initially blunted in the small intestinal phase with a reduction in recovered glucose at $T_{[75]}$ of 75.5% (P=0.030), 62.7% (P=0.047) and 63.8% (P=0.045) at 125, 250 and 500mg respectively after the first 15 minutes of the small intestinal phase.

With 500mg of FMC3 alginate there were statistically significant increases in the amount of glucose recovered at $T_{[120]}$ and $T_{[150]}$ of 57.3%(P=0.007) and 129.8%(P=0.012) respectively. At 125 and 250mg FMC3 there were no significant changes to corn starch digestion between $T_{[90]}$ and $T_{[150]}$.

However by the final timepoint $T_{[180]}$ there were statistically significant increases in glucose recovered at all concentrations of FMC3 with increases of 45.7% (P=0.024), 42.2% (P=0.002) and 129.8% (P=0.031) at 125, 250 and 500mg respectively.
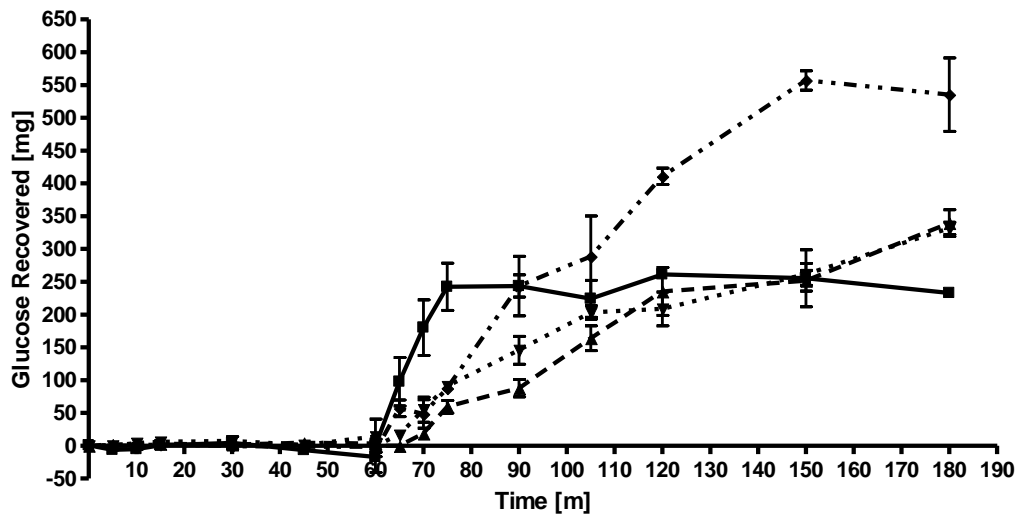
Figure 147 – Corn Starch digestion in a model gut system with and without FMC3 Alginate. The graph shows total glucose recovered from model gut system after TCA (Trichloroacetic Acid) precipitation to stop enzyme activity and Methanol-KCl precipitation to remove undigested starch. 1g of Native Corn Starch was digested alone (Control Digestion) and in the presence of varying concentrations of FMC3. Control digestion is represented as as (■) and digestion with FMC3 at 125mg as (▲), 250mg (▼) and 500mg (●). All samples were tested in triplicate, errors are shown as standard deviation.

Although visually alginates SF120 and H120L shown in Figure 148 and Figure 149 respectively suggest that they may be following a similar pattern of blunted carbohydrate digestion in the initial phase of digestion, and an increase in glucose yield in the final stages of the simulated small intestine, there were no statistically significant changes. Furthermore the results with 500mg of SF120 were highly variable suggesting the possibility of experimental error.
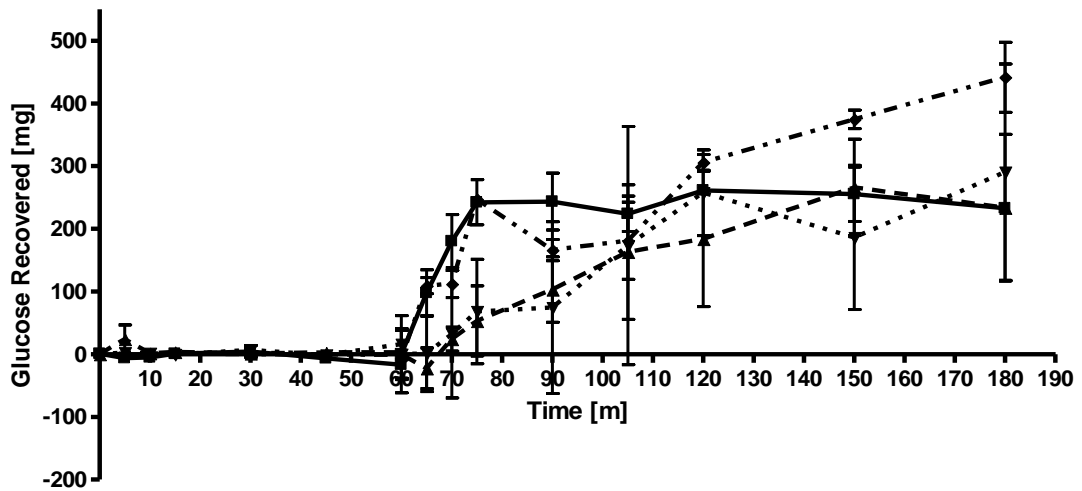
Figure 148 – Corn Starch digestion in a model gut system with and without SF120 Alginate. The graph shows total glucose recovered from model gut system after TCA (Trichloroacetic Acid) precipitation to stop enzyme activity and Methanol-KCl precipitation to remove undigested starch. 1g of Native Corn Starch was digested alone (Control Digestion) and in the presence of varying concentrations of SF120. Control digestion is represented as as (■) and digestion with SF120 at 125mg as (▲), 250mg (▼) and 500mg (●). All samples were tested in triplicate, errors are shown as standard deviation.
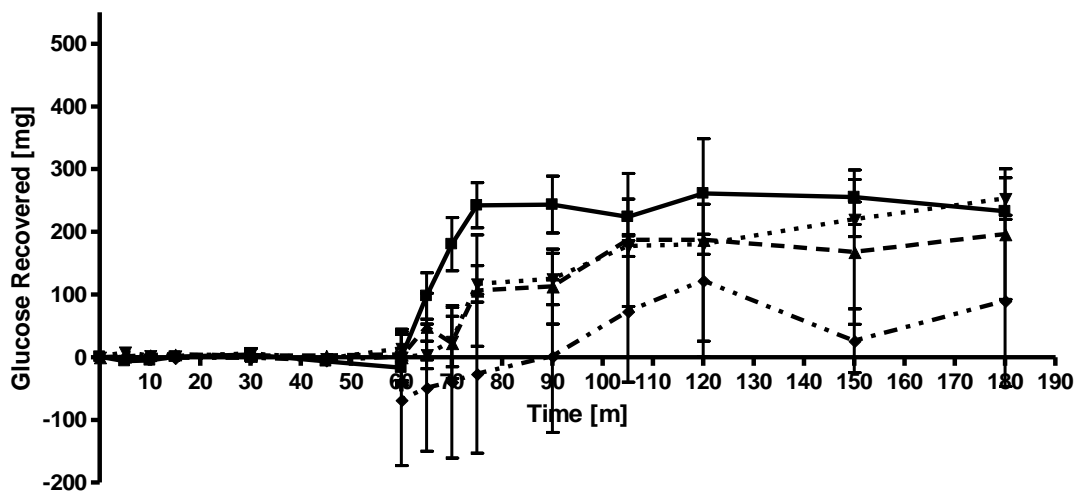
Figure 149 – Corn Starch digestion in a model gut system with and without H120L Alginate. The graph shows total glucose recovered from model gut system after TCA (Trichloroacetic Acid) precipitation to stop enzyme activity and Methanol-KCl precipitation to remove undigested starch. 1g of Native Corn Starch was digested alone (Control Digestion) and in the presence of varying concentrations of H120L. Control digestion is represented as as (■) and digestion with H120L at 125mg as (▲), 250mg (▼) and 500mg (●). All samples were tested in triplicate, errors are shown as standard deviation.

263

6.4   Protein Digestion in The Model Gut

In order to distinguish the exact site of the effects of exogenous compounds on protein digestion, the gastric and pancreatic phases of digestion were analysed separately. This was done so there was a known amount of protein substrate entering the small intestinal phase.

6.4.1   Gastric Protein Digestion

Figure 150 shows a control digestion of 0.5g of BSA in the gastric phase of the model gut system. Between $T_{[0]}$ and $T_{[45]}$ there is a more or less linear breakdown of the protein substrate, after which, digestion begins to plateau in the final 15 minutes of the assay up to $T_{[60]}$. As can be seen, approximately 500mg of digested protein is recovered in the assay. This 100% recovery rate suggests that all protein substrate is digested within 60 minutes, and is accurately quantified by the assay system.
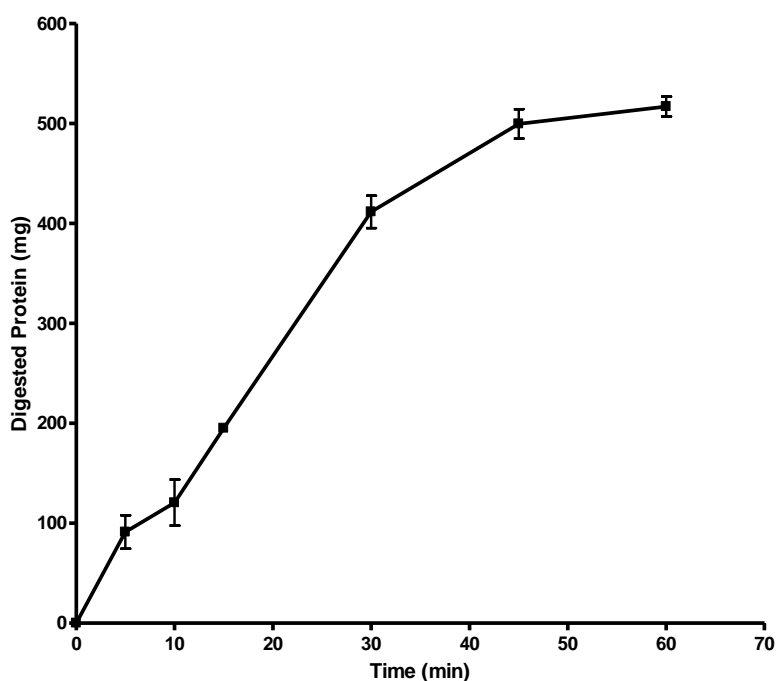
Figure 150 – Bovine Serum Albumin digestion in gastric phase of a model gut system. 0.5g BSA was digested (Control Digestion). The graph shows total protein recovered from model gut system after TCA (Trichloroacetic Acid) precipitation to stop enzyme activity and remove undigested polypeptides. Control digestion is represented as (■). All samples were tested in triplicate, errors are shown as standard deviation.

Pentosan polysulphate (SP54) was used as the positive inhibition control. Pentosan polysulphate is a highly sulphated polysaccharide, and sulphated polysaccharides have been shown to have anti-pepsin activity, both *in vitro* and *in vivo*.

Three concentrations of pentosan polysulphate (SP54) were tested in the gastric phase of the model gut in order to validate the detection of inhibition (Figure 151). At all tested concentrations of 50mg, 100mg and 200mg pentosan polysulphate there was significant inhibition of gastric proteolysis at all time points from $T_{[5]}$ onwards.

At T[5], 50, 100 and 200mg of pentosan polysulphate significantly inhibited the gastric digestion of protein by 62.5% (P=0.005), 90.1% (P=0.003) and 90.5% (P=0.002) respectively.

At $T_{[60]}$ by the end of the gastric phase, 50, 100 and 200mg of pentosan polysulphate significantly inhibited the gastric digestion of protein by 54.1% (P=0.0001), 78.9% (P=0.001) and 87.6% (P=0.0004) respectively. This showed a dose responsive inhibition of gastric proteolysis by pentosan polysulphate.

Figure 151 – Bovine Serum Albumin digestion in gastric phase of a model gut system with and without SP54. The graph shows total protein recovered from model gut system after TCA (Trichloroacetic Acid) precipitation to stop enzyme activity and remove undigested polypeptides. 0.5g BSA was digested alone (Control Digestion) and in the presence of varying concentrations of SP54. Control digestion is represented as as (■) and digestion with SP54 at 125mg as (▲), 250mg (▼) and 500mg (●). All samples were tested in triplicate, errors are shown as standard deviation.

In vitro assays described in Chapter 3 demonstrated that alginates were potent inhibitors of pepsin activity, and that this inhibition was related to increasing levels of mannuronic acid. In order to investigate if this inhibitory effect was likely to persist *in vivo*, alginate inhibition of protein digestion was investigated in the model gut system.

Four alginates were tested for their effect on the simulated gastric digestion of alginates; FMC3, FMC13, SF120 and H120L. With all tested alginates there was a significant inhibition of protein digestion in the gastric phase.

By the end of the simulated gastric phase, FMC13 was the weakest of the four alginates tested (Figure 152). By $T_{[60]}$ after an hour of simulated digestion with 125, 250 and 500mg of FMC13, proteolytic digestion was reduced by 23.4% (P=0.021), 52.2% (P=0.040) and 43.5% (P=0.013) respectively, as compared to a control.

This represented a trend of recovery towards the amount of protein digestion in the control. At timepoints $T_{[30]}$ and $T_{[45]}$ there was a larger percentage terms inhibition as compared to control. At $T_{[30]}$ after an hour of simulated digestion with 125, 250 and 500mg of FMC13 proteolytic digestion was reduced by 52.8% (P=0.004), 75.7% (P=0.004) and 62.7 (P=0.0008) respectively. At T[45] after an hour of simulated digestion with 125, 250 and 500mg of FMC13 proteolytic digestion by 52.8% (P=0.004), 70.9% (P=0.001499) and 73.06 (P=0.01846).
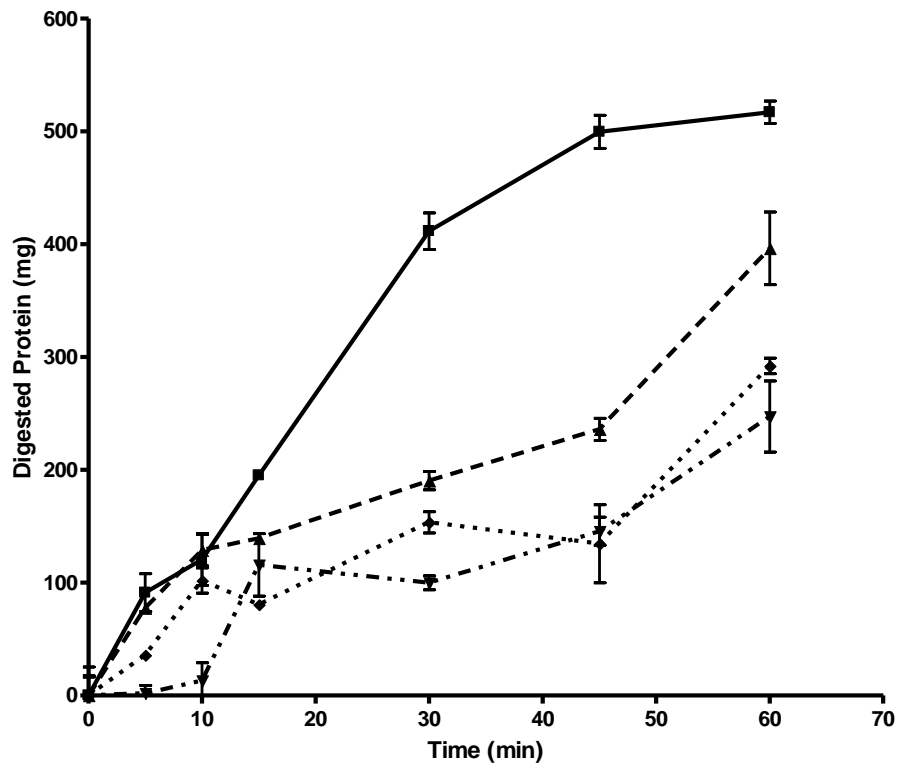
Figure 152 – Bovine Serum Albumin digestion in gastric phase of a model gut system with and without FMC13 Alginate. The graph shows total protein recovered from model gut system after TCA (Trichloroacetic Acid) precipitation to stop enzyme activity and remove undigested polypeptides. 0.5g BSA was digested alone (Control Digestion) and in the presence of varying concentrations of FMC13. Control digestion is represented as as (■) and digestion with FMC13 at 125mg as (▲), 250mg (▼) and 500mg (●). All samples were tested in triplicate, errors are shown as standard deviation.

FMC3 showed a similar inhibition profile to FMC13 (Figure 153). At $T_{[30]}$, protein digestion was reduced by 51.9% (P=0.0002), 69.6% (P=0.013) and 48.0% (P=0.016002) as compared to control with 125mg, 250mg and 500mg of FMC3 alginate respectively. At $T_{[45]}$, protein digestion was reduced by 50.4% (P=0.005263), 64.0 % (P=0.015) and 47.2% (P=0.0004) as compared to control with 125mg, 250mg and 500mg of FMC3 alginate respectively. By the final timepoint at $T_{[60]}$, protein digestion was reduced by 20.2% (P=0.029), 64.8% (P=0.024) and 55.1% (P=0.035) as compared to control with 125mg, 250mg and 500mg of FMC3 alginate respectively.

At all three of these timepoints where significant inhibition was achieved, the highest level of inhibition is with the intermediate concentration of alginate 250mg, with 125mg and 500mg yielding lower levels of inhibition. It is to be expected that at lower concentrations of alginate there would be lower levels of inhibition, however it is

267

somewhat counter-intuitive that at the higher concentration of 500mg FMC3, that the inhibition is lower than with 250mg.

Figure 153 – Bovine Serum Albumin digestion in gastric phase of a model gut system with and without FMC3 Alginate. The graph shows total protein recovered from model gut system after TCA (Trichloroacetic Acid) precipitation to stop enzyme activity and remove undigested polypeptides. 0.5g BSA was digested alone (Control Digestion) and in the presence of varying concentrations of FMC3. Control digestion is represented as as (■) and digestion with FMC3 at 125mg as (▲), 250mg (▼) and 500mg (●). All samples were tested in triplicate, errors are shown as standard deviation.

As can be seen from Figure 154, inhibition of protein digestion with alginate SF120 was varied, but at all timepoints after $T_{[15]}$, the highest levels of inhibition were achieved with the highest concentration of 500mg SF120. At $T_{[30]}$, protein digestion was reduced by 35.4% (P=0.010), 47.3% (P=0.033) and 62.1% (P=0.002) as compared to control with 125mg, 250mg and 500mg of SF120 alginate respectively. At $T_{[45]}$, protein digestion was reduced by 60.8% (P=0.0033408), 37.5% (P=0.003) and 70.2% (P=0.019) as compared to control with 125mg, 250mg and 500mg of SF120 alginate respectively. By the final timepoint at $T_{[60]}$, protein digestion was reduced by 32.9% (P=0.0025), 30.8% (P=0.007) and 50.5% (P=0.001) as compared to control with 125mg, 250mg and 500mg of SF120 alginate respectively.

Figure 154 – Bovine Serum Albumin digestion in gastric phase of a model gut system with and without SF120 Alginate. The graph shows total Protein recovered from model gut system after TCA (Trichloroacetic Acid) precipitation to stop enzyme activity and remove undigested polypeptides. 0.5g BSA was digested alone (Control Digestion) and in the presence of varying concentrations of SF120. Control digestion is represented as as (■) and digestion with FMC3 at 125mg as (▲), 250mg (▼) and 500mg (●). All samples were tested in triplicate, errors are shown as standard deviation.

The results seen from the biopolymer H120L were somewhat different to what was seen with the other alginate samples (Figure 155). With the higher concentrations of alginate H120L at 250mg and 500mg there was an increase in the rate of protein digestion at $T_{[5]}$, and with 500mg an increase also at $T_{[10]}$. At $T_{[5]}$ there was an increase in protein digestion of 71.8% with 250mg H120L and of 154% with 500mg, although neither of these increases were statistically significant. At $T_{[10]}$ there was an increase in the digested protein yield of 145% with 500mg H120L, this was shown to be statistically significant (P=0.038). From $T_{[30]}$ onwards the data for H120L is more similar to what was seen with the other alginate samples, whereby there is a reduced level of protein digestion at all timepoints for all alginates. At $T_{[60]}$ there were reductions of 55.6%, 50.4% and 65.25% at 125mg, 250,mg and 500mg respectively.

It is unclear from the data whether the increases in protein digestion seen in the first 15 minutes of protein digestion represent a real phenomenon, or are experemental artefacts, as only one of the data points was statistically significant. It may be that alginate is

269

interacting with the protein substrate and forming a physical gel that is separating the simulated gut contents into two phases and reducing the reaction volume in the remaining solution. This could be a possible explanation for an initial increase in rate, which is then overcome as the free substrate is depleted and the remaining substrate is bound to alginate.
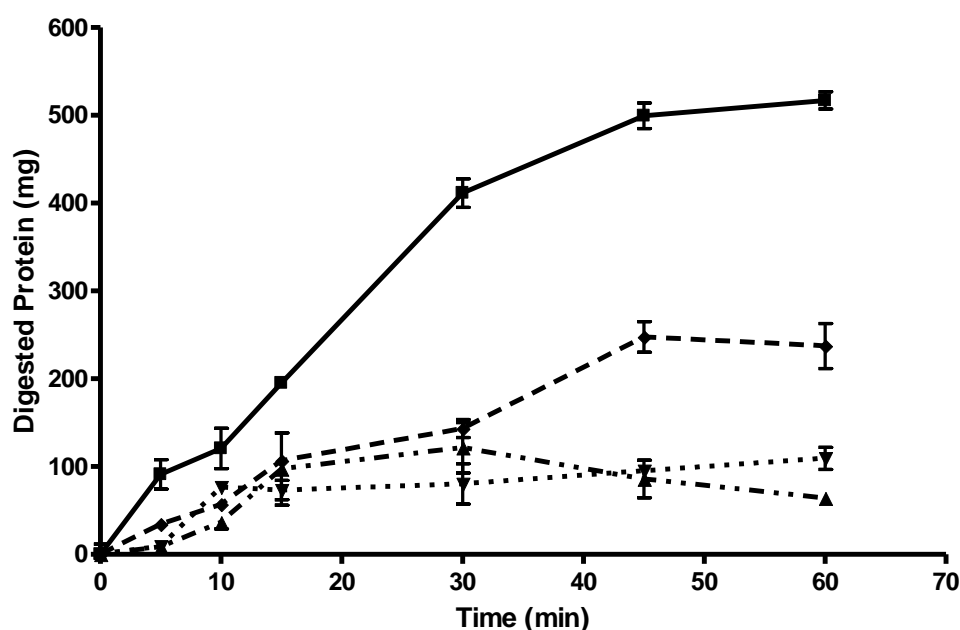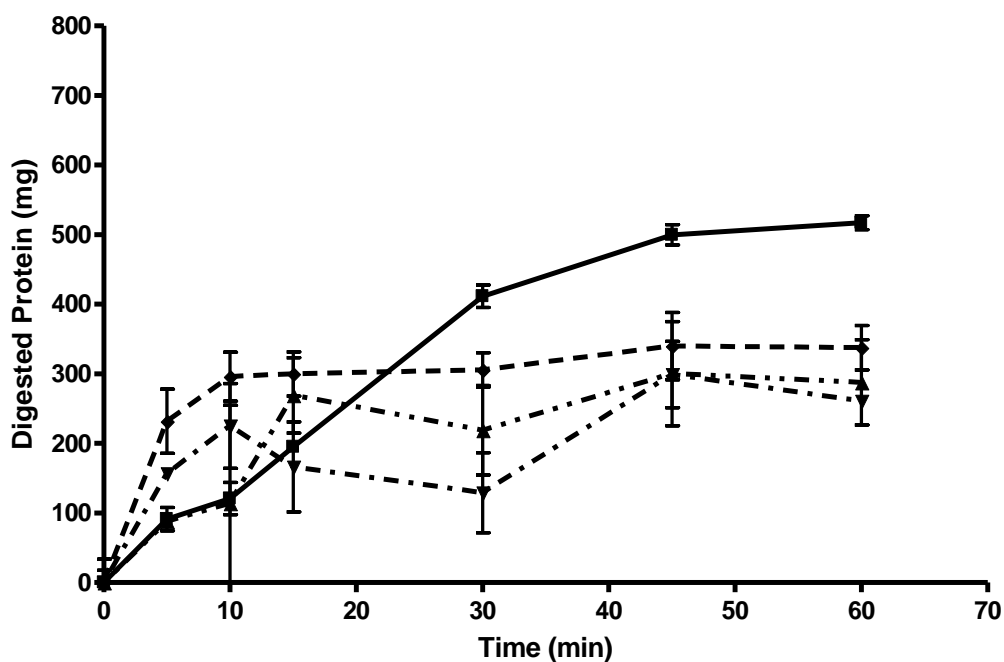

Figure 155 – Bovine Serum Albumin digestion in gastric phase of a model gut system with and without H120L Alginate. The graph shows total protein recovered from model gut system after TCA (Trichloroacetic Acid) precipitation to stop enzyme activity and remove undigested polypeptides. 0.5g BSA was digested alone (Control Digestion) and in the presence of varying concentrations of H120L. Control digestion is represented as as (■) and digestion with H120L at 125mg as (▲), 250mg (▼) and 500mg (●). All samples were tested in triplicate, errors are shown as standard deviation.

6.4.2   Pancreatic Phase Protein Digestion

In Chapter 4, the effects of alginate on trypsin were investigated. Only marginal variations in trypsin activity could be shown to be statistically significant. It was shown that pH dependent viscosity interactions may be the reason why protein substrate was unavailable for digestion by pepsin in an acidic environment, but trypsin digestion at a neutral pH was unaffected.

However, the physiological environment in which proteolytic digestion occurs in the small-intestine is considerably more complex than the environment simulated in the

microplate assays. Firstly, the substrate has passed through the salivary and gastric phases and mixed with various digestive secretions and enzymes.

Figure 156 shows a control digestion of 1g of BSA in the model gut system. During the gastric phase of digestion between $T_{[0]}$ and $T_{[60]}$, gastic pepsin has been omitted from the simulated gastric juice, and there is consequently no significant protein digestion in the gastric phase. After $T_{[60]}$ the simulation enters the small-intestinal phase, porcine bile is added to the digestive mixture and pancreatic secretions containing active proteolytic enzymes are pumped in. During the first hour of small-intestinal digestion, between $T_{[60]}$ and $T_{[120]}$ there is a more or less linear breakdown of the protein substrate, after which, digestion begins to plateaux in the final 60 minutes of the assay up to $T_{[180]}$. As can be seen in Figure 156 there is a 100% recovery of protein in the small-intestinal phase, although there is some variation.
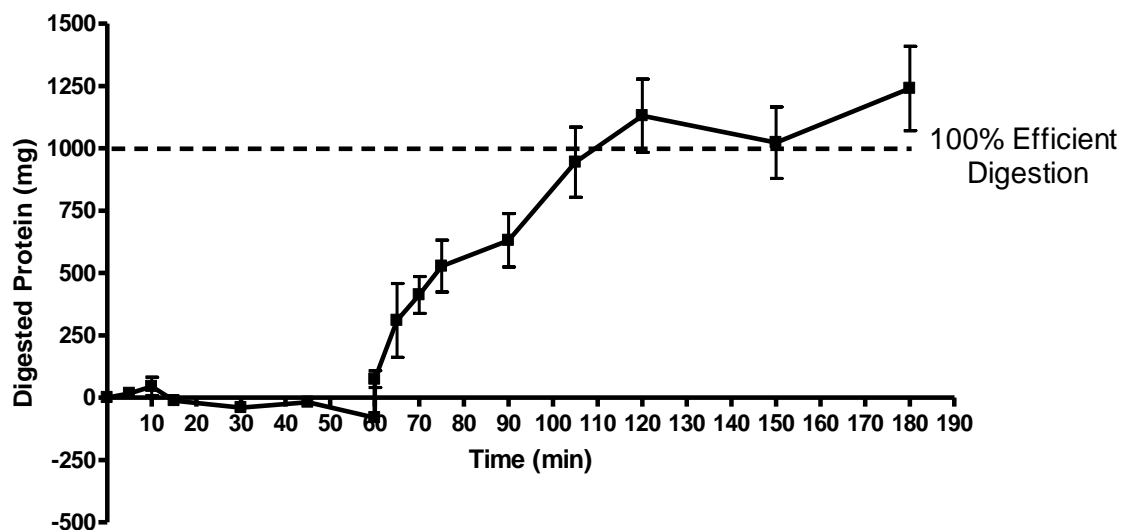
Figure 156 – Bovine serum albumin (BSA) digestion in the small-intestinal phase of a model gut system. The graph shows total Protein recovered from model gut system after TCA (Trichloroacetic Acid) precipitation to stop enzyme activity and remove undigested polypeptides. Control digestion of 1g BSA is represented as (■). All samples were tested in triplicate, errors are shown as standard deviation.

Soybean Trypsin Inhibitor (SBTI) was used as the positive inhibition control (Figure 157). Three concentrations of SBTI were tested in the model gut in order to validate the detection of inhibition of proteolysis. At all tested concentrations of 125mg, 250mg and 500mg SBTI, there was no difference in proteolytic activity throughout the gastric phase of digestion.

However as would be expected, during the small-intestinal phase, the addition of SBTI to the digestive mixture downregulated proteolytic activity and reduced the amount of digested protein recovered from the assay. From $T_{[70]}$ onwards the addition of 250 and 500mg yielded statistically significant inhibition at all timepoints until the end of the assay.

With 500mg SBTI, at $T_{[70]}$ inhibition of 79.3% was achieved. From $T_{[75]}$ until $T_{[180]}$, inhibition of proteolytic activity was between 90.6 and 100% and statistically significant at all time-points. With 250mg SBTI, statistically significant inhibition of over 60.1% was achieved at all timepoints after $T_{[70]}$. With 125mg of SBTI, statistically significant inhibition of proteolytic digestion was achieved between $T_{[70]}$ and $T_{[120]}$ ranging from 59.25-100%, however at $T_{[150]}$ and $T_{[180]}$ the reduction in protein digestion relative to control could not be shown to be statistically significant. These data showed a dose responsive inhibition of simulated small intestinal protein digestion, with maximum inhibition achieved at 500mg SBTI.
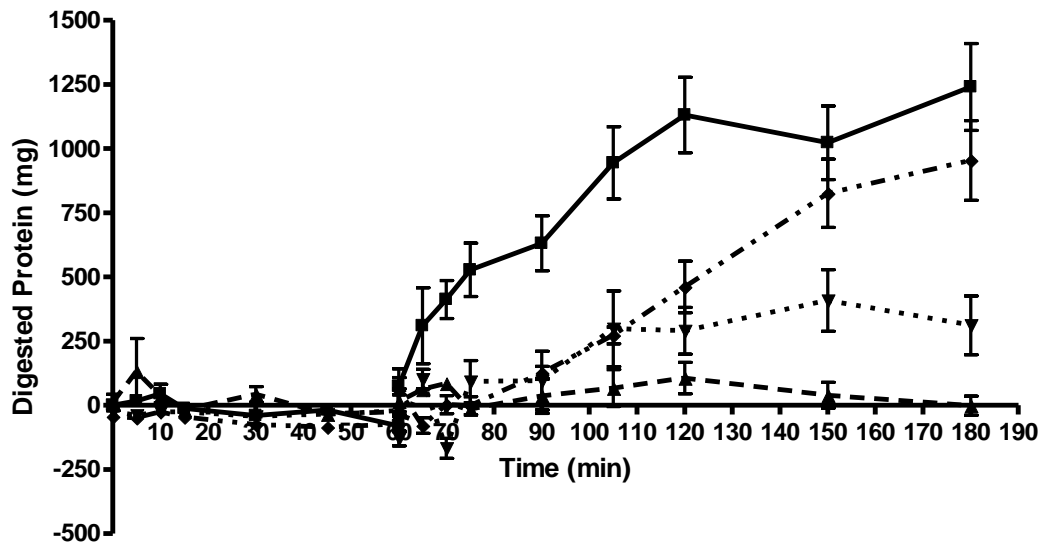
Figure 157 – Bovine serum albumin (BSA) digestion in the small-intestinal phase of a model gut system with and without SBTI. The graph shows total protein recovered from model gut system after TCA (Trichloroacetic Acid) precipitation to stop enzyme activity and remove undigested polypeptides. 1g BSA was digested alone (Control Digestion) and in the presence of varying concentrations of SBTI. Control digestion is represented as as (■) and digestion with SBTI at 125mg as (▲), 250mg (▼) and 500mg (●). All samples were tested in triplicate, errors are shown as standard deviation.

Four alginates were tested for their effects on protein digestion in the small-intestinal phase of the model gut system (Figure 158-Figure 161). While there were variations in levels of protein digestion with the addition of alginate, none of these deviations from the relative control time-point could be shown to be statistically significant.
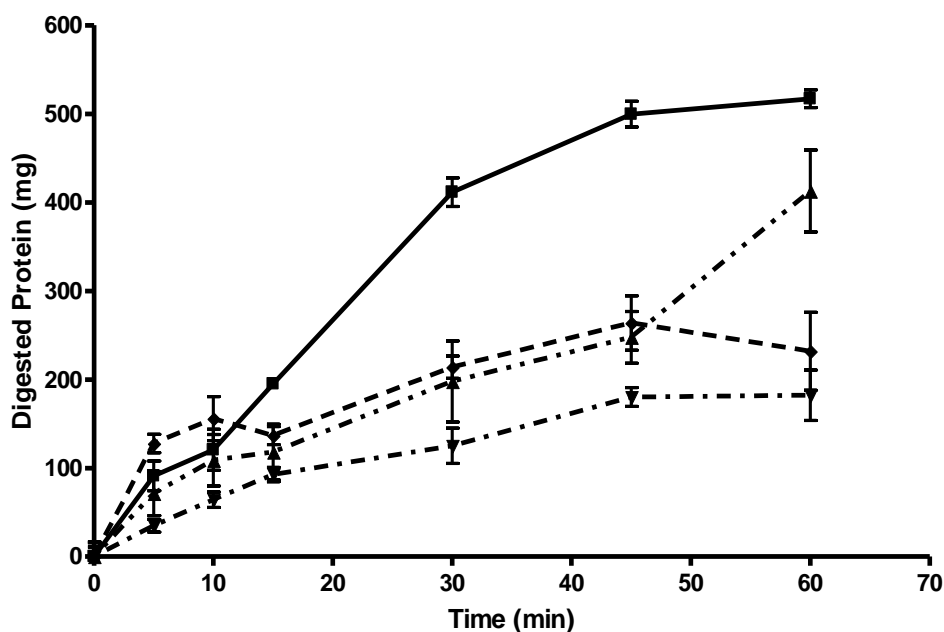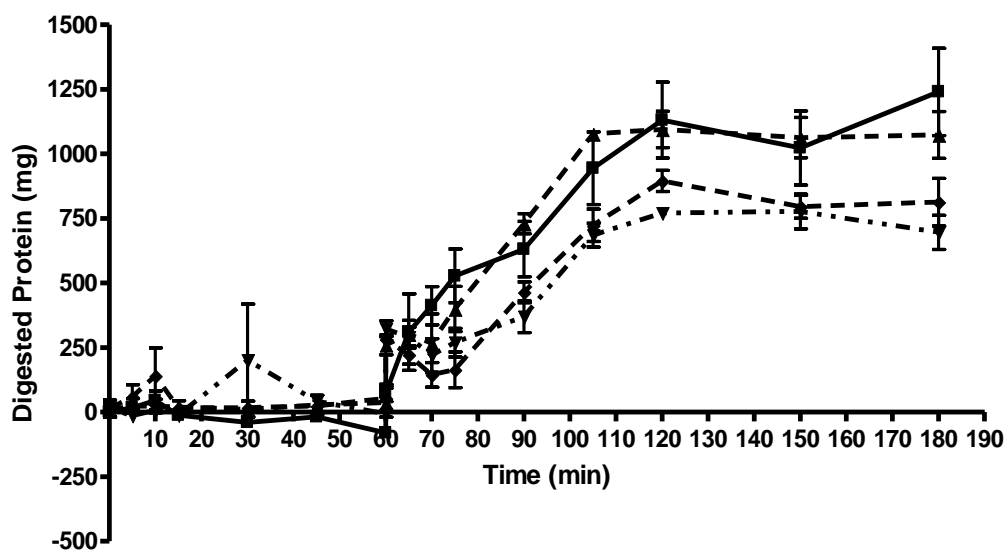
Figure 158 – Bovine serum albumin (BSA) digestion in the small-intestinal phase of a model gut system with and without FMC3 Alginate. The graph shows total protein recovered from model gut system after TCA (Trichloroacetic Acid) precipitation to stop enzyme activity and remove undigested polypeptides. 1gBSA was digested alone (Control Digestion) and in the presence of varying concentrations of FMC3. Control digestion is represented as (■) and digestion with FMC3 at 125mg as (▲), 250mg (▼) and 500mg (●). All samples were tested in triplicate, errors are shown as standard deviation.
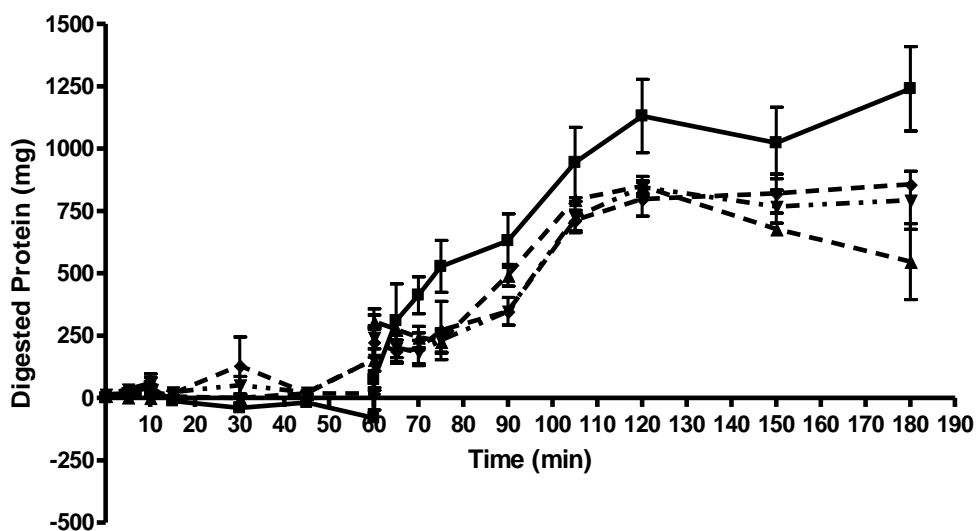
Figure 159 – Bovine serum albumin (BSA) digestion in the small-intestinal phase of a model gut system with and without FMC13 Alginate. The graph shows total protein recovered from model gut system after TCA (Trichloroacetic Acid) precipitation to stop enzyme activity and remove undigested polypeptides. 1gBSA was digested alone (Control Digestion) and in the presence of varying concentrations of FMC13. Control digestion is represented as (■) and digestion with FMC13 at 125mg as (▲), 250mg (▼) and 500mg (●). All samples were tested in triplicate, errors are shown as standard deviation.
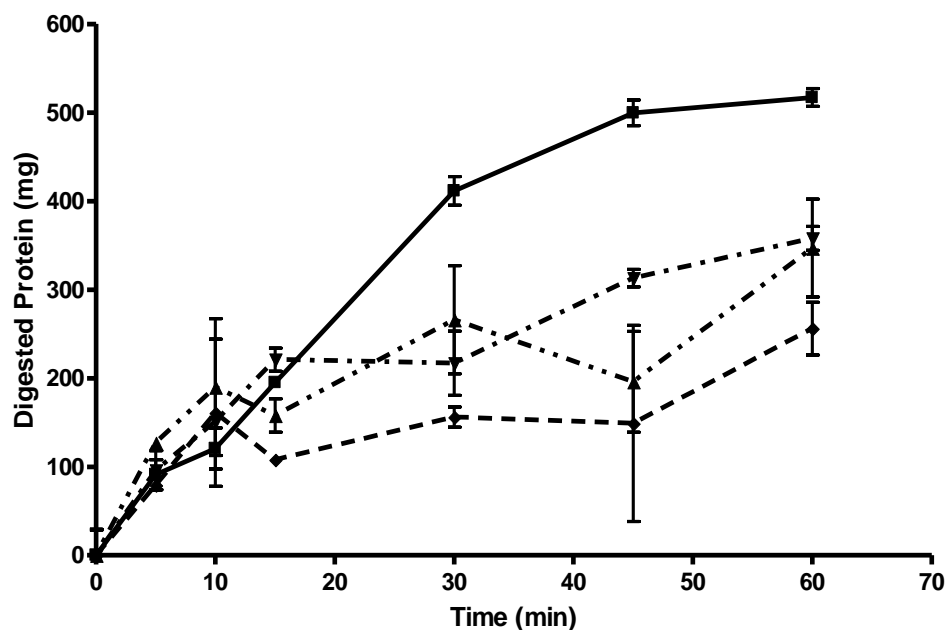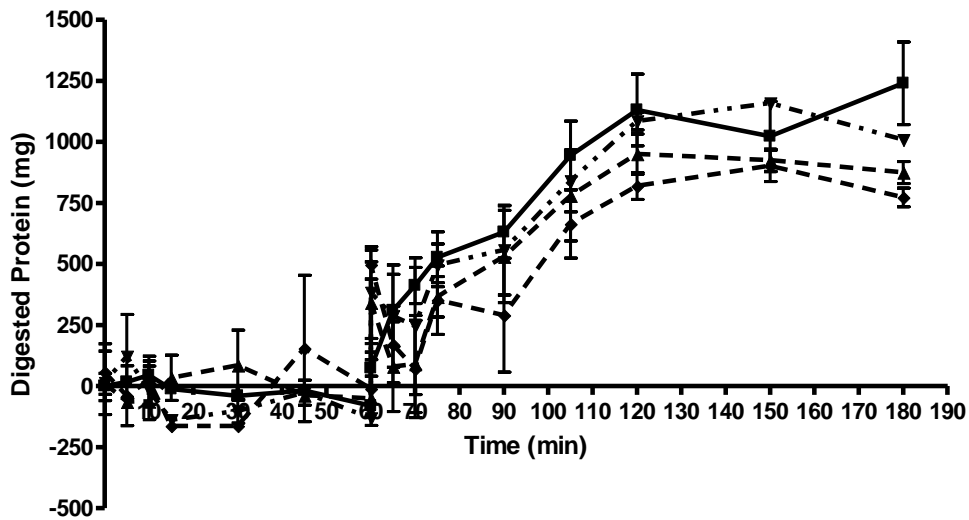
Figure 160 – Bovine serum albumin (BSA) digestion in the small-intestinal phase of a model gut system with and without SF120 Alginate. The graph shows total protein recovered from model gut system after TCA (Trichloroacetic Acid) precipitation to stop enzyme activity and remove undigested polypeptides. 1gBSA was digested alone (Control Digestion) and in the presence of varying concentrations of SF120. Control digestion is represented as (■) and digestion with SF120 at 125mg as (▲), 250mg (▼) and 500mg (●). All samples were tested in triplicate, errors are shown as standard deviation.
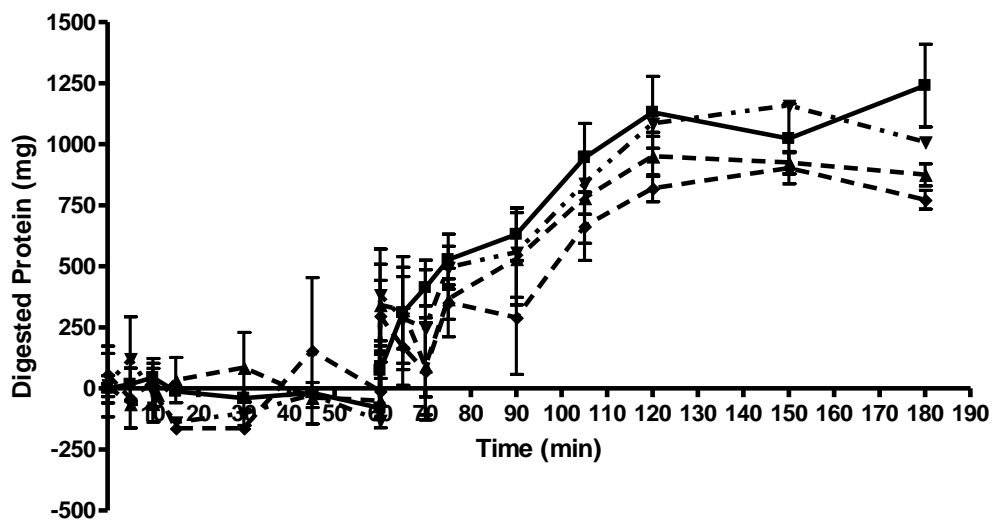
Figure 161– Bovine serum albumin (BSA) digestion in the small-intestinal phase of a model gut system with and without H120L Alginate. The graph shows total protein recovered from model gut system after TCA (Trichloroacetic Acid) precipitation to stop enzyme activity and remove undigested polypeptides. 1gBSA was digested alone (Control Digestion) and in the presence of varying concentrations of H120L. Control digestion is represented as (■) and digestion with SF120 at 125mg as (▲), 250mg (▼) and 500mg (●). All samples were tested in triplicate, errors are shown as standard deviation.

6.5 Discussion

A novel model gut system has been designed to simulate the conditions of macronutrient digestion *in vitro.* The digestion and absorption of macronutrients can be assayed in a simple, controlled and reproducible system. The inhibition of fat and protein digestion by alginate has been demonstrated in a physiologically relevant model. Using the synthetic gut model described, the effects of further dietary fibres and bioactive compounds on the digestion of macronutrients can be tested. This data can be used to inform further studies looking at using bioactive compounds as modulators of macronutrient digestion and uptake in the human diet, with potential applications for health and disease.

The conditions of the synthetic digestive tract were based on conditions reported in the literature and was a continuation of previous development of the model gut system by Dr Mathew Wilcox, Dr Iain Brownlee and Professor Jeffrey Pearson. The purpose of the simulated gastrointestinal digestion was to investigate the effects reported in Chapter 3-Chapter 5, and to investigate if these effects could be replicated in a physiologically relevant system. Some of the regulatory effects were consistent between the microplate assays and the synthetic gastrointestinal environment however there were instances where the effects of the exogenous regulators differed in the model gut system.

As reported by Dr Matthew Wilcox, specific alginates have been shown to inhibit the action of pancreatic lipase *in vitro*. The inhibitory effect has been shown to be linked to alginate structure, with guluronic-acid rich alginates tending to inhibit more strongly.

Glyceryl Trioctanoate was used as a substrate for fat digestion, and release of free glycerol from the triglyceride molecule was used as a marker of digestion. The assay system was validated using Orlistat as a positive inhibition control which showed potent dose dependent inhibition. Five alginate samples in total were tested in the model gut system.

Alginate samples FMC3 and FMC13 had no significant effect on the digestion of glyceryl trioctanoate at any of the tested time points. FMC13 is a mannuronic-acid rich alginate, therefore low in G-residues (F[G]=0.34), and therefore would not be expected to be a potent inhibitor of fat digestion based on the reports that G-rich alginates make the most potent inhibitors. FMC3 alginate on the other hand is a guluronic acid rich alginate (F[G]=0.68) and would be predicted to be a strong inhibitor of fat digestion.

Alginate LFR560, a guluronic acid rich alginate performed as predicted (F[G]=0.633), with a strong dose dependent dependent inhibition of gyceryl trioctanoate digestion.

Alginates SF120 and H120L showed an inhibitory effect on fat digestion, however the effect was not as potent, the inhibition profiles were markedly different and no dose dependent effects were seen. Over the first hour of small-intestinal digestion there was no significant change to the digestion profile of glyceryl trioctanoate in the presence of alginate H120L or SF120. However during the second hour of small intestinal digestion, significant reductions in glycerol release were seen as compared to control. This culminated in net reductions in fat digestion from 33-58% with alginate H120L depending upon dose and 38-52% for alginate SF120. Again this data was inconsistent with previous observations that G-rich alginates are more potent inhibitors of fat digestion, as SF120 is a g-rich alginate (F[G]=0.664), and H120L is an M-Rich alginate (F[G]=0.45), yet they showed very similar inhibition profiles.

There are a number of potential explanations for the unexpected and varied results seen with alginates in the artificial gut system. The lipase assays conducted by Wilcox *et al* which showed the potential of alginate to inhibit lipase were undertaken in highly controlled, 'simple' single enzyme conditions, so that a distinct effect can be seen, and causally related to the test sample. The Simulated model gut system however aims to pertain to physiological gastro-intestinal conditions and as such is a much more complex environment containing a diverse range of chemicals, enzymes and other digestive secretions. Whole porcine bile, and porcine pancreatin were used in the model gut system. Bile contains a complex mix of bile salts, cholesterol, billirubin, lecithin and mucus and porcine pancreatin contains the full range of enzymes found in the small intestine. Alginate has been shown to interact with bile acids and other digestive enzymes [57]. It is therefore possible that these interactions affect or disrupt the ability of alginate to inhibit lipase, although the mechanism of alginate inhibition of lipase remain unknown.

Furthermore, the microplate assays conducted by Wilcox *et al* were conducted in a pH-buffered environment of pH7.3. However during the Gastric phase of the model gut system, the pH is highly acidic, as the simulation passes into the small intestinal phase, the pH is raised by the addition of porcine bile, and the addition of pancreatic secretions rich in bicarbonate causeing a gradual neutralisation and raising of the pH. As discussed in the introduction, alginate forms an acid-gel at an acidic pH during which the alginate

molecules form strong interchain reactions. This gelling may provide an explanation in the case of SF120 and H120L why the alginate has no effect on fat digestion during the initial hour of small-intestinal digestion, but causes significant inhibition over the second hour. It may be that over the course of the small intestinal phase as the pH is raised by the addition of pancreatic secretion, the gelling effect is lost, and alginate becomes free and available to interact with pancreatic lipase in order to inhibit it.

That LFR560 does not show this same 'lag' in inhibition may be explained by the fact that it has a considerably lower molecular weight of 34700 as compared to 195000 for SF120 and 397000 for H120L and therefore would not form a strongly interlinked gel.

A further difference between the *in vitro* microplate assays and the model gut system is the motion of the model gut system which is stirred at a frequency of 0.05Hz to simulate the motion of the digestive tract. Although this stirring does not accurately model the physiological shearing, mixing and churning caused by gastric motility and peristaltic motion, it recognises that digestion does not occur in a static environment. This motion is therefore a further change from the microplate assays, and the introduction of physical forces may have effects on the way alginate is able to form interactions with lipase and fat substrates.

A range of triglyceride substrates have been tested in the model gut system, with varying lengths of fatty acid chains (data not included). However in this study, only Glyceryl Trioctanoate was investigated in relation to alginate activity due to time constraints. In the original work on alginate inhibition of pancreatic lipase, two types of assays were carried out; one with Olive Oil as the substrate, containing a varied mix of triglycerides, and one with DGGR (1,2 Di-o-laulryl-rac-glycero-3-(glutaric acid 6-methyl resorufin ester)) a synthetic substrate.

Alginate showed potent inhibition of fat digestion in both of these assays, however it is possible that the inhibition of pancreatic lipase is substrate specific, and favours the inhibition of particular triglycerides and that there is a relationship between fatty acid chain length and degree of inhibition. The way in which alginate interacts with triglycerides of different fatty acid chain lengths is being investigated elsewhere.

Alginate is not the only biopolymer that has been shown to inhibit the activity of pancreatic lipase. Wilcox, 2010 also showed that pectin, carrageenan and cellulose were also cpable of inhibiting fat digestion by lipase *in vitro*.

Pectins were capable of inhibiting lipase activity by up to 24.7±6.3%, inhibition of lipase by pectin was shown to be related to levels of esterification [5]. This is supported in the literature by the findings of Isaksson *et al* 1982, and Kumar *et al* 2010, who also showed inhibition of lipase by pectin to be linked to lower levels of esterification [229, 282] . Kumar *et al* argue that the carboxyl groups of pectin interact with the active site residues of the lipase enzyme, protonating them and disrupting the catalytic mechanism. This explains why increasing levels of esterification reduces inhibition, as the number of carboxyl groups is decreased. It was argued by Wilcox 2010, that a similar mechanism may be the cause of alginate inhibition of lipase, as alginates are similarly rich in carboxyl groups [5]. No data is available for pectin inhibition of lipase in a model gut system, but in a separate study, Isaksson et al, 1983 showed that the inclusion of 5% pectin in the diet of rats increased, fat content in ileostomy effluent samples, suggesting a decrease in fat digestion [283]. Chitan and chitosan, both cationic polymers have been shown to inhibit lipase activity [284, 285]. However, other polymers including carrageenan have been shown to activate lipase activity.

Pectin, cellulose and carrageenans have not been tested in the model gut system, but data from *in vitro* assays [5], animal studies [283] and unpublished human data suggests that alginates and other biopolymers have potential to reduce fat digestion and uptake, and may have the potential to be used as a treatment for obesity. `

An assay for carbohydrate digestion was developed and validated using Acarbose as the positive inhibition control. Corn Starch was used in the assays described herein in the native form, but the assay has also been validated with potato starch and wheat starch both in the native and gelatinised form [data not included].

As was commented upon in the results section, 1g of native corn starch was used as the carbohydrate substrate, but in the control digestion, only approximately 25% of this is recovered. This may be down to under-reporting of the digestion of carbohydrate in the assay system. As described in the methodology, after sampling and removal of undigested starch, the digestion products which would consist of mono-,di- and short oligo- saccharide chains were exhaustively digested down to monosaccharides using α-glucosidase. However a major digestion product of starch digestion is α-limit dextrim, breakdown of which requires the brush border isomaltse to cleave the α(1-6) bonds of α-limit dextrin [286]. As synthetic pancreatin does not contain brush-border isomaltase,

it is possible that these breakdown products are not fully broken down to mono-saccharides. Secondly, it is possible that during the methanol KCl precipitation to remove undigested starch, that some digestion products, particularly the larger oligo-saccharides are also pulled out of solution.

However, it is possible that not all of the starch is broken down in the assay system. As discussed by Zhang *et al* 2006, starch is classified into rapidly digestible starch, slowly digestible starch, and resistant starch, depending upon how quickly glucose is released. Starch consists of highly ordered and structured molecules, which in the native crystaline form which reduces their solubility and ability to interact with other molecules [287]. Digestion of starch generally requires disruption of the crystalline structure of starch granules which normally occurs through food processing and cooking. Having said this, starch macromolecules – as a source for plant energy storage – must be accessible to metabolic enzymes. Hydrolysis of native starch is accepted as a two-phase system; first the rapidly digested non-granular starch, and then the slowly digested crystalline granules. Native starch generally contains between 15-45% crystalline material, so only between 55-85% of starch would be readily accessible for α-amylase hydrolysis [287]. It may therefore be that the initial spike in starch digestion seen at the beginning of the small-intestinal phase is the non-crystalline rapidly digestable starch being hydrolysed, after which the granular native starch is either resistant to digestion, or very slowly digested.

Microplate screening and kinetic assays had shown alginate to be capable of increasing the activity of α-amylase *in vitro* and that alginates high in mannuronic acid tended to be better activators.

Four alginates were tested for their effects on Corn Starch digestion in the model gut system; FMC3, FMC13, SF120 and H120L. Although visibly altering the digestion kinetics of corn starch digestion, there were no significant changes caused be SF120 or H120L. FMC3 and FMC13 on the other hand both showed similar regulatory profiles, with an initial inhibition of Corn starch digestion for the first 15 minutes of the small intestinal phase, after which digestion recovered to normal control levels. At the lower concentrations of alginate of 125mg and 250mg, both FMC3 and FMC13 showed no significant changes from control, but at the highest concentration of 500mg with both of

these alginates there was an activatory effect, and by the final time-point the amount of glucose recovered had significantly increased.

This activatory affect suggests that the fact that only 25% of starch substrate was reported in the control digestion is due in part at least due to some of that substrate starch remaining resistant to digestion, and that with the addition of 500mg of FMC13 there is an interaction which renders the carbohydrate more accessible to digestion. With the addition of 500mg FMC13, by the final timepoint of the small intestinal face, approximately 60% of substrate starch has been efficiently released. Further investigations of this are required, to confirm conclusively that this is the cause of the reported levels of starch digestion being lower than expected.

The initial inhibition of carbohydrate digestion seen in the initial 15 minutes of the small intestinal phase is not consistent with the results described in Chapter 5 that alginates increase the activity of α-amylase *in vitro*. It is however consistent with the numerous reports in the literature that dietary fibres including alginates have anti-hyperglycaemic effect *in vivo* [288]. As discussed in Chapter 5, mechanisms for this hypoglaecaemic effect are thought to include delayed gastric emptying and inhibition of the sodium-glucose cotransporter. However, neither of these processes are modelled in the currently described model gut system.

In the microplate assays described in Chapter 5, potato starch is used as the substrate, whereas corn starch has been used in the gut modelling, therefore further investigations are required to see if there are differences in the way in which alginate effects the digestion of carbohydrates from different sources. The addition of alginate may reduce carbohydrate digestion via a viscosity effect, slowing down the pedisis of particles and reducing the accessibility of α-amylase to substrate, decreasing the chance of a successful enzyme-substrate reaction [140]. Furthermore the way in which alginate interacts with α-amylase and its carbohydrate substrates across the pH range requires further investigation.

The inhibitory effect seen with FMC3 and FMC13 did not continue beyond the first 15 minutes of the small intestinal phase, after which there were no significant differences to control activity at 125 and 250mg alginate. However, with 500mg of both FMC13 and FMC3 there was an increase in carbohydrate breakdown by the final time-point of T[180]. This suggests that there are multiple processes occurring, and that inhibitory effects prevail in the initial phase of small-intestinal, but are overcome and with

sufficient alginate activation effects are seen. As was discussed in Chapter 4, alginates have a pH dependent rheological behaviour, forming gels at low pH and viscous liquids at neutral pH, so as alginates pass from the gastric phase to the small intestinal phase, the change in pH will alters their structural characteristics, and therefore behaviour. Further investigations are reguired to investigate how alginate affects lipase activity across the pH range.

As discussed in Chapter 3 and Chapter 4, alginates had been shown to inhibit pepsin activity in *in vitro* microplate assays, but have no effect on trypsin. Protein digestion was investigated in the model gut system in order to investigate the effects of alginate in a physiologically relevant system. Gastric pepsin is the enzyme responsible for proteolytic digestion in the stomach, it was therefore expected that the results from Chapter 3 would be predictive of what occurs in the gastric phase of the simulation. Small intestinal protein digestion however is a more complex process mediated by multiple proteases secreted from the pancreas and activated in the proteolytic enzyme cascade; Trypsin, chymotrypsin, elastase, carboxypeptidases A and B. It was therefore important to investigate how alginate interacts with the complex multi-enzyme environment.

As described in section 6.4, the gastric and small-intestinal phases of digestion were examined separately, so that the site of any regulatory effects can be identified. Inhibition in the gastric phase was validated with pentosan polysulphate as a positive inhibition control, and Soybean Trypsin Inhibitor was used as a positive inhibition control for small intestinal proteolytic digestion.

Four alginates were tested in the gastric phase of the model gut system. As predicted from the microplate assays in Chapter 3, all four of these alginates (FMC3, FMC13, H120L and SF120) caused significant inhibition of pepsin mediated gastric protein digestion, with the High-M alginate inhibiting to a significantly greater extent than the High-G alginates. While there was variation in small intestinal phase protein digestion, none of the alginates tested caused any statistically significant changes.

These results support the findings discussed in Chapter 5 that there is a pH-dependent interaction between alginate and protein substrate which affects proteolytic digestion at acidic pH, but has no effect on proteolytic digestion in the neutral environment of the small intestine.

Further investigations would be required into the effect that alginate has on the other proteolytic enzymes of the small intestine, as it may be that alginate is affecting the rate of chymotrypsin, elastase or carboxypeptidase, but that the redundant capacity of the small intestinal proteases mean that the addition of alginate has no affect on net proteolytic digestion.

The observation of alginate-inhibition of protein digestion occurs in the gastric phase is consistent with reports in the literature of pH dependent interactions between proteins and carbohydrates [56, 191-193]. The data reported herein supports the theory that carbohydrates, and alginates specifically display general protein binding behaviour. This adds weight to the theory that inhibitor-substrate interactions between alginate and protein are formed as the pH is lowered taking the protein below it's iso-electric point and allowing electrostatic charges to form, leading to protein-alginate gellation. Furhermore this theory provides an explanation for the fact that protein digestion is inhibited in the gastric phase, as substrate is bound by alginate, but not in the small intestinal phase here these interactions do not form at a near neutral pH.

Chapter 7

General Discussion

7.1 Background & aims

The current investigation into the effects of alginate and other bioactive compound was based on the work of Wilcox *et al* 2010 which showed that specific alginates can inhibit pancreatic lipase by up to 70% depending upon their structure [5]. Alginate is now being investigated as a potential anti-obesity agent in human weight loss trials.

As the digestion and absorption of the major macronutrients fat, protein and carbohydrate is a central factor in health and metabolic diseases, using exogenous compounds such as alginate to modulate the activity of the major digestive enzymes present a paradigm for treatment of nutrition related disorders.

This project therefore aimed to develop methodologies which could be used to investigate alginate and other bioactive compounds as regulators of digestive enzymes. To this end, a 3-step process was developed to test the action of biopolymers on the major enzymes of macronutrient digestion, pepsin, trypsin, α-amylase and lipase:

i. High Throughput Analysis

ii. Model Gut Analysis

iii. Selected Kinetic Analysis
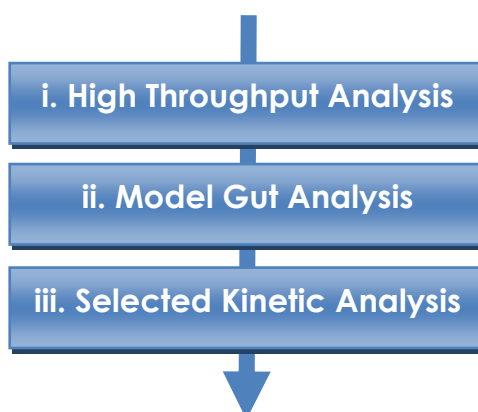
7.2 Discussion

Alginates have been shown to have the ability to modify the activity of multiple digestive enzymes *in vitro* and affect the digestion profile of major macronutrients in a physiologically relevant model gut system. Some of these functional effects have been shown to be linked to structural characteristics of alginates [5, 281, 289, 290].

Through the use of an N-terminal Proteolysis assay it was possible to determine that alginate was a potent inhibitor of pepsin activity, but had no significant effect on trypsin.

The strongest inhibition of pepsin observed was with alginate H120L which reduced pepsin activity to 53.9% ($\pm$9.53SD) of normal activity. It was shown that the potency of inhibition correlated with alginate structure, a strong positive correlation between alginate F[M] and levels of pepsin inhibition, supporting the findings of Strugala *et al* 2005[7]. Furthermore an increasing proportion of contiguous G-Blocks was shown to be negatively associated with inhibition of pepsin, with [n(g>1)], F[GG] and F[GGG] all negatively correlating with pepsin inhibition. The composition of alginates as large negatively charged polymeric molecules able to form gels and intramolecular interactions, can result in inhibition flexibility. Alginates have been shown to be capable of binding to both enzyme and substrate.

A small number of the catalogue of tested alginate samples were observed to have a statistically significant effect on trypsin, the largest of these effects was only approximately a 10% inhibition by FMC5. However generally alginate had no statistically significant effects on trypsin activity and those that were observed were negligible and not supported by the selected kinetic analysis.

Protein digestion was investigated in the physiologically relevant model gut system, and the results shown were consistent with what was predicted from the single enzyme microplate investigations. Protein digestion was inhibited in the gastric phase of digestion by up to 46.1%, however no significant changes to proteolytic digestion were observed in the simulated small intestinal phase, as would be expected as they do not inhibit trypsin. However this data also suggests that alginates do not have any effect on the activity on the other proteolytic digestive enzymes of the small intestine. The reasons for this will be discussed later.

Due to the distinctly different inhibition profiles for pepsin and trypsin, the manner in which alginates and protein substrates interact across the pH range was investigated rheologically. Profound rheological ineractions were observed at acidic pHs, but no pattern of rheological interaction was observed at neutral pH; with all alginate samples tested, a protein-alginate co-precipitate was formed at acidic pH, but not at a neutral pH.

Protein-carbohydrate interactions are common in biology, and widely reported *in vitro* [56]. SP54, heparin sulphate, and other highly sulphated polysaccharides are known to inhibit pepsin activity [179, 180]. Non-specific protein binding has also been observed with polysaccharides, raising the possibility of inhibitor-substrate interactions being involved in pepsin inhibition. Protein-carbohydrate interactions occur at low pH. As the pH is lowered and protein is taken below its iso-electric point, negative charges are lost and the protein becomes positively charged. Positively charged protein then form interactions with negative charges on the carbohydrate and carbohydrate-protein complexes form, leading to gelation [196].

Alginate is a negatively charged polymer, capable of forming such electrostatic interactions with positively charged proteins at low pH [197]. Alginate may associate with protein through hydrogen bonding at hydroxyl groups; charge-charge interactions with δ- carboxyl groups, and the negatively charged COO- group of the alginate, although this group would become protonated at low pH. The pH sensitivity of the synergism between alginate and proteins suggests that these electrostatic interactions are important in inhibition and that ionisation plays a key role.

This theory also provides a clue as to why high-M alginates tend to be better inhibitors of pepsin activity than high-G alginates. High-G alginates form stiff rigid gels at low pH and strongly bind divalent cations, forming strong interchain associations. High-M alginates on the other hand form much weaker gels, with more flexible alginate chains. Cations would compete for COO- groups on the alginate chain, meaning less COO- groups will be free to interact with a protein substrate. Furthermore alginate gels with stronger interchain associations, will be freer to interact with protein substrate. The chain flexibility of High-M alginates will also allow the polymer chain to be more supple and therefore be more capable of mirroring the structure of the protein molecules and forming interactions.

The binding to protein and formation of a precipitate with alginate would remove protein substrate from solution and make the protein substrate unavailable to pepsin, thereby inhibiting pepsin activity. While at neutral pH the protein substrate remains available for proteolysis. This explains why no inhibition of trypsin activity was observed. Furthermore this supports the model gut data described in Chapter 6 whereby inhibition of proteolysis by alginate was reported in the gastric phase of digestion, but not in the small intestinal phase.

Trypsin is not the only enzyme present in the small intestine responsible for proteolytic digestion (Table 3), yet no significant change in protein digestion in the small intestinal phase of the model gut was observed. This suggests that alginate has no effect on the cumulative activity of trypsin, chymotrypsin, elastase and the carboxypeptidases. It also confirms the theory that at the pH levels seen in the small intestinal phase, there are no protein-alginate interactions that make substrate unavailable for enzymatic digestion.

A number of other biopolymers were tested for regulatory activity towards the proteolytic enzymes [Data not included]. Some were shown to be potent inhibitors of pepsin activity in the order Fucoidan>Carrageenan>Alginate. Alginates higher in mannuronic acid residues tended to be stronger inhibitors, and with fucoidan and carrageenan a relationship was observed whereby a high degree of sulphation was associated with potent inhibition of pepsin activity.

Sulphated polysaccharides have previously been shown to inhibit pepsin as was discussed with SP54 and heparin. Furthermore, anti-peptic effects have been observed *in vivo, with heparin* reducing peptic ulceration in rats and guinea-pigs [179, 185, 186]. Th mechanism of sulphated polysaccharide inhibition of pepsin is also due to electrostatic interactions forming between molecules, but in this case between the sulphate groups of the carrageenan and positively charged regions of the protein [194, 195]. The interactions between substrate and biopolymer were again shown to be pH sensitive, as neither carrageenan or fucoidan significantly affected trypsin activity. This further supports the argument that at low pH, interactions occur between positively charged protein molecules and negative charges on carbohydrate polymers.

Sunderland *et al* 2000 reported a direct interaction between alginate and pepsin whereby pepsin was pulled out of solution by alginate during centrifugation. This suggested direct binding of pepsin as a possible mechanism of inhibition [57]. However, a more general protein binding interaction has been described herein. This does not however rule out a direct interaction between alginate and pepsin, and it may be that both alginate binding of substrate and enzyme occur in concert to inhibit proteolysis.

Alginates rich in hydroxyl and carboxyl groups capable of forming hydrogen bonding and charge:charge interactions with pepsin active site residues in a similar mechanism to pepstatin inhibition. Pepstatin inhibits pepsin activity by strongly binding and blocking access to the active site. By forming electrostatic interactions alginate may similarly block substrate binding.

Furthermore, these interactions with active site residues may act to disrupt the catalytic mechanism. Carboxyl groups have been shown to be important in enzyme inhibition, as in the case of pectin and lipase, and similarly it is possible that similar interactions may form with the active site Asp32 residue of pepsin, disrupting the acid-base pair of Asp32-Asp215, and preventing nucleophillic attack on the scissile peptide bond. Even if direct interactions are not formed, the presence of large negative charges in proximity of the active site may be sufficient to disrupt the charge relay mechanism or prevent regeneration of the catalytic nucleophile.

It is unlikely that these same interactions would occur with trypsin at a near neutral pH as the carboxyl groups of alginate would not be protonated, and would therefore be unable to act as proton donors. Furthermore substrate binding by trypsin is highly specific and has a strong preference for cleavage sites, it is therefore unlikely that an alginate molecule could form a stable interaction and mimic substrate binding in the same way that soyabean trypsin inhibitor does. Furthermore the active site of trypsin is enclosed within the centre of the two domains of the globular trypsin protein and has a negatively charged substrate binding pocket, as alginates are large negatively charged polymers, they would be repelled from the trypsin substrate binding site due to charge:charge repulsion and moreover have poor accessibility to the active site binding pocket due to size [291].

As discussed in the Aims & Approaches section in Chapter 2, the ability to modulate protein digestion and absorption by eliciting an increase or decrease in pepsin activity has potential therapuetic benefits. However what has been reported in the current study is that alginates, fucoidan and sulphated carrageenans have the ability to inhibit gastric proteolysis, but have no effect on small-intestinal protein digestion.

Gastric emptying depends upon the breakdown of the food matrix by pepsin hydrolysis, inhibition of pepsin activity by alginates will impair this breakdown. Delayed gastric emptying has been reported with the administration of Proton Pump Inhibitors, a reduction in proteolytic activity slows the gastric breakdown of food, which is thought to have implication for GORD as well as human nutrition [292]. PPIs are administered in order suppress gastric secretion and reduce acidity of refluxate, however the reduced acidity decreases pepsin activity and slows the process of gastric proteolysis.

It has previously been asserted that protein malabsorption due to gastric acid suppression is probably negligible, this assertion is based on the fact that total protein

digestion has been shown to be largely unaffected by total gastrectomy or pernicious anemia [293]. However in a separate study of 16 healthy subjects, it was shown that gastric acid suppression with the PPI Omeprazole delayed and reduced protein assimilation. Protein digestion was measured using ^{14}C-octanoic acid/^{13}C-egg white breath test. Evenepoel et al 1998, suggest that impaired gastric digestion means substrates passing into the small intestine are less accessible to small-intestinal hydrolytic enzymes. Furthermore an increase in phenol and p-cresol production by fermentation of unabsorbed protein by the colonic microflora is indicative of protein malabsorption [294].

While this observation was not supported by the observations seen in the model gut system in Chapter 6 that small intestinal proteolysis was unaffected by addition of alginate or fucoidan, it must be remembered that the model gut simulation is an incomplete model of the physiological complexity of digestion. Firstly the model does not attempt to and is not capable of simulating the processes that mediate gastric emptying *in vivo*; the model therefore does not have the capacity to mimic how a resilient food matrix in the gastric phase of digestion would delay food delivery into the simulated small intestinal phase. Furthermore, small intestinal proteolytic digestion was examined independently of gastric protein digestion by the complete omission of gastric pepsin. Therefore, in the small intestinal analysis of protein digestion, neither sample nor control had been exposed to gastric pepsin hydrolysis. This means that the model does not account for a more intact test meal reaching the small intestinal phase of the simulation. Therefore *in vivo* alginate and fucoidan may have an anti-proteolytic effect in the small intestinal phase through both delayed gastric emptying and protection of protein substrate in the food matrix after passage into the small intestine. In order to investigate these hypotheses, *in vivo* studies would be required.

Accelerated gastric emptying has been implicated in a particular subset of patients with functional dyspepsia, and the retardation of gastric emptying may be of clinical value to them [295]. Furthermore, if alginate and fucoidan can be used to affect the rate of food delivery to the small intestine through delayed gastric emptying, and retard the degradation of the food matrix they have potential to slow the rate of nutrient release and uptake, which has implications beyond just protein digestion.

It has been shown that the initial rise in post-prandial blood glucose is directly related to the rate of gastric emptying and that rapid gastric emptying can be an excaserbating

factor in diabetes [296]. PPI administration has been shown to improve glycaemic control, although the exact mechanism remains unclear [297].

Furthermore delayed gastric emptying has been associated with increased sensation of fullness and satiety following a meal, which may have implications for decreasing calorific intake and energy yield of a meal [298].

Carbohydrate digestion was also affected by the presence of alginate in the reaction mixture. In the microplate assays of α-amylase activity, addition of alginate increased α-amylase by a maximum of 41.1±8.42%. In the microplate high-throughput assays, no statistically significant relationship was shown between any of the structural characteristics of alginate and levels of activation. However from the kinetic testing, significant positive correlations were shown between maximum velocity of reaction and frequency of mannuronic acid residues of alginate.

Alginates chelate divalent cations such as calcium, and it is possible that alginate present Ca++ to the α-amylase enzyme, or interaction with the α-amylase enzyme through this calcium binding site and stabilise calcium binding [255].

As was seen with protein and alginate, it is possible that alginate-substrate interactions play a role in this regulatory effect. Interactions between alginate and starch have been previously reported; Richardson *et al* showed that alginate can interact with starch so as to disrupt gellation [256]. Furthermore it was shown in the current experiments that the addition of corn, wheat and potato starch to an H120L alginate solution greatly reduced alginate viscosity. It may be therefore that a mechanism by which alginate increases the activity of α-amylase is by disrupting the gel network of starch, increasing the surface area of starch substrate that is available for α-amylase to act upon.

These reports of α-amylase activation go against what has widely been reported in the literature stating that dietary fibres have protective affects against diabetes [44]. However, these reports of activation were in a pH controlled single-enzyme environment, and as can be seen from the model gut system, this activation was not wholly replicated in a physiological simulation. In the first 15 minutes of the small-intestinal phase of the model gut simulation there was a short-lived inhibition, after which carbohydrate digestion returned to control levels. With two of the alginates

tested, there was an increase in carbohydrate digestion by the final time-point at the highest tested dose of alginate, but not at lower doses.

The data for the model gut simulations is more consistent with data that has been presented in the literature, suggesting that dietary fibres including alginate have anti hyperglycaemic effects *in vivo.* Epidemioplogical studies have shown high long term intake of dietary fibre is associated with decreased risk of diabetes [44], and specific anti-hyperglycaemic effects have been shown with certain dietary fibres. Anti-diabetic and anti-hyperglycaemic effects have widely been reported *in vivo*. Guar gum, partially hydrolysed guar gum and alginate have been shown to reduce post-prandial hyperglycaemia if diabetic rats and have a significant hypoglycaemic effect in humans [139, 252].

Suggested mechanisms for these anti-diabetic and anti-hyperglycaemic effects include; delayed gastric emptying, stabilisation of the food matrix, viscosity effects and inhibition of sodium-glucose cotransporter. Gastric emptying presents a rate limiting step on carbohydrates being delivered to the small intestine for breakdown and subsequent uptake. Stabilisation of the food matrix is thought to both delay gastric emptying, and retard the action of enzymatic hydrolysis after transit to the small intestine. Fibre viscosity is thought to affect carbohydrate digestion both through a delaying effect on gastrointestinal transit time, and by viscous fibre reducing the accessibility of carbohydrolytic enzymes to the substrate, and also by reducing the rate of glucose diffusion through the lumen for uptake [140]. Kimura *et al* 1996, advance a theory for a specific mechanism by which alginate exerts its hypoglycaemic effect by inhibiting the sodium glucose transporter [252].

Breakdown of starch into maltose, maltotriose and α-limit dextrin is thought to occur very rapidly and within 10 minutes of transit into the duodenum; because duodenal digestion of carbohydrate is so rapid, an increase in amylolytic activty will have a marginal effect on the speed of carbohydrate digestion and other factors such as gastric emptying will be the rate limiting step [258]. As carbohydrate digestion predominantly occurs in the duodenum, the rate at which carbohydrates are delivered to the duodenum will therefore be the determining factor in the rate of carbohydrate digestion. Torsdottir *et al* 1991 showed that gastric emptying was significantly delayed by alginate supplementation This is likely to be the determining factor which resulted in the anti

hyper-glycaemic effect, as reduced blood glucose rise correlated with slowed gastric emptying [257].

Alginate has been shown to inhibit sodium absorption in the small intestine and increase Na+ excretion during digestion [252, 259]. Sodium is essential for intestinal absorption of glucose, as glucose uptake occurs through the sodium glucose co-transporter and reduced glucose uptake and the hypoglycaemic effect of alginates may be due to in part to alginate making sodium unavailable to the NaGluc Cotransporter [260]. It was suggested by Kimura *et al* 1996, suggest that the net hypoglycaemic effect of alginate may be due to a combination of alginate gelling in the stomach, delaying gastric emptying, and reduced sodium uptake in the small intestine inhibiting the action of the sodium-glucose co-transporter [252]. Furthermore increased viscosity of the gut lumen contents caused by alginate may reduce the accessibility of amylase to it's substrate, and reduces the rate of glucose diffusion through the lumen for uptake [140].

The gastrointestinal tract is a complex environment with these multiple, physical, physiological and chemical processes working in transit, and it is therefore likely that while alginate has an activatory effect on α-amylase activity in isolation, in the complex environment of the GI tract, this activation is overcome by the cumulative inhibitory effects described above. These results further underline the need to look at the processes of digestion in their totality, and test effects in physically relevant situations and ultimately *in vivo.*

The way in which alginate and other bioactive compounds affect the digestion of fat has been studied by this research group at length previously. Alginates have shown the ability to inhibit the action of pancreatic lipase by up to 70% *in vitro*, this has been correlated to the structure, with alginates high in guluronic acid tending to be the more potent inhibitors [5, 299].

Alginate is now being investigated in human trials as a potential treatment for obesity. Using bread as a delivery vehicle, the effects of alginate on total fat digestion and post-prandial blood triglycerides has been investigated (unpublished data). A further investigation is due to be undertaken titled "Designing the most effective vehicle to deliver alginate to effectively reduce fat digestion and absorption".

In Chapter 6 of this current study an assay is described to investigate the digestion of triglycerides in the simulated model gut system. Data reported in the current study is for how alginate affects the digestion of a single triglyceride (glycerol trioctanoate), and only one of the alginates tested was shown to yield dose-responsive inhibition of alginate. However, other work undertaken in this lab using the methodology has investigated the was alginate effects the digestion of other triglyceride substrates, and a mixed-triglyceride substrate mixture.

While alginates have been previously shown to be potent inhibitors of pancreatic lipase *in vitro,* model gut analysis described herein was varied. Alginate samples FMC3 and FMC13 had no significant effect on the digestion of glyceryl trioctanoate. Alginates LFR560, SF120 and H120L all showed significant inhibition of glyceryl trioctanoate digestion. Only glyceryl trioctanosate was tested as a substrate for inhibition of fat digestion, therefore further investigations are necessary to investigate the specificity of alginate inhibition to different triglycerides.

It was argued by Wilcox, 2010, that alginate inhibits lipase activity according to a similar mechanism reported in pectin inhibition of lipase, whereby carboxyl groups of the polymer protonate key active site residues of the Lipase enzyme, disrupting catalytic activity [5] [229].

7.3   Future Scope

As stated previously, the aim of this project was to develop a 3-step methodology to investigate the effects of exogenous compounds on the digestion of the major macronutrients. These assays were developed and used to analyse the bioactive properties of alginate, fucoidan, pectin and carrageenan. These assays have demonstrated wider utility in a number of collaborations including the analysis of the bioactive properties of seaweed and seaweed extracts and the investigation of pepsin as an aggressor in GORD.

These assay systems and methodological approach provide a template for investigating the paradigm of exogenous compounds as inhibitors of digestive enzyme activity and the development of novel therapeutics and food additives targeting macronutrient digestion.

Furthermore the model gut system developed in this lab provides a physiologically relevant model of the digestive tract. The Royal Society of Edinburgh has recognised the value of this model to industry and awarded an Enterprise Fellowship to continue development of the model as a commercial venture.

Nutrition research has been identified as a key strategic priority by the BBSRC both in terms of food security and in understanding the role of diet and the mechanisms that underpin health and disease [8]. The MGS provides a controlled, reproducible and cost-effective method of investigating dietary therapeutic interventions in a physiologically relevant system. *In vitro* MGS are an ethical alternative to animal studies and therefore appeal to companies who wish to avoid the negative publicity of animal studies. MGS also provide robust physiologically relevant mixed model which can be used to inform and improve human studies.

The MGS provides a higher-throughput primary screening method by which compounds can be ruled in or out as effective therapeutic agents and a system of analysis for looking at bioactive effects. As with pharmacological studies, randomised, double blinded control trials in human populations are the gold standard of nutrition studies, however cost and complexity are often prohibitive [262]. Smaller scale human studies can also be costly and difficult. A small outlay in cost on preliminary MGS trials will provide companies and research groups with data that can be used to investigate efficacy, dosage, delivery methods and allow them to make decisions that will potentially save costs and improve results without using animal models.

294

Due to the cost, ethics and scale of *in vivo* studies a range of *in vitro* methods have been developed to model digestion. Single enzyme analysis can identify novel enzyme inhibitors, but is insufficient to draw conclusions about the effects *in vivo*. A number of model gut systems have been developed to study different aspects of digestion and GI physiology, however this is the only known model in which a continuous profile of fat, carbohydrate and protein digestion from mouth to small intestine can be gained. Other models that have been developed look at; bioavailability and bioaccessibility of contaminants [300], digestion of allergens [301] study of pre and probiotics [302], models of gut motility, peristaltic motion and physiological mixing and shearing [303], enzymatic digestion [303], substrate digestion and interaction [269], intestinal microbiota [304], water and nutrient absorption [276]and drug delivery [305].

Nutrition research is also of great interest to industry. In 2012 the global consumer health market was US$203 Billion, with $87 billion of the market being vitamin and dietary supplements, and $13billion in weight management products [306]. Furthermore, the 'Health and Wellness' food industry is worth a further US$628 billion with weight management food and beverages valued at US$144 billion globally [307, 308]. A key aim of industry is therefore to develop novel health foods and dietary interventions.

According to Euromoniter International, "Consumer health innovation is thriving, as manufacturers introduce creative new formulations, delivery formats and positioning". In a study of the Research and Development spending of 25 of the world's largest food companies with turnovers ranging from 11-256 $billion, 6 companies responded with R&D spends of; Unilever 2.6%, Cadbury Schweppes 0.9%, Kraft 1.2%, Nestlé 1.6%, Yum! 0.3% [309].

Furthermore the introduction of EFSA (European Food Standards Agency) requires a much higher threshold of scientific evidence for food health claims in the EU. This means that costly and financially risky human studies must be undertaken to support health claims. A key benefit of this methodological approach is therefore that it provides a robust and physiologically relevant *in vitro* approach for the identification and validation of potential bioactive samples, and can be used to provide data that can be used to improve and inform human studies.

In terms of progressing the current work, there are a number of areas requiring further investigation. It would be of interest to investigate the way in which each enzyme responds to the presence of biopolymer samples across the pH range at which each enzyme is active. It would also be useful to investigate inhibition and activation with smaller blocks of alginate of 10-20 residues. This would help to elucidate if the effects seen were due to large intermolecular interactions with substrate, or by specific interaction with the enzyme active sites or allosteric regulation.

As the data in **Error! Reference source not found.** showed, whole seaweeds and non-alginate extracts of seaweed were capable of regulating enzyme activity, it would therefore be of value to further investigate the purity of alginate samples to ensure there is no contamination with other molecules such as polyphenols.

It would also be of value to further investigate the mechanism of inhibition using Fourier Transform Infrared Spectroscopy (FTIR) and Quartz-Crystal Microbalance with Dissipation (QCM-D). These techniques would allow clear determination of which components of the reaction the bioactive is interacting with.

Chapter 8
Appendix

Alginate Structural Characteristics *Figure 162a-f   Structural characteristics of all alginate samples*
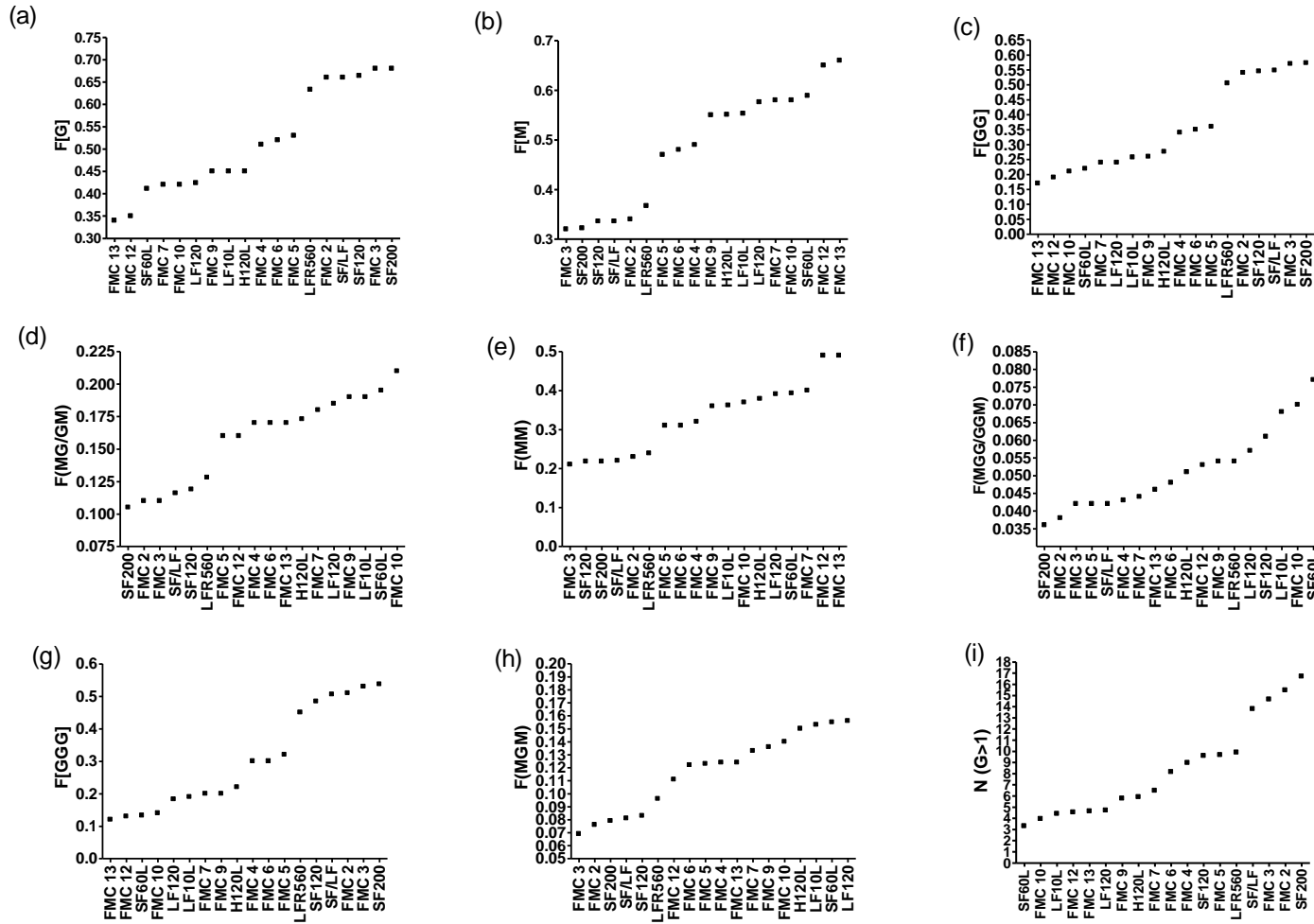
8.2   Models of Enzyme Inhibition

$E \; + \; S \; \leftrightarrow \; ES \; \rightarrow \; P \; + \; E$

$+$

I

$\updownarrow$

EI

Velocity

V_{max}

V_{max}

K_m

Substrate Concentration

$\dfrac{1}{v_0}$

$\dfrac{1}{V_{max}}$

$\dfrac{1}{V_{max}}$

$\dfrac{-1}{K_m}$

$\dfrac{1}{s}$
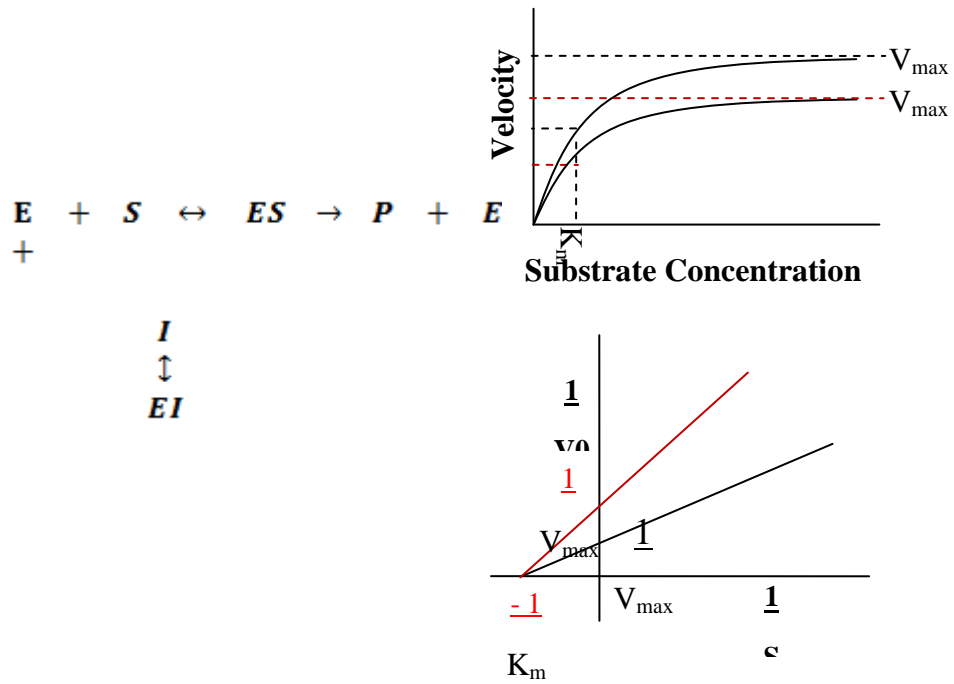
Figure 163a   Reversible competitive inhibition

$E \; + \; S \; \leftrightarrow \; ES \; \rightarrow \; P \; + \; E$

$+ \qquad\qquad +$

$I \qquad\qquad\quad I$

$\updownarrow \qquad\qquad\quad \updownarrow$

$EI \; + \; S \; \leftrightarrow \; EIS$

Velocity

V_{max}

V_{max}

K_m K_m

Substrate Concentration

$\dfrac{1}{v_0}$

$\dfrac{1}{s}$
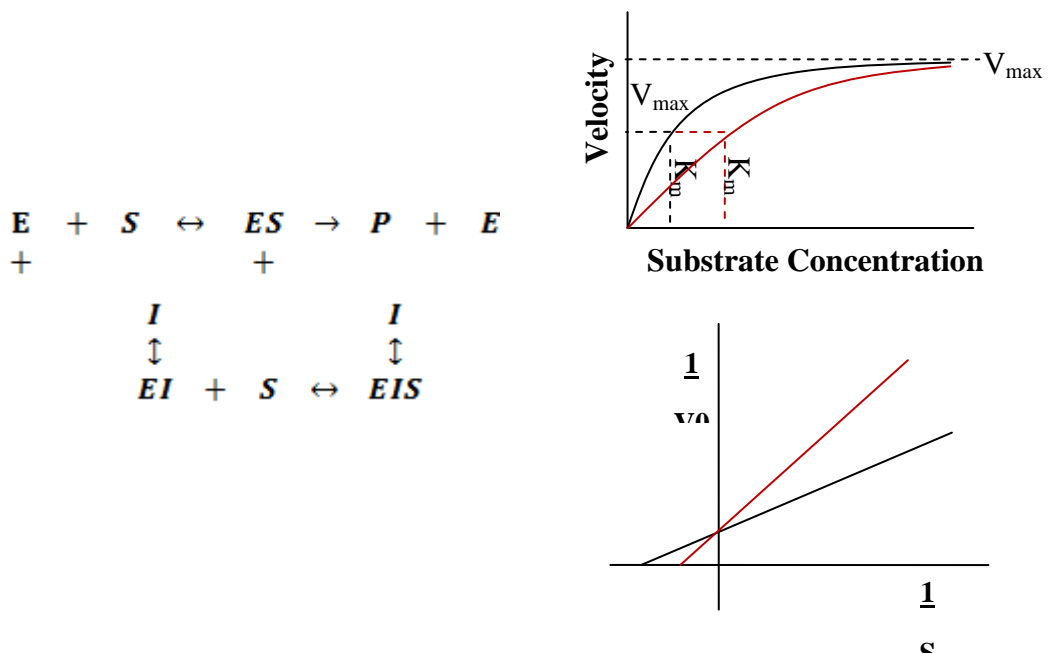
Figure 164b   Non-Competitive Reversible inhibition

$E + S \leftrightarrow ES \rightarrow P + E$

$+$

I

$\updownarrow$

EIS

Velocity

V_{max}
V_{max}

K_m K_m **Substrate**

$\dfrac{1}{V_0}$

$\dfrac{1}{S}$

Figure 165c   Uncompetetive Inhibition

EI

$+$

I

$+$

$E + S \leftrightarrow ES \rightarrow P + E$

$+$ $+$

I I

$\updownarrow$ $\updownarrow$

$EI + S \leftrightarrow EIS$

Velocity

V_{max}
V_{max}

K_m K_m **Substrate**

$\dfrac{1}{V_0}$

$\dfrac{1}{S}$
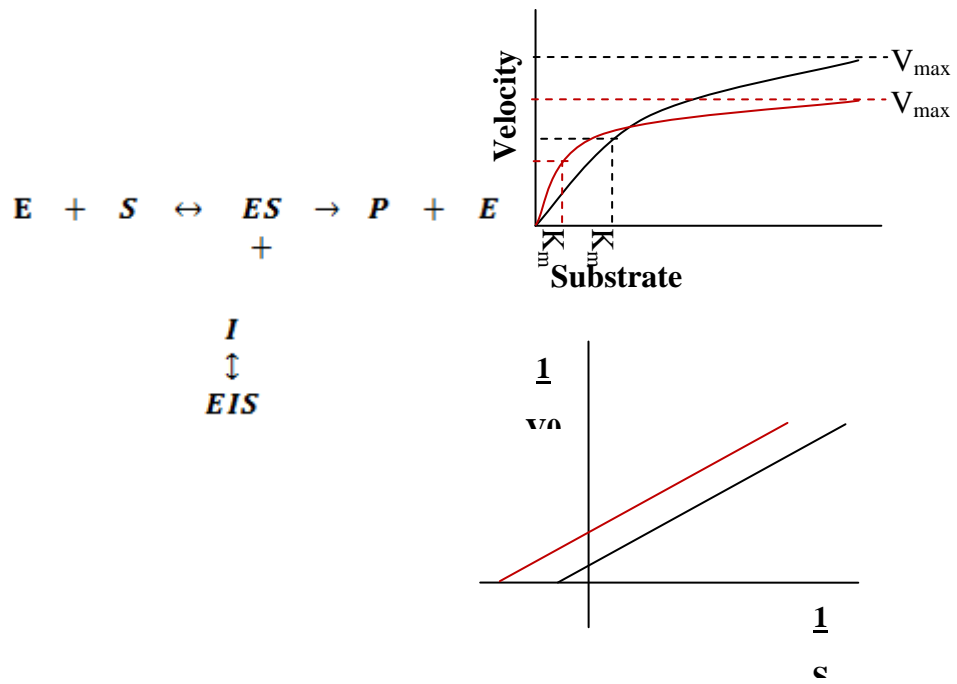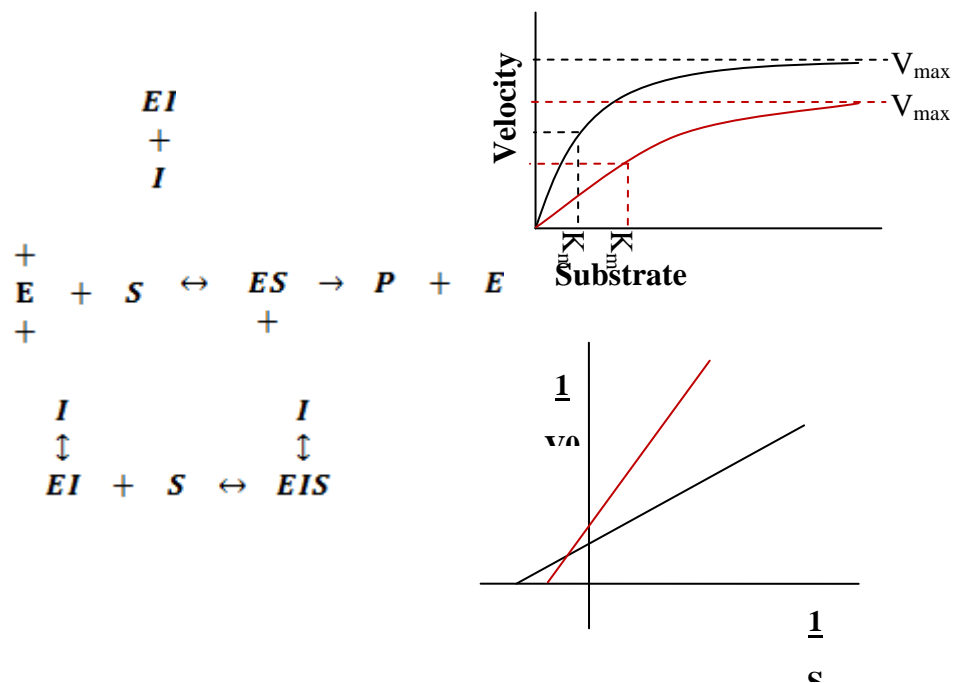
Figure 166d   Mixed Inhibition

8.3   Enzyme Activation

Enzyme activation is a less well studied field than inhibition, but shares many of the principles and methods of analysis.

8.3.1   Non-essential Activation

Enzyme activation can be described as essential or non-essential. Essential activation occurs when the presence of the activator is required for the reaction to take place, for example if the binding of a metal ion is essential for enzyme activity. The current study does not deal with essential activators.

Non-essential activation is when the reaction would take place without the presence of the activator, although at a slower rate.

Non-essential activation occurs in the same manner as enzyme inhibition with regard to the enzyme kinetics. Just that rather than decreasing the activity of the enzyme, activity is enhanced. A similar model of activation can be employed:

$$
\begin{array}{ccccccc}
E & + & S & \leftrightarrow & ES & \rightarrow & P & + & E \\
+ & & & & + \\
A & & & & A \\
\updownarrow & & & & \updownarrow \\
EA & + & S & \leftrightarrow & EAS & \rightarrow & P & + & E
\end{array}
$$
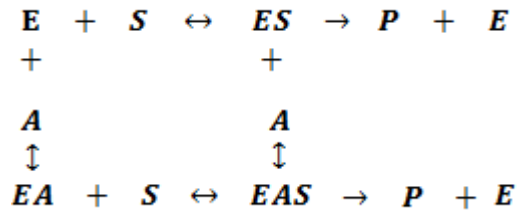
As can be seen from the diagram above, the product can be produced via two alternative paths; the non-activated route, which is the normal enzyme reaction, or the activated route.

8.3.2   Affect on Enzyme Kinetics

Three possible scenarios of activation are hypothesised below:

8.3.2.1 Increased affinity of enzyme for substrate.

This would cause an increased rate of reaction at low substrate concentrations, but would be saturated out at higher substrate concentrations and the V_{max} would be unchanged:
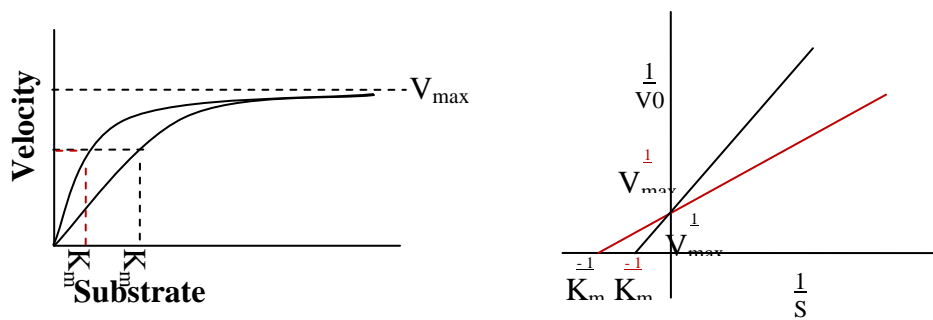
Figure 167 Generalised kinetic model for activation with increased affinity.

8.3.2.2 Increased enzyme activity with no change in affinity:

In this scenario, the enzyme becomes more active towards the substrate and the maximum velocity is increased, but there is no change in enzyme-substrate affinity and the K_m remains the same. This would occur when the rate of ES complex formation and dissociation are at in the same proportions in the activated and unactivated scenarios:

$$K_m = \frac{(K_2 + K_3)}{K_1}$$
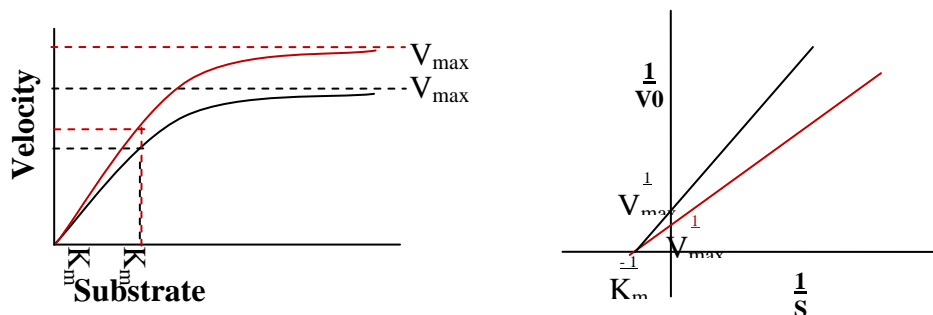
Figure 168 Generalised kinetic model for activation with no increase in affinity

8.3.2.3 Mixed Activation

When both substrate-enzyme affinity and maximum velocity are increased.
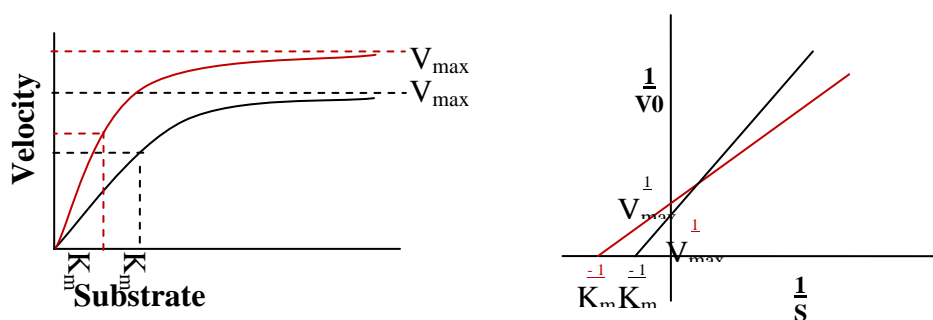
Figure 169 Generalised kinetic model for mixed activation

Chapter 9

Bibliography

1. WHO, *Obesity and Overweight Statistics*. 2006: World Health Organisation. p. Fact sheet N°311 September 2006; World Health Organisation.
2. Department of Health and the Department for Children, S.a.F., *Programme Budgeting Guidance 2006–07*. 2008, Department of Health
3. Lucas KH and Kaplan-Machlis B, *Orlistat--a novel weight loss therapy*. Ann Pharmacotherapy, 2001. **35**(3): p. 314-328.
4. Martin AE and Montgomery PA, *Acarbose: an alpha-glucosidase inhibitor*. Am J Health Syst Pharm, 1996. **53**: p. 2277–90.
5. Wilcox, M., *Bioactive Alginates*, in *ICAMB*. 2010, Newcastle University: Newcastle Upon Tyne.
6. Wilcox, M., et al., *The inhibition of pancreatic lipases*. 2009.
7. Strugala, V., et al., *Inhibition of pepsin activity by alginates in vitro and the effect of epimerization*. Int J Pharm, 2005. **304**(1-2): p. 40-50.
8. BBSRC, *The Age of Bioscience Strategic Plan 2010-2015*. 2010, BBSRC.
9. Power and Schulkin, *The Evolution of Obesity*. 2009, Baltimore: The Johns Hopkins University Press.
10. Wadden TA and Stunkard AJ, *Handbook of obesity treatment*. 2004: Guilford Press.
11. Ayyad C and Andersen T, *Long-term efficacy of dietary treatment of obesity: a systematic review of studies published between 1931 and 1999*. Obes Rev, 2000. **1**(2): p. 113-9.
12. Buchwald H, et al., *Bariatric surgery: a systematic review and meta-analysis*. Jama, 2004. **292**(14): p. 1724-37.
13. Haddock, C.K., et al., *Pharmacotherapy for obesity: a quantitative analysis of four decades of published randomized clinical trials*. Int J Obes Relat Metab Disord, 2002. **26**(2): p. 262-73.
14. Srishanmuganathan, J., et al., *National trends in the use and costs of anti-obesity medications in England 1998-2005*. J Public Health (Oxf), 2007. **29**(2): p. 199-202.
15. de Castro, J.J., et al., *A randomized double-blind study comparing the efficacy and safety of orlistat versus placebo in obese patients with mild to moderate hypercholesterolemia*. Rev Port Cardiol, 2009. **28**(12): p. 1361-74.
16. Padwal RS and Majumdar SR, *Drug treatments for obesity: orlistat, sibutramine, and rimonabant*. Lancet, 2007. **369**(9555): p. 71-7.
17. Weibel, E.K., et al., *Lipstatin, an inhibitor of pancreatic lipase, produced by Streptomyces toxytricini. I. Producing organism, fermentation, isolation and biological activity*. J Antibiot (Tokyo), 1987. **40**(8): p. 1081-5.
18. Cudrey, C., et al., *Inactivation of pancreatic lipases by amphiphilic reagents 5-(dodecyldithio)-2-nitrobenzoic acid and tetrahydrolipstatin. Dependence upon partitioning between micellar and oil phases*. Biochemistry, 1993. **32**(50): p. 13800-8.

19. Al-Suwailem AK, et al., *Safety and Mechanism of Action of Orlistat (Tetrahydrolipstatin) as the First Local Antiobesity Drug.* Journal of Applied Sciences Research, 2006. **2**(4): p. 205-208.

20. Hadvary P, et al., *The lipase inhibitor tetrahydrolipstatin binds covalently to the putative active site serine of pancreatic lipase.* Journal of Biological Chemistry, 1991. **266**(4): p. 2021-2027.

21. Hadváry P, Lengsfeld H, and Wolfer H, *Inhibition of pancreatic lipase in vitro by the covalent inhibitor tetrahydrolipstatin.* Biochem J., 1988. **256**(2): p. 357-361.

22. Tiss, et al., *Inhibition of human pancreatic lipase by tetrahydrolipstatin: Further kinetic studies showing its reversibility.* Journal of Molecular Catalysis, 2009. **58**(1-4): p. 7.

23. Haiker H, et al., *Rapid exchange of pancreatic lipase between triacylglycerol droplets.* Biochim Biophys Acta., 2004. **1682**(1-3): p. 72-79.

24. Bo-Linn GW, et al., *Starch blockers; their effect on calorie absorption from a high-starch meal.* N Engl J Med, 1982 **307**(23): p. 1413-6.

25. Udani J, Hardy M, and Madsen DC, *Blocking Carbohydrate Absorption and Weight Loss: A Clinical Trial Using Phase 2™ Brand Proprietary Fractionated White Bean Extract.* Alternative Medicine Review, 2004. **9**(1): p. 63-69.

26. Subramanian R, Asmawi MZ, and Sadikun AS, *In vitro α-glucosidase and α-amylase enzyme inhibitory effects of Andrographis paniculata extract and andrographolide* 2008. **55**(2): p. 391-398.

27. Celleno L, et al., *A Dietary Supplement Containing Standardized Phaseolus vulgaris Extract Influences Body Composition of Overweight Men and Women* Int J Med Sci, 2007: p. 45-52.

28. Buonocore V, et al., *Interaction of wheat monomeric and dimeric protein inhibitors with alpha-amylase from yellow mealworm (Tenebrio molitor L. larva).* Biochem J, 1980. **187**(3): p. 637-45.

29. Martins JC, et al., *Solution structure of the main alpha-amylase inhibitor from amaranth seeds.* Eur J Biochem, 2001. **268**(8): p. 2379-89.

30. Champ MM, *Non-nutrient bioactive substances of pulses.* Br J Nutr, 2002. **88 Suppl 3**: p. S307-19.

31. Chiasson JL, et al., *Acarbose for prevention of type 2 diabetes mellitus: the STOP-NIDDM randomised trial.* Lancet, 2002. **359**(9323): p. 2072-7.

32. Bischoff H, *The mechanism of alpha-glucosidase inhibition in the management of diabetes.* Clin Invest Med, 1995. **18**(4): p. 303-11.

33. Brunkhorst C, Andersen C, and Schneider E, *Acarbose, a pseudooligosaccharide, is transported but not metabolized by the maltose-maltodextrin system of Escherichia coli.* J Bacteriol, 1999. **181**(8): p. 2612-9.

34. Arungarinathan G, McKay GA, and Fisher M, *Drugs for diabetes: part 4 acarbose.* Br J Cardiol, 2011. **18**(2): p. 78−81.

35. Mertes, G., *Safety and efficacy of acarbose in the treatment of Type 2 diabetes: data from a 5-year surveillance study.* Diabetes Res Clin Pract, 2001. **52**(3): p. 193-204.

36. Trowell, H., et al., *Letter: Dietary fibre redefined.* Lancet, 1976. **1**(7966): p. 967.

37. Brownlee IA, et al., *Alginate as a source of dietary fiber.* Crit Rev Food Sci Nutr, 2005. **45**(6): p. 497-510.

38. Schaafsma G, *Health claims, options for dietary fibre.*, in *Dietary fibre: bio-active carbohydrates for food and feed.*, J.W.v.d. Kamp, Asp, N. G., Miller Jones, J., Schaafsma, G. , Editor. 2003, Wageningen Universiteit (Wageningen University).

39.   Steffen, L.M., et al., *Associations of whole-grain, refined-grain, and fruit and vegetable consumption with risks of all-cause mortality and incident coronary artery disease and ischemic stroke: the Atherosclerosis Risk in Communities (ARIC) Study.* Am J Clin Nutr, 2003. **78**(3): p. 383-90.

40.   Anderson JW, et al., *Health benefits of dietary fiber* Nutrition Reviews, 2009. **67**(4): p. 188-205.

41.   Wolk, A., et al., *Long-term intake of dietary fiber and decreased risk of coronary heart disease among women.* Jama, 1999. **281**(21): p. 1998-2004.

42.   Whelton, S.P., et al., *Effect of dietary fiber intake on blood pressure: a meta-analysis of randomized, controlled clinical trials.* J Hypertens, 2005. **23**(3): p. 475-81.

43.   He, J., et al., *Effect of dietary fiber intake on blood pressure: a randomized, double-blind, placebo-controlled trial.* J Hypertens, 2004. **22**(1): p. 73-80.

44.   Montonen, J., et al., *Whole-grain and fiber intake and the incidence of type 2 diabetes.* Am J Clin Nutr, 2003. **77**(3): p. 622-9.

45.   Lairon, D., et al., *Dietary fiber intake and risk factors for cardiovascular disease in French adults.* Am J Clin Nutr, 2005. **82**(6): p. 1185-94.

46.   Bingham SA, et al., *Dietary fibre in food and protection against colorectal cancer in the European Prospective Investigation into Cancer and Nutrition (EPIC): an observational study.* Lancet, 2003. **361**(9368): p. 1496-501.

47.   Lubin, F., et al., *Lifestyle and ethnicity play a role in all-cause mortality.* J Nutr, 2003. **133**(4): p. 1180-5.

48.   Lloveras, G., et al., *Food consumption and nutrient intake in relation to smoking.* Med Clin (Barc), 2001. **116**(4): p. 129-32.

49.   K Ikeda and T. Kisano, *In vitro inhibition of digestive enzymes by indigestible plant polysaccharides.* Cereal Chemistry, 1983. **60**(4): p. 260-263.

50.   Schneeman, B.O. and D. Gallaher, *Changes in small intestinal digestive enzyme activity and bile acids with dietary cellulose in rats.* J Nutr, 1980. **110**(3): p. 584-90.

51.   Dunaif, G. and B.O. Schneeman, *The effect of dietary fiber on human pancreatic enzyme activity in vitro.* Am J Clin Nutr, 1981. **34**(6): p. 1034-5.

52.   El Kossori, et al., *Comparison of effects of prickly pear (Opuntia ficus indica sp) fruit, arabic gum, carrageenan, alginic acid, locust bean gum and citrus pectin on viscosity and in vitro digestibility of casein.* Journal of the Science of Food and Agriculture, 2000. **80**(3): p. 359-364.

53.   Langhout, D.J. and J.B. Schutte, *Nutritional implications of pectins in chicks in relation to esterification and origin of pectins.* Poult Sci, 1996. **75**(10): p. 1236-42.

54.   Cavaliere H, Floriano I, and Medeiros-Neto G, *Gastrointestinal side effects of orlistat may be prevented by concomitant prescription of natural fibers (psyllium mucilloid).* Int J Obes Relat Metab Disord, 2001. **25**(7): p. 1095-9.

55.   Eastwood, M.A. and E.R. Morris, *Physical properties of dietary fiber that influence physiological function: a model for polymers along the gastrointestinal tract.* Am J Clin Nutr, 1992. **55**(2): p. 436-42.

56.   Dickinson E, *Stability and rheological implications of electrostatic milk protein–polysaccharide interactions.* Trends in Food Science & Technology, 1998. **9**(10): p. 347-354.

57.   Sunderland AM, Dettmar PW, and Pearson JP, *Alginates inhibit pepsin activity in vitro; A justification for their use in gastro-oesophageal reflux disease (GORD).* Gastroenterology, 2000. **118**(4): p. 347.

58. N, S., Mahoney RR, and Pellett PL, *Effect of guar gum, lignin and pectin on proteolytic enzyme levels in the gastrointestinal tract of the rat: a time-based study.* J Nutr, 1986. **116**(5): p. 786-94.

59. Percival E and Young M, *The polysaccharides of green, red and brown seaweeds: Their basic structure, biosynthesis and function.* European Journal of Phycology, 1979. **14**(2): p. 103 - 117.

60. Ertesvag, H., et al., *Mannuronan C-5-epimerases and their application for in vitro and in vivo design of new alginates useful in biotechnology.* Metab Eng, 1999. **1**(3): p. 262-9.

61. Boyd A and Chakrabarty AM, *Role of alginate lyase in cell detachment of Pseudomonas aeruginosa.* Appl Environ Microbiol, 1994. **60**(7): p. 2355-9.

62. TCC, *The alginate industry: general background.* 1979, The Competition Commission; The Monopolies and Mergers Commission.

63. Panikkar R and Brasch DJ, *Composition and block structure of alginates from New Zealand brown seaweeds.* Carbohydrate Research, 1996. **293**(1): p. 119-132.

64. Levitt, G., et al., *The effects of kelp harvesting on its regrowth and the understorey benthic community at Danger Point, South Africa, and a new method of harvesting kelp fronds.* African Journal of Marine Science, 2002. **24**: p. 71-85.

65. ISP, *Alginates - Products for Scientific Water Control* 2000: ISP (International Speciality Products).

66. Remminghorst, U. and B.H. Rehm, *Bacterial alginates: from biosynthesis to applications.* Biotechnol Lett, 2006. **28**(21): p. 1701-12.

67. Soon-Shiong, P., et al., *Long-term reversal of diabetes by the injection of immunoprotected islets.* Proc Natl Acad Sci U S A, 1993. **90**(12): p. 5843-7.

68. Khan, S., et al., *Overcoming drug resistance with alginate oligosaccharides able to potentiate the action of selected antibiotics.* Antimicrob Agents Chemother, 2012. **56**(10): p. 5134-41.

69. Draget, K., O. Smidsrod, and G. Skjak-Braek, *Alginates from Algae*, in *Biopolymers*, E.J.V. A. Steinbüchel, Martin Hofrichter, Sophie De Baets, Editor. 2002 Wiley-VCH.

70. King AH, *Brown seaweed extracts (alginates)* Food hydrocolloids, 1983. **2** p. 115

71. Draget, K.I., G. Skjak-Braek, and O. Smidsrod, *Alginate based new materials.* Int J Biol Macromol, 1997. **21**(1-2): p. 47-55.

72. Draget, K.I., et al., *Small-angle X-ray scattering and rheological characterization of alginate gels. 3. Alginic acid gels.* Biomacromolecules, 2003. **4**(6): p. 1661-8.

73. Smidsrod O. and D. K.L., *Chemistry and physical properties of alginates.* Carbohydrate European, 1996; . **14**: p. 6-13.

74. Erickson RH, Y. S., and M.D. Kim, *Sigestion and absorption of dietary protein.* Annu. Rev. Med., 1990. **41**: p. 133-139.

75. Rees, D., *Shapely polysaccharides. The eighth Colworth medal lecture.* Biochem J. , 1972. **126**(2): p. 257-73.

76. Braccini I and P. S, *Molecular basis of C(2+)-induced gelation in alginates and pectins: the egg-box model revisited.* Biomacromolecules, 2001. **2**(4): p. 1089-96.

77. Atkins EDT, et al., *Crystalline structures of poly-D-mannuronic and poly-L-guluronic acids.* Journal of Polymer Science Part B: Polymer Letters, vol., 1971. **9**(4): p. 311-316.

78. Draget KI, et al., *Swelling and partial solubilization of alginic acid gel beads in acidic buffer* Carbohydrate Polymers, 1996. **29**(3): p. 209-215.

79. Draget, K.I., G. Braek, and O. Smidsrod, *Alginic acid gels: the effect of alginate chemical composition and molecular weight.* Carbohydrate Polymers, 1994. **25**: p. 31-38.

80. Hartmanna, M., et al., *Enzymatic modification of alginates with the mannuronan C-5epimerase AlgE4 enhances their solubility at low pH* Carbohydrate Polymers, 2006. **63**(2): p. 257-262

81. Evans, D.F., et al., *Measurement of gastrointestinal pH profiles in normal ambulant human subjects.* Gut, 1988. **29**(8): p. 1035-41.

82. Pedersen AM, et al., *Saliva and gastrointestinal functions of taste, mastication, swallowing and digestion.* Oral Dis., 2002. **8**(3): p. 117-129.

83. Mese H and M. R., *Salivary secretion, taste and hyposalivation.* J Oral Rehabil, 2007. **34**(10): p. 711-723.

84. Germann WJ and Stnfield CL, *Principles of human physiology*. 2005: Pearson Education.

85. IT, B., *The role of pancreatic enzymes in digestion.* Am J Clin Nutr, 1973. **26**(3): p. 311-25.

86. Roxas M, *The Role of Enzyme Supplementation in Digestive Disorders.* Alternative Medicine Review, 2008. **13**(4): p. 307-314.

87. Westergaard H and Dietschy JM, *The mechanism whereby bile acid micelles increase the rate of fatty acid and cholesterol uptake into the intestinal mucosal cell.* J Clin Invest., 1976. **58**(1): p. 97-108.

88. Stamp, D. and G. Jenkins, *An Overview of Bile-Acid Synthesis, Chemistry and Function*, in *Bile Acids: Toxicology and Bioactivity*, G.J.a.L.J. Hardie, Editor. 2008, RSC Publishing.

89. Caspary WF, *Absorption: general aspects and tranport mechanisms in the small intestine*, in *Structure and function of the small intestine*. 1987, Excerpta Medica: Amsterdam. p. 63-68.

90. Johnson IT and G. JM, *Effect of gel-forming gums on the intestinal unstirred layer and sugar transport in vitro.* Gut, 1981. **22**(398-403): p. 398-403.

91. Vickerstaff J and Janice M, *Digestion, diet, and disease: irritable bowel syndrome and gastrointestinal function*. 2004: Rutgers University Press.

92. Mu H and H. CE, *The digestion of dietary triacylglycerols.* Progress in Lipid Research, 2004. **43**(2): p. 105-33.

93. Iqbal J and Hussain MM, *Intestinal lipid absorption* Am J Physiol Endocrinol Metab, 2009. **296**(6): p. 1183-1194.

94. Hamosh M and Scow RO, *Lingual Lipase and Its Role in the Digestion of Dietary Lipid.* J Clin Invest, 1973 **52**(1): p. 88-95.

95. Fredrikzon BO and Bläckberg L, *Lingual Lipase an Important Lipase in the Digestion of Dietary Lipids in Cystic Fibrosis?* Pediatric Research, 1980. **14**: p. 1387-1390.

96. Fredrikzon B and Hernell O, *Role of feeding on lipase activity in gastric contents.* Acta Paediatr Scand, 1977 **66**(4): p. 479-84.

97. Liao TH, Hamosh P, and H. M., *Fat Digestion by Lingual Lipase: Mechanism of Lipolysis in the Stomach and Upper Small Intestine.* Pediatr Res, 1984 **18**(5): p. 402-409.

98. Armand M, et al., *Digestion and absorption of 2 fat emulsions with different droplet sizes in the human digestive tract.* Am J Clin Nutr, 1999. **70**(6): p. 1096-1106.

99. Jenkins GJ, et al., *Bile Acids: Toxicology and Bioactivity (Issues in Toxicology*. 2008: Royal Society of Chemistry.

100. Elsenhans B and C. WF, *Resorption von Kohlenhydraten*, in *Handbuch der inneren Medizin Volume 3*. 1983 p. 139-156.

101. Rosenblum JL, Irwin CL, and A. DH., *Starch and glucose oligosaccharides protect salivary-type amylase activity at acid pH.* Am J Physiol., 1988 **254**: p. 775-780.

102. Holmes R and Lobley RW, *Intestinal brush border revisited.* Gut, 1989. **30**: p. 1667-1678.

103. Swagerty DL, Walling AD, and Klein RM, *Lactose Intolerance.* Am Fam Physician, 2002. **65**(9): p. 1845-1851.

104. Wright EM, Martín MG, and T. E., *Intestinal absorption in health and disease--sugars.* Best Pract Res Clin Gastroenterol., 2003. **17**(6): p. 943-956.

105. Srichamroen A, *Intestinal Transport of Monosaccharides.* Naresuan University Journal, 2007. **15**(2): p. 127-135.

106. WH, K. and D. JM, *Adaptive regulation of sugar and amino acid transport by the vertebrate intestine. .* American Journal of Physiology - Gastrointestinal and Liver Physiology, 1983. **245**: p. 443-462.

107. Traber PG, *Carbohydrate assimilation.*, in *Textbook of Gastroenterology*. 2004, Lippincott Williams & Wilkins: New York.

108. Wright, E., *Intestinal absorption in health and disease—sugars.* Best Practice & Research Clinical Gastroenterology, 2003. **17**(6): p. 943-956.

109. Ikeda TS, et al., *Characterization of a Na+/glucose cotransporter cloned from rabbit small intestine.* The Journal of Membrane Biology, 1989. **110**(1): p. 87-95.

110. Expasy. 2010; Available from: http://www.expasy.ch/.

111. Herriott, R.M., *Isolation, Crystallization, and Properties of Swine Pepsinogen.* J Gen Physiol, 1938. **21**(4): p. 501-540.

112. Hirschowitz, B.I., *Pepsinogen.* Postgrad Med J, 1984. **60**(709): p. 743-50.

113. Van Dyke, R., *Mechanisms of digestion and absorption of food.* Annu. Rev. Med., 1989. **41**: p. 133-139.

114. Caspary, W., *Physiology and pathophysiology of intestinal absorption.* Am J Clin Nutr, 1992. **55**(1): p. 299-308.

115. Rinderknecht H, *Activation of pancreatic zymogens. Normal activation, premature intrapancreatic activation, protective mechanisms against inappropriate activation.* Dig Dis Sci., 1986. **31**(3): p. 314-321.

116. Bröer S, *Amino acid transport across mammalian intestinal and renal epithelia.* Physiol Rev., 2008 **88**(1): p. 249-286.

117. Tanner J, *Cells and the Growth of Tissues*, in *Foetus Into Man: Physical Growth from Conception to Maturity*. 1989.

118. Krondl M and Anderson GH, *Conceptual models.*, in *Diet and Behaviour: Multidisciplinary Approaches.* 1990, Springer-Verlag London.

119. Booth SL, et al., *Environmental and Societal Factors Affect Food Choice and Physical Activity: Rationale, Influences, and Leverage Points.* Nutrition Reviews, 2009. **59**(3): p. 21-36.

120. Blundell JE and Halford JCG, *Regulation of nutrient supply: the brain and appetite control* Proceedings of the Nutrition Society, 1994. **53**: p. 407-418.

121. Blundell JE, *Pharmacological approaches to appetite suppression.* Trends Pharmacol Sci, 1991. **12**: p. 147-157.

122. Davis JD and Smith GP, *Learning to sham feed: behavioral adjustments to loss of physiological postingestional stimuli.* Am J Physiol Regul Integr Comp Physiol 2, 1990. **259**: p. 1228-1235.

123. Woods SC, *Gastrointestinal satiety signals I. An overview of gastrointestinal signals that influence food intake.* Am J Physiol Gastrointest Liver Physiol, 2004 **286**(1): p. 7-13.

124. Näslund E and Hellström PM, *Appetite signaling: from gut peptides and enteric nerves to brain.* Physiology & Behavior, 2007. **92**(1-2): p. 256-62.

125. Smith, G.P., C. Jerome, and R. Norgren, *Afferent axons in abdominal vagus mediate satiety effect of cholecystokinin in rats.* Am. J. Physiol, 1985. **249**: p. 638-641.

126. Inui A, et al., *Ghrelin, appetite, and gastric motility: the emerging role of the stomach as an endocrine organ.* The FASEB Journal, 2004. **18**(3): p. 439-456.

127. Cummings DE, et al., *A preprandial rise in plasma ghrelin levels suggests a role in meal initiation in humans.* Diabetes, 2001. **50**(1714-1719): p. 1714.

128. Schmid DA, et al., *Ghrelin stimulates appetite, imagination of food, GH, ACTH, and cortisol, but does not affect leptin in normal controls.* Neuropsychopharmacology, 2005 **30**(6): p. 1187-1192.

129. Kojima M and Kangawa K, *Ghrelin: Structure and Function.* Physiological Reviews, 2005. **85**(2): p. 495-522.

130. Friedman JM, *The Function of Leptin in Nutrition, Weight, and Physiology.* Nutrition Reviews, 2002. **60**(10): p. 1-14.

131. Rogers PJ and Blundell JE, *Separating the actions of sweetness and calories: Effects of saccharin and carbohydrates on humger and food intake in human subjects.* . Physiology and Behavior, 1989. **45**: p. 1093-1099.

132. Kershaw EE and Flier JS, *Adipose Tissue as an Endocrine Organ.* The Journal of Clinical Endocrinology & Metabolism, 2004. **89**(6): p. 2548-2556.

133. Seip M and Trygstad O, *Generalized lipodystrophy, congenital and acquired (lipoatrophy).* Acta Paediatr Suppl., 1996 **413**: p. 2-28.

134. Shaw JE, Sicree RA, and Z. PZ., *Global estimates of the prevalence of diabetes for 2010 and 2030.* Diabetes Res Clin Pract., 2010 **87**(1): p. 4-14.

135. Nolan CJ, Damm P, and P. M., *Type 2 diabetes across generations: from pathophysiology to prevention and management.* Lancet., 2011 **378**: p. 169-181.

136. Roglic G, Unwin N, and B. PH., *The burden of mortality attributable to diabetes: realistic estimates for the year 2000.* Diabetes Care, 2005. **28**(2130-2135): p. 2130.

137. Nielsen, J.E. and T.V. Borchert, *Protein engineering of bacterial alpha-amylases.* Biochim Biophys Acta, 2000. **1543**(2): p. 253-274.

138. Kuriki, T. and T. Imanaka, *The concept of the alpha-amylase family: structural similarity and common catalytic mechanism.* J Biosci Bioeng, 1999. **87**(5): p. 557-65.

139. Saeed S, et al., *Antihyperglycemic and antihyperlipidemic effects of guar gum on streptozotocin-induced diabetes in male rats.* Pharmacogn Mag., 2012. **8**(29): p. 65-72.

140. Dall'alba V, et al., *Improvement of the metabolic syndrome profile by soluble fibre - guar gum - in patients with type 2 diabetes: a randomised clinical trial.* Br J Nutr., 2013 **3**: p. 1-10.

141. Jenkins D, et al., *Unabsorbable carbohydrates and diabetes: Decreased postprandial hyperglycaemia.* . Lancet, 1976: p. 172-174.

142. Domínguez-Muñoz JE, *Pancreatic exocrine insufficiency: Diagnosis and treatment.* Journal of Gastroenterology and Hepatology, 2011. **26**(2): p. 12-16.

143. Cavaliere H, Floriano I, and Medeiros-Neto G, *Gastrointestinal side effects of orlistat may be prevented by concomitant prescription of natural fibers (psyllium mucilloid).* International Journal of Obesity, 2001. **25**: p. 1095-1099.

144. DiMagno EP, Go VLW, and S. WHJ., *Relations between pancreatic enzyme outputs and malabsorption in severe pancreatic insufficiency. .* N. Engl. J. Med., 1973. **288**: p. 813-815.

145. Safdi M, et al., *The effects of oral pancreatic enzymes (Creon 10 capsule) on steatorrhea: a multicenter, placebo-controlled, parallel group trial in subjects with chronic pancreatitis.* Pancreas, 2006. **33**: p. 156-162.

146. Proesmans M and DeBoeck K, *Omeprazole, a proton pump inhibitor, improves residual steatorrhea in cystic fibrosis patients treated with high dose pancreatic enzymes. .* Eur. J. Pediatr., 2003. **162**: p. 760-763.

147. Dukehart MR, Dutta SK, and V. J, *Dietary fiber supplementation: effect on exocrine pancreatic secretion in man.* American Journal of Clinical Nutrition, 1989. **50**(5): p. 1023-1028.

148. Dutta K and H. J., *Dietary fiber in pancreatic disease: effect of high fiber diet on fat malabsorption in pancreatic insufficiency and in-vitro study ofthe interaction ofdietary fiber and pancreatic enzymes.* Am J Clin Nutr, 1985. **4**: p. 517-525.

149. Gonzalez NJ and I. LL., *Evaluation of pancreatic proteolytic enzyme treatment of adenocarcinoma of the pancreas, with nutrition and detoxification support. .* Nutr Cancer, 1999. **33**: p. 117-124.

150. de Fonseka A and Kaunitz J, *Gut sensing mechanisms* Current Gastroenterology Reports, 2009. **11**: p. 442-447.

151. Pearson, J.P., *Pepsin*, in *Effects, Diagnosis and Management of Extra-esophageal Reflux*, B.J. Toohill, Nikki, Editor. 2010, Nova Science Publishers: Milwaukee.

152. Touitou E and Barry BW, *Enhancement in Drug Delivery*. 2007, NW: CRC Press.

153. Langguth P, Merkle HP, and Amidon GL, *Oral absorption of peptides: the effect of absorption site and enzyme inhibition on the systemic availability of metkephamid.* Pharm Res, 1994 **11**(4): p. 528-535.

154. Berg JM, Tymoczko JL, and Stryer L, *Section 8.5, Enzymes Can Be Inhibited by Specific Molecules.*, in *Biochemistry. 5th edition.* 2002, W H Freeman: New York.

155. Fujinaga M, et al., *Crystal structure of human pepsin and its complex with pepstatin.* Protein Sci., 1995 **4**(5): p. 960-972.

156. Cooper JB, et al., *X-ray analyses of aspartic proteinases. II. Three-dimensional structure of the hexagonal crystal form of porcine pepsin at 2.3 A resolution.* J Mol Biol, 1990. **214**(1): p. 199-222.

157. Fusek M and Větvička V, *Aspartic proteinases: physiology and pathology.* 1995 CRC Press.

158. Pearson JP, et al., *Pepsin* in *Effects, Diagnosis and Management of Extra-Esophageal Reflux*. 2010, Nova Science Publishers. p. 29-41.

159. Sinkovits, A.F., et al., *Understanding the structure-function role of specific catalytic residues in a model food related enzyme: Pepsin.* Enzyme and Microbial Technology, 2007. **40**(5): p. 1175-1180.

160. Szecsi PB, *The aspartic proteases.* Scand J Clin Lab Invest Suppl., 1992. **210**: p. 5-22.

161. Powers JC, Harley AD, and Myers DV, *Subsite specificity of porcine pepsin.* Adv Exp Med Biol, 1977. **95**: p. 141–157.

162. Hamuro Y, et al., *Specificity of immobilized porcine pepsin in H/D exchange compatible conditions.* Rapid Commun Mass Spectrom., 2008 **22**(7): p. 1041-1046.

163. Schechter, I. and A. Berger, *On the size of the active site in proteases. I. Papain.* Biochem Biophys Res Commun, 1967. **27**(2): p. 157-62.

164. Seijffers, M., *Partial Characterization of Human Pepsin I, Pepsin IIA, Pepsin IIB, and Pepsin III.* Biochemistry 1964. **3**(9): p. 1203.

165. Piper DW and Fenton BH, *pH stability and activity curves of pepsin with special reference to their clinical importance.* Gut, 1965. **6**(5): p. 506-8.

166. Dee, D., et al., *Comparison of solution structures and stabilities of native, partially unfolded and partially refolded pepsin.* Biochemistry, 2006. **45**(47): p. 13982-13992.

167. Dettmar PW, et al., *Pepsin inhibition by alginates.* 2003.

168. Lin Y, Means GE, and Feeney RE, *The action of proteolytic enzymes on N,N-dimethyl proteins. Basis for a microassay for proteolytic enzymes.* J Biol Chem, 1969. **244**(3): p. 789-93.

169. Onsøyen E, *Alginates*, in *Thickening and Gelling Agents for Food.* 1997. p. 22-24.

170. Parikh, S., *Biomarkers of Reflux*, in *ICaMB.* 2012, Newcastle University.

171. Dettmar PW, et al., *Rapid onset of effect of sodium alginate on gastro-oesophageal reflux compared with ranitidine and omeprazole, and relationship between symptoms and reflux episodes.* Int J Clin Pract, 2006. **60**(3): p. 275-83.

172. Strugala, V., et al., *The role of an alginate suspension on pepsin and bile acids - key aggressors in the gastric refluxate. Does this have implications for the treatment of gastro-oesophageal reflux disease?* J Pharm Pharmacol, 2009. **61**(8): p. 1021-8.

173. Goldberg, H.I., et al., *Role of acid and pepsin in acute experimental esophagitis.* Gastroenterology, 1969. **56**(2): p. 223-30.

174. Dangin M, et al., *The digestion rate of protein is an independent regulating factor of postprandial protein retention.* Am J Physiol Endocrinol Metab. 2001 Feb;280(2):E340-8., 2001. **280**(2): p. 340-348.

175. Lambers TT, van den Bosch WG, and de Jong S, *Fast and Slow Proteins: Modulation of the Gastric Behavior of Whey and Casein In Vitro.* Food Digestion, 2013. **4**(1): p. 1-6.

176. Hall, W.L., et al., *Casein and whey exert different effects on plasma amino acid profiles, gastrointestinal hormone secretion and appetite.* British Journal of Nutrition, 2003. **89**(2): p. 239-248.

177. Yamamoto, A., et al., *Effects of Various Protease Inhibitors on the Intestinal-Absorption and Degradation of Insulin in Rats.* Pharmaceutical Research, 1994. **11**(10): p. 1496-1500.

178. Hutton, D.A., et al., *Separation of pepsins in human gastric juice: analysis of proteolytic and mucolytic activity.* Biochem. Soc. Trans., 1986. **14**

179. Bianchi RG and Cook DL, *Antipeptic and Antiulcerogenic Properties of a Synthetic Sulfated Polysaccharide (Sn-263).* Gastroenterology, 1964. **47**: p. 409-14.

180. Cook DL and Drill VA, *Pharmacological Properties of Pepsin Inhibitors.* Ann N Y Acad Sci, 1967. **140**(2): p. 724-733.

181. Balaji SK, et al., *An improved process for the preparation of pentosan polysulfate or salts thereof*, in *Alembic Pharmaceuticals Limited*, A.P. Limited, Editor. 2012.

182. Yung-Chi C and Prusoff WH, *Relationship between the inhibition constant (KI) and the concentration of inhibitor which causes 50 per cent inhibition (I50) of an enzymatic reaction ☆.* Biochem Pharmacol, 1973. **22**(23): p. 3099-3108.

183. El Aouad N, et al., *A new natural Pepstatin from Kitasatospora (Actinomycetales).* Planta Medica, 2011. **77**: p. 59.

184. Fujinaga, M., et al., *Crystal structure of human pepsin and its complex with pepstatin.* Protein Sci, 1995. **4**(5): p. 960-72.

185. Turner MD, *Pepsinogens and pepsins.* Gut, 1968. **9**: p. 134-138.

186. Shay, H., et al., *A simple method for the uniform production of gastric ulceration in the rat.* Gut, 1945. **5**: p. 43-61.

187. Tersariol, I.L., et al., *Proteinase activity regulation by glycosaminoglycans.* Braz J Med Biol Res, 2002. **35**(2): p. 135-44.

188. Ermolieff, J., et al., *Heparin protects cathepsin G against inhibition by protein proteinase inhibitors.* J Biol Chem, 1994. **269**(47): p. 29502-8.

189. Kainulainen V, et al., *Syndecans, heparan sulfate proteoglycans, maintain the proteolytic balance of acute wound fluids.* Journal of Biological Chemistry, 1998. **273**: p. 11563-11569.

190. Lindahl U, et al., *Evidence for a 3-O-sulfated D-glucosamine residue in the antithrombin-binding sequence of heparin.* Proceedings of the National Academy of Sciences, 1980. **77**: p. 6551-6558.

191. Olson ST, Halvorson HR, and Björk I, *Quantitative characterization of the thrombin-heparin interaction. Discrimination between specific and nonspecific binding models.* . Journal of Biological Chemistry, 1991. **266**(6342-6352).

192. Almeida PC, et al., *Cathepsin B activity regulation. Heparin-like glycosaminogylcans protect human cathepsin B from alkaline pH-induced inactivation.* J Biol Chem, 2001. **276**(2): p. 944-51.

193. Olson ST, Halvorson HR, and Bjork I, *Quantitative characterization of the thrombin-heparin interaction. Discrimination between specific and nonspecific binding models.* J Biol Chem, 1991. **266**(10): p. 6342-52.

194. Grindrod J and Nickerson TA, *Effect of Various Gums on Skimmilk and Purified Milk Proteins.* J Dairy Sci, 1968. **51**(6): p. 834-841.

195. Payens TAJ, *Light Scattering of Protein Reactivity of Polysaccharides Especially of Carrageenans.* J Dairy Sci, 1972. **55**(2): p. 141-150.

196. De Jong and Hubertus GA, *New Hunger Supressing Food Compositions.* 2008.

197. Then C, et al., *Production of Alginate by Azotobacter vinelandii in semi-industrial scale using batch and fed-batch cultivation systems.* Journal of Advanced Scientific Research, 2012. **3**(4): p. 45-50.

198. Smidsrod, O. and K.I. Draget, *Chemistry and physical properties of alginates.* Carbohydrates in Europe, 1996. **14**: p. 7-13.

199. Puente, X.S., et al., *A genomic view of the complexity of mammalian proteolytic systems.* Biochem Soc Trans, 2005. **33**(Pt 2): p. 331-4.

200. Di Cera, E., *Serine proteases.* IUBMB Life, 2009. **61**(5): p. 510-5.

201. Erickson, R.H. and Y.S. Kim, *Digestion and absorption of dietary protein.* Annu Rev Med, 1990. **41**: p. 133-9.

202. Rinderknecht H, *Activation of pancreatic zymogens. Normal activation, premature intrapancreatic activation, protective mechanisms against inappropriate activation.* Dig Dis Sci, 1986. **31**(3): p. 314-21.

203. Hedstrom L, *Serine protease mechanism and specificity.* Chem Rev., 2002. **102**(12): p. 4501-4524.

204. Polgar, L., *The catalytic triad of serine peptidases.* Cell Mol Life Sci, 2005. **62**(19-20): p. 2161-72.

205. Rawlings ND and S. G, *Handbook of Proteolytic Enzymes (Third Edition).* Academic Press, 2012.

206. Krieger, M., L.M. Kay, and R.M. Stroud, *Structure and Specific Binding of Trypsin - Comparison of Inhibited Derivatives and a Model for Substrate Binding.* J Mol Biol, 1974. **83**(2): p. 209-&.

207. Robert H and B. W, *Structural basis of the activation and action of trypsin.* Accounts of Chemical Research 11.3, 1978: p. 114-122.

208. Cunningham, J.L., *Molecular-Kinetic properties of crystalline diisopropyl phosphoryl trypsin.* J. Biol. Chem., 1954. **211**: p. 13-19.

209. Fehlhammer, H., W. Bode, and R. Huber, *Crystal structure of bovine trypsinogen at 1-8 A resolution. II. Crystallographic refinement, refined crystal structure and comparison with bovine trypsin.* J Mol Biol, 1977. **111**(4): p. 415-38.

210. Leiros HK, et al., *Trypsin specificity as elucidated by LIE calculations, X-ray structures, and association constant measurements.* Protein Sci., 2004 **13**(4): p. 1056-70.

211. Bode W and Schwager P, *The single calcium-binding site of crystallin bovin beta-trypsin.* FEBS Lett, 1975. **56**(1): p. 139-43.

212. Graf, L., et al., *Selective alteration of substrate specificity by replacement of aspartic acid-189 with lysine in the binding pocket of trypsin.* Biochemistry, 1987. **26**(9): p. 2616-23.

213. Craik, C.S., et al., *Redesigning trypsin: alteration of substrate specificity.* Science, 1985. **228**(4697): p. 291-7.

214. Hedstrom, L., *An overview of serine proteases.* Curr Protoc Protein Sci, 2002. **Chapter 21**: p. Unit 21 10.

215. Berg JM, Tymoczko JL, and Stryer L, *Biochemistry Fifth Edition.* 2002: W. H. Freeman.

216. Kunitz, M. and J.H. Northrop, *Inactivation of Crystalline Trypsin.* J Gen Physiol, 1934. **17**(4): p. 591-615.

217. Grillet AM, Wyatt NB, and G. LM, *Polymer Gel Rheology and Adhesion*, in *Rheology*, D.J.D. Vicente, Editor. 2012.

218. Dickinson E, *Stability and rheological implications of electrostatic milk protein-polysaccharide interactions.* Trends in Food Science and Technology, 1998. **9**(10): p. 347-354.

219. Rheotec, *Introduction to Rheology*, Rheotec, Editor., Rheotec.

220. Koide, T. and T. Ikenaka, *Studies on soybean trypsin inhibitors. 1. Fragmentation of soybean trypsin inhibitor (Kunitz) by limited proteolysis and by chemical cleavage.* Eur J Biochem, 1973. **32**(3): p. 401-7.

221. Blow DM, Janin J, and Sweet RM, *Mode of action of soybean trypsin inhibitor (Kunitz) as a model for specific protein-protein interactions. .* Nature, 1974 **249**(452): p. 54-57.

222. Blow DM, Janin J, and Sweet RM, *Mode of action of soybean trypsin inhibitor (Kunitz) as a model for specific protein–protein interactions.* Nature 249, 54 - 57 (03 May 1974), 1974. **249**: p. 54-57.

223. Enswick JW, et al., *Use of Benzamidine as a Proteolytic Inhibitor in the Radioimmunoassay of Glucagon in Plasma.* J. Clin. Endocrinol. Metab., 1972 **35**: p. 463-467.

224. Katona G, et al., *Crystal Structure Reveals Basis for the Inhibitor Resistance of Human Brain Trypsin.* J Mol Biol, 2002. **315**: p. 1209-1218.

225. Steffen, L.W. and B.W. Steffen, *Improved method for measuring fibrinogen in plasma, with use of a plasmin inhibitor.* Clin Chem, 1976. **22**(3): p. 381-3.

226. Grillet AM, W.N., Gloe LM, *Polymer Gel Rheology and Adhesion*, in *Rheology*, D.J.D. Vicente, Editor. 2012.

227. Taylor C, et al., *Mucous Systems Show a Novel Mechanical Response to Applied Deformation.* Biomacromolecules, 2005. **6**(3): p. 1524-1530.

228. Ferry, J., *Viscoelastic Properties of Polymers, 3rd Edition.* 1980: Wiley-Blackwell.

229. Kumar A and Chauhan GS, *Extraction and characterisation of pectin from apple pomace and its evaluation as lipase (steapsin) inhibitor.* Carbohydrate Polymers, 2010. **82**(2): p. 454-459.

230. Brownlee, I.A., et al., *Mucosal protective properties of dietary fibre may be mediated through an interaction with mucus.* Gut, 2001. **49**(Suppl III): p. 2440.

231. Braccini, I., R.P. Grasso, and S. Perez, *Conformational and configurational features of acidic polysaccharides and their interactions with calcium ions: a molecular modeling investigation.* Carbohydr Res, 1999. **317**(1-4): p. 119-30.

232. Smidsrod O., D.K.L., *CHEMISTRY AND PHYSICAL PROPERTIES OF ALGINATES* CARBOHYDRATE EUROPEAN 1996; . **14**: p. 6-13.

233. Madsen F, Eberth K, and Smart JD, *A rheological assessment of the nature of interactions between mucoadhesive polymers and a homogenised mucus gel.* 19, 1998: p. 1083-92.

234. Chen L and Subirade M, *Alginate-whey protein granular microspheres as oral delivery vehicles for bioactive compounds.* Biomaterials, 2006. **27**(26): p. 4646-54.

235. Reseland, J.E., et al., *Proteinase inhibitors induce selective stimulation of human trypsin and chymotrypsin secretion.* J Nutr, 1996. **126**(3): p. 634-42.

236. Vihinen M and Mantsiila P, *Microbial Amylolytic Enzymes.* Critical Reviews in Biochemistry and Molecular Biology, 1989. **24**(4): p. 329-418.

237. Vihinen M and Mantsala P, *Microbial amylolytic enzymes.* Crit Rev Biochem Mol Biol, 1989. **24**(4): p. 329-418.

238. Granger M, Abadie B, and Marchis-Mouren G, *Limited action of trypsin on porcine pancreatic amylase: characterization of the fragments.* FEBS LETTERS, 1975. **56**: p. 189-193.

239. Brayer GD, Luo Y, and Withers SG, *The structure of human pancreatic alpha-amylase at 1.8 A resolution and comparisons with related enzymes.* Protein Sci, 1995. **4**(9): p. 1730-42.

240. Butterworth PJ, Warren FJ, and Ellis PR, *Human a-amylase and starch digestion: An interesting marriage.* Starch, 2011. **63**: p. 395-405.

241. Sogaard, M., et al., *Site-directed mutagenesis of histidine 93, aspartic acid 180, glutamic acid 205, histidine 290, and aspartic acid 291 at the active site and tryptophan 279 at the raw starch binding site in barley alpha-amylase 1.* J Biol Chem, 1993. **268**(30): p. 22480-4.

242. Takase, K., et al., *Site-directed mutagenesis of active site residues in Bacillus subtilis alpha-amylase.* Biochim Biophys Acta, 1992. **1120**(3): p. 281-8.

243. Davies, G. and B. Henrissat, *Structures and mechanisms of glycosyl hydrolases.* Structure, 1995. **3**(9): p. 853-9.

244. Wakim J, Robinson M, and Thoma JA, *The active site of porcine-pancreatic alpha-amylase: Factors contributing to catalysis* Carbohydrate Research, 1969. **10**(4): p. 487-503.

245. Rydberg EH, et al., *Mechanistic Analyses of Catalysis in Human Pancreatic R-Amylase: Detailed Kinetic and Structural Studies of Mutants of Three Conserved Carboxylic Acids.* Biochemistry, 2002. **41**: p. 4492-4502.

246. Ishikawa K, Matsui I, and Honda K, *Substrate-Dependent Shift of Optimum pH in Porcine Pancreatic a-Amylase-Catalyzed Reactions.* Biochemistry , 29, 7 1 19-7 12, 1990. **29**: p. 7119-7123.

247. Wang X, et al., *Structure-antioxidant relationships of sulfated galactomannan from guar gum. .* Int J Biol Macromol, 2010. **46**: p. 59-66.

248. Holt, S., et al., *Effect of gel fibre on gastric emptying and absorption of glucose and paracetamol.* Lancet, 1979. **1**(8117): p. 636-9.

249. Jenkins, D.J., et al., *Dietary fibres, fibre analogues, and glucose tolerance: importance of viscosity.* Br Med J, 1978. **1**(6124): p. 1392-4.

250. Jenkins, D.J.A., et al., *Dietary fibre, lente carbohydrates and the insulin-resistant diseases.* British Journal of Nutrition, 2000. **83**(Suppl. 1): p. S157-S163.

251. Jenkins, D.J.A., et al., *Soluble fiber intake at a dose approved by the US Food and Drug Administration for a claim of health benefits: serum lipid risk factors for cardiovascular disease assessed in a randomized controlled crossover trial.* American Journal of Clinical Nutrition, 2002. **75**(5): p. 834-839.

252. Kimura, Y., K. Watanabe, and H. Okuda, *Effects of soluble sodium alginate on cholesterol excretion and glucose tolerance in rats.* Journal of Ethnopharmacology, 1996. **54**(1): p. 47-54.

253. Sumner, J., *Dinitrosalicylic acid: A reagent for the estimation of sugar in normal and diabetic urine.* The Journal of Biological Chemistry, 1921. **47**: p. 5-9.

254. Ruhlmann, A., et al., *Pancreatic trypsin inhibitor (Kunitz). II. Complexes with proteinases.* Cold Spring Harb Symp Quant Biol, 1972. **36**: p. 148-50.

255. Brayer, G.D., Y. Luo, and S.G. Withers, *The structure of human pancreatic alpha-amylase at 1.8 A resolution and comparisons with related enzymes.* Protein Sci, 1995. **4**(9): p. 1730-42.

256. Shi X and BeMiller JN, *Effects of food gums on viscosities of starch suspensions during pasting.* Carbohydrate Polymers, 2002. **50**(1): p. 7-18.

257. Torsdottir, I., et al., *A small dose of soluble alginate-fiber affects postprandial glycemia and gastric emptying in humans with diabetes.* J Nutr, 1991. **121**(6): p. 795-9.

258. Alvarado F, *Sodium-driven transport. A re-evaluation of the sodium-gradient hypothesis. ,* in *Intestinal ion transport.* 1976, MTP Press: Lancaster. p. 117-152.

259. Kato, H., et al., *Abstract papers*, in *Annual Meeting of the Japanese of Society of Nutrition and Food Science,* . Kyoto. p. 246.

260. Peerce, B.E. and E.M. Wright, *Sodium-induced conformational changes in the glucose transporter of intestinal brush borders.* Journal of Biological Chemistry, 1984. **259**: p. 14105-14112. .

261. Torgerson, J.S., et al., *XENical in the Prevention of Diabetes in Obese Subjects (XENDOS) Study: A randomized study of orlistat as an adjunct to lifestyle changes for the prevention of type 2 diabetes in obese patients.* Diabetes Care, 2004. **27**(1): p. 155-161.

262. Visioli F, *Can experimental pharmacology be always applied to human nutrition?* International Journal of Food Sciences and Nutrition, 2012(63): p. 10–13.

263. Wickham M, Faulks R, and Mills C, *In vitro digestion methods for assessing the effect of food structure on allergen breakdown.* Mol Nutr Food Res., 2009 **53**(8): p. 952-958.

264. Baker DH, *Animal models in nutrition research.* J Nutr, 2008. **138**(2): p. 391-6.

265. Festing, S. and R. Wilkinson, *The ethics of animal research. Talking Point on the use of animals in scientific research.* EMBO Rep, 2007. **8**(6): p. 526-30.

266. Oomen, A.G., et al., *Comparison of five in vitro digestion models to study the bioaccessibility of soil contaminants.* Environ Sci Technol, 2002. **36**(15): p. 3326-34.

267. Mainville, I., Y. Arcand, and E.R. Farnworth, *A dynamic model that simulates the human upper gastrointestinal tract for the study of probiotics.* Int J Food Microbiol, 2005. **99**(3): p. 287-96.

268. Kong F and Singh RP, *A Human Gastric Simulator (HGS) to Study Food Digestion in Human Stomach.* Journal of Food Science, 2010. **75**: p. E627–E635.

269. Reis, P.M., et al., *Influence of Surfactants on Lipase Fat Digestion in a Model Gastro-intestinal System.* Food Biophys, 2008. **3**(4): p. 370-381.

270. Minekus, M., et al., *A computer-controlled system to simulate conditions of the large intestine with peristaltic mixing, water absorption and absorption of fermentation products.* Applied Microbiology and Biotechnology, 1999. **53**(1): p. 108-14.

271. Blanquet S, et al., *A dynamic artificial gastrointestinal system for studying the behavior of orally administered drug dosage forms under various physiological conditions.* Pharm Res, 2004. **21**(4): p. 585-91.

272. Wickham MJS, et al., *The Design, Operation, and Application of a Dynamic Gastric Model*, D. Technologies, Editor. 2012.

273. Schulze, K., *Imaging and modelling of digestion in the stomach and the duodenum.* Neurogastroenterol Motil, 2006. **18**(3): p. 172-83.

274. Minekus M and Havenaar R, *In vitro model of an in vivo digestive tract.* 1996.

275. Company, N.E., *The First Quantitative Evidence Proving The Efficacy Of Supplemental Enzymes*, in *National Enzyme Company*. 2004.

276. Minekus, M., et al., *A computer-controlled system to simulate conditions of the large intestine with peristaltic mixing, water absorption and absorption of fermentation products.* Applied Microbiology & Biotechnology, 2000. **53**(1): p. 108.

277. Savalle B, Miranda G, and Blissier JP, *In Vitro Simulation of Gastric Digestion of Milk Proteins.* J Agric Food Chem, 1989. **37**: p. 1336-1340.

278. Chiang CC, et al., *Development of a Dynamic System Simulating Pig Gastric Digestion.* Asian-Aust. J. Anim. Sci., 2008. **21**(10): p. 1522.

279. Hansen, M.B., *Neurohumoral control of gastrointestinal motility.* Physiol Res, 2003. **52**(1): p. 1-30.

280. Wiechelman, K.J., R.D. Braun, and J.D. Fitzpatrick, *Investigation of the bicinchoninic acid protein assay: identification of the groups responsible for color formation.* Anal Biochem, 1988. **175**(1): p. 231-7.

281. Wilcox, M.D.B., I. A.;Dettmar, P. W.;Pearson, J. P. ;, *The inhibition of pancreatic lipases.* 2009.

282. Isaksson, G., I. Lundquist, and I. Ihse, *In vitro inhibition of pancreatic enzyme activities by dietary fiber.* Digestion, 1982. **24**(1): p. 54-9.

283. Isaksson, G., et al., *Influence of dietary fiber on exocrine pancreatic function in the rat.* Digestion, 1983. **27**(2): p. 57-62.

284. Han, L.K., Y. Kimura, and H. Okuda, *Reduction in fat storage during chitin-chitosan treatment in mice fed a high-fat diet.* Int J Obes Relat Metab Disord, 1999. **23**(2): p. 174-9.

285. Tsujita, T., et al., *Inhibition of lipase activities by basic polysaccharide.* J Lipid Res, 2007. **48**(2): p. 358-65.

286. Zhang, G., Z. Ao, and B.R. Hamaker, *Slow digestion property of native cereal starches.* Biomacromolecules, 2006. **7**(11): p. 3252-8.

287. Oates CG, *Towards an understanding of starch granule structure and hydrolysis.* Trends in Food Science & Technology, 1997. **8**(11).

288. Ohta, A., et al., *The alginate reduce the postprandial glycaemic response by forming a gel with dietary calcium in the stomach of the rat.* International Journal for Vitamin and Nutrition Research, 1997. **67**(1): p. 55-61.

289. Sunderland, A.M., P.W. Dettmar, and J.P. Pearson, *Alginates inhibit pepsin activity in vitro; A justification for their use in gastro-oesophageal reflux disease (GORD).* Gastroenterology, 2000. **118**(4): p. 347.

290. Dettmar PW, H.F., Sunderland AM, Pearson JP, *Pepsin inhibition by alginates.* 2003.

291. Katona G, B.G., Hajdu J, GraÂf L, *Crystal Structure Reveals Basis for the Inhibitor Resistance of Human Brain Trypsin.* J Mol Biol, 2002. **315**: p. 1209-1218.

292. Sanaka, M., T. Yamamoto, and Y. Kuyama, *Effects of proton pump inhibitors on gastric emptying: a systematic review.* Dig Dis Sci, 2010. **55**(9): p. 2431-40.

293. Parkman HP and Jones MP, *Tests of Gastric Neuromuscular Function.* Gastroenterology, 2009 **136**(5): p. 1526-1543.

294. Evenepoel, P., et al., *Evidence for impaired assimilation and increased colonic fermentation of protein, related to gastric acid suppression therapy.* Aliment Pharmacol Ther, 1998. **12**(10): p. 1011-9.

295. Delgado-Aros, S., et al., *Contributions of gastric volumes and gastric emptying to meal size and postmeal symptoms in functional dyspepsia.* Gastroenterology, 2004. **127**(6): p. 1685-94.

296. Samsom, M., et al., *Diabetes mellitus and gastric emptying: questions and issues in clinical practice. .* Diabetes Metab. Res. Rev., 2009. **25**: p. 502-514.

297. Mefford IN and Wade EU, *Proton pump inhibitors as a treatment method for type II diabetes.* Med Hypotheses., 2009 **73**(1): p. 29-32.

298. Bergmann JF, et al., *Correlation between echographic gastric emptying and appetite: influence of psyllium.* Gut, 1992 **33**(8): p. 1042-3.

299. Wilcox MD, et al., *The modulation of pancreatic lipase activity by alginates [In Press].* Journal of Food Chemistry 2013.

300. Oomen, A.G., et al., *Comparison of Five In Vitro Digestion Models To Study the Bioaccessibility of Soil Contaminants.* Environmental Science & Technology, 2002. **36**(15): p. 3326-3334.

301. Faulks R and Wickham M, *Dynamic gastric model.* 2012.

302. Mainville, I., Y. Arcand, and E.R. Farnworth, *A dynamic model that simulates the human upper gastrointestinal tract for the study of probiotics.* International Journal of Food Microbiology, 2005. **99**(3): p. 287-296.

303. Kong F and Singh RP, *A human gastric simulator (HGS) to study food digestion in human stomach.* J Food Sci, 2010. **75**(9): p. 627-35.

304. Molly, K., et al., *Validation of the Simulator of the Human Intestinal Microbial Ecosystem (SHIME) Reactor Using Microorganism-associated Activities.* Microb Ecol Health Dis, 1994. **7**(4): p. 191-200.

305. Blanquet S, et al., *A dynamic artificial gastrointestinal system for studying the behavior of orally administered drug dosage forms under various physiological conditions.* Pharm Res., 2004. **21**(4): p. 585-91.

306. International, E., *New Product Development Trends in Consumer Health 2013.* 2013, Euromonitor International

307. International, E., *Future of Weight Management with Stevia, CLA and Satiety Food and Drinks: Functional Approach versus Calorie Reduction.* 2011, Euromonitor International: Euromonitor International.

308. International, E., *Health and Wellness Global Briefings*, in *GLOBAL BRIEFING SERIES.* 2012, Euromonitor International.

309. Lang T, Rayner G, and Kaelin E, *The food industry, diet, physical activity and health: A review of the reported commitments and practice of 25 of the worlds largest food companies.* 2006, City University London: City University London.